HAROKOPIO UNIVERSITY

SCHOOL OF ENVIRONMENT, GEOGRAPHY AND APPLIED ECONOMICS

DEPARTMENT OF GEOGRAPHY

Late Pleistocene to Holocene Climate and Environmental Changes in Greece: Evidence from Glacial Processes and multi proxy Records

Doctoral Thesis

Aris-Dimitrios Leontaritis

Athens, 2020

ΧΑΡΟΚΟΠΕΙΟ ΠΑΝΕΠΙΣΤΗΜΙΟ

ΣΧΟΛΗ ΠΕΡΙΒΑΛΛΟΝΤΟΣ, ΓΕΩΓΡΑΦΙΑΣ ΚΑΙ ΕΦΑΡΜΟΣΜΕΝΩΝ ΟΙΚΟΝΟΜΙΚΩΝ

ΤΜΗΜΑ ΓΕΩΓΡΑΦΙΑΣ

Κλιματικές και Περιβαλλοντικές μεταβολές κατά το Άνω Πλειστόκαινο-Ολόκαινο στην Ελλάδα: Ενδείξεις από παγετώδεις διεργασίες και πολλαπλές ιζηματολογικές καταγραφές

Διδακτορική Διατριβή

Άρης – Δημήτριος Λεονταρίτης

Αθήνα, 2020

HAROKOPIO UNIVERSITY

SCHOOL OF ENVIRONMENT, GEOGRAPHY AND APPLIED ECONOMICS

DEPARTMENT OF GEOGRAPHY

This doctoral dissertation was examined by the following 7-member committee:

Petros Katsafados (Supervisor)
Asociate Professor, Department of Geography, Harokopio University

Phil Hughes,
Professor, School of Environment, Education and Development, University of Manchester

Katerina Kouli
Associate Professor, Faculty of Geology and Geoenvironment, National and Kapodistrian University of Athens

Kosmas Pavlopoulos
Professor, Department of Geography and Planning, Sorbonne University Abu Dhabi

Eythymios Karympalis
Professor, Department of Geography, Harokopio University

Adriano Ribolini
Associate Professor, Department of Earth Sciences, University of Pisa

Konstantinos Vouvalidis
Associate Professor, Department of Geology, Aristotle University of Thessaloniki

ΧΑΡΟΚΟΠΕΙΟ ΠΑΝΕΠΙΣΤΗΜΙΟ

ΣΧΟΛΗ ΠΕΡΙΒΑΛΛΟΝΤΟΣ, ΓΕΩΓΡΑΦΙΑΣ ΚΑΙ ΕΦΑΡΜΟΣΜΕΝΩΝ ΟΙΚΟΝΟΜΙΚΩΝ

ΤΜΗΜΑ ΓΕΩΓΡΑΦΙΑΣ

Η Διδακτορική Διατριβή εξετάστηκε από την κάτωθι Επταμελή Επιτροπή:

Πέτρος Κατσαφάδος (Επιβλέπουσα/Επιβλέπων)
Αναπληρωτής Καθηγητής, Τμήμα Γεωγραφίας, Χαροκόπειο Πανεπιστήμιο

Philip D. Hughes,
Professor, School of Environment, Education and Development, University of Manchester

Κατερίνα Κούλη
Αναπληρώτρια Καθηγήτρια, Τμήμα Γεωλογίας και Γεωπεριβάλλοντος, ΕΚΠΑ

Κοσμάς Παυλόπουλος
Professor, Department of Geography and Planning, Sorbonne University Abu Dhabi

Ευθύμιος Καρύμπαλης
Καθηγητής, Τμήμα Γεωγραφίας, Χαροκόπειο Πανεπιστήμιο

Adriano Ribolini
Associate Professor, Department of Earth Sciences, University of Pisa

Κωσταντίνος Βουβαλίδης
Αναπληρωτής Καθηγητής, τμήμα Γεωλογίας, ΑΠΘ

The approval of this doctoral thesis by the department of Geography does not imply acceptance of the author’s opinions.

Η έγκριση της διδακτορικής διατριβής από το τμήμα Γεωγραφίας του Χαροκοπείου Πανεπιστημίου δεν υποδηλώνει και αποδοχή των απόψεων του συγγραφέα.

Ο Άρης Δημήτριος Λεονταρίτης

δηλώνω υπεύθυνα ότι:

1) Είμαι ο κάτοχος των πνευματικών δικαιωμάτων της πρωτότυπης αυτής εργασίας και από όσο γνωρίζω η εργασία μου δε συκοφαντεί πρόσωπα, ούτε προσβάλει τα πνευματικά δικαιώματα τρίτων.

2) Αποδέχομαι ότι η ΒΚΠ μπορεί, χωρίς να αλλάξει το περιεχόμενο της εργασίας μου, να τη διαθέσει σε ηλεκτρονική μορφή μέσα από τη ψηφιακή Βιβλιοθήκη της, να την αντιγράψει σε οποιοδήποτε μέσο ή/και σε οποιοδήποτε μορφότυπο καθώς και να κρατά περισσότερα από ένα αντίγραφα για λόγους συντήρησης και ασφάλειας.

This work is dedicated to the wild and beautiful Greek nature and still unspoilt and wonderful mountains.
And like this they shall remain in the difficult years yet to come.

Mountains have been and will always be home to the eternal spirit of freedom and of its unspoken wilderness;
refuge for the poor and the persecuted,
for all the bandits and all the Robin Hoods,
for all the partisans that dared to defy power and fight for political and social justice.

Abstract

The objective of this thesis is to address temporal gaps in the glacial history of the Pindus Mountains in northwest Greece with new insights from the study of the glacial record of Mt Mavrovouni and its connection with the respective records in southern Greece and in the Balkans. The glacial geomorphology of Mt Mavrovouni was mapped and the timing of Late Pleistocene glaciations was constrained by cosmogenic ^{36}Cl exposure ages from ophiolitic glacial boulders within a well-preserved glacial/periglacial sequence. These ages indicate that the most extensive Late Pleistocene glaciers reached their terminal positions at 26.6 ± 6.6 ka suggesting a Late Pleistocene local glacial maximum close in timing to the Last Glacial Maximum (27-23 ka). This timing was confirmed by ^{36}Cl ages from limestone glacial boulders in a similar study in the nearby Mt Tymphi. The consistency of these ages validates the theoretical suitability of cosmogenic ^{36}Cl exposure dating on ophiolites while it constitutes the only chronology of Late Pleistocene glaciations on the mountains of Greece that is independent from inherent issues in surface exposure dating of limestones such as weathering rates of rock surfaces. At the same time the geochronological framework of Late Pleistocene glaciations in the Pindus mountains in northwest Greece is now one of the best dated in western Balkans. New evidence and a detailed review of glacial studies in the mountains of Greece provided a new synthesis of our current understanding of the Quaternary glacial history of Greece. The ice cover during the largest Middle Pleistocene glaciations (MIS 12/ MIS 6) was more extensive than previously thought. Latest evidence from Mt Tymphi, Mt Smolikas and Mt Chelmos along with findings of other glacial studies in western Balkans suggests that valley glaciers radiated from central ice field/ice caps throughout this region during the most extensive Middle Pleistocene glaciations. Ice extent was considerably smaller during the Last Glacial Cycle (MIS 5d – MIS 2) whereas during the Holocene only very small glaciers formed in some deep-cirques thanks to strong local topographical and climatic controls. Finally, an analysis of regional palaeoclimatic records showed that moisture supply of the atmospheric systems seems to have been the most critical factor for the formation of glaciers in the mountains of Greece. Moreover, the Late Pleistocene Equilibrium Line Altitudes across Greece indicate a wetter climate in southern Greece that can be attributed to different palaeoatmospheric circulation mechanisms in central Mediterranean that forced moisture supply into a SW-NE track.

Keywords: Quaternary climate change; chlorine-36 cosmogenic dating; geomorphology; glacial history; Greece

Εκτεταμένη Περίληψη

Το Τεταρτογενές, χαρακτηρίζεται από κλιματικές εξάρσεις με ένα σημαντικό αριθμό παγετωδών και μεσοπαγετωδών κύκλων (Ehlers και Gibbard, 2003). Αυτές οι εξάρσεις αποτυπώνονται έντονα στο γεωλογικό αρχείο μέσω των ενδείξεων των επαναλαμβανόμενων προωθήσεων και υποχωρήσεων των παγετώνων: μεγάλα παγετωνικά καλύμματα σε υψηλότερα γεωγραφικά πλάτη και αλπικοί παγετώνες σε ορεινές περιοχές (Ivy-Ochs και Briner, 2014). Οι παγετώνες αποκρίνονται στις κλιματικές αλλαγές και ιδιαίτερα στη θερμοκρασία και το ύψος των κατακρημνίσεων καθώς επηρεάζεται το ισοζύγιο μάζας τους με αποτέλεσμα την προώθηση ή την υποχώρηση του μετώπου τους (Oerlemans, 2005). Έτσι η έκταση τους κατά το παρελθόν που αποτυπώνεται στις παγετωνικές αποθέσεις και γεωμορφές (Fuchs και Owen, 2008) ταυτόχρονα αποτυπώνει και τις αντίστοιχες αλλαγές στο παλαιοκλίμα (Ivy-Ochs και Briner, 2014).

Η περιοχή της Μεσογείου, βρίσκεται σε μια πολύ σημαντική γεωγραφική θέση για την κατανόηση των κλιματικών αλλαγών στο βόρειο ημισφαίριο κατά το Τεταρτογενές καθώς βρίσκεται αμέσως ανατολικά του Β. Ατλαντικού Ωκεανού και είναι ευθυγραμμισμένη με τα μέσα προς χαμηλά γεωγραφικά πλάτη (Hughes και Woodward, 2017). Έτσι, ένας σημαντικός αριθμός σύγχρονων ερευνών επικεντρώνεται σε αυτή την περιοχή και ιδιαίτερα στη χρονολόγηση και τη χαρτογράφηση της έκτασης των παλαιοπαγετώνων στα βουνά της Μεσογείου.

Η Ελλάδα είναι μια ιδιαίτερα ορεινή μεσογειακή χωρά, με το 42% της ηπειρωτικής επιφάνειάς της να χαρακτηρίζεται ως ορεινή (Bassiouka, 2011). Η τοπογραφία της χαρακτηρίζεται από την οροσειρά της Πίνδου, η οποία εκτείνεται από τα ΒΔ προς τα ΝΑ (Figure 1). Οι κυριότερες κορυφές της ξεπερνούν τα 2200 m σε υψόμετρο και αμέτρητες δευτερεύουσες κορυφές ξεπερνούν τα 1800 m σε υψόμετρο. Υπάρχει πληθώρα ενδείξεων για την ύπαρξη Τεταρτογενών παγετώνων (Figure 1; Table 1), όπως υπέδειξαν και οι πρωτοπόροι ερευνητές στις αρχές του 20ου αι. όπως οι Niculescu (1915), Cvijic (1917), Sestini (1933), Mistardis (1937a) και Messerli (1967).

Η μελέτη της αλληλουχίας των παγετωνικών αποθέσεων στο όρος Τύμφη στη Β. Πίνδο είναι μια από τις πρώτες προηγμένες παλαιοπαγετωνικές έρευνες στις ορεινές περιοχές της Μεσογείου και πλέον χαρακτηρίζεται από μια σειρά πολύ καλών γεωχρονολογήσεων (Woodward et al., 2004; Hughes et al., 2006a, 2006b; Woodward και Hughes, 2011; Allard et al., 2020). Τα αποτελέσματα των ερευνών αυτών οδήγησαν στον καθορισμό της Χρονοστρωματογραφίας της Πίνδου (Hughes et al. 2006a). Ωστόσο όταν ξεκίνησε η παρούσα

έρευνα (2015-2016), οι προηγμένες έρευνες που περιλάμβαναν δεδομένα απόλυτων χρονολογήσεων περιορίζονταν γεωγραφικά στη Β. Ελλάδα και συγκεκριμένα στο όρος Τύμφη. Επιπροσθέτως, το γεωχρονολογικό πλαίσιο στη Β. Πίνδο καθοριζόταν από απόλυτες χρονολογήσεις μόνο για τις παλαιότερες και εκτενέστερες παγετωνικές φάσεις κατά το Μέσο Πλειστόκαινο (ισοτοπικό στάδιο ή MIS 12 – MIS 6) ενώ οι νεότερες και πιο περιορισμένες φάσεις είχαν αποδοθεί στο Ανώτερο Πλειστόκαινο μέσω της σχετικής χρονολόγησής τους και της θέσης/υψομέτρου τους. Η έλλειψη περαιτέρω δεδομένων απόλυτης χρονολόγησης των παγετωνικών φάσεων του Ανώτερου Πλειστόκαινου αποτελούσε λοιπόν ένα σημαντικό κενό στη χρονοστρωματογραφία της Πίνδου που οδήγησε στην έναρξη νέων ερευνών, συμπεριλαμβανομένης της παρούσης, τόσο στη βόρεια όσο και στη νότια Ελλάδα. Τα τελευταία χρόνια, νέα δεδομένα δημοσιεύθηκαν τόσο από τη Ν. Ελλάδα (Όρος Χελμός στην Πελοπόννησο - Pope et al., 2017; Pavlopoulos et al., 2018) αλλά και από τον Όλυμπο στα ΒΑ (Styllas et al., 2018) και την Τύμφη στα ΒΔ (Allard et al., 2020), παρέχοντας ένα πιο συμπαγές γεωχρονολογικό πλαίσιο για την παγετωνική ιστορία των βουνών της Ελλάδας (Figure 1, Table 1). Μια εκτενής βιβλιογραφική ανασκόπηση των ερευνών αυτών παρατίθεται στο κεφάλαιο 3.

Αντικείμενο Έρευνας

Στο πλαίσιο αυτό, η παρούσα έρευνα επικεντρώνεται στη μελέτη παγετωνικών αποθέσεων του Ανώτερου Πλειστόκαινου στη ΒΔ Ελλάδα σε μια προσπάθεια ολοκλήρωσης της χρονοστρωματογραφίας της Πίνδου από μια γεωχρονολογική σκοπιά. Ταυτόχρονα, η μελέτη της παγετωνικής ιστορίας της Ν. Ελλάδας αποσκοπεί στη γεωγραφική επέκταση αυτού του γεωχρονολογικού πλαισίου στην υπόλοιπη Ελλάδα. Έτσι, ο βασικός στόχος της έρευνας αυτής είναι η χρονολόγηση των παγετωνικών αποθέσεων που αποδίδονται στο Ανώτερο Πλειστόκαινο σε τρεις περιοχές μελέτης: το όρος Μαυροβούνι στην Β. Πίνδο, ο Χελμός στην Πελοπόννησο και ο Παρνασσός στη Στερεά Ελλάδα (βλ. Figure 1 για τοποθεσίες).

Συνοπτικά, συγκεκριμένοι στόχοι της έρευνας αυτής είναι:

i. η χρονολόγηση με κοσμογονικά ισότοπα ^{36}Cl των παγετωνικών και περιπαγετωνικών αποθέσεων που αποδίδονται κατά το Ανώτερο Πλειστόκαινο και συγκεκριμένα κατά το LGM/Late-Glacial στο όρος Μαυροβούνι. Η εφαρμογή της μεθόδου αυτής εφαρμόζεται για πρώτη φορά σε οφιολιθικά πετρώματα.

ii. η ανακατασκευή της έκτασης των παλαιοπαγετώνων και των ισοϋψών γραμμών ισορροπίας μάζας (Equilibirium Line Altitudes ή ELAs) με χρήση εξειδικευμένων εργαλείων GIS (π.χ. Pellitero et al., 2015, 2016)

iii. Η χρονολόγηση ασβεστολιθικών παγετωνικών αποθέσεων στο όρος Χελμός με τη μέθοδο OSL (Optically Stimulated Luminescence)

iv. Η προκαταρκτική παγετωνική γεωμορφολογική έρευνα στον Παρνασσό

v. η ερμηνεία των αποτελεσμάτων και η συσχέτισή τους με άλλες μελέτες στην Ελλάδα και τα ευρύτερα Βαλκάνια

vi. η σύγκριση του παγετωνικού χρονικού με άλλα παλαιοκλιματικά αρχεία και ιδιαίτερα με αλληλουχίες γύρης, αναδεικνύοντας τη σημασία του στο ευρύτερο παλαιοκλιματικό πλαίσιο της Μεσογείου

Αποτελέσματα και συμπεράσματα

Η παγετωνική γεωμορφολογία του όρους Μαυροβούνι χαρτογραφήθηκε λεπτομερώς και το χρονικό των παγετωνικών φάσεων κατά το Ανώτερο Πλειστόκαινο προσδιορίστηκε μέσω της απόλυτης χρονολόγησης οφιολιθικών παγετωνικών λίθων με τη μέθοδο κοσμογενών ισοτόπων χλωρίου (^{36}Cl) σε μια παγετωνική/περιπαγετωνική ακολουθία αποθέσεων. Οι ηλικίες που προέκυψαν έδειξαν ότι οι παγετώνες είχαν φθάσει στις τελικές τους θέσεις 26.6 ± 6.6 ka πριν από σήμερα, υποδηλώνοντας ότι το τοπικό παγετωνικό μέγιστο κατά το Ανώτερο Πλειστόκαινο έλαβε χώρα κοντά στο Παγκόσμιο Παγετωνικό Μέγιστο (LGM: 27-23 ka), κάτι που επιβεβαιώθηκε από μια πρόσφατη αντίστοιχη μελέτη στο γειτονικό ασβεστολιθικό όρος Τύμφη (Allard et al., 2020). Η συνοχή των ηλικιών αυτών επικυρώνει τη θεωρητική καταλληλόλητα της επιλεγμένης μεθόδου για τη χρονολόγηση οφιολιθικών δειγμάτων ενώ ταυτόχρονα αποτελεί τη μοναδική γεωχρονολόγηση παγετωνικών αποθέσεων στην Ελλάδα που είναι απαλλαγμένη από τις εγγενείς αβεβαιότητες της χρονολόγησης ασβεστολιθικών δειγμάτων όπως ο ρυθμός αποσάθρωσης. Ως άμεση συνέπεια της επικύρωσης της εφαρμοσιμότητας της απόλυτης χρονολόγησης με τη μέθοδο κοσμογενών ισοτόπων χλωρίου σε οφιολιθικά πετρώματα, ανοίγει η προοπτική της χρονολόγησης της ακολουθίας των παγετωνικών αποθέσεων στο επίσης οφιολιθικό όρος Σμόλικας, η οποία είναι η πιο ολοκληρωμένη που έχει καταγραφεί στην Ελλάδα.

Στον Χελμό, η χρονολόγηση μια μοραίνας σε υψόμετρο 1900-2050 m a.s.l. στην κοιλάδα Σπανόλακος με τη μέθοδο OSL έδωσε ηλικίες απόθεσης πριν από 89-86 ka που θα μπορούσαν να υποδεικνύουν μια ακόμα παγετωνική φάση στην Πελοπόννησο κατά το MIS5b. Ωστόσο, δεν υπάρχουν αντίστοιχες ενδείξεις από άλλα βουνά στην Ελλάδα και τα Βαλκάνια και επομένως μέχρι να υπάρξουν περισσότερα δεδομένα που να την επιβεβαιώνουν, η υπόθεση αυτή θα πρέπει να αντιμετωπίζεται με επιφύλαξη.

Ταυτόχρονα, η λεπτομερής ανασκόπηση των προηγούμενων παγετωνικών μελετών αλλά και νέες παρατηρήσεις οδήγησαν σε μια νέα σύνθεση της Τεταρτογενούς παγετωνικής ιστορίας της Ελλάδας η οποία αποτυπώνεται στην πρώτη οργανωμένη βάση δεδομένων για τις παλαιοπαγετωνικές έρευνες στην Ελλάδα (Table 21). Η ανάλυση και η συζήτηση πάνω σε αυτή την βάση δεδομένων οδήγησε στην διορατικότερη κατανόηση μας των παγετωνικών φάσεων στα βουνά της Ελλάδας. Τα κυριότερα στοιχεία για την κάθε περίοδο συνοψίζονται ως εξής:

Α. Μέσο Πλειστόκαινο

- Οι πιο εκτενείς παγετωνικές φάσεις πιθανότατα έλαβαν χώρα κατά το Μέσο Πλειστόκαινο και συγκεκριμένα κατά το MIS 12 (Skamnellian Stage) και το MIS 6 (Vlasian Stage). Η παγοκάλυψη κατά τις παγετωνικές αυτές φάσεις ήταν μεγαλύτερη από όσο είχε αρχικά εκτιμηθεί. Τα πιο πρόσφατα ευρήματα από τα βουνά της Ελλάδας αλλά και των Βαλκανίων υποδηλώνουν ότι εκτενή πεδία πάγου κυριαρχούσαν στους ορεινούς όγκους κατά τις περιόδους αυτές τροφοδοτώντας παγετώνες προς τις χαμηλότερες κοιλάδες, ανεξαρτήτως προσανατολισμού.
- Τα παλαιοκλιματικά/παλαιοοικολογικά αρχεία των νότιων Βαλκανίων υποδεικνύουν ψυχρές αλλά υγρές κλιματικές συνθήκες κατά τα αρχικά στάδια των παγετωνικών περιόδων MIS 12 και MIS 6, τις οποίες ακολούθησαν ιδιαίτερα ψυχρές και άνυδρες συνθήκες. Αυτό υποδεικνύει ότι ο σχηματισμός των παγετώνων θα πρέπει να έλαβε χώρα κατά τα αρχικά και πιο υγρά στάδια των σφοδρών αυτών παγετωνικών περιόδων. Μάλιστα, η ανάλυση του παλαιοκλιματικού αρχείου της λίμνης Οχρίδας για τα τελευταία 1,36 εκ. χρόνια (Wagner et al., 2019) έδειξε ότι οι περίοδοι ενισχυμένων χειμερινών κατακρημνίσεων συμπίπτει με περιόδους χαμηλής ηλιακής ακτινοβολίας στο βόρειο ημισφαίριο, υποδεικνύοντας ιδιαίτερα ευνοϊκές συνθήκες για το σχηματισμό εκτενών παγετώνων και παγοκαλυμάτων.

Β. Τελευταία Παγετώδης Περίοδος (Tymphian Stage MIS 5d-2)

- Η παγοκάλυψη ήταν σαφώς μικρότερη κατά την τελευταία παγετώδη περίοδο, ενώ κατά το Ολόκαινο επιβίωσαν πολύ μικροί παγετώνες σε βαθιά έγκοιλα στον Όλυμπο χάριν της ισχυρής επίδρασης τοπικών τοπογραφικών και κλιματικών παραγόντων
- Το γεωχρονολογικό πλαίσιο των παγετωνικών φάσεων στην Πίνδο είναι ένα από τα καλύτερα χρονολογημένα στα Βαλκάνια. Το τοπικό παγετωνικό μέγιστο κατά το Ανώτερο Πλειστόκαινο έλαβε χώρα κοντά στο Παγκόσμιο Παγετωνικό Μέγιστο

(LGM: 27-23 ka) όπως υποδεικνύουν οι συνεπείς ηλικίες με κοσμογενή ισότοπα χλωρίου (36Cl) τόσο από το οφιολιθικό όρος Μαυροβούνι, όπου η σταθεροποίηση των πιο εκτενών παγετώνων κατά το Ανώτερο Πλειστόκαινο έλαβε χώρα 26.6 ± 6.6 ka πριν από σήμερα, όσο και από την ασβεστολιθική Τύμφη, όπου την ίδια περίοδο οι πιο εκτενείς παγετώνες είχαν καταλάβει τις τελικές τους θέσεις πριν από 29.0 ± 3.0 - 25.7 ± 2.6 ka ενώ είχαν ήδη υποχωρήσει εντός εγκοίλων σε μεγαλύτερα υψόμετρα στα 24.5 ± 2.4 ka (Allard et al., 2020). Ο χρονικός αυτός προσδιορισμός του τοπικού παγετωνικού μεγίστου κατά το Ανώτερο Πλειστόκαινο είναι συνεπής με τα αποτελέσματα των αναλύσεων των ποτάμιων ιζημάτων του ποταμού Βοϊδομάτη κατάντι των παγετωνικών λεκανών της Τύμφης καθώς και με το αρχείο γύρης από τη γειτονική λίμνη Παμβώτιδα, το οποίο υποδεικνύει υγρές και ψυχρές κλιματικές συνθήκες, κατάλληλες για το σχηματισμό παγετώνων, πριν από 30-25 ka (Allard et al., 2020).

- Στο όρος Χελμός στην Πελοπόννησο, έρευνες έδειξαν ότι οι παγετώνες κατά το Ανώτερο Πλειστόκαινο έφτασαν στη μεγαλύτερη έκτασή τους πριν από 36.5 ± 0.9 - 28.6 ± 0.6 ka (Pope et al., 2017 με επαναϋπολογισμό ηλικιών σύμφωνα με Allard et al., 2020), ενώ καταγράφεται υποχώρηση και σταθεροποίηση τους στα 22.2 ± 0.3 - 19.6 ± 0.5 ka (Pope et al., 2017). Αυτό υποδεικνύει ότι πιθανότατα τα ψηλότερα έγκοιλα του Χελμού καταλαμβάνονταν από παγετώνες κατά το MIS 3 και το MIS 2 και η θέση τους διακυμαίνονταν σαν απόκριση στις μεταβαλλόμενες κλιματικές συνθήκες και ιδιαίτερα στις αλλαγές σε επίπεδο χιλιετηρίδων μεταξύ ψυχρών/άνυδρων και δροσερών/υγρών συνθηκών στην περιοχή.
- Η χρονολόγηση με χρήση κοσμογενών ισοτόπων χλωρίου (36Cl) τόσο των περιπαγετωνικών αποθέσεων στο όρος Μαυροβούνι στα 20.0 ± 5.0 ka αλλά και των παγετωνικών αποθέσεων (τερματικές μοραίνες στην ΒΑ Τύμφη) στα 18.0 ± 1.9 ka (Allard et al., 2020) υποδεικνύουν μη ευνοϊκές συνθήκες για το σχηματισμό παγετώνων κατά τη μεταβατική περίοδο από το LGM προς το Late-glacial, αλλά αρκετά ψυχρές και υγρές για τη διατήρηση πεδίων αιώνιου χιονιού (perennial nevé fields) και μικρών παγετώνων σε τοπογραφικά ευνοϊκές θέσεις.
- Καθώς τα βουνά της βόρειας Πελοποννήσου (Χελμός, Ερύμανθος) και τα βουνά της βόρειας Ελλάδας (Β. Πίνδος, Όλυμπος) διαφέρουν περισσότερο από 2ο σε γεωγραφικό πλάτος, το κλίμα θα αναμενόταν θερμότερο στην Πελοπόννησο. Ωστόσο η ανάλυση πληθώρας δεδομένων από μια σειρά μετεωρολογικών σταθμών από άλλους ερευνητές

έδειξε ότι οι σύγχρονες μέσες μηνιαίες θερμοκρασίες στην Ελλάδα εξαρτώνται σχεδόν αποκλειστικά από τα υψόμετρο και ελάχιστα από το γεωγραφικό πλάτος. Έτσι, οποιεσδήποτε συστηματικές διαφορές στα υψόμετρα των ισοϋψών γραμμών ELA θα πρέπει να αποδίδονται σε διαφορές στις κατακρημνίσεις παρά σε επικρατούσες θερμοκρασιακές διαφορές. Η ανάλυση των περιφερειακών παλαιοκλιματικών αρχείων έδειξε ότι οι κατακρημνίσεις είναι ο πιο καθοριστικός παράγοντας δημιουργίας παγετώνων. Ταυτόχρονα, μελετώντας σύγχρονα δεδομένα κατακρημνίσεων αποκαλύφθηκε ότι οι διάφοροι ορεινοί όγκοι στην Ελλάδα χαρακτηρίζονται από πολύ διαφορετικά μοτίβα κατακρημνίσεων. Ο υετός και οι χιονοπτώσεις στα βουνά της Πίνδου σχετίζονται ισχυρά με συστήματα καιρού από τα δυτικά/βορειοδυτικά ενώ τόσο ο Χελμός όσο και ο Όλυμπος δέχονται λιγότερη υγρασία από τη ΒΔ Ελλάδα και το περισσότερο χιόνι κατακρημνίζεται από πλούσια σε υγρασία νοτιοδυτικά συστήματα από τη Μεσόγειο και νοτιοανατολικά συστήματα από το Αιγαίο Πέλαγος αντίστοιχα.

– Λαμβάνοντας υπόψη την τεκτονική ανύψωση τα τελευταία 30ka, οι ισοϋψείς γραμμές ELA των παγετώνων πριν αλλά και κατά τη διάρκεια του LGM στην Τύμφη και στον Χελμό φαίνεται να βρίσκονταν στα ~1990-2000 m πάνω από τη σημερινή επιφάνεια της θάλασσας και κατ'επέκταση μπορούμε να συμπεράνουμε ότι οι παγετώνες κατά την περίοδο αυτή σχηματίστηκαν στα δυο βουνά υπό παρόμοιες κλιματικές συνθήκες. Όσον αφορά το τέλος της τελευταίας παγετώδους περιόδου (Late-glacial), οι παγετωνικές αποθέσεις από αυτή την περίοδο απαντώνται σπάνια στα βουνά της Ελλάδας και έχουν καταγραφεί και χρονολογηθεί μόνο στον Όλυμπο (φάση HS1: 15.6-14.2 ka, φάση YD: 12.6 - 12.0 ka) και τον Χελμό (φάση YD: 12.6-10.2 ka). Οι ισοϋψείς γραμμές ELA για τους παγετώνες αυτούς δείχνουν μια ενδιαφέρουσα τάση. Έτσι, ενώ στη βόρεια Ελλάδα οι παγετώνες είναι απόντες από την Τύμφη, στο Σμόλικα οι παγετώνες που αποδίδονται στη Νεώτερη Δρυάδα (YD) χαρακτηρίζονται από μια μέση ELA στα 2372 m a.s.l. και στον Όλυμπο οι μοραίνες που αντιστοιχούν στο YD υποδεικνύουν ισοϋψείς σε ELA μεγαλύτερα από 2300 m a.s.l., στον Χελμό στην Πελοπόννησο οι παλαιοπαγετωνες κατά το YD είχαν πολύ χαμηλότερα ELA στα 2174 m a.s.l. Αυτές οι διαφορές στα ELA υπονοούν σημαντικά υγρότερο κλίμα στη νότια Ελλάδα σε σχέση με τη βόρεια κατά την περίοδο αυτή. Το φαινόμενο αυτό μπορεί να αποδοθεί σε διαφορετικούς μηχανισμούς ατμοσφαιρικής κυκλοφορίας στην κεντρική Μεσόγειο που οδηγούσε τα βροχοφόρα συστήματα σε μια νοτιοδυτική-νοτιοανατολική τροχιά.

Acknowledgements

I would like to specially thank my supervisor Kosmas Pavlopoulos for his open-mindedness in believing in my abilities to complete this research although I had a different academic background. His unlimited support throughout this period and his rare ethical/academic attitude is outstanding. The same stands for Katerina Kouli who I would also like to thank heartfully for her support in anything I might have needed during these years. I also wish to thank Phil Hughes for his input and advice during my research and for his support in my first steps in the wonderful world of paleaoglaciers. Thank you to Petros Katsafados for taking responsibility of my PhD research during the last months and Constantin Athanassas for his contribution in this research and especially for the hard work during the sampling field trip on Mt Mavrovouni in October 2017. Special thanks also to Adriano Ribolini and Matteo Spagnolo for their collaboration in publishing part of this research and for the wonderful and very insightful field trip in the Maritime Alps in 2019. I would also like to heartfully thank Shasta Marrero for her invaluable help with testing and confirming the suitability of the CRONUS online calculator for the calculation of ^{36}Cl exposure ages oh ophiolitic samples and Ramon Pellitero for his help with the use of the GLARE tool. Many thanks also to George Panayiotopoulos of the beloved Metsovion Interdisciplinary Research Centre for sharing his super-useful aerial videos of Mt Mavrovouni. Limited space permits me to mention only a few of the many people who came out with me on numerous field trips and insightful hiking trips in numerous mountains throughout the world: Miltos Karamanlis (an expert in glacial sediments by this time!), Dimitris Verdelis, Thomas Chatzigeorgiou, Panos Giannopoulos, Katerina Moutoupa, and Francesca Marchina. I am also thankful to the Kalaitzis family for letting me use of their family house in Konitsa as a base for a number of field trips in Epirus. Many thanks to everyone in Munti Smolikas guesthouse for their warm hospitality. I would also like to mention that the encouragement and advice of Giannis Pantekis and Fotini Pomoni has been really helpful at the very first steps of pursuing a doctoral research project on paleaoglaciers. Thanks to Penelope Matsouka and Ivy Adamakopoulou of Anavasi Editions for their support with digital and hard-copies of their precious maps. Moreover, without the flexibility in my engineering job in the National Technical University of Athens I would not be able to complete this research. Thus, I would like to thank Sotiris Karellas and my colleagues Tryfon Roumpedakis, Stratis Varvagiannis and Platon Pallis for their understanding and support. Most of all, I thank my partner Elena Dalamara for her support, understanding and patience as well as for accompanying me in some quite rough field trips throughout this research.

Contents

List of Figures

List of Tables

Chapter 1. Introduction

The Quaternary period, the last 2.58 million years of Earth history, is characterized by extremes in climate with a number of glacial and interglacial cycles (Ehlers and Gibbard, 2003). These extremes are vividly indicated in the geologic record by the evidence for repeated advances and retreats of glaciers: the large ice sheets that occur in the higher latitudes and the alpine glaciers of mountainous regions (Ivy-Ochs and Briner, 2014). The study of the current and past climatic cycles through glaciers and palaeoglaciers was consolidated by the influential Glacial Theory of Louis Agassiz (1840) and has evolved into one of the most important fields of Quaternary research worldwide. The acceptance of the glacial theory in the mid- 19th century led to the observation of former glacial deposits throughout Europe and as far south as the mountains of the Mediterranean region (Hughes, 2004): here, glacial features were first described in the Pyrenees by Penck (1885), in the Lebanon by Diener (1886), on the Balkan peninsula by Cvijic (1898) and in Greece by Niculescu (1915) and Cvijic (1917).

The Mediterranean region is situated in an important geographical position for understanding Quaternary climate change in the northern hemisphere, immediately to the east of the North Atlantic Ocean and aligned along the low mid-latitudes (Hughes and Woodward, 2017). Much of modern research is devoted to this region and the timing of glaciations in the Mediterranean mountains in particular.

In the last three decades, the advances in geochronological dating techniques, especially in terrestrial cosmogenic nuclide (TCN) exposure dating of glacial boulders and bedrock surfaces led to a significant increase in glacial studies across the Mediterranean region. Other methods widely used include the radiocarbon dating of relatively young landforms (<50ka), the luminescence dating of glacial and glacio-fluvial outwash deposits and uranium series dating of secondary carbonates in glacial and glacio-fluvial deposits (Fuchs and Owen, 2008). As a result, it is now possible for researchers to explore patterns in the large number of dates now available to better understand the regional patterns of glacial advance and retreat and their wider palaeoenvironmental significance (Balco, 2020; Hughes and Woodward, 2017 and references therein)

However, as it often happens in science, the publication of a scientific study creates more questions than it answers. In other words, sometimes the more things we understand about a scientific hypothesis, the more complex it becomes. For example, the legendary astronomical theory of Milankovic (1941) for ice ages posits that quasiperiodic expansions and contractions

of Northern Hemisphere ice sheets are driven by variations in Earth's orbital geometry and axial inclination (obliquity 41-kyr cycles and precession 23- and 19-kyr cycles) that influence the amount of summer insolation received at northern high latitudes (Tzedakis et al., 2017). Although this theory provided great insight into the causes of climate oscillations through the earth history and was generally in accordance with records of changing ice volume and climate, it was not able to fully predict and explain the domination of a 100-kyr cycle in climate variance in the Middle and Late Pleistocene (Hay et al., 1976; Tzedakis et al., 2017). Moreover, it has not been clear how astronomical forcing translates into the observed sequence of interglacials. It was only recently, that a plausible theory that was also verified by the climatic and ice-volume records was developed by Tzedakis et al. (2017). In short, this theory is based on the idea that complete deglaciation does not depend only on the intensity of summer insolation but also on the time elapsed since the previous deglaciation, taking into account the fact that time contributes to glacial instability through glaciological or carbon-cycle processes. The simplest possible model was developed to describe and predict whether a particular insolation peak led to the onset of an interglacial throughout the past 2.58 Myr. The results showed that the succession of interglacial onsets that has occurred is one of a small set of possibilities Tzedakis et al., 2017). Nevertheless, the development of an extended astronomical theory of ice ages is still incomplete.

In this context, further research is needed in order to overcome contradictions in the developing theories and move towards the understanding of Quaternary climatic variability and its implications to the Earth and its ecosystems.

1.1 The Mountains of Greece and their glacial history

Mainland Greece is highly mountainous with 42% of its surface characterized as mountainous (Bassiouka, 2011). Its topography is dominated by the Pindus mountain range that extends from NNW to SSE (Figure 1). The mountains of Greece represent part of the Alpine–Himalayan orogenic system that formed due to the collision between the African and Eurasian plates (Aubouin, 1959; Angelier, 1978; King et al., 1997; Jolivet and Faccenna, 2000; van Hinsbergen et al., 2009). Its main peaks exceed 2200 m a.s.l. and countless minor peaks exceed 1800 m a.s.l. in altitude.

Evidence of former glaciation episodes is abundant throughout the mountains of Greece (Figure 1; Table 1) and was first identified by pioneer researchers/geographers at the beginning of the 20th century such as Niculescu (1915), Cvijic (1917), Sestini (1933), Mistardis (1937a)

and Messerli (1967). It has been argued that glacial evidence is confined only on the higher parts of mountains that exceed 2200 m a.s.l. (Woodward and Hughes, 2011; Boenzi and Palmentola, 1997). However, even though the Geological Sheets of the Greek Institute for Geological and Mineral Exploration (IGME) often misinterpret glacial deposits, in reality some mountains even below 2000 m a.s.l. have been glaciated in the past while glacial sediments within mountain valleys have been found down to 700 m a.s.l. (Pavlopoulos et al., 2018), implying that glacial extent was greater than previously thought.

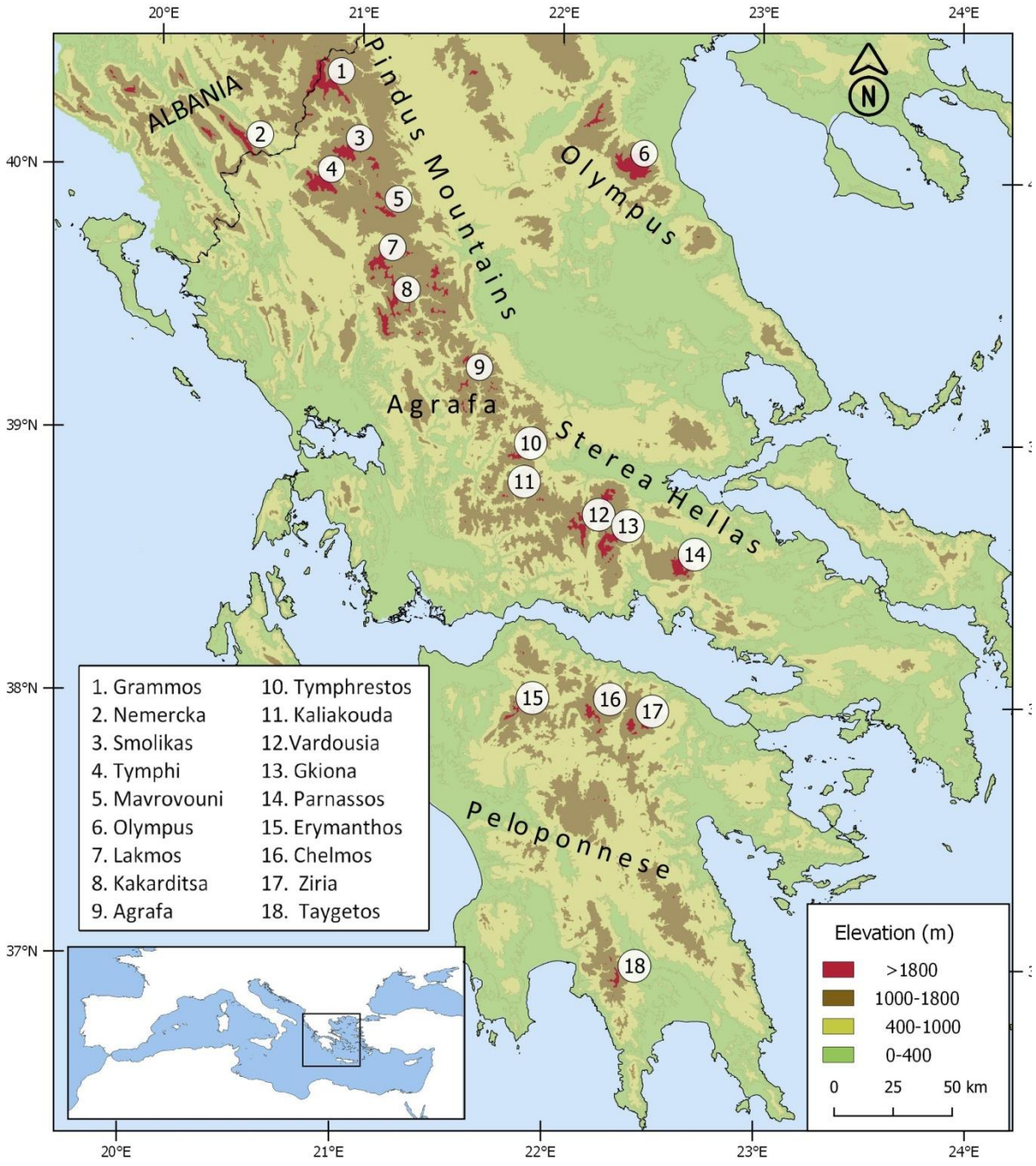

Figure 1. The mountains of Greece. The numbered mountains are those with identified glacial evidence (from Leontaritis et al., 2020)

Table 1. References table for the glaciated mountains shown in Figure 1 (modified from Leontaritis et al., 2020)

Massif	References	Massif	References
1. Grammos	Bourcart (1922) Louis (1926)	2. Nemercka	Louis (1926)
3. Smolikas	Niculescu (1915) Mistardis (1937a) Boenzi et al. (1992) Hughes (2004) Hughes et al. (2006c)	4. Tymphi	Mistardis (1935) Palmentola et al. (1990) Smith et al. (1998) Woodward et al. (2004) Hughes et al. (2006a) Allard et al. (2020)
5. Mavrovouni	Present research	6. Olympus	Cvijić (1917) Wiche (1956) Messerli (1967) Faugeres (1969) Smith et al. (1997) Manz (1998) Styllas et al. (2006; 2008)
7. Lakmos	Sestini (1933)	8. Kakarditsa	Sestini (1933)
9. Agrafa	Hunt and Sugden (1964)	10. Tymphrestos	Klebelsberg (1932)
11. Kaliakouda	Mistardis (1937a)	12. Vardousia	Maull (1921) Mistardis (1937a)
13. Gkiona	Mistardis (1937a) Pechoux (1970)	14. Parnassos	Renz (1910) Maull (1921) Mistardis (1937a) Pechoux (1970)
15. Erymanthos	Mistardis (1937a)	16. Chelmos	Philippson (1892) Maull (1921) Mistardis (1937a, 1937b, 1937c, 1946); Mastronuzzi et al. (1994) (Pope et al., 2017) Pavlopoulos et al. (2018)
17. Ziria	(Pope et al., 2017)	18. Taygetos	Maull (1921) Mistardis (1937a) Mastronuzzi et al. (1994) Pope (2010) Kleman et al. (2016)

The glacial sequence in northwest Greece (Mount Tymphi) is one of the first mountainous areas in the Mediterranean where the full progression from pioneer to advanced glacial research took place and is very well dated (Woodward et al., 2004; Hughes et al., 2006a, 2006b; Woodward and Hughes, 2011; Allard et al., 2020). The result of these studies led to the definition of the Pindus Chronostratigraphy (Hughes et al. 2006a). However, at the time this research was initiated (2015-2016), advanced glacial studies including radiometric or other dating data was -from a geographic perspective- limited to Northern Greece and Mt Tymphi in particular. As regards the geochronology of the glacial sequence on Mt Tymphi though, whilst glacial deposits on Mt Tymphi and Mt Smolikas had been ascribed to different glacial Stages spanning from Middle Pleistocene and MIS 12 to the Late Pleistocene and the Younger Dryas, their geochronological constraint had been achieved only for the Middle Pleistocene Stages (MIS 12 and MIS 6). The lack of further dating data from the Late Pleistocene glacial phase(s) constituted an important temporal gap of the contemporary chronostratigraphy of the Pindus Mountains which led to the initiation of further studies, including the present one, both in Northern and Southern Greece.

In this perspective, the present research focused on Late Pleistocene deposits in northern, Greece in an effort to complete the Pindus Chronostratigraphy from a geochronological perspective. At the same time studying the glacial history of southern Greece aimed at expanding geographically this chronology to the rest of Greece. In recent years new dating data has been published from southern Greece (Mt Chelmos in the Peloponnese - Pope et al., 2017; Pavlopoulos et al., 2018) from Mt Olympus in the northeast (Styllas et al., 2018) and from Mt Tymphi in the northwest (Allard et al., 2020) providing a robust chronological framework for the mountains of Greece (Figure 1; Table 1). A complete review of the glacial studies in Greece is presented in Chapter 3.

It should be noted that although the glacial record on the mountains of Greece constitutes a significant and relatively well-studied paleoclimatic archive, it remains only partially explored.

1.2 Glacial studies and past climates

Glaciers change volume, and thus thickness and length, in response to changes in air temperature and precipitation (Oerlemans, 2005). In other words, glaciers respond to climatic changes and therefore to changes in their mass balance, with a consequent advance or retreat of the glacier’s front. Their former extents therefore record past changes in climate. Moreover, even though many studies use marine sediments and ice cores to reconstruct past climate

variations, neither of these types of records, provides information on the locations or specific extents of glaciers on continents, nor how patterns of ice distribution have varied spatially with time (Ivy-Ochs and Briner, 2014). The former extents of glaciers are however documented by terrestrial glaciogenic sediments and landforms (Fuchs and Owen, 2008). In this context, mapping and dating of past ice margins based on evidence such as moraines and associated landforms (outwash plains, kettles, eskers, trim-lines, erratic boulders etc.) provide valuable information which can be used to gain a better understanding of landscape evolution and palaeoclimate change (Owen et al. 2002; Svendsen et al. 2004). Apart from the determination of glacial advance and retreat phases which provide qualitative indications of favourable/unfavourable conditions for glacial development, quantitative climatic data can be inferred by the mass balance of former glaciers with the use of empirical equations that link temperature and precipitation at the Equilibrium Line Altitude (ELA) like the one proposed by Boettcher and Ohmura (2018). The glacial record can thus be compared with modern climate data to generate information on the nature of winter moisture supply and summer temperatures during Pleistocene cold stages (Hughes and Woodward, 2017).

1.3 The significance of the glacial record of Greece and the Balkans in Mediterranean Quaternary studies

The former glacial environments in the mountains of Greece and the Balkans, similarly to other mountains in the Mediterranean during glacial episodes, are dynamic landscape systems that are highly responsive to regional or local climate variability and due to their geographical position in the mid-latitudes they are very important for palaeoclimate research (Oliva et al., 2019; Hughes and Woodward, 2017; Tzedakis et al., 2004; Regato and Salman, 2008; Woodward, 2009; Vogiatzakis, 2012).

The data retrieved from glacial studies of the Mediterranean mountains usefully complement the rich body of proxy climate data that has been retrieved from other Mediterranean archives (Woodward, 2009), including lacustrine sediments (e.g. Sadori et al., 2016; Wulf et al., 2018), speleothems (e.g. Luetscher et al., 2015) and the marine sedimentary record (e.g. Grant et al., 2012). Overall, the chronology and reconstruction of palaeoglaciers can provide a regional perspective on how and when glaciers responded to past climate oscillations across the Mediterranean, and how hemispherical/regional climate changes were modulated at the regional to local scale in terms of air temperature and precipitation.

As regards precipitation and palaeoatmospheric circulation patterns across the central-eastern Mediterranean, the underlying mechanisms of change and their persistence are poorly elucidated (Kuhlemann et al., 2008). Thus, a proxy record that covers multiple glacial–interglacial cycles and is sensitive to changes in the Mediterranean hydroclimate is key to addressing long-standing questions regarding the underlying mechanisms, such as timing and amplitude of precipitation variability under different climate boundary conditions (Wagner et al., 2019).

The glacial records of the Balkans, and Greece in particular, could prove very useful in answering these questions both due to their geographical position and the availability of numerous well-dated proxies in the region (Figure 2), such as the LC21 marine sediment core from the Aegean Sea (Grant et al., 2012) and the lacustrine pollen records from Tenaghi Philippon (Wulf et al., 2018), Lake Ioannina (Tzedakis et al., 2002), Lake Ohrid (Sadori et al., 2016; Wagner et al., 2019) and Lake Prespa (Panagiotopoulos et al., 2014). For example, changes in the regime of westerly atmospheric depressions generated both in the North Atlantic, and in central Mediterranean along with southward outbreaks of the polar front (Florineth and Schlüchter, 2000; Lionello et al., 2006; Kuhlemann et al., 2008) and the consequent southerly track of atmospheric depressions through the Mediterranean (Florineth and Schlüchter, 2000; Luetscher et al., 2015; Oliva et al., 2019) could have affected glacier viability on the mountains of Greece. At the same time these changes would also be recorded in proxy records.

Overall, while a number of glacial deposits have been identified in the mountains of Greece (Figure 1) only some have been successfully dated to Late Pleistocene and particularly to the LGM and Late-glacial and the response of glaciers in the mountains of Greece to these cold events remains largely understudied. Reconstructed former glaciers relative to the few dated moraines indicate climatic conditions that could fit with regional, Mediterranean-wise palaeoclimatic models. However, palaeoprecipitation, which most likely played a key role in this region, and which can be obtained through the reconstruction of glaciers ELA relative to dated deposits, has essentially never been quantified. This kind of information would be very useful for the reconstruction of the palaeoclimate of the eastern Mediterranean and as a test for regional circulation models. Understanding where, when and why Mediterranean glaciers reached their maxima during the last glacial cycle is not only important for understanding the local and regional dynamics of the glacial climate during this period, but also the sediment and meltwater delivery to river systems, the dynamics of Mediterranean refugia, and the

environmental context of Middle and Upper Palaeolithic archaeological records (Hughes and Woodward, 2008, 2017; Allard et al., 2020).

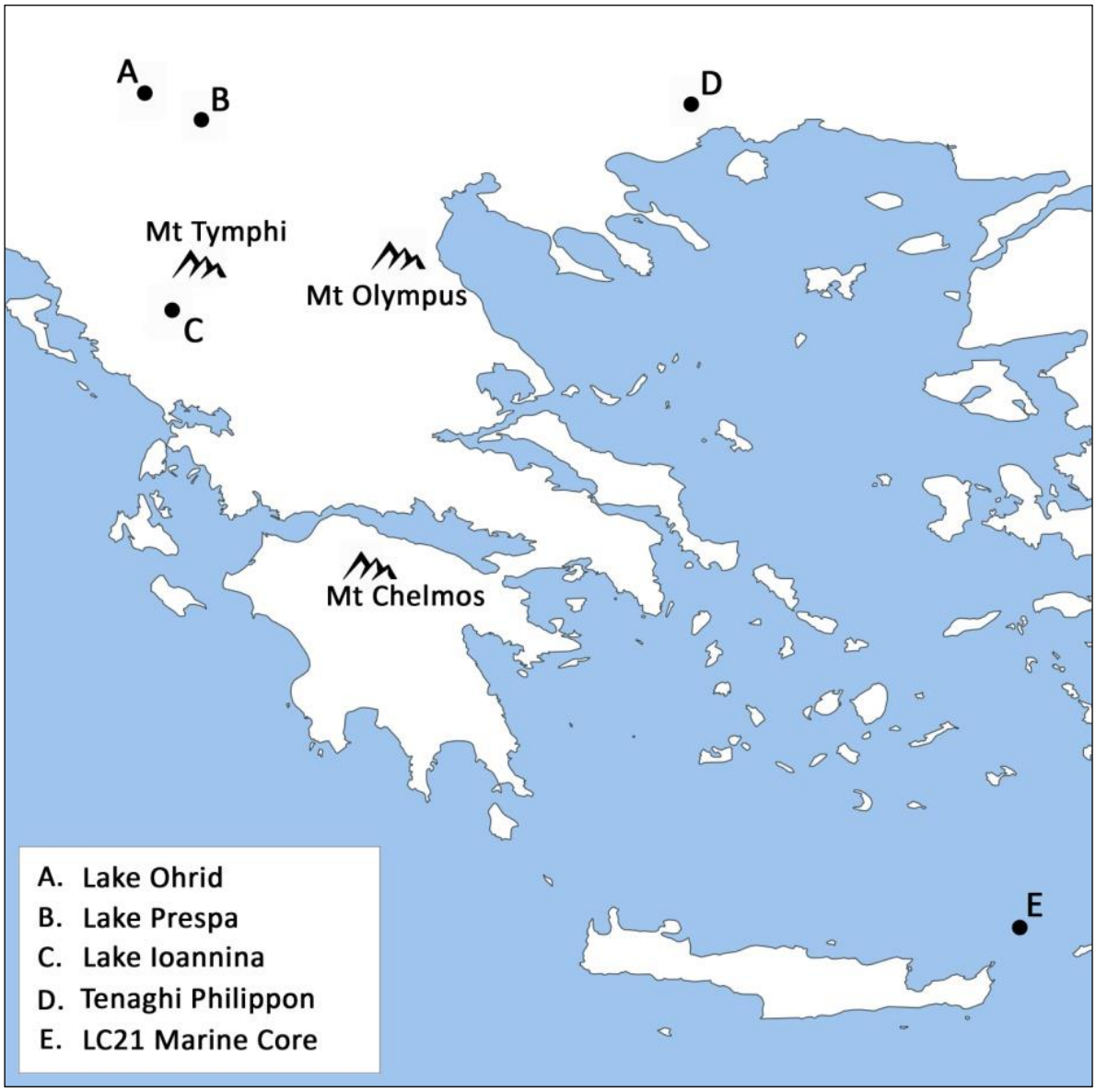

Figure 2. Major regional palaeoclimatic and palaeoenvironmental proxies in relation to best dated glaciated mountains in Greece (from Leontaritis et al., 2020)

1.4 Study areas and aims of this research

As already analysed, the present research focuses on Late Pleistocene deposits in northern, central and southern Greece in an effort to address both temporal and geochronological gaps in the glacial chronology of the mountains of Greece. Thus, the core objective of this research is to constrain the age of Late Pleistocene glacial deposits - focusing on the LGM and the Late-

glacial - in two key-locations: Mt Mavrovouni in northern Greece and Mt Chelmos in Peloponnese in the south (see Figure 1 for locations).

The ambition is firstly to complete the Pindus chronological framework in northwest Greece by a full glacial geomorphological study of the ophiolitic Mt Mavrovouni in the Pindus Mountains combined with geochronological control of the high-altitude deposits. Given their morphostratigraphy, altitude and orientation and according to the glacial-research background in the mountains of Greece presented in Chapter 3 these deposits are expected to be Late Pleistocene in age. Mt Mavrovouni has been selected as the main study area, mainly for its well-preserved high-altitude glacial sequence, for its proximity to Mt Tymphi and for its relatively good accessibility (Chapter 4). Moreover, its ophiolitic lithology makes it ideal for both testing the applicability of ^{36}Cl dating on ophiolites and for providing limestone-independent geochronological control of Late Pleistocene deposits in the mountains of Greece.

Overall, Mt Mavrovouni is the ideal alternative to the already identified but undated glacial sequence on Mt Smolikas (see section 3.1.2) which bares the same characteristics: it is also ophiolitic and is located in the very near proximity of Mt Tymphi. However, a sampling campaign on the rather inaccessible highlands of Mt Smolikas would require complicated logistics, while a much larger number of samples to be dated would be required in order to provide effective geochronological control on this extended glacial sequence. Given the uncertainties in the applicability of ^{36}Cl dating of ophiolites (see Chapter 2) and the increased funds that are required for an advanced glacial study on Mt Smolikas, such an option was out of range for this research project.

The aim is, then to expand this geochronology to the south, by studying Mt Chelmos in the Peloponnese. Mt Chelmos was selected as the most appropriate -for glacial studies- mountain in the Peloponnese due to its well-preserved and almost complete glacial sequence and for its accessibility (Chapter 5).

The new glacial studies for Mt Olympus (Styllas et al., 2018) in the northeast and for Mt Chelmos (Pope et al., 2017) that were published in the course of this research were partly controversial (see 2.3), highlighting the importance of a firmly-grounded comparison and interpretation of the results from these studies and the reconstruction of the palaeoclimatic conditions across Greece at these times. A very useful tool for the achievement of this goal would be the creation of a key geographical link for Late Pleistocene glaciations between the well-studied Pindus mountains/Mt Olympus in northern Greece and Mt Chelmos in the south. Such a link would allow for the comparison and interpretation of the results from these studies

and the reconstruction of the palaeoclimatic conditions across Greece at these times. Taking into consideration that the glacial sedimentary records in the mountains of central Greece (Mt Parnassus, Mt Gkiona, and Mt Vardousia - Figure 1) had already been identified as a potentially important archive of former glacial episodes that has not yet been studied (Pavlopoulo et al., 2018; see also section 3.4), it was decided that this link could be realised by focusing on one of these mountains. As high-altitude glacial deposits are best preserved on Mt Parnassus, the massif was selected as the third study area of this research (Chapter 6). Work on this study area was limited to a preliminary geomorphological study as an outline for a future research project.

Finally, it should be mentioned that new observations and glacial evidence recorded by the author in different mountains outside the study areas mentioned above, are presented alongside the review of the glacial studies in Greece in 2.3. This evidence does not necessarily constitute part of systematic research but it has been considered meaningful to be included in this thesis as they provide further insights and pose new research questions in the Quaternary glacial history of Greece.

1.4.1 Particular objectives

In summary, the particular objectives of this research are:

vii. the cosmogenic exposure dating of likely LGM/Late-Glacial moraines and pronival ramparts on the ophiolitc Mt Mavrovouni

viii. the application of ^{36}Cl cosmogenic exposure dating on ophiolitic boulders for the first time in order to prove its applicability in these lithologies

ix. the development of an independent geochronological control of Late Pleistocene deposits in the mountains of Greece, providing the first ages from non-limestone glacial boulders from Mt Mavrovouni and testing the existing ^{36}Cl ages form limestone samples

x. the reconstruction of the extent and equilibrium line altitudes of the studied palaeoglaciers with specialised GIS tools (e.g. Pellitero et al., 2015, 2016)

xi. the optically stimulated luminescence (OSL) dating of limestone-derived morainic deposits on Mt Chelmos

xii. the preliminary glacial geomorphological study of Mt Parnassus focusing on high altitude and thus probably Late Pleistocene in age evidence

xiii. the interpretation of the results and their correlation with other glacial studies in the southern and northern mountains of Greece, as well as in the wider Balkans, in order test and provide inputs for palaeoclimate models

xiv. the comparison of the glacial chronology with other palaeoclimatic records and especially pollen sequences, highlighting possible correlations and the significance of these records in a wider palaeoclimatic perspective.

Chapter 2. Methodology

2.1 Geomorphological mapping

Geomorphological mapping is a well-established method for examining earth surface processes and landscape evolution in a range of environmental contexts. In glacial research, it constitutes a crucial tool for palaeoglaciological reconstructions, providing an essential geomorphological framework for establishing glacial chronologies (Chandler et al., 2018). The general approach involved detailed, thematic geomorphological mapping with an emphasis on glacial and periglacial landforms and processes. Such a reductionist approach is helpful in ensuring a map is not 'cluttered' with less relevant data that may in turn make a multi-layered map unreadable (Kraak and Oremling, 2010; Chandler et al., 2018).

In this context, the idealised approach proposed by Chandler et al. (2018) for glacial geomorphologic mapping in alpine environment which involves several consultations of remotely-sensed data and field mapping was to a certain extent followed (Figure 3). This methodology provides a robust approach to mapping that has been broadly used in previous studies (e.g. Benn and Ballantyne, 2005; Brynjólfsson et al., 2014; Schomacker et al., 2014).

Accordingly, the first step for the geomorphological mapping in the study areas was the collection and reconnaissance analysis of available digital and printed topographic maps (e.g. commercial topographic maps, maps from the Hellenic Army Geographical Service or Open Street Maps - OSM) the regional 1:50,000 Geological Sheets of the Greek Institute for Geological and Mineral Exploration (IGME) and high-resolution satellite imagery (Google Earth, Bing Maps). The Digital Elevation Model (DEM, also known as Digital Terrain Model or DTM and as Digital Surface Model or DSM) in the case of Mavrovouni was provided by the Hellenic Cadastre at a resolution of 5 m whereas on Mt Chelmos the DEM provided by the Hellenic Cadastre was enriched by digitizing contours from high resolution maps. After identifying possible glacial and periglacial features from this material and mapping some of the clearer features, a detailed mapping fieldwork plan was developed. In the field, already mapped as well as new glacial, erosional, glaciofluvial and periglacial landforms and sediments were verified, mapped and recorded using a GPS device over numerous fieldtrips. Field mapping began with traverses of the study area starting from higher ground, where an overview can be gained, and proceeded by crossing valley axes and cirque floors, enabling the viewing and assessment of landforms from as many perspectives, angles and directions as possible (Demek, 1972).

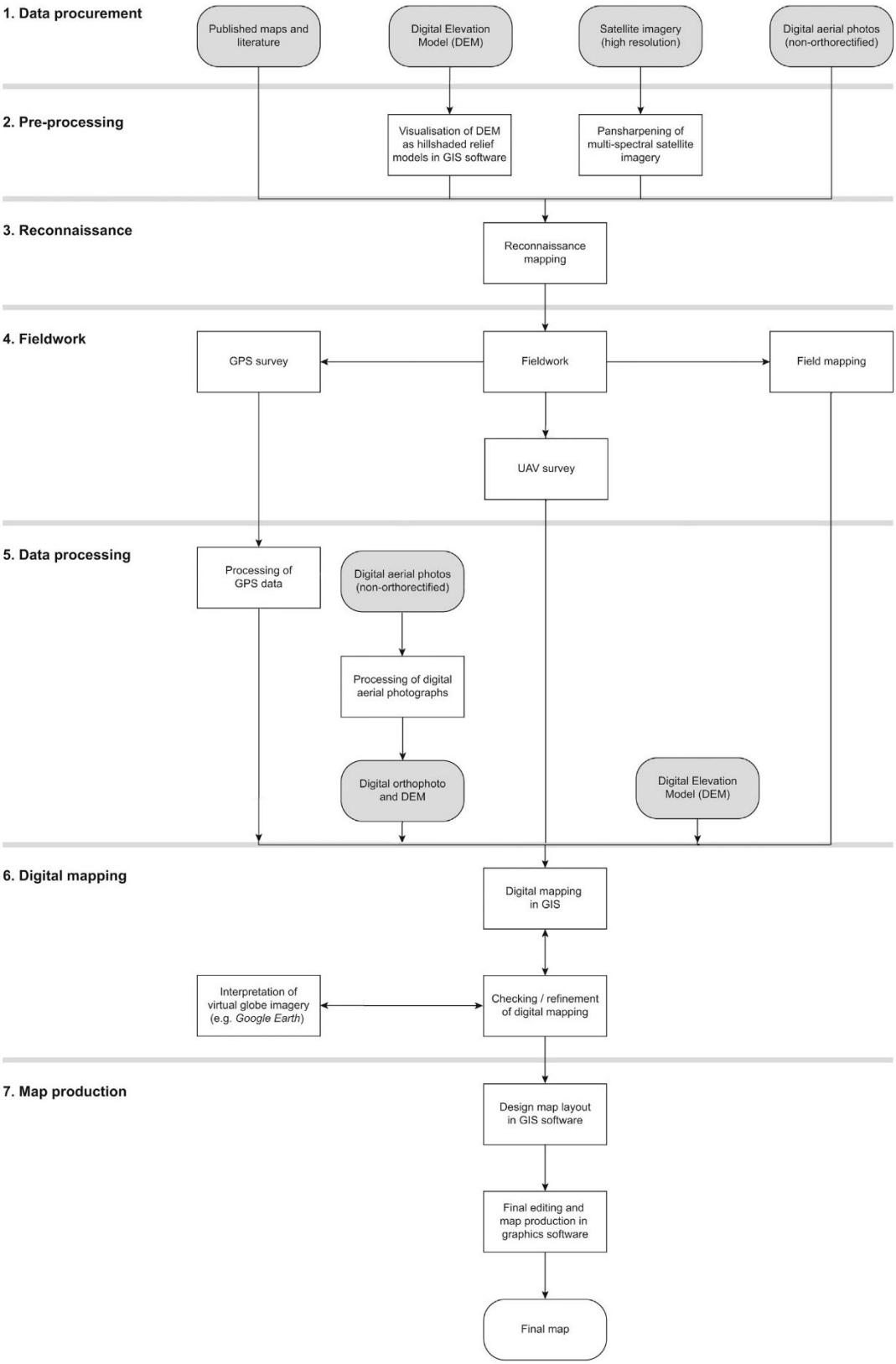

Figure 3. Applied workflow diagram of the glacial geomorphological mapping process in the study areas. Modified from the idealized flow chart for glacial geomorphological mapping in alpine environments by Chandler et al. (2018). DEM: Digital Elevetion Model; UAV: Unmanned Aerial Vehicle; GPS: Global Positioning System; GIS: Geographic Information System

Additionally, on Mt Mavrovouni (Chapter 4) aerial videos and pictures were taken with the use of unmanned aerial vehicle (UAV or a drone in common language) in a specific valley. This material proved very useful both in finalising the geomorphological mapping and in interpreting the different landforms and deposits along the valley. In the case of Mt Chelmos, a detailed orthophoto was also created by using ALOS (Advanced Land Observing Satellite) PRISM imagery as described in detail in Pavlopoulos et al. (2018) and in Chapter 5.

The digital mapping and the creation of the glacial geomorphological maps were conducted in an open source GIS (Geographical Information Systems) environment (QGIS). Additionally, for Mt Chelmos a semi-automated geomorphological mapping approach was followed as described in detail in Pavlopoulos et al. (2018) and in Chapter 5. In both study areas the geographical entities were classified according to their characteristics following the rules of cartographic generalization, abstraction and simplification (Gustavsson, 2006). Specifically, discrete levels of information were generated concerning topographical, hydrographical, geological and geomorphological features. As regards glacial and periglacial features in particular, they were further classified in different morphostratigraphic units following the principles of morphostratigraphy described next.

2.1.1 Morphostratigraphic classification of glacial and periglacial features

Stratigraphy is the science dealing with the description of all rock bodies (including sediments) and their organisation into distinctive, useful, mappable units based on their properties or attributes (Salvador, 1994). Hence, morphostratigraphy refers to the application of stratigraphic principles to geomorphology (Lukas, 2006) and it can be defined as the subdivision of sedimentary units based on surface form (Frye and Willman, 1962). However, in practice, morphostratigraphical units are rarely defined without using at least some lithological criteria (Bowen, 1978). For example, glacial units may be recognised by lithological criteria incorporating a range of sedimentological characteristics, such as striated subrounded boulders, diamicton exposures or erratic lithology, but separated by morphological criteria, such as moraine position (Hughes, 2010a). Clearly these units are not directly comparable to standard lithostratigraphical units, where vertical and lateral changes, as well as relationships to other units, can generally be observed unambiguously (Rawson et al., 2002) and therefore morphostratigraphical units should only be given informal status (Richmond, 1959). Moreover, the apparently simple external morphology of some landforms, such as ice-marginal formations, commonly hides internal complexities of sediment sequences preserved beneath or within them (Rawson et al., 2002). For this reason, whilst morphostratigraphy

might prove to be very useful, it should never be regarded as a substitute forother more precise types of stratigraphical units, such as lithostratigraphy and allostratigraphy (Rawson et al., 2002).

Nevertheless, morphostratigraphy is especially useful for glacial geomorphologic studies as it allows for the utilization of spatial relationships between individual landforms to assign them to events or periods (Lukas, 2006). Due to the limited availability of dateable sites or material and for economic reasons, it is feasible to date only some representative landforms within a study area and thus, the necessity of extrapolating characteristic geomorphological evidence from dated sites to those that remain undated arises in most glaciated areas (Lowe and Walker, 1997; Benn and Ballantyne, 2005; Lukas, 2006). This approach has been successfully applied in glacial geomorphology worldwide, underlying many glacier reconstructions (e.g. Colhoun, 1988; Lemmen and England, 1992; Chadwick et al., 1997; Lehmkuhl, 1998; Richards et al., 2000). In the present research, the stratigraphic classification of glacial and periglacial features in different units was based upon morphostratigraphy which proved crucial for local (i.e. within the same massif) and regional (e.g. within the Epirus region in Greece) morphostratigraphic correlations which allowed for extrapolating available geochronologies into a robust age model for the glacial history of Greece.

2.2 Geochronology

The use of glacial sediments and landforms in order to infer the nature and magnitude of past glaciations and thus past climatic conditions requires a robust temporal framework. Relative dating methods, such as the use of morphostratigraphy, are very useful for a first placement of glacial evidence in temporal order but absolute dating methods are of fundamental importance in establishing independent chronologies (Wagner, 1998; Fuchs and Owen, 2008). Some of the most widely applied methods include, lichenometry, tephrochronology, varve chronologies, dendrochronology, amino acid geochronology, palaeomagnetism, radiocarbon, luminescence, K/Ar, Ar/Ar, U-series, terrestrial cosmogenic nuclide (TCN) surface exposure and fission track dating (Brigham-Grette, 1996). The application of these dating methods varies considerably and only a few are suitable for targeting Middle to Late Pleistocene deposits such as those considered in this thesis. Radiocarbon dating is the most widely-used for the Quaternary, but prerequisites the existence of well-preserved organic matter within the sediment or on the landforms which can be very scarce within the rather sterile and extremely active geomorphic systems associated with glacial environments (Fuchs and Owen, 2008). Moreover, this method is limited to the last 50 kyr because of the relatively short half-life of

^{14}C (Ivy-Ochs and Kober, 2008). Other methods, such as lichenometry and dendrochronology have found a wide range of applications but are quite limited in time span whereas palaeomagnetism, K/Ar, Ar/Ar and U-series dating which have been successfully used for longer timescales (>10 ka) require appropriate dateable material, which is often difficult to find (Fuchs and Owen, 2008).

Luminescence dating has been used in a great number of various types of palaeoenvironmental and landscape evolution studies. Although it has been argued that it could prove very useful also in directly dating glacial deposits as suggested by a number of successful studies, its application in this field has been limited due to concerns in the detection and handling of insufficiently bleached sediments associated with the nature of glacial processes (Fuchs and Owen, 2008).

Sites unsuitable for luminescence techniques, such as sediments that have not been exposed to light long enough, may be dated with cosmogenic nuclide methods (Ivy-Ochs and Kober, 2008). During the last three decades, there has been a great increase in the use of Terrestrial Cosmogenic Nuclides (TCN) surface exposure dating of glacial landforms and erosion rates but to be accurate, this method requires stable surfaces, little or measurable weathering and shielding by snow cover, exclusion of inherited TCNs due to prior exposure and other factors which sometimes are hard to achieve in glacial environments (Putkonen and Swanson, 2003; Ivy-Ochs and Kober, 2008).

2.2.1 Dating methods applied in the study areas

Overall, TCN, luminescence and U-series are the most commonly used methods for dating glacial deposits. The U-series method has a great potential in placing glaciation phases within the 100ka glacial cycle in the scale of climate variance in the Middle and Late Pleistocene (i.e. to determine the Glacial Stage and Marine Isotope Stage associated with glacial activity) as it has been showcased by influential glacial studies in Greece and the Balkans (e.g. Woodward et al., 2004; Hughes et al., 2006a; Hughes et al., 2010) but is of less use in determining the exact timing of glacial phases within the same glacial period (e.g. the Last Glacial Cycle) which is the aim of this research.

In this research both luminescence and TCN dating methods were applied in order to constrain the timing of deposition of glacial sediments in the study areas. A short summary of the characteristics, physical principles and application suitability on glacial deposits for the TCN and Luminescence methods is given in section 2.2.2 and 2.2.3 respectively, whilst

thorough reviews of both methods are provided in a series of landmark publications such as those of Gosse and Phillips (2001), Ivy-Ochs and Kober (2008), Fuchs and Owen (2008), Rhodes (2011) and Balco (2020).

On Mt Mavrovouni in the Pindus mountains in northwest Greece, the cosmogenic ^{36}Cl exposure dating method was applied on ophiolitic glacial boulders along moraine and pronival rampart ridges which are expected to be Late Pleistocene in age. This method was chosen over luminescence and cosmogenic ^{10}Be or ^{26}Al as the entirely ophiolitic lithology of the massif excludes the presence of quartz, feldspar or secondary calcites that are necessary for the application of these methods (Fuchs and Owen, 2008; Ivy-Ochs and Kober, 2008). Noble gases isotopes (^{3}He and 21Ne) were also excluded due to their usefulness for longer time scales (>50ka; Ivy-Ochs and Kober, 2008) than the targeted glacial and periglacial deposits that are expected to be pre-LGM to LGM (35-23ka) to Late-glacial (<20ka) in age. On the other hand, ^{36}Cl exposure dating can be used for any rock type or mineral separate under most conditions (Ivy-Ochs and Kober, 2008) and it was hence chosen for this application.

Cosmogenic ^{36}Cl exposure dating is well-proven in limestone-dominated environments in the mountains of Greece (e.g. Pope et al., 2017; Styllas et al., 2018; Allard et al., 2020) and in principle it should also be applicable on ophiolites. However, its application on mid to highly serpentinized ophiolitic rocks (i.e. silicate rocks with high concentrations of Mg and Fe and very low to insignificant concentrations of Ca, K and Ti) such as those dominating the glaciated valleys on Mt Mavrovouni, is challenging as the main production of cosmogenic ^{36}Cl atoms is expected to mainly take place from neutron capture of stable Cl in the rock and Fe spallation (see section 2.2.2), which are processes that are not fully explored and are sources of uncertainty (Gosse and Phillips, 2001; Marrero et al., 2016b; Moore and Granger, 2019). This application is attempted for the first time, and although theoretically this should not cause any major issues, it is an element of innovation. The confirmation of the suitability of ^{36}Cl dating on this kind of lithologies would have significant impact on our dating capacity of glacial and other sediments with this method. Moreover, the resulting ages would constitute the only geochronology of Late Pleistocene glaciations on the mountains of Greece that is independent from inherent issues in ^{36}Cl surface exposure dating of limestones such as the erosion rate of rock surfaces (Sarikaya et al., 2020). The importance of independent age constraints is also stressed by Ivy-Ochs and Kober (2008).

On Mt Chelmos in Peloponnese in southern Greece, the Optically Stimulated Luminescence (OSL) dating method was implemented to directly date limestone-derived

subglacial till within a termino-lateral moraine. Although ^{36}Cl dating would also be applicable in this case, the OSL method for the dating of glacial sediments was chosen for reasons of diversity in the methodology of this research.

Details on samples collection and characteristics, application of the methods and obtained results are given in Chapter 4 and Chapter 5 for Mt Mavrovouni and Mt Chelmos respectively.

2.2.2 Terrestrial Cosmogenic Nuclides (TCN)

In the last decades surface exposure dating using cosmogenic nuclides has emerged as a powerful tool in Quaternary geochronology and landscape evolution studies (Ivy-Ochs and Kober, 2008). Cosmogenic nuclides are produced in rocks due to reactions induced by cosmic rays and upon this principle several earth science applications for the accumulation of cosmogenic isotopes were predicted by Lal and Peters (1967). However, it was not until the development of accelerator mass spectrometry (AMS) that routine measurement of terrestrial cosmogenic nuclides became feasible (Elmore and Phillips, 1987). Hence, depending on rock or landform weathering rates the determination of the exposure history of landforms ranging in age from a few hundred years to tens of millions of years is possible whereas the number of nuclides available (the radionuclides ^{10}Be, ^{14}C, ^{26}Al, and ^{36}Cl and the stable noble gases ^{3}He and ^{21}Ne) allows almost every lithology to be dated (Ivy-Ochs and Kober, 2008). The selection of the appropriate nuclide is controlled by the estimated exposure duration of the surface being investigated, and the nature of the study, whereas the choice of lithologies can restrict the nuclides used (Gosse and Phillips, 2001).

Cosmogenic-nuclide exposure dating has been attempted on thousands of glacial landforms located in all continents (Balco, 2020), including boulders on moraines (e.g. Gosse et al., 1995; Finkel et al., 2003; Balco and Schafer, 2006) and buried glacial deposits (e.g. Balco et al., 2005), boulders on glacial outwash fans (e.g. Phillips et al., 1997), boulders on the former margins of ice-dammed lakes (Davis et al., 2006), boulders deposited during catastrophic outburst of ice-dammed lakes (Cerling et al., 1994; Reuther et al., 2006) as well as rates of glacial retreat and depth of subglacial erosion upon ice-moulded bedrock (e.g. Guido et al., 2007; Hippe et al., 2014)

2.2.2.1 Physical principles of TCN dating

Cosmogenic nuclides (^{3}He, ^{10}Be, ^{21}Ne, ^{26}Al, ^{36}Cl) accumulate predictably in minerals exposed at the Earth's surface due to nuclear reactions induced by cosmic ray particles (Dunai and Lifton, 2014). The property that makes cosmic-ray-produced nuclides valuable for

geochronology is that they are produced only at the Earth's surface or very close to it (Balco, 2020). Therefore, measuring their concentrations allows determination of how long rocks or sediment have been exposed at or near the surface of the Earth (Lal 1991; Gosse and Philips, 2001).

The Earth is constantly being bombarded by cosmic rays and interactions of high-energy cosmic ray particles with nuclei in the Earth's atmosphere result in a cascade of secondary particles and especially neutrons and short-lived muons (Gosse and Philips, 2001; Ivy-Ochs and Kober, 2008). Cosmogenic nuclides build up in rocks due to the interactions of cosmic rays with atoms in minerals which include high energy spallation, muon-induced reactions and low-energy (epithermal and thermal) neutron capture (Lal and Peters, 1967). A spallation reaction is a high-incident energy process in which a secondary cosmic ray neutron collides with a target nucleus within a mineral and breaks from it several lighter particles, leaving a lighter residual nucleus (i.e. the cosmogenic nuclide) in the mineral lattice (Templeton, 1953). Muonic interactions producing TCN mainly involve the capture of slow negative muons by charged nuclei, although coulombic interactions of fast muons also contribute (Lal, 1988). They can also indirectly release neutrons, through a variety of reactions, which can in turn generate nuclides such as ^{36}Cl through low-energy neutron absorption (Stone et al., 1998), whereas highly energetic muons can also interact spallogenically (Gosse and Phillips, 2001). Low energy neutrons include thermal and epithermal neutrons whose path is described by Brownian motion due to random collisions with atomic nuclei in the medium, ultimately being absorbed by the nuclei of atoms they encounter and resulting in the formation of thermal-neutron-produced cosmogenic nuclides (Gosse and Phillips, 2001). As the mechanisms of low-energy neutron production and difuusion within the rock are still not fully understood, this pathway of cosmogenic nuclides production is a source of uncertainty (Gosse and Phillips, 2001; Marrero et al., 2016b).

As regards the production of cosmogenic ^{36}Cl in particular, production from spallation takes place mainly from Ca and K and to a lesser extent from Ti and Fe (the combined contributions from Ti and Fe are typically less than 1-2% in samples excluding oxide mineral separates; Marrero et al., 2016b) whereas the muon-induced reactions take place in Ca and K but their contribution to total ^{36}Cl production is proportionally much smaller than spallation (Stone et al., 1998; Marrero et al., 2016a). In rocks with sufficient natural Cl (^{35}Cl and ^{37}Cl), ^{36}Cl is produced through low-energy (thermal and epithermal) neutron capture on ^{35}Cl (Gosse and Phillips, 2001; Ivy-Ochs and Kober, 2008). However, the much higher production rate of Ca

and K spallation compared to low-energy neutron capture means that in rocks with high Ca and K content the production of ^{36}Cl will be spallation-dominated regardless the natural Cl content (Marrero et al., 2020). On the other hand, in rocks with considerable Cl content but negligible Ca and K content such as the highly serpentinized ophiolites that were dated on Mt Mavrovouni in this research, the ^{36}Cl production will be dominated from low-energy neutron capture on authigenic ^{35}Cl whereas depending on Fe and Ti concentrations, spallation from these elements might also have a higher contribution than a total of 1-2% mentioned above.

2.2.2.2 Calculation of Exposure Ages

In order to calculate the exposure ages of rock samples the total production rate of ^{36}Cl needs to be determined. However, as each rock has a different chemistry, the ^{36}Cl production rates must be calculated individually for each type of reaction and for each element (Ivy-Ochs and Kober, 2008), which requires the accurate measurement of rock composition. First of all, the determination of major element oxides concentrations such as CaO, K_2O, Fe_2O_3 and TiO_2 is needed for the calculation of the spallation and muon-induced production rates. Additionally, concentrations of trace elements of B, Gd, and Sm must be determined as these elements are strong neutron absorbers and influence the proportion of low-energy neutrons that are available for neutron capture reactions (Ivy-Ochs and Kober, 2008). U and Th concentrations are also needed to correct for subsurface non-cosmogenic neutron-capture ^{36}Cl production (Fabryka-Martin, 1988). Major/minor element and trace element concentrations are usually determined using ICP-ES (Inductively Coupled Plasma Emission Spectrometry) and ICP-MS (ICP - Mass Spectrometry).

A crucial issue for the calculation of the ^{36}Cl production rates from low-energy neutron capture reactions, is the determination of the total rock Cl concentration in samples. A significant improvement in ^{36}Cl methodology is the implementation of isotope dilution: by adding a spike of known isotopic composition but different from the natural ratio of ^{35}Cl:^{37}Cl which is about 3:1, both the total rock Cl concentration and ^{36}Cl can be determined in a single target using AMS, by measuring the $^{37}Cl/^{35}Cl$ and the $^{36}Cl/Cl$ ratios (Elmore et al., 1997; Ivy-Ochs and Kober, 2008). This has led to marked improvements in both precision and accuracy in cosmogenic ^{36}Cl dating results (Desilets et al., 2006).

Other considerations in the calculation of exposure ages include the shielding by surrounding land or the seasonal snow cover that reduce the cosmic ray flux to the sampling site leading to lower ^{36}Cl production rates which can produce overestimated exposure ages (Ivy-Ochs and Kober, 2008). In general, the effect of typical topographic obstructions is small

because the incoming cosmic radiation is strongly concentrated near the vertical, but the shielding effect may be accentuated if the sampled surface is sloped toward a major topographic obstruction (Gosse and Phillips, 2001). Land-shielding corrections are usually done with field measurements following Dunne et al. (1999) and Gosse and Phillips (2001) and the use of nowadays available online calculators (e.g. http://hess.ess.washington.edu/math/) The calculation of topographic shielding factors is also possible through dedicated DTM-based GIS tools (e.g. Li, 2018; available online at https://web.utk.edu/~yli32/programs.html). As regards snow cover, the shielding effect depends on the average values of the annual duration of snow cover, of its thickness and of its density, but reasonable estimates can be made for the degree of snow cover shielding over the long term (Gosse and Phillips, 2001).

Finally, where field evidence indicates that rock surface weathering (erosion) has been significant, an assumed or measured erosion (denudation) rate needs to be used for the calculation of ages (Ivy-Ochs and Kober, 2008). The effect of erosion on cosmogenic nuclide accumulation does not depend on the erosion rate, but rather on the total erosion depth (Gosse and Phillips, 2001). Significant erosion can be defined as an appreciable fraction of the apparent attenuation length, on the order of 15 or 20 cm rock depth and therefore assumptions of negligible erosion are probably generally adequate for surface-exposure dating studies in the late Quaternary age range (Gosse and Phillips, 2001). Inheritance is defined as the presence of a non-zero cosmogenic nuclide concentration in the rock surface at the beginning of the exposure period that is of interest and can lead to overestimations of ages (Ivy-Ochs and Briner, 2014). These inherited cosmogenic isotopes would then have been produced during previous exposure to cosmic rays.

The most widely used calculators of exposure ages for different available cosmogenic nuclides and scaling models include the production rates and calculation code of Marrerro et al. (2006a, 2006b) incorporated in the online Cronus Calculator (http://cronus.cosmogenicnuclides.rocks) and the Excel spreadsheet and production rates of Schimelpfennig et al. (2009, 2011).

2.2.2.3 Moraine dating

Surface exposure dating with cosmogenic nuclides is especially well suited to the dating of moraines and such landforms ranging in age from hundreds of years to hundreds of thousands of years in both hemispheres have been dated (e.g. Barrows et al., 2002; Kaplan et al., 2004; Briner et al., 2005; Ivy-Ochs et al., 2006; Balco and Schafer, 2006). As the boulders transported by a glacier and deposited on moraines originate from collapsed rock walls in the accumulation

area and from rocks plucked from beneath the glacier's base they are mostly fresh, never-before-exposed rocks (Ivy-Ochs and Briner, 2014). As the glacier retreats from its terminal position near the moraine, deposition ceases, and cosmogenic nuclides build up in the boulders of the moraines. Therefore, exposure dating of a boulder on the moraine crest can well approximate the time since the glacier last contributed sediments to the moraine (Ivy-Ochs and Briner, 2014). This is the ideal case (Figure 4a). However, there are two principal geological factors that can lead to erroneous deposition ages (Heyman et al., 2011): inheritance due to exposure prior to glaciation yielding older exposure ages than the true age of deposition (Figure 4b) and incomplete exposure due to post-depositional shielding, yielding younger exposure ages than the true age of deposition (Figure 4c).

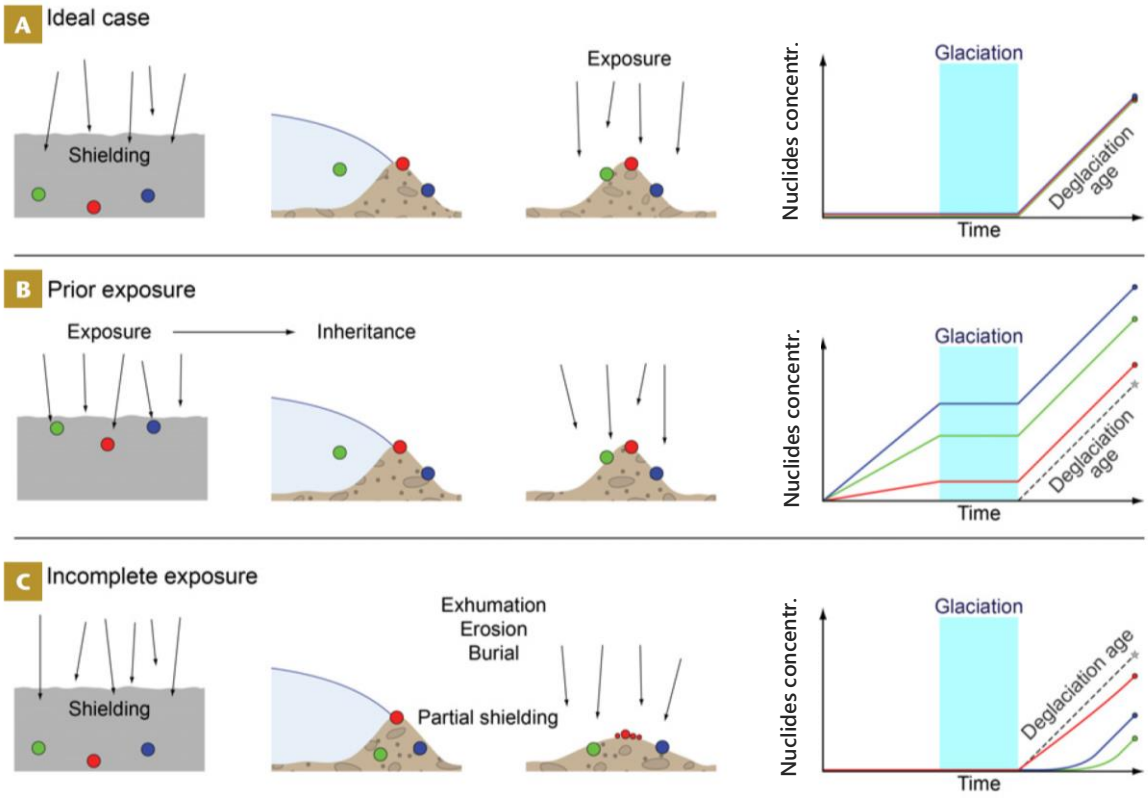

Figure 4. Schematic of possible prior exposure and incomplete exposure of boulders deposited on moraines and relationships between ages of boulders and the true depositional age of moraines. On the right-hand side, the buildup of cosmogenic nuclides with time in the respective boulder surfaces (green, red, blue circles) is shown: ***a)****(up): Ideal case where the sampled boulder has been completely shielded from cosmic rays prior to glaciation and continuously exposed since deglaciation exposure – yielded age same as true age of deposition,* ***b)*** *(middle): inheritance due to exposure of the sampled boulder to cosmic rays prior to glaciation – yielded age exceeds the true age of deposition ," and* ***c)****(bottom): sampled boulder disintegrated or exhumed after moraine deposition leading to incomplete exposure of sampled boulder due to partial post-depositional shielding from cosmic rays - yielded age younger than the true age of deposition. [Modified from Heyman et al. (2011) and Ivy-Ochs and Briner (2014)].*

Several studies compiling ages from sites across the globe suggest that marked inheritance in moraine boulders is rare (Heyman et al., 2011) due to the excessive erosional features of glaciers and relatively short transport distances compared to fluvial sediments (Schmidt et al., 2011; Sarikaya et al., 2020). Incomplete exposure on the other hand is more likely to be an issue, especially in old degraded moraines where boulders may have been exhumed or toppled. (Ivy-Ochs and Briner, 2014). Such effects may be reduced by cautious selection of sampled boulders. Stable - broad and large boulders that are well embedded in relatively stable moraine crests are more suitable -and when possible, they also need to be high enough (>1.5 m high) to ensure they have protruded above the matrix all the way since moraine deposition (Hallet and Putkonen, 1994; Putkonen and Swanson, 2003; Putkonen and O'neal, 2006). In general, the spread in ages amongst the exposed boulders increases with moraine age due to longer periods of erosion processes and boulders exhumation (Zreda et al., 1994; D'Arcy et al., 2019) This may make interpretation of the deposition age of moraines difficult (Kaplan et al., 2005; Smith et al., 2005). In such cases a detailed scrutiny of the landforms and morphostratigraphic relationships is required and, in some cases, the oldest age can usually be assumed to be geomorphologically the most reasonable to be closest to the moraine deposition age (Ivy-Ochs and Kober, 2008). It should be noted that taking a mean of all ages is not necessarily the best choice (Ivy-Ochs et al., 2007).

Finally, the fact that a glacier may fluctuate about the terminal moraine for centuries to millennia resulting in complex nested moraine formations that might have been additionally modified by post-depositional fluvial erosion and that lateral moraines can also have a composite architecture that reflects to repeated glaciation phases, makes the detailed field mapping of the landforms to be dated a prerequisite for judicious sampling (Ivy-Ochs and Kober, 2008; Ivy-Ochs and Briner, 2014).

2.2.3 Luminescence dating

Dating of sediments using optically stimulated luminescence (OSL) has become important for studying Earth surface processes, and this technique continues to develop rapidly. A group of closely linked luminescence methods can be used to estimate the time since grains of quartz and feldspar were last exposed to daylight by detecting their subsequent response to environmental ionizing radiation exposure (Rhodes, 2011). Luminescence dating can be readily applied to most terrestrial sediments and can be used to date sediments on timescales from a few years to 200ka, encompassing the entire Late Quaternary (Fuchs and Owen, 2008; Rhodes, 2011). As this dating method defines the timing of sedimentation, in most instances it

directly dates landform formation, and is potentially extremely accurate (Lian and Roberts, 2006). Moreover, errors of OSL dating within a few percent of the age can be achieved and therefore represents one of the most potentially useful and applicable dating methods for defining the age of late Quaternary glacial and associated sediments and landforms (Fuchs and Owen, 2008). However, OSL dating has not yet been widely applied to glacial sediments despite its usefulness and applicability as shown by a number of studies such as in the Himalaya (Spencer and Owen, 2004), the European Alps (e.g. Bavec et al., 2004; Klasen et al., 2007) and the Alps of New Zealand (Preusser et al., 2005). The application of OSL dating is particularly valuable when combined with TCN surface exposure dating of moraines (e.g. Spencer and Owen, 2004).

The limited use of luminescence dating probably reflects a common concern that glacial and associated sediments have not been reset by sufficient daylight exposure during the last process of sediment reworking before deposition (Fuchs and Owen, 2008). Insufficient daylight exposure results, if undetected, result in age overestimation (Duller et al., 1995). Most studies dealing with palaeoenvironmental reconstruction of glacial environments have therefore concentrated on dating proglacial glaciofluvial or glaciolacustrine sediments, which are considered less likely to have insufficient bleaching problems compared to glacial sediments and ice-contact sediments (Fuchs and Owen, 2008). Nevertheless, the double whammy of rapid deposition along with poor quartz characteristics which makes glacial deposits challenging to date has been a driver of technical innovation for OSL (Rhodes, 2011) and recent advances in luminescence dating techniques enable the production of reliable ages (Duller, 2006).

2.2.3.1 Physical principles of luminescence dating

Luminescence dating is a radiometric dating method that is based on the time-dependent accumulation of electrons at traps within the crystal lattice of minerals such as quartz and feldspar (Fuchs and Owen, 2008). Natural environmental ionizing radiation, derived from radioactive isotopes within the sediment and cosmic radiation, causes charge (electrons and holes) to become trapped when grains are buried in the ground, as bonding electrons are excited from their valence positions, and a small fraction become trapped within the crystal lattice of minerals (Rhodes, 2011). A short daylight exposure (in the range of 1 to 100 s) is sufficient to reduce certain electron trap, effectively resetting the luminescence dating clock (bleaching), and the subsequent gradual increase in trapped charge population in response to the prevailing radiation flux provides the basis for dating (Rhodes. 2011). The storage of trapped charge

within the crystal lattice is similar to the action of a rechargeable battery (Figure 5), forming an attractive analogy (Duller 2008). One important distinction is that in luminescence dating, charging occurs very slowly (10 – 10^5 years), but charge removal happens very quickly (1–100 s) during both bleaching and OSL measurement (Rhodes, 2011).

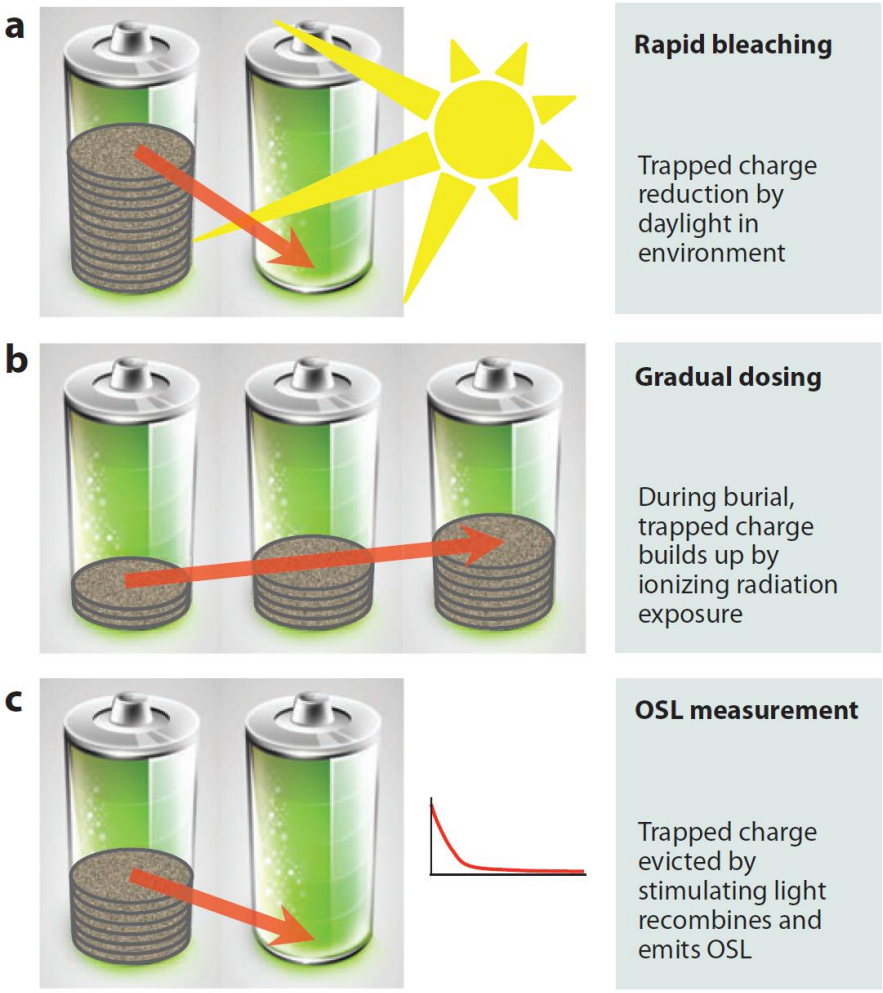

Figure 5. The rechargeable battery forms a useful analogy to help understand optically stimulated luminescence (OSL) dating. Gray plates show charge level: ***a)*** *(up): Daylight releases trapped charge during grain movement over periods of seconds to minutes,* ***b)****(bottom): charge is slowly built up as a small fraction of electron-hole pairs produced by low levels of environmental radiation are trapped in the mineral lattice and* ***c)****(bottom): after sample collection and preparation, intense stimulating light releases charge from light-sensitive traps, which recombines emitting a luminescence signal in the form of an OSL decay (shown). [From Rhodes (2011) based on an illustration by Duller (2008)].*

The release of the trapped electrons results in a detectable luminescence signal, the intensity of which is a measure of the number of radiation-induced electrons, which in turn is dependent upon the rate of natural ionizing radiation (dose rate) and duration of burial (Wagner, 1998; Lian and Roberts, 2006). Trapped charge concentration is assessed by laboratory measurements, in which minerals are stimulated with heat or light to release the trapped

electrons (Fuchs and Owen, 2008) and create the luminescence signal (equivalent dose), which consists of a rapidly decaying light emission as electrons are evicted (Bailey et al. 1997). Natural radiation flux, or dose rate, may be determined with a choice of methods (e.g. Adamiec and Aitken, 1998).

The type of luminescence dating is distinguished on the basis of the stimulation method, such that stimulation by heat is Thermoluminescence (TL -not used so often nowadays), stimulation by visible light is optically stimulated luminescence (OSL) which is applied on quartz and stimulation by infrared light is infrared stimulated luminescence (IRSL) which is applied in feldspar (Fuchs and Owen, 2008).

2.2.3.2 Calculation of luminescence ages

The three principal parameters required for the calculation of the luminescence age are (a) the natural luminescence signal measurement, (b) an assessment of sensitivity (luminescence signal response to applied radiation dose), and (c) the determination of the burial dose rate experienced by each sample (Rhodes, 2011). The first two parameters are combined into a single procedure that provides the applied dose acquired over the period of interest, which represents the equivalent dose (De measured in Gy) of accumulated radiation energy in the crystal during burial (Rhodes, 2011; Fuchs and Owen, 2008). The mean ionizing radiation dose rate (D measured in $Gy \cdot yr^{-1}$) can be derived from direct measurements or measured concentrations of radioisotopes.

The luminescence age (La) is then calculated by the equation:

$$La\ (yr) = \frac{De(Gy)}{D\ (Gy\ \cdot yr^{-1})}$$

2.3 Glacier reconstructions and ELA calculations

A geographic information system (GIS) approach was used for the reconstruction of palaeoglaciers on Mt Mavrovouni (Chapter 4). In particular, the surface and thickness of the former glaciers were reconstructed using the GlaRe toolbox, a semi-automated GIS tool based on the numerical technique of Benn and Hulton (2010) and developed by Pellitero et al. (2016). The approach is based on user-given basal shear stress value along the flowline of the glacier (default value 100 kPa in accordance with Paterson, 1994; Rea and Evans, 2007), which in turn can either be defined automatically by the toolbox according to the user given glacier limits and the DEM or it can be user-defined. Palaeoglacier limits were established based on

geomorphological field evidence such as terminal and lateral moraines. Where evidence was absent or fragmentary a rough outline of the palaeoglacier limits was established based on usual valley glaciers rheology.

The equilibrium line altitudes (ELAs) of former glaciers were automatically calculated with the adaptation of the classic area– altitude balance ratio (AABR) method which accounts for both glacier hypsometry and mass balance gradients (Osmaston 2005). The method was applied in another dedicated GIS tool developed by Pellitero et al. (2015) using a balance ratio (BR) of 1.6, which is the average obtained on present-day glaciers in other Mediterranean mountains (Rea 2009).

Chapter 3. Review of glacial geomorphologic studies and new evidence on the mountains of Greece

A significant number of glacial geomorphologic studies has been conducted in the mountains of Greece and therefore it is essential to provide a summary and an overview of this studies that form the background of this research. A part of this review has been recently published in a journal article (Leontaritis et al., 2020). Where it has been considered meaningful and helpful for future studies, additional evidence collected by the author has been added although by no means does this evidence constitute part of systematic research.

3.1 The Pindus Range in northwest Greece

The extensive glacial landforms and sediments in the mountains of northern Greece attracted the attention of the first pioneer explorers (Figure 1 and Table 1). In the northernmost part of Epirus, on the Greek-Albanian borders, cirques and moraines have been described on the mainly ophiolitic Mt Grammos (2520 m a.s.l.) (Bourcart, 1922; Louis, 1926). Further south, with ophiolites and flysch still dominating local lithology, stands Mt Smolikas (2637m a.s.l.) the second highest mountain of Greece after Mt Olympus (2918 m a.s.l.). Evidence of its former glaciation was first identified by Niculescu (1915) and Mistardis (1937a) while the first detailed geomorphological mapping was conducted by Boenzi et al. (1992).

Some 15km to the south lies the impressive Mt Tymphi (2497 m a.s.l.- limestone) with probably the most extensive and well-preserved glacial deposits in Greece (Mistardis, 1937a; Woodward and Hughes, 2011). Mistardis (1935) was the first to report glacial evidence on Mt Tymphi while detailed geomorphological mapping was first conducted by Palmentola et al. (1990) and later on by Smith et al. (1998) who used satellite imagery to map the extent of glacial deposits. Just 20km to the west, on the borders with Albania, impressive glacial cirques and moraines were also observed by Louis (1926) on Mt Nemercka (2482 m a.s.l. - limestone). On the ophiolitic Mt Mavrovouni (2157 m a.s.l.), about 15km in the south-east of Mt Tymphi, a complete glacial sequence has been recorded and dated by the author which is part of this research and is described in detail in Chapter 4. Finally, Sestini (1933) identified further south the traces of the extensive former glaciation of Mt Kakarditsa (2429 m a.s.l. - limestone) and Mt Lakmos (2295 m a.s.l. - limestone).

The first advanced study of the Pindus Mountains was the geomorphological study of Mt Tymphi and Mt Smolikas by Hughes (2004, 2006a, 2006c) and Woodward et al. (2004), which

was supported by geochronological control for what proved to be Middle Pleistocene glaciation phases. This provided the initial chronological framework for glaciations in Greece (Hughes et al., 2005). After these first advanced studies in northern Greece, the lack of further evidence from the last cold stage in Greece (MIS 5d - MIS 2; Hughes et al., 2006a) constituted an important gap in the glacial chronology of the Pindus Mountains that led to further studies in Mt Olympus and the Peloponnese that focused on Late Pleistocene deposits (see next sections).

The temporal framework for the glaciations of the North Pindus mountains however, was further constrained only years later by the contribution of Allard et al. (2020) who provided cosmogenic exposure ages for the - up to that moment - undated Late Pleistocene glacial deposits, thus providing a constraint on the timing of the respective glaciations. The studies on Mt Tymphi and Mt Smolikas are presented in detail next.

3.1.1 Mt Tymphi

Mt Tymphi is mainly formed of Palaeocene and Upper Eocene crystalline limestones that dominate its upper slopes. However, older Upper Jurassic/Senonian limestones and dolomites are also exposed on the cliffs of the northern escarpments of the highest peaks (Hughes et al., 2017). Upper Eocene/Miocene flysch is generally restricted to the lower mountain slopes and was mostly situated outside the main areas of glacier erosion (IGME, 1970). Combined glacial and karstic processes on the other hand have formed a classic glacio-karst system (Hughes et al., 2006e).

Numerous glacial and periglacial landscape features were recorded on Mount Tymphi including cirques, deep ice-scoured troughs, limestone bedrock pavements, rock glaciers and extensive and well-preserved moraine complexes including lateral, terminal and hummocky moraines. Sketch maps of the glacial geomorphology were published in Palmentola et al. (1990) and this pioneering work was then improved upon with more detailed mapping by Hughes (2004). An extensive dating program followed: secondary calcites contained in the older and most extensive recorded glacial deposits were radiometrically dated by means of uranium series (Figure 10), first published by Woodward et al. (2004) then followed-up by Hughes (2004) and Hughes et al. (2006a). These data formed the basis for the definition of the glacial sequence on the Pindus Mountains (Hughes et al., 2005, 2006a).

Correlating the results of the aforementioned studies with cold stage intervals recorded in the ca. 425ka long lacustrine pollen sequence at the nearby Lake Ioannina (Tzedakis, 1994; Tzedakis et al., 2002), the glacial chronostratigraphy for the Pindus Mountains was defined.

Three main glacial stages correlated with the marine isotope record have been identified (Hughes, 2004; Hughes et al., 2005, 2006a). These stages are summarised in Table 2.

Table 2. The Pindus Chronostratigraphy as defined by Hughes et al. (2005, 2006a)

The Pindus Chronostratigraphy		
Stage Name	MIS Age	Equivalent glacial phase to northern Europe
Skamnellian Stage	MIS12 ca. 480-430 ka	Elsterian Stage
Vlasian Stage	MIS 6 ca. 190-130 ka	Saalian of northern Europe
Tymphian Stage	MIS 5d – MIS 2 ca. 110-11.7 ka	Weichselian Stage

3.1.1.1 Middle Pleistocene Glacial Phases

These studies on Mt Tymphi provided abundant and clear geomorphological evidence and good geochronological control for extensive glacier formation during the first two Middle-Pleistocene stages (MIS 12/MIS 6). As it can be seen in Figure 6, extensive valley glaciers during the Skamnellian Stage extended down to altitudes of 850 m a.s.l. and 700 m a.s.l. on its southern and north/north-eastern slopes respectively with a mean ELA of 1741m a.s.l. (Hughes et al., 2006a). Aspect appears to have had insignificant effect on the overall distribution of the glaciers. Thus, factors such as shading and lee-slope accumulation also appear not to have been dominant controls on glacier development during these glaciations (Hughes et al., 2007). The moraines from this glaciation have deeply weathered soil profiles with profile development indices (PDIs) ranging from 51.8 to 61 (Hughes et al., 2006a). The PDIs were measured and scored following the methods of Harden (1982). In short, this index is used to quantitatively measure the degree of soil profile development taking as well into account its weathering degree. The higher the value of the PDI of the soil that covers the moraines, the older the deposits are.

As the deposits from this glacial stage are traversed by mountain tracks and village roads around Tsepelovo, Skamnelli and Vrysochori (Figure 6), good-quality exposures are commonly present in the lower altitude zone of the sediments. Such exposures in the tills show that the glacial sediments are dominated by limestone-derived sediments with a minor flysch component (Hughes et al., 2006e). They contain subrounded limestone boulders of a wide size

range, cobbles and gravels commonly dispersed in a fine-grained matrix rich in sands, silts and clays (Woodward and Hughes, 2011). Most interestingly, detailed sedimentological analyses of the diamicton sequences within these moraines, indicated that stacked diamicts separated by gravels related to meltout and glacial retreat record at least three phases of former glacial advance and retreat (Hughes et al., 2006e). Evidence of the later Vlasian Stage is confined to mid-valley positions (mean ELA 1862 m a.s.l.) with rather weathered soil profiles as the PDIs range from 29.8 to 38.3 (Hughes et al., 2006a).

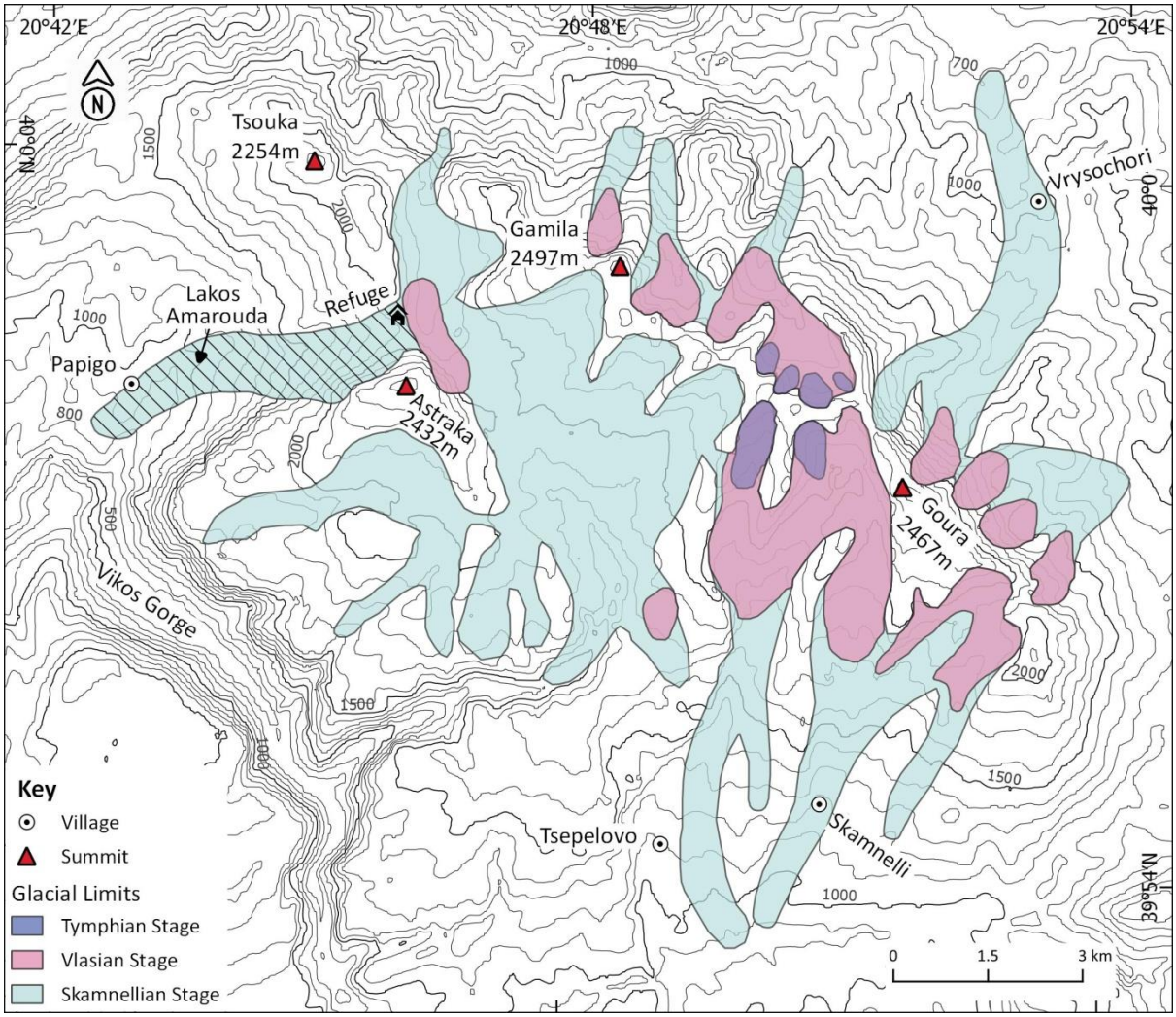

Figure 6. Glacial extent during the different Stages of the Pindus Chronostratigraphy on Mt Tymphi. Denoted Tymphian Stage glacial extent refers to LGM glaciers after retreat from the positions held during the local pre-LGM Late Pleistocene glacial maximum according to Allard et al. (2020). Hatched area denotes a lobe glacier according to the new evidence presented here. Skamnellian Stage extent increased to a near-ice-cap configuration accordingly (map modified from Hughes et al., 2007).

New evidence

New observations, which even though are not part of systematic research, are included here as supplementary material that could have important implications on the interpretation of the well-documented glacial studies on Mt Tymphi. In particular, evidence from sediments with similar characteristics to the subglacial tills exposed near Tsepelovo and Skamnelli was found in the Lakkos Amarouda valley above the village of Papigo in the north-western part of the massif (Figure 6 and Figure 8). These deposits contain various sizes of subrounded limestone boulders commonly dispersed in a fine-grained matrix rich in sands and have been thrusted over the flysch bedrock (Figure 7). They extend all the way from 1450m to 800m near the villages Papigo and Mikro Papigo (Figure 8) along with scattered glacial boulders (Figure 9). This glacier would have originated from the ice-scoured northern crags of Astraka. However, perched glacial boulders and till were also identified on the col near the refuge of Astraka at the head of the valley, implying that this former glacier breached the watershed and was an outlet lobe of a larger plateau ice-field rather than a stand-alone valley glacier (Figure 6 and Figure 8). If this was the case, the extent of glaciation during the most extensive Middle Pleistocene glacial phase is likely to have been underestimated. Thus, it is very likely that during the Skamnellian Stage Mt Tymphi was glaciated by a plateau ice field with valley glaciers radiating from a central ice dome centred over the plateau between Astraka and Gamila. Similar ice configurations occurred over Mt Chelmos in the Peloponnese (Pope et al., 2017) and over the mountains of Montenegro (Hughes et al., 2010, 2011).

Figure 7. A road-side exposure of till sediments near the village of Papigo (Photo: June 2017).

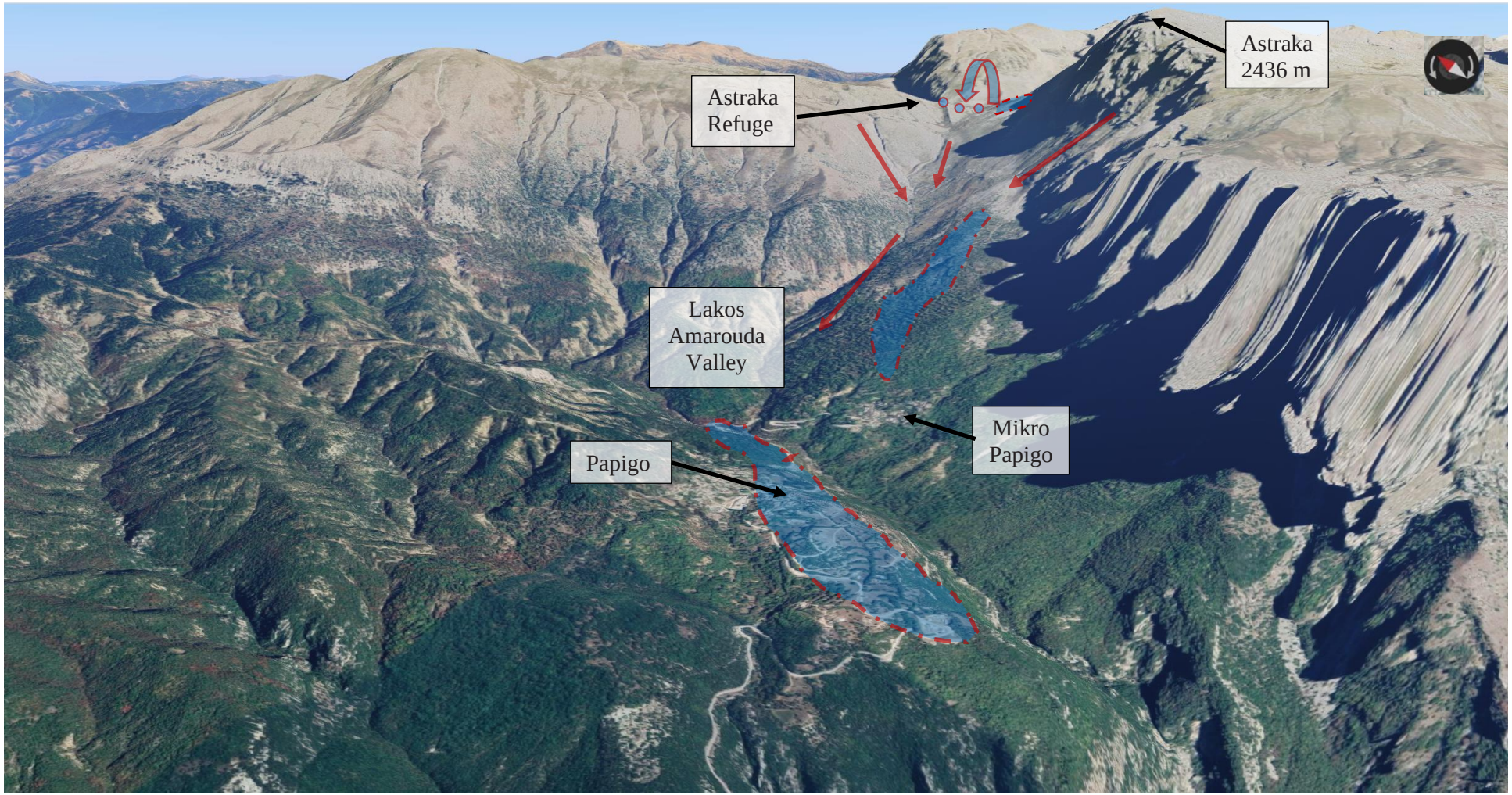

Figure 8. Glacial evidence in the Papigo region depicted on virtual globe imagery (Google Earth). Red Arrows denote the ice flow direction, dashed polygons correspond to till units and spheres to areas with glacial boulders. The curved arrow denotes the Astraka refuge col where the ice cap broke the watershed. Based on field work during autumn 2016- summer 2017.

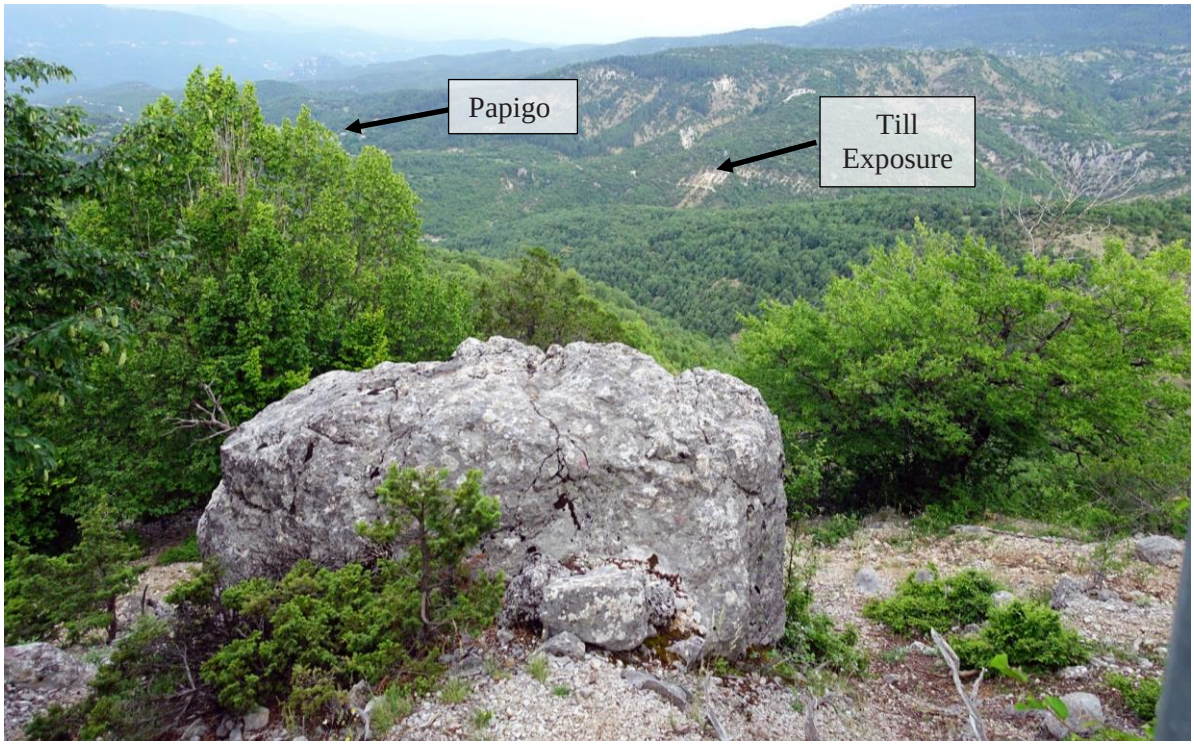

Figure 9. Glacier boulder within the till unit above Mikro Papigo (see Figure 8). The location of the roadside exposure of the till unit near Papigo can also be seen in the background (Photo: June 2017).

3.1.1.2 Late Pleistocene Glaciations

As regards the Tymphian Stage – the last cold stage in Greece - the evidence implied a much more restricted glacier development. The youngest deposits formed in the highest cirques above 1800 m a.s.l. are well preserved but are limited to rock glaciers and small moraines (Hughes et al., 2003; Hughes, 2004). These deposits are well within the limits of the Vlasian Stage deposits and show only very limited evidence of pedogenic weathering (PDIs of 7.8 to 9.0) (Hughes et al., 2006a). Therefore, they were ascribed to the last cold stage even though at this point there were no radiometric or cosmogenic dating data (Hughes, 2004; Hughes et al., 2006a, 2006c). More marginal glacial conditions during these later cold stages appear to have forced glaciers to occupy locally-favourable topographic settings with northern and eastern aspects (Hughes et al., 2007). These glacial limits however that are presented in Figure 6, were later identified by Allard et al. (2020) as LGM positions of glaciers after retreat from their maximum extent during the local Late Pleistocene glacial maximum prior to the LGM. This work is summarised next.

The lack of geochronological data for the Tymphian Stage led to dedicated research on the Late Pleistocene deposits found on the upper valleys of Mt Tymphi by Allard et al. (2020). In this work there are presented 27 ^{36}Cl ages from glacial boulders that address both a significant geographical gap in Mediterranean glacial chronologies and a temporal gap in the glacial

history of this region by targeting the previously undated Late Pleistocene record (Allard et al., 2020). Most samples were collected from glacial boulders within terminal and lateral moraines expanding between 1700 m and 2050 m a.s.l. in the Laccos Megalon Litharion and the Tsioumako valleys (Figure 10). These deposits mark the extent of Late Pleistocene glaciers on the southern side of Mount Tymphi. Some more samples were collected from a pair of terminal moraines within the north-oriented Laccos cirque. The main glacial features that were sampled are presented in Figure 11.

As regards the Laccos Megalon Litharion valley samples were taken from two moraines: a high altitude one at ~ 2000 m a.s.l. and a lower altitude one at ~ 1710 m a.s.l. The yielded ages – excluding outliers - span from 14 ± 1.4 to 24.5 ± 2.4 ka and 15.7 ± 1.9 to 25.7 ± 2.6 ka in the upper and the lower moraine respectively (Allard et al., 2020). Similarly, in the Tsioumako valley, three samples at ~1770 m a.s.l. reported ages of 29.0 ± 3.0 ka, 15.5 ± 1.7 ka and 18.9 ± 1.9 ka (Allard et al., 2020). The authors argue that the oldest age is likely to most closely represent the true age of the moraines whilst younger ages have been assumed to represent a period of moraine degradation and boulder exhumation. This assumption has been based on the facts that these moraines are not cemented, making them susceptible to hillslope processes while at the same time they do not have sharp crests providing some evidence for degradation and boulder exhumation. Moreover, other methods of landform age interpretation such as the mean age can lead to significant inaccuracy where incomplete exposure and erosion are the main geological uncertainties (Applegate et al., 2010; D'Arcy et al., 2019). In this perspective the oldest ages from the Tsioumako valley and the lower moraine in the Laccos Megalon Litharion valley are considered to represent the most extensive Late-Pleistocene glacier extent whilst the oldest age from the upper moraine in the Laccos Megalon Litharion valley is considered to represent a distinct glacial retreat phase during which glaciers were confined within the upper cirques of the valleys.

The samples from the terminal moraines between 1420 and 1435 m a.s.l. in the Laccos cirque yielded ages between 6.7 ± 0.9 ka and 18.0 ± 1.9 ka (Allard et al., 2020). Glaciers in this cirque were perhaps longer sustained in these low altitudes by avalanching and wind-blown snow accumulation and topographic shading from the steep Goura cliffs (>1000 m tall). Even though these ages could represent a younger Late Pleistocene glacial advance phase, this interpretation should be regarded in view of the paucity of chronological data on the northeast side of the Tymphi massif and therefore more data are needed to build a more robust age model (Allard et al., 2020).

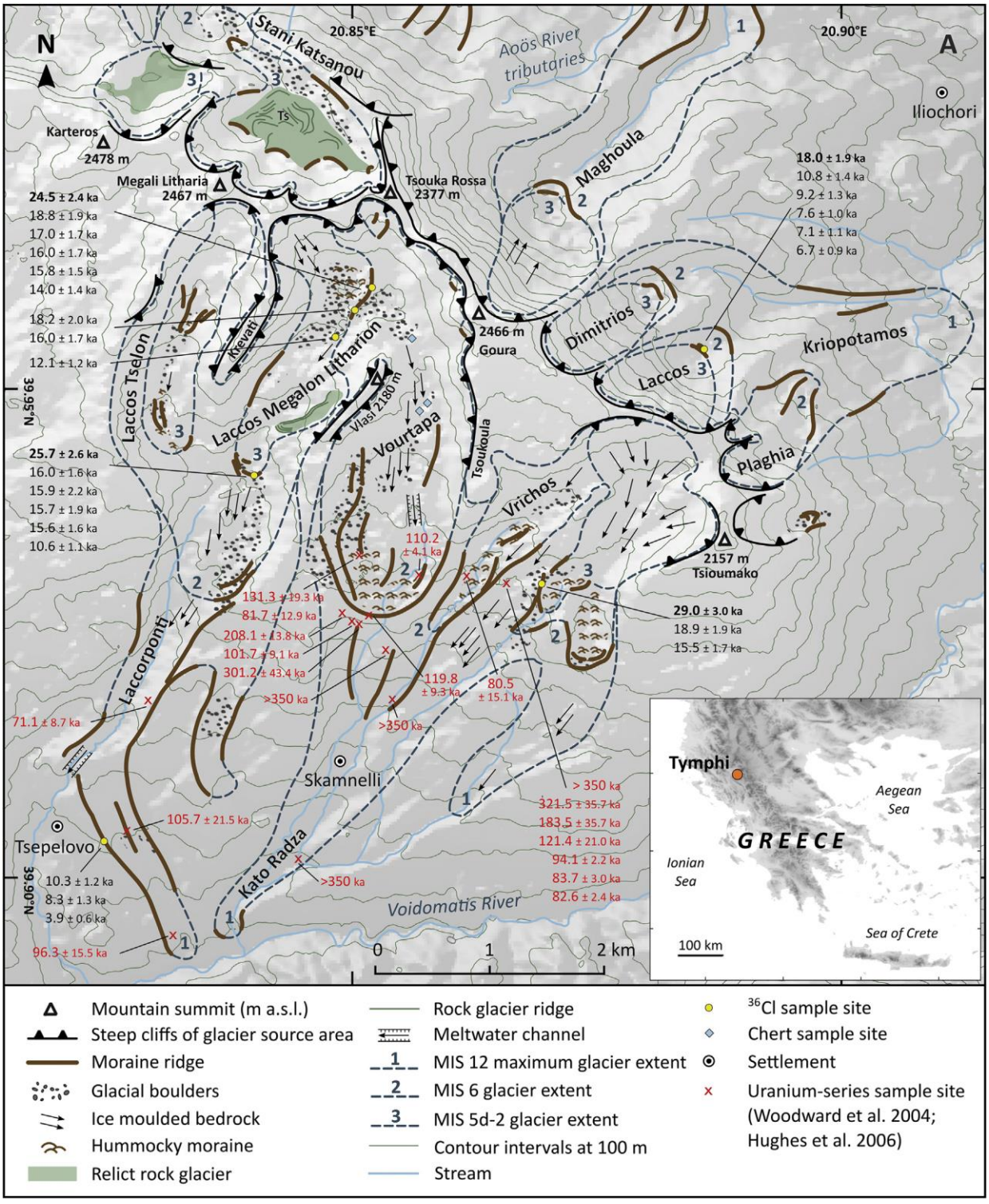

Figure 10. Glacial geomorphological map of Mount Tymphi, Epirus, northwest Greece. The location and ^{36}Cl ages of moraine boulders (black lettering - Allard et al., 2020) are identified along with uranium-series sample sites and ages from secondary carbonates within glacial deposits (red lettering - Woodward et al., 2004; Hughes et al., 2006a). The maximum extent of glaciation during MIS 12 (Skamnellian Stage), MIS 6 (Vlasian Stage) and MIS 5d-2 (Tymphian Stage) is denoted by morphostratigraphic units 1, 2 and 3 respectively (from Allard et al., 2020).

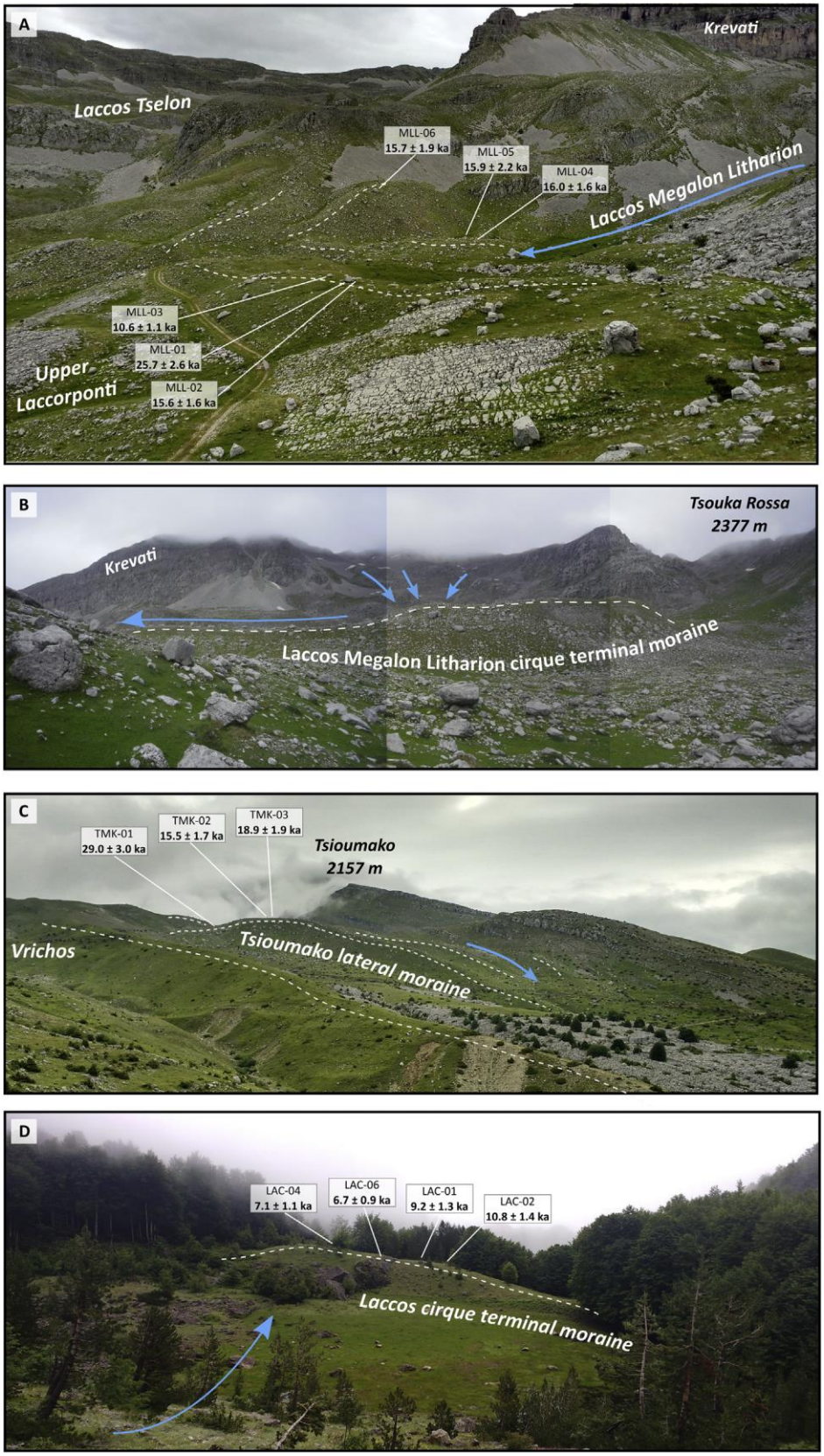

Figure 11. Glacial landforms at sampling sites and yielded ^{36}Cl ages on Mount Tymphi according to Allard et al. (2020): ***A)*** *Looking northwest towards the Laccos Megalon Litharion lower valley terminal moraine.* ***B)*** *Looking northwest towards the Laccos Megalon Litharion cirque terminal moraine and lateral moraine.* ***C)*** *Looking northeast towards the Tsioumako lateral moraine.* ***D)*** *Looking northeast within the Laccos cirque at the inner terminal moraine (from Allard et al., 2020).*

3.1.1.1 Summary and glacier reconstructions

In summary, during the cold stages of the last glacial cycle, the glaciers of Mount Tymphi were restricted to the cirques and upper valleys between 1700 and 2350 m. The updated glaciers reconstructions of Allard et al. (2020) are depicted in Figure 12. The largest glaciers on Mt Tymphi during the Tymphian Stage (MIS 5d-2), reached their terminal positions no later than 29.0 ± 3.0 - 25.7 ± 2.6 ka. The mean ELA for this stage was 2016 m a.s.l. (Allard et al., 2020) uncorrected for tectonic uplift and sea-level change. Glaciers had retreated to the high cirques by 24.5 ± 2.4 ka, during Heinrich Stadial 2., with an ELA of 2231 m a.s.l. (Allard et al., 2020). During this period of glacier retreat, rock glaciers formed below small glaciers in the Tsouka Rossa cirques (Hughes et al. 2003) under cold and drier conditions. Initial results also suggest that small glaciers persisted in the northeast cirques at 18.0 ± 1.9ka although more evidence is needed in order to confirm this. A mean ELA of 1596 m a.s.l. was calculated for these glaciers (Allard et al., 2020), although glacier formation was controlled by slope angle, aspect, topographic shielding and avalanching snow accumulation and therefore these values should not be used for comparison between different massifs. Indicatively, extensive snow patches remain today on this side of the massif during the summer months, fed by avalanching snow and shaded by the Goura cliffs (Allard et al., 2020).

The identified glacial Stages and sub-phases, morphostratigraphic units, altitudinal extent of geomorphological evidence and age models according to all the presented studies on Mt Tymphi are summarised in Table 3.

Table 3. Pleistocene glacial phases and morphostratigraphic units on Mt Tymphi (see text for references)

Phase	Age (Correlations)	PDI	Orientation/mean ELA Deposits Altitude
Tymphian Stage (Unit 3)	18.0 ± 1.9 ka	-	NE/1596 m a.s.l. 1420-1435 m a.s.l.
	24.5 ± 2.4 ka (retreat phase)	7.8 - 9	S / 2231 m a.s.l. 2150-2350 m a.s.l.
	29.0 ± 3.0 - 25.7 ± 2.6 ka		S,N / 2016 m a.s.l. 1700-1850 m a.s.l.
Vlasian Stage (Unit 2)	MIS 6; ca. 190-130 ka	29 - 38.3	S /N 1862 m a.s.l. 1100-1350 m a.s.l.
Skamnellian Stage (Unit 1)	MIS12; ca. 480-430 ka	51.8 - 61	N,S / 1741 m a.s.l. Down to750 m a.s.l.

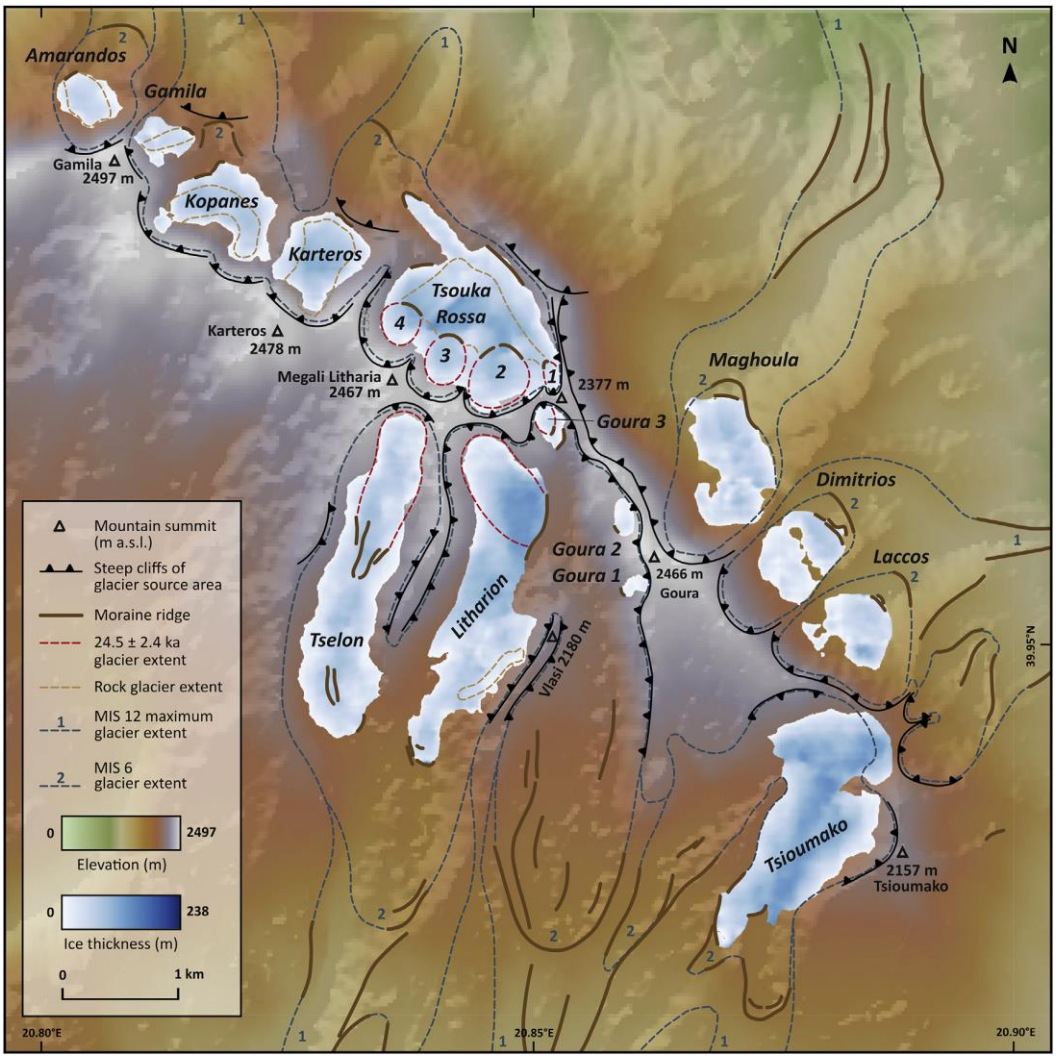

Figure 12. Reconstruction of the maximum extent of Late Pleistocene Tymphian Stage glaciers (25.7 ± 2.6-29 ± 3.0 ka) on Mount Tymphi. Dotted red lines show Late Pleistocene glacier extents at 24.5 ± 2.4 ka, after glacier retreat and dotted brown lines show rock glaciers that developed during the same period. The extent of previous glaciations during MIS 12 (Skamnellian Stage) and MIS 6 (Vlasian Stage) are denoted by morphostratigraphic units 1 and 2 respectively (from Allard et al., 2020).

3.1.2 Mt Smolikas

Mt Smolikas is the second tallest mountain in Greece at 2637 m a.s.l. and lies just 15km to the north of Mt Tymphi. However, its ophiolitic geology means it is less complex in form as it is a generally rounded mountain with fewer cirques and deep valleys cut in to it compared to Mt Tymphi (Hughes, 2004). Mt Smolikas is part of the Pindus ophiolite complex (Jones and Robertson, 1991), part of a nappe which is tectonically overthrust onto the Eocene flysch of the Pindus Zone. Its ophiolites consist of serpentinites, harzburgites and dunites which are traversed by pyroxinite and gabbro veins. Jurassic schists and limestones are also present locally, at the overthrust nappe of the ophiolitic complex (IGME, 1987). Simple sketch maps of the glacial geomorphology of Smolikas were provided in the pioneering work of Boenzi et

al. (1992) and this was followed-up with more detailed mapping and sedimentological investigations by Hughes (2004).

Glacial geomorphological features are less well preserved than on Mt Tymphi and the glacial sequence in some cirque-valley systems is typically more fragmented (Hughes et al., 2006e). Evidence of a complete glacial sequence has been documented only on its northern slopes, while near its highest peaks well-developed cirques and glacial deposits within them have been recorded (Hughes et al., 2006d). Most importantly, four discrete phases of Pleistocene glacial activity are recorded on Mt Smolikas (Hughes et al., 2006c) implying that there is one more, younger stage of glaciation here that is absent on Mt Tymphi (Figure 13; Table 4).

Table 4. Pleistocene glacial phases of Mt Smolikas (see Figure 13 for locations and text for references)

Phase	Age (Correlations)	Orientation / mean ELA Deposits Altitude
Late-glacial/Younger Dryas (Unit 4)	MIS 2; 17.5-11.7 ka	N / 2372 m 2300-2400 m
Tymphian Stage (Unit 3)	MIS 2; 29.0 - 25.7 ka	N – NE– SE / 2241 m 2000-2200 m
Vlasian Stage (Unit 2)	MIS 6; ca. 190-130 ka	N / 1997 m 1100-1350 m
Skamnellian Stage (Unit 1)	MIS12; ca. 480-430 ka	N / 1680 m 1000 m

Traces of vast glacier formation have so far been documented only in the Vathylakos valley on its northern slopes that has been correlated based on morphostratigraphy and altitude to the Skamnellian/Vlasian Stages on Mt Tymphi (Hughes, 2004; Hughes et al., 2006c). This deep ice-scoured valley is headed by typical glacial cirques near its tallest peaks which exceed 2600 m a.s.l. in altitude (Figure 14) and ends up in some thick diamicton deposits at an altitude of 1000 m a.s.l. near the village of Aghia Paraskevi (Figure 13; Woodward and Hughes, 2011). These deposits are traversed by a road revealing a 30 m thick vertical section of ophiolite-derived unconsolidated sediments with a minor limestone component (Hughes et al., 2006e). A detailed sedimentological analysis of the diamicton sequences by Hughes et al. (2006e) within these deposits revealed three stacked subglacial till facies separated by facies related to meltout. Moreover, the boundary between glaciotectonized units and undeformed original

glacial deposits was considered as lithostratigraphic division between the different glacial units (Hughes et al., 2006e). Therefore, based on the morphostratigraphic sequence on Mt Tymphi, the lowest non-deformed unit (Unit 1 – ELA 1680 m a.sl.) was ascribed by Hughes (2004) to the Skamnellian Stage (MIS 12) while the pair of glaciotectonized units deposited about 500 m up-valley (Unit 2 – ELA 1997 m a.s.l.) were ascribed to at least two glacier advance/retreat cycles during the Vlasian Stage (MIS 6). The latter phase is also related with similar deposits that form clear ridges upvalley between 1100 and 1350 m a.s.l. (Hughes et al., 2006c).

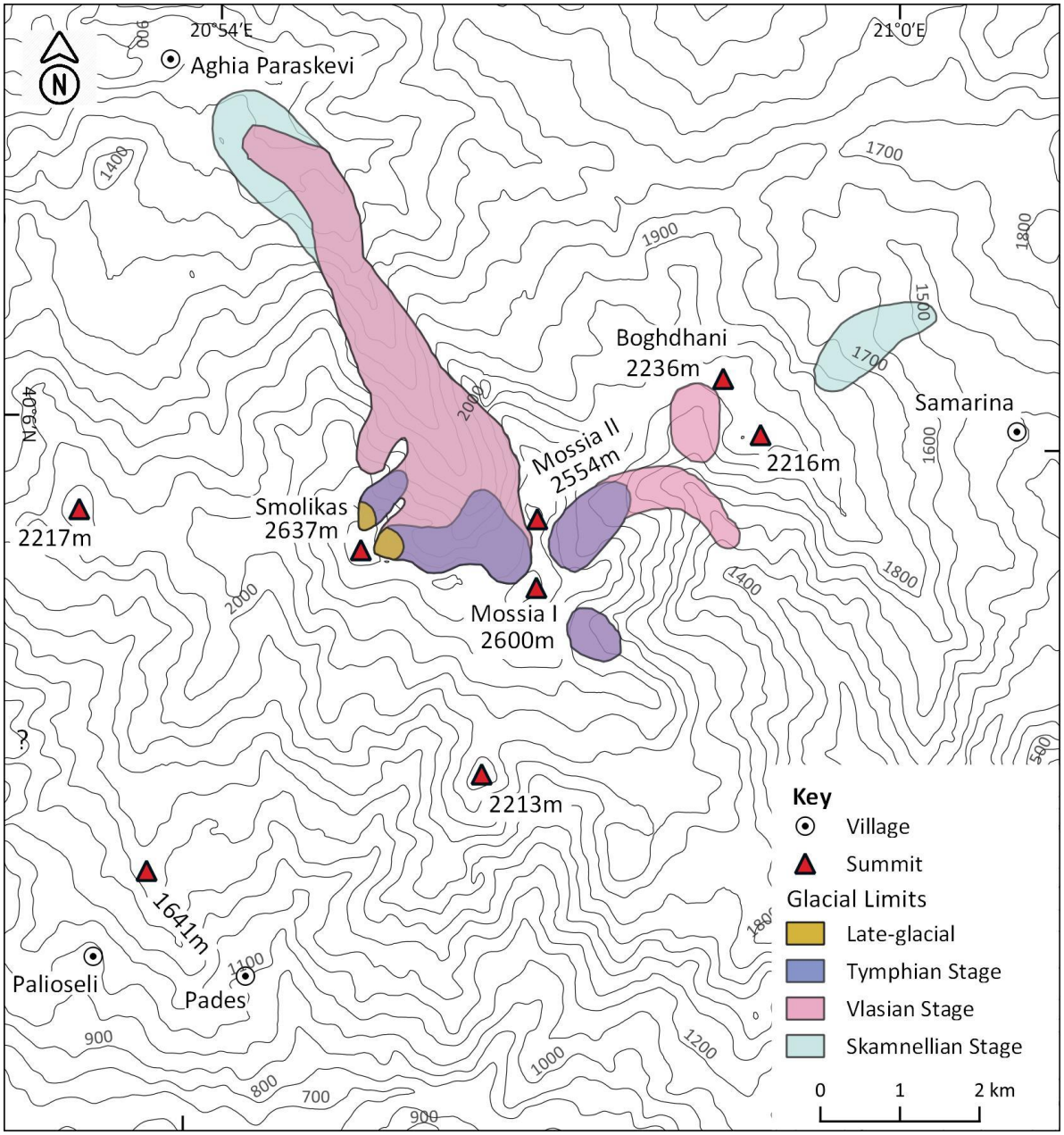

Figure 13. Glacial extent during the different Stages of the Pindus Chronostratigraphy on Mt Smolikas according to so far published studies (adapted from Leontaritis et al., 2020 – map composition based on Hughes et al., 2007)

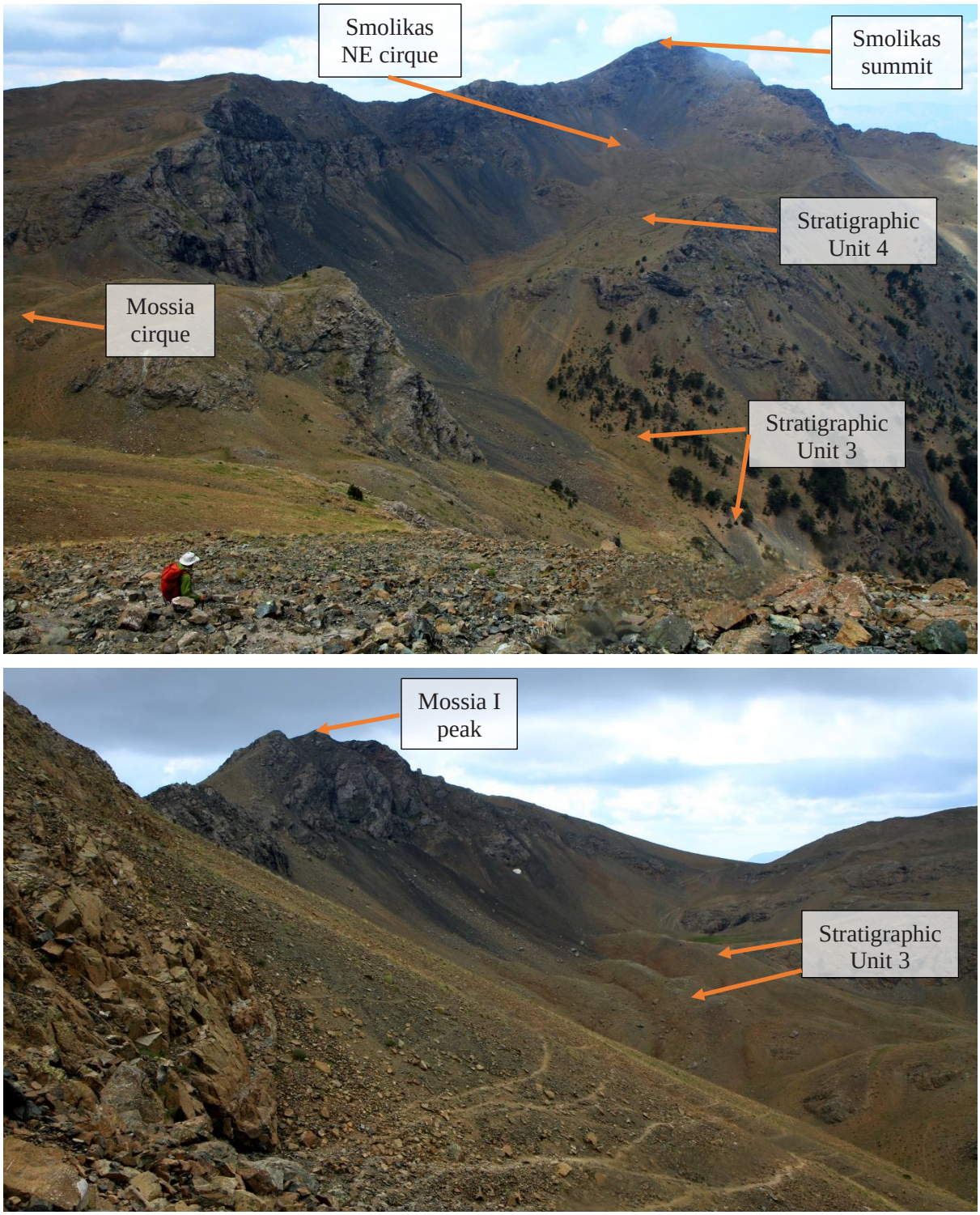

Figure 14. ***Up:*** *the impressive NE cirque below the summit of Mt Smolikas (2637 m a.s.l.) and the upper western branch of the ice-scoured Vathylakos valley. Two distinct morphostratigraphic groups have been identified here (3 and 4) which have been correlated to glacial activity around the LGM and the Late-glacial/Younger Dryas respectively (Hughes et al., 2006c). The eastern branch of the valley can be seen in the left side of the picture and is headed by the Mossia cirque.* ***Bottom:*** *the deposits within the Mossia cirque below the homonymous peaks Mossia I & II have been ascribed to morphostratigraphic unit 3 which are attributed to morphostratigraphic unit 3 and glacial activity around the LGM by Hughes et al. (2006c). (Photos: August 2019)*

Elsewhere on Mt Smolikas, the glacial sequence is fragmentary due to the high erosion and numerous landslides of the ophiolitic bedrock. Therefore, morphostratigraphic correlations of low to mid altitude deposits that could be Middle Pleistocene in age is difficult to establish. Moreover, it was originally assumed, that there are no glacial erosional or depositional features on the southern slopes of Mt Smolikas (Hughes, 2004; Hughes et al., 2006c). This was based on the lack of obvious cirques or troughs in topographic maps and the mapping of Hughes (2004, 2006c) generally agreed with the earlier observations of Boenzi et al. (1992).

The next two groups of moraines in the Vathylakos valley (Figure 13 and Figure 14) occur at 2000 to 2150 m a.s.l. (Unit 3 – mean ELA of 2241 m a.s.l; Hughes, 2004) and 2300-2400 m a.s.l. (Unit 4 –mean ELA of 2372 m a.s.l.; Hughes, 2004). These two suites of moraines are separated by hummocky moraines and perched boulders that were most probably deposited upon glacial retreat. Unit 3 deposits have been correlated with the Tymphian Stage on Mt Tymphi (MIS 5d – MIS 2) and probably predate the LGM (Hughes et al., 2006c). Moreoever, under the light of the latest ^{36}Cl chronology from Tymphian Stage moraines on Mt Tymphi (Allard et al., 2020; see also section 3.1.1.2) this morphostratigraphic group could be more precisely ascribed to glacial activity close to the LGM between 29.0 and 25.7 ka. Apart from the Vathylakos valley, glacier deposits within the Mossia cirques (Figure 14; 2150-2200 m a.s.l.) below the summits of Mossia I&II (2600 m a.s.l. and 2554 m a.s.l. respectively) were also ascribed to morphostratigraphic Unit 3 based on their altitude and morphostratigraphic position (Hughes et al., 2006c).

Arguably, some of the most interesting features on Mt Smolikas are the high-altitude glacial deposits of morphostratigraphic Unit 4. These glacial landforms exceed in altitude the floors of the highest cirques on Mt Tymphi by 200 m and therefore could postdate the youngest moraines on Mount Tymphi (24.5 ka – Allard et al., 2020). It has been argued that they could have been formed after the local Late Pleistocene glacier maximum and the last cold stage - during the Late-glacial (17.5-11.7 ka; Rasmussen et al., 2006; 2014) - and in particular that they might be Younger Dryas in age (Hughes, 2004; Hughes et al., 2006c). This argument is well supported by more recent findings on Mt Olympus and Mt Chelmos (see next sections) but still needs to be confirmed by cosmogenic exposure dating. Historical satellite imagery from late summer (September) appears to confirm that there are no permanent snowfields on Smolikas, unlike on Mount Olympus (Hughes, 2018). Based on this evidence and snow melt modelling, Hughes (2018) argued that pronival ramparts that are present against the north-facing cliffs of Smolikas are also likely to be Late-glacial in age with no glacial or nival features

dating to the Holocene. Again, this hypothesis requires further testing using cosmogenic exposure dating.

3.1.3 New evidence from Mt Smolikas

The new evidence from Mt Smolikas that is presented here regards some diamicton sediments that are interpreted as sub-glacial till and moraines both in the southern and northern slopes of the mountain.

3.1.3.1 Northern Slopes

The evidence considering the northern slopes regards the identification of terminal and lateral moraines in the Mesopotamos and the Koutsoura valleys, that are located to the west and parallelly to the Vathylakos valley (Figure 15).

Koutsoura valley

The evidence in the Koutsoura valley (Figure 15) regards some terminolateral moraines at 1100 m a.s.l. which are characterised by some very thick accumulations of proglacial till (>40m) (Figure 16a). These deposits have been incised by the Koutsoura stream which divides them into two sections, revealing good exposures of the deposits (Figure 16b). The key characteristic of these moraines is that their lithology is ophiolitic. In terms of composition, this till unit is very similar to the Vathylakos lower undeformed till unit described by Hughes et al. (2006e; see also section 3.1.2) that has been ascribed to MIS 12. The clasts within the diamicton deposits are sub-rounded and striated and range in size between gravels and massive boulders >80 cm in diameter. These clasts are supported by a sandy to muddy matrix. However, an important remark is that in contrast to the Vathylakos lateral moraines ascribed to MIS 12 which are unconsolidated, these deposits are lithified in places (Figure 16c). This could indicate that they are older in age compared to the ones in Vathylakos.

These deposits were considered as the lowermost depositional limit of Skamnellian Stage (MIS 12) glaciers originating from the Vathylakos valley (Hughes 2004; Hughes et al., 2006c). An alternative interpretation could also be possible though. These till sediments could be ascribed to a previous glacial interval if it is proved that they are stratigraphically older than the MIS 12 deposits as indicated by their partial lithification. However, as the Vathyakos formation deposits are partly nested into the deposits of the Koutsoura valley formation they are difficult to be distinguished from their morphology and a detailed sedimentological analysis is required. In any case, under the lack of further evidence and a detailed study of these deposits

the adaptation of such an assumption would be speculative. Therefore, the approach of Hughes at al. 2006c has been followed regarding the ascription of both the lower undeformed unit in the Vathylakos valley and the deposits in the Koutsoura valley in the same morphostratigraphic unit and its correlation with Skamnellian Stage (MIS 12) in Mt Tymphi. The respective ice limits according to the new mapping of the Koutsoura and Vathylakos deposits are depicted in Figure 15.

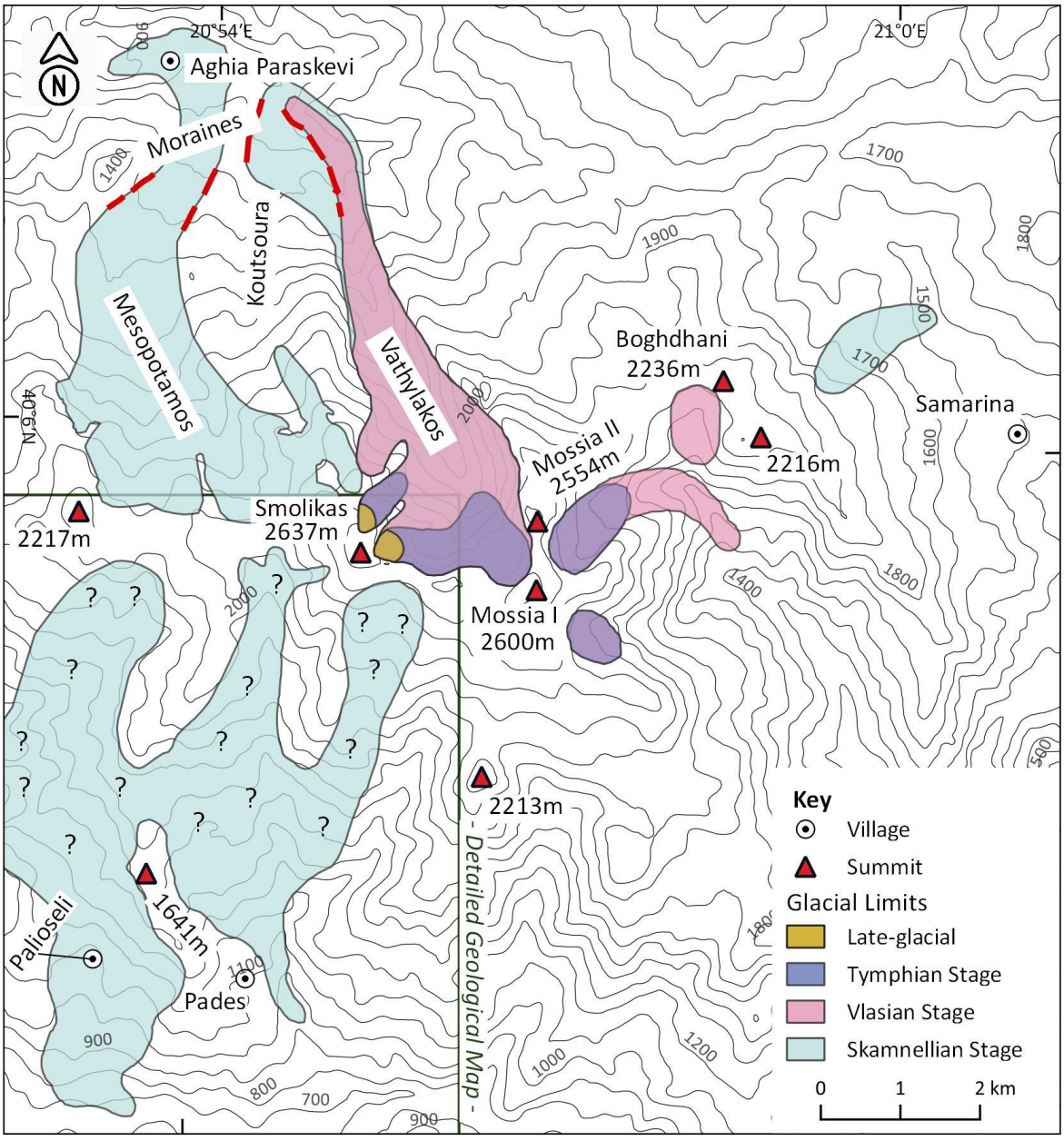

Figure 15. Glacial Stages and updated glacier extent according to new evidence on Mt Smolikas. While the identified till units indicate the lower glacial limits, the ice configuration depicted here represents only an approximate logical assumption according to local geomorphology. Moraine ridges on the northern slopes are denoted with red dashed lines whereas the detailed geological map tile along with the mapped till units on the southern slopes of the massif are shown in Figure 20. (Modified from Hughes et al., 2017)

Figure 16. ***a) (Top)****: Looking west towards the western part of the deposits (~40 m tall) from a track bisecting the eastern section of the deposits in the Koutsoura valley. Notice the person on the track for scale,* ***b) (Middle)****: trackside exposure at the same point and* ***c) (Bottom):*** *lithified till within the eroded inner flank of the western section of the deposits (Photos: August 2019)*

Mesopotamos valley

The lithology of the upper Mesopotamos valley (above 1600 m a.sl.) is dominated by ophiolites while in lower elevations the bedrock is mainly composed of flysch. Most importantly, there are several outcrops of Jurassic limestone along the lower part of the valley (IGME, 1987) and this is reflected in the lithology of the moraines that have been identified in this valley (Figure 15; Figure 17).

*Figure 17. The eastern **(top)** and western **(bottom)** moraine ridges in the Mesopotamos valley are characterized by limestone clasts and boulders (see Figure 15 for location). Ophiolite-derived sediments are limited to smaller clasts and to the fine material of the matrix supporting the deposits. The moraine has been deposited on Flysch bedrock (Photos: August 2019).*

Apart from their rich content in ophiolite-derived sediments similarly to the moraines in Vathylakos and Koutsoura valley, these moraines are characterised by the presence of limestone clasts and large (>1.5 and up to 4 m in diameter), glacially transported boulders within their deposits as well as on the valley floor between the two moraines (Figure 17).

These two moraines are much more restricted in height compared with the moraines in Vathylakos and Koutsoura valleys that exceed 30m and this could be attributed to the much larger width of the Mesopotamos valley that probably resulted in a considerably thinner glacier compared to the Vathylakos valley glacier. The composition of the deposits is similar to the subglacial till unit in the southern slopes of Mt Smolikas that is described in the next section. They are characterized by clast-rich lithology with sandy to muddy matrix. The fine-grained material is mainly ophiolite-derived and is unconsolidated. The clasts on the other hand are subrounded and striated and their lithology ranges from ophiolite to limestone, with the ophiolitic clasts and boulders being much smaller in size compared to limestone ones. It should be noted that although it is here argued that these sediments are glacial in origin as it has been, in the geological sheets of IGME (1987) the whole valley between 1600 and 800m a.s.l. is marked as a land-sliding area.

Figure 18. Glacially transported limestone boulder in the village of Aghia Paraskevi. The village is built on till composed of ophiolite and limestone-derived sediments from the uplands of Mt Smolikas whereas the bedrock of the area around the village is dominated by flysch.
(Photo: August 2019)

The down-valley depositional limits of this unit have been recorded at 850 m a.s.l. below the village of Agia Paraskevi (Figure 15) that is actually built upon glacial deposits between 900 and 1000 m a.s.l. (Figure 18). This till formation must have been deposited by the Koutsoura valley glacier originating from the upper northern slopes of the mountain. The watershed could be the upper limit but an ice-cap configuration should not be excluded. It should be mentioned that although there are no cirques or glacially steepened headwalls present, there is plenty of glacial evidence such as glacial boulders and fragmentary morainic deposits along the upper valley. A similar lack of ice-steepened headwalls of formerly glaciated valleys has also been observed in the nearby, also ophiolitic, Mt Mavrovouni (Chapter 4).

3.1.3.2 Southern Slopes

The road connecting the villages of Vrysochori and Palioseli traverses the northern bank of the Aoos Gorge on the lowermost slopes of Mt Smolikas exposing good sections of diamicton sediments at an altitude range between 650m to 1050m (Figure 19 and Figure 20). Similar deposits were also observed near the village of Palioseli at 1140m and it is most probable that these are of glacial origin. These sediments are characterized by clast-rich lithology with sandy to muddy matrix (Figure 19a). The fine-grained material is mainly ophiolite-derived and is unconsolidated, resembling the matrix of the Vathylakos and the Mesopotamos till/moraine formations that are mentioned above. The clasts are subrounded and striated and their lithology ranges from ophiolite to limestone. The ophiolitic clasts and boulders are much smaller in size compared to limestone probably due to the several cracks and joints present in the parent bedrock. This sediment unit lies on flysch (Figure 19b).

As it can be seen in the geological map of the region (Figure 20), ophiolite within the studied basin occurs at higher altitudes (1400-2100 m a.sl.) while limestone mainly appears in the 1350-1500 m a.s.l. altitude zone. Therefore, the ophiolite-derived sediments must have been transported a further distance down-valley compared with the limestone material, although both lithologies represent erratic material since they are lying on top of flysch bedrock in the lower valley areas. Taking also into account the composition of the sediments, gravitational or fluvial deposition could be excluded, implying a glacial origin. In particular, these sediments might be subglacial till from a glacier originating from the above slopes. However, it should be noted that neither a cirque nor a typically deepened ice-scoured glacial valley is present above these deposits. Therefore, while this till unit indicates the lower glacial limits, the ice configuration depicted in Figure 15 represents only an approximate logical assumption according to local geomorphology and the position of the lower glacial deposits.

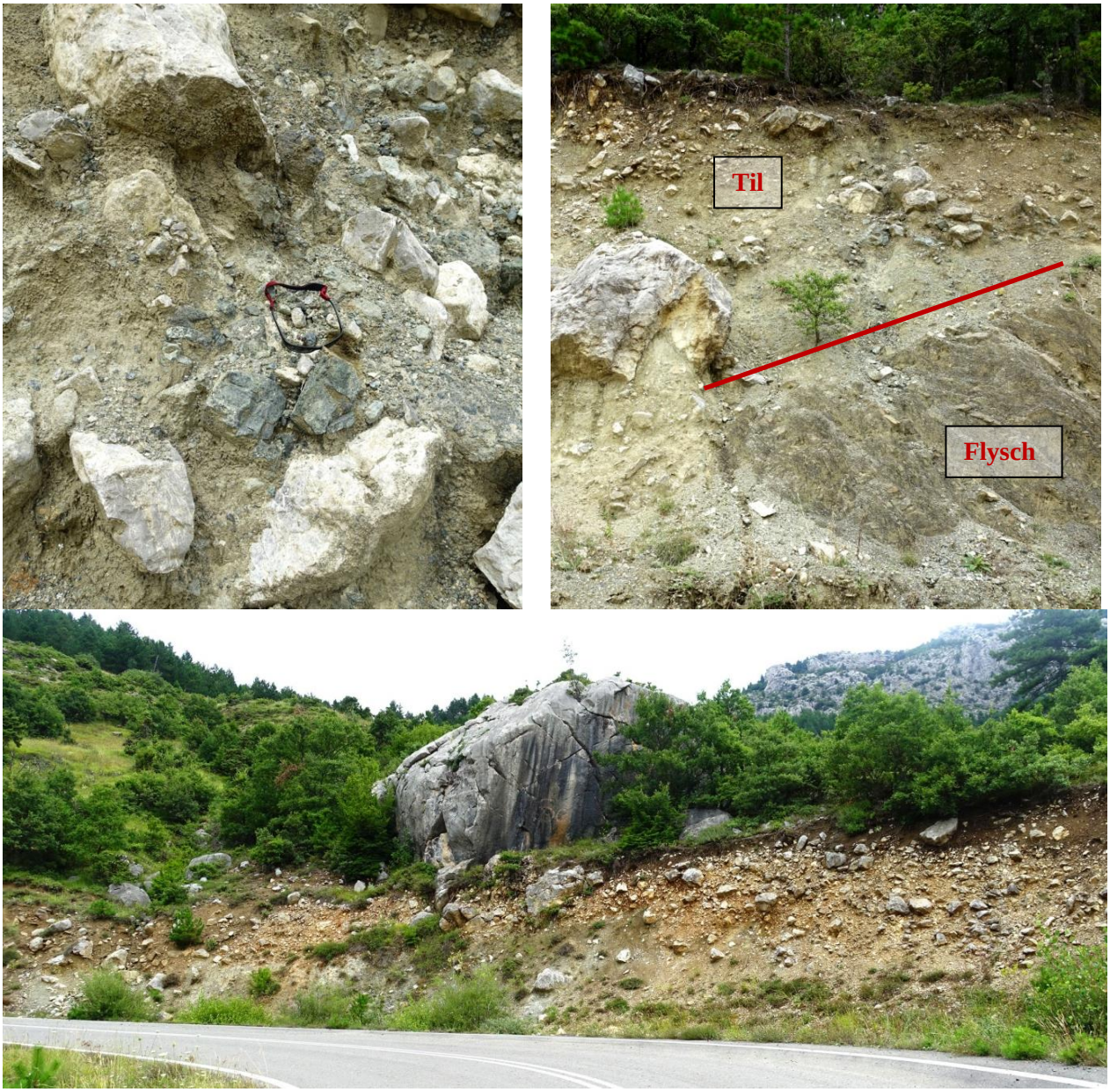

Figure 19. Road-side exposure of till sediments on the lowermost southern slopes of Mt Smolikas: ***a) (Top left)****: note the sand and mud rich matrix and the mixed limestone/ophiolite subrounded clasts - sunglasses for scale****; b) (Top right)****: the limestone/ophiolite diamicton deposits derived from higher altitudes have been thrusted over the underlying flysch bedrock;* ***c) (Bottom)****: a massive erratic boulder (Photos: July 2017).*

Another till unit is reported on the local geological sheet of the Greek Institute for Geological and Mineral Exploitation (IGME, 1987) above the village of Pades which can be attributed to the same glacial phase (Figure 20). In the geological map of IGME (1987) the deposits are mapped with the symbol for glacial deposits but labelled on the same geological map by the code for terraces of carbonate debris, which is inconsistent with local geomorphology and lithology. These deposits are also mapped as scree in Hughes (2004) following the IGME Geological Sheet.

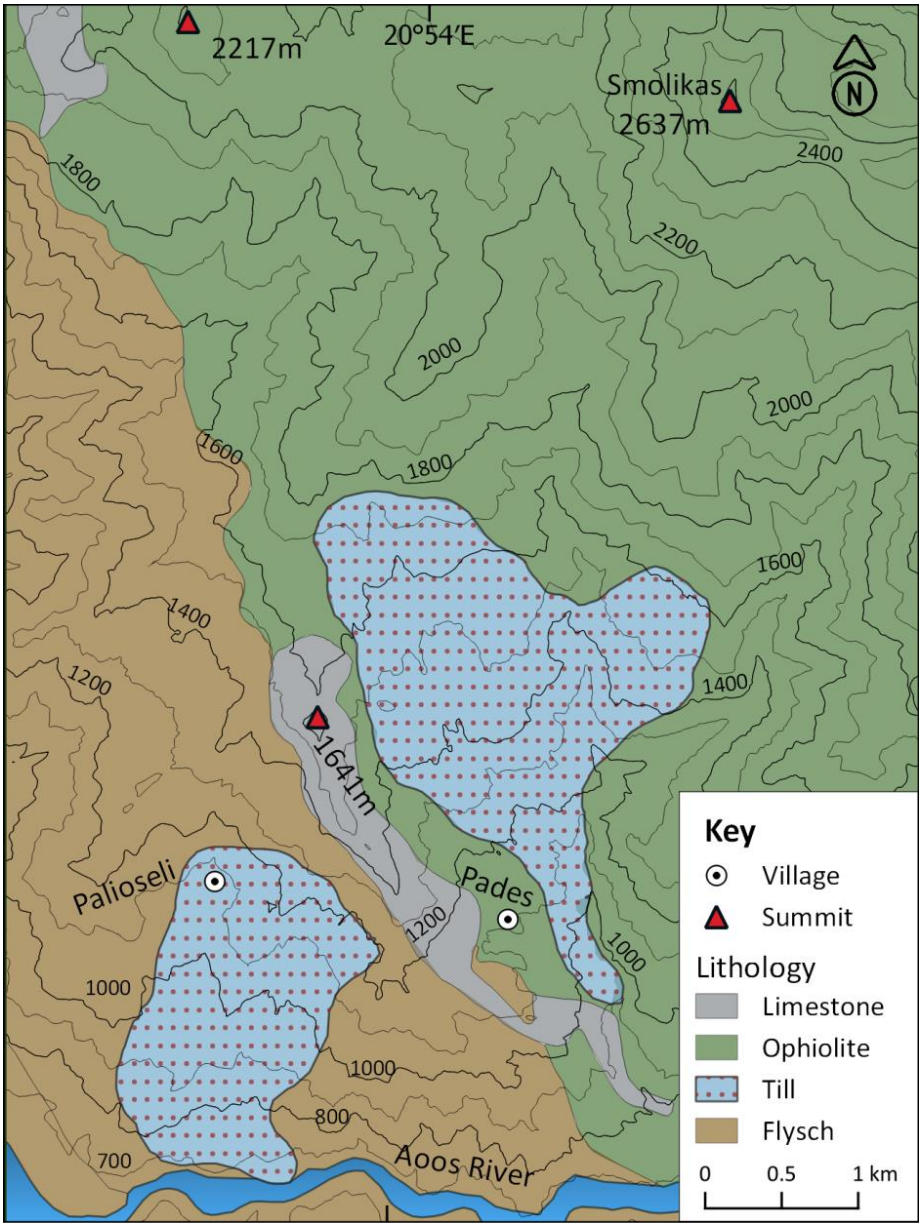

Figure 20. Detailed geological map of the southern slopes of Mt Smolikas within the Palioseli/Pades region on southern Mt Smolikas where new glacial evidence has been identified. Till units drawn upon new evidence and the local 1:50,000 geological sheet of IGME (1987). The Lithology has been based on the same geological sheet. See text for further details.

However as new evidence indicates, these deposits are indeed diamicton deposits of glacial origin and are similar in sedimentological composition to those described above (e.g.) and are therefore interpreted here as subglacial till. In particular these sediments are ophiolite-derived and are characterized by clast-rich lithology and unsorted gravels supported by a sandy matrix which remains unlithified (Figure 21). The clasts are striated and subrounded and vary in sizes with the bigger boulders exceeding 50 cm in diameter. Similar exposures can be found throughout this area and are generally in agreement with the limits of the unit denoted in the IGME geological sheet (1:50:000; IGME, 1987).

Figure 21. ***a) (Top)****: Roadside exposure of diamicton deposits within the village of Pades at an altitude of 1160 m a.s.l.;* ***b) (Bottom)****: detail of the same till exposure (Photos: January 2020)*

It should be noted that in this case the valley above these deposits is headed by the ice-steepened NW flanks and semi-developed cirques below the Smolikas summit at 2637 m a.s.l. However, the valley has undergone significant erosion and its lower parts are V-shaped making it difficult to distinguish their glacial origin as well as the glacier limits within the valley. Therefore, the glacier configuration depicted in Figure 15, is an approximation based on local geomorphology and the position of the identified till unit.

3.1.3.3 Conclusions and interpretation of new evidence

The lack of typical glacial geomorphology (i.e. ice-scoured deepened valleys headed by ice-steepened cirques) in the upper parts of some of the glaciated valleys described above has so far led researchers (e.g. Boenzi et al., 1992; Hughes, 2004; Hughes et al. 2006c; 2007) to identify with caution the glacial deposits on Mt Smolikas. This tactic is safe from a scientific point of view but the conservative approach in this case proved to result in underestimating the limits of former glacial extent on the massif. Nevertheless, in the nearby ophiolitic Mt Mavrovouni (2157 m a.s.l.), moraines and other glacial deposits have been recorded in down-valley positions whereas no glacial cirques or ice-steepened slopes are present at the head of the valleys (see Chapter 4). At the same time, ophiolite-derived till is prone to post-depositional fluvial erosion and other mass wasting processes and therefore it is not so often well-preserved.

Moreover, on neighbouring Mt Tymphi some areas also display sedimentary evidence of glaciation in lower valley areas but no cirque forms in upper areas (Hughes et al 2007a). This is the case on the slopes of the Astraka peak (Figure 6) where a Skamnellian Stage plateau ice-field occupied the area to the south of Astraka, forming moraines in lower valleys but no cirques in the upper valley areas (Hughes et al., 2006a). A similar situation may be envisaged for Smolikas with a plateau ice-field or ice cap emanating, producing valley glaciers but no cirques. This may also be compounded by the fact that cirques tend to be more weakly developed in ophilolite terrains, whereas cirques in limestone areas are deeper, longer and more enclosed (Hughes et al., 2007).

In terms of altitude, this phase of glacial activity could be correlated with the Skamnellian Stage (MIS 12) in Mt Tymphi (Table 4) on the basis of altitude and morphostratigraphic position, while the till units can be interpreted as the lower limits of the most extensive Middle Pleistocene glaciers. However, the absence of distinct glacial or periglacial features in the slopes above the two till units makes it very difficult at this point to establish the exact glacial limits. In Figure 15, the drawn glacial extent depicts just an approximate assumption of what could be a logical ice configuration that deposited the identified till units. Further evidence is needed in order to confirm the observations presented here as well as to explore further evidence in other valleys -especially in the eastern part of the massif where the glacial sequence is fragmentary (see Figure 13) - and eventually clear out the ice limits on Mt Smolikas. It should be noted that a plateau ice field with valley glaciers radiating from a central ice dome centered over the tallest peaks of the massif cannot be excluded.

In any case, a significant conclusion based on the new sedimentological observations is that glaciers on Mt Smolikas also formed on its southern slopes and not only on its northern slopes as it was up to now believed. This implies that as was the case on nearby Mt Tymphi, slope orientation does not seem to have played a significant role on the formation of glaciers during the most extensive Middle Pleistocene glacial phase. Therefore, these findings reveeal new perspectives on the study of glacial history of Mt Smolikas and north Pindos in general and open up the possibility that plateau ice fields dominated the palaeoglacier geometry of the most extensive glacial phases, such as during the Skamnellian Stage, resulting in outlet glaciers forming on all slope orientations.

3.2 Mt Olympus (north Greece)

Mount Olympus is the highest mountain of Greece and the second highest of the Balkan peninsula reaching an elevation of 2918 m a.s.l. It is located in north Greece just 18 km west of the Aegean Sea shoreline and comprises a relatively small (surface area: 550 km2,) and isolated massif separated from adjacent lower mountains by shallow topographic depressions (Styllas et al., 2016). The lithology of the massif is characterized by a metamorphosed and deformed sequence of limestones of Triassic and Cretaceous to early Tertiary age, overlain by a late Eocene flysch. High Pleistocene uplift rates up to 1.6 mm/yr have been reported (Nance, 2010). In the higher part of the mountain lies an extensive limestone plateau between 2200 and 2700 m a.s.l. surrounded by several peaks (Smith et al., 1997). Evidence of former glaciation is abundant: clearly shaped cirques and morainic deposits can be found at the head of its deep valleys both above and below the plateau. This glacial evidence was identified and reported in the first pioneering studies of the mountain (Cvijić, 1917; Wiche, 1956; Messerli, 1967; Faugeres, 1969).

The first detailed field mapping on Mount Olympus and the surrounding piedmont zone was carried out by Smith et al. (1997). In this study they identified evidence of former extensive ice caps on the high-altitude plateaus of Mt Olympus as well as glacial deposits within a number of glacially scoured valleys headed by typical glacial cirques (Figure 22). Three discrete sedimentary packages (units 1–3) related to glacial activity in the uplands have been identified in the area—each capped by a distinctive soil. The maximum glaciation was characterised by an upland ice cap, extensive valley glaciation and piedmont lobes in the surrounding lowlands. A second glaciation involved the development of upland ice and valley glaciers that did not reach the piedmont. A third, and most recent, glaciation was restricted to valley heads and glaciers that extended to mid-valley positions.

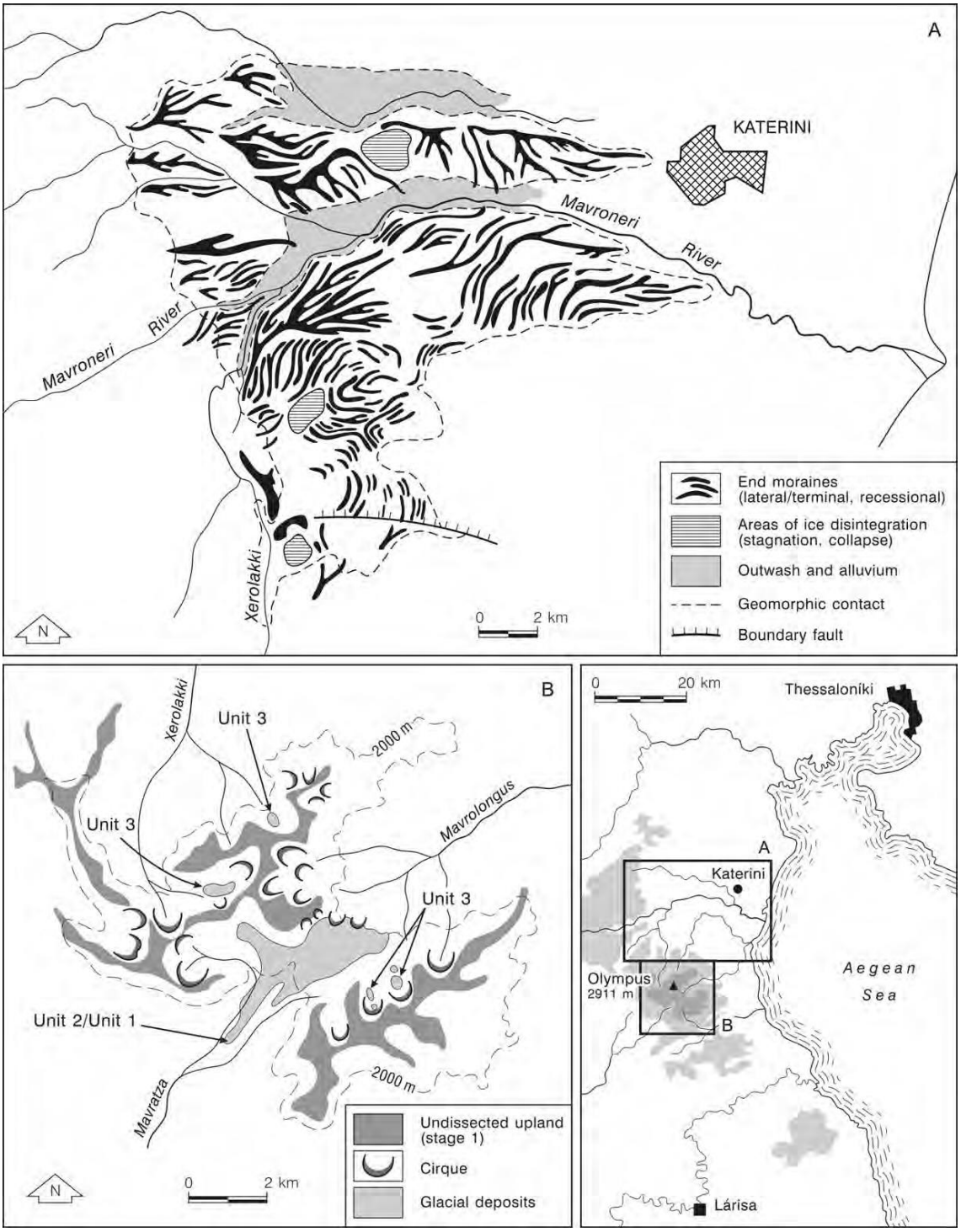

Figure 22. Geomorphological maps of the glaciated uplands of Mount Olympus in northeast Greece showing the landscape near the town of Katerini (A) and the cirques and glacial deposits of the Bara plateau close to the summit (B) (from Woodward and Hughes, 2011 - based on the maps of Smith et al., 1997).

The lack of radiometric data directed Smith et al. (1997) towards a tentative correlation model for the timing of glacial phases based on the weathering of the soil profiles on those three sedimentary units. The quantification of weathering using pedogenic maturity indices

(PDI) after Harden (1982) allowed for the correlation with a poorly dated - for modern standards - sequence of alluvial sediments in the nearby Larisa Basin by Demitrack (1986). In short, this index is used to quantitatively measure the degree of soil profile development taking as well into account its weathering degree. The correlation of these sediments placed unit 1 before 200ka (interpreted as deposition within MIS 8), and unit 2 within MIS 6 (Table 5). The sediments of unit 3, representing the last major glaciation of the massif which was restricted to valley heads, were placed within MIS4 to MIS2 (Smith et al., 1997).

Table 5. Comparison of PDIs of sedimentary units and respective age model for Mt Olympus (tentative age model and PDIs after Smith et al. 1997) and Mt Tymphi (U-series ages and PDIs after Hughes et al., 2006a)

Mt Olympus			Mt Tymphi		
Sedimentary Unit	PDI	Age	Glacial Stage	Age	PDI
3	5-13.2	MIS8	Tymphian Stage (Unit 3)	MIS 5d – MIS 2	7.8 - 9
2	38	MIS6	Vlasian Stage (Unit 2)	MIS 6	29 - 38.3
1	50.8 -81.7	MIS4-2	Skamnellian Stage (Unit 1)	MIS12	51.8 - 61

However, even though these ages are generally in agreement with the dated glacial deposits in other mountains, this archive should be viewed with caution in terms of reliability for regional correlation and comparisons due to both the poor chronological control of the Larisa basin alluvial sequence and the difficulties of making valid comparisons of soil profile development when sites are located at different altitudes in contrasting geomorphological settings (Woodward and Hughes, 2011). Moreover, comparison of ELAs elsewhere in Greece with those reconstructed for Mount Olympus is difficult since ELA reconstructions presented in Smith et al. (1997) are very unclear and contradictory (Hughes, 2004).

The PDIs obtained from soils developed on glacial deposits on Mt Tymphi (Hughes et al., 2006a) and Mt Olympus (Smith et al. 1997) are in any case comparable, since they have been scored with the same methods of Harden (1982) and at the same time it is likely that soils in these two areas have undergone similar rates and styles of weathering given the similar geology and relatively short distance between the sites (Hughes, 2004). In this perspective, it should be noted that the oldest deposits on Mt Olympus (Unit 1) have deeply weathered soil profiles with profile development indices (PDIs) in the range of 50.8 to 81.7 (Smith et al. 1997) and compare with values between 51.8 to 61 obtained for soils developed on the oldest glacial deposits on Mount Tymphi (Table 5). Similarly, for unit 2 and unit 3 deposits, the scored PDIs of 38.0 and

5-13.2 respectively compare with the respective values of PDIs obtained for soils developed on Vlasian Stage (29-38.3) and Tymphian Stage glacial deposits (7.8-0) on Mt Tymphi.

Therefore, the oldest and most extensive deposits (unit 1) could rather safely be correlated to the Middle Pleistocene stages of the well dated chronostratigraphy of the Pindus mountains in north-western Greece (see section 3.1.1). In particular they could be related with the oldest and most extensive Skamnellian Stage (MIS 12) although such a claim should be done with caution. Similarly, unit 3 deposits can be correlated with the Tymphian Stage of the Pindus Chronostratigraphy as suggested also by the latest study on Mt Olympus by Styllas et al. (2018), which is presented in detail next. The geomorphological context of Unit 2 deposits though is rather blurry so it would be quite risky to attempt a correlation based on PDIs only.

What is notable about the most extensive phase of glaciation that correspond to unit 1 deposits is that according to the work of Smith et al. (1997) glaciers formed piedmont lobes that extended as low as 100 m a.s.l.. This was a radical revision of the early work of Faugères (1969) and Messerli (1967) where it was concluded that glaciers on Mount Olympus did not descend to altitudes lower than 1600 m a.s.l. Faugeres (1967) interpreted most of the lowest piedmont deposits as fluvial deposits and alluvial fans. Hughes (2004) argued that whilst there is evidence of glaciation as low as 850 m a.s.l. on Mount Tymphi (Woodward et al. 2004), nowhere in Greece are glacial deposits recorded as low as argued by Smith et al. (1997) for Mount Olympus. Moreover, the interpretations by Smith et al. (1997) were contradictory to the recorded extent of glaciation in the Pindus Mountains to the west which back in 2004 was the best studied glacial sequence in the Mediterranean. On these grounds, the interpretations of Smith et al. (1997) were disregarded as not plausible and the question of Middle Pleistocene glaciation extent on Mt Olympus has since remained open.

Recent observations by the author seem to reopen this research questions. As stated at the beginning of this chapter, these observations are not part of systematic research and are rather included in this thesis as supplementary material that could help future glacial research in the mountains of Greece. Diamicton deposits that could be interpreted as glacial in origin (till) have been identified right at the outlet of the Ourlias river at an altitude of 260 m a.s.l. on the eastern piedmont of the massif and ~14 km SW of Katerini (Figure 22). These deposits can be seen in Figure 23 and Figure 24. It should be noted that the diamicton deposits depicted in Figure 24 sit on top of a partly lithified and stratified sedimentary unit that could possibly be of fluvial/glaciofluvial origin. This unit has been deeply incised by later fluvial activity revealing a sedimentary unit with what could be described as a complex sedimentation history.

Exposures of similar sedimentary units can be found near the outlets of many valleys in the east/northeast piedmont of the mountain. Systematic research is in any case needed in order to proceed with meaningful interpretations of such complex sedimentary units.

Figure 23. Diamicton deposits dominated by rounded and sub-rounded limestone boulders and supported by a sand matrix, forming an obvious unconformity with the underlying bedrock. Road-side exposure near the outlet of the Ourlias stream and the homonymous canyon at the eastern piedmont of Mt Olympus. These deposits can be interpreted as till (Photo: August 2019)

Figure 24. Diamicton deposits on top of very thick (up to 40 m) accumulation of partly lithified and stratified sedimentary unit of fluvial/glaciofluvial origin (?) at the outlet of the Ourlias stream and the homonymous canyon (northern bank) at the eastern piedmont of Mt Olympus (Photo: August 2019)

Figure 25. The uplands of Mt Olympus bare traces of very extended glaciations in the past. Here are depicted two aspects of the ice polished and scoured NE flanks of the Rema Naoum valley that also drains the Megala Kazania cirque (Figure 26, Figure 27). The whole area seems to have been covered by an extensive ice cap rather than by glaciers confined within the boundaries of certain valleys. The orange dot has been placed as a point of reference between the two pictures. Notice that even though this rocky elevation is well above the valley floor, it is clearly scoured and polished by ice indicating that this former ice cap was several hundred meters thick (Photos: September 2020).

It could be stated that the above-mentioned deposits are far too low in altitude (260 m a.s.l.) compared with the Skamnellian Stage deposits on Mt Tymphi that only came down to an altitude of 700 m a.s.l. (see section 3.1.1). However, the valleys were glaciers formed on Mt Tymphi are headed by peaks that hardly exceed 2400 m in altitude whereas on Mt Olympus there are several peaks that exceed 2800 m. Moreover, Mt Olympus has at least two high altitude plateaus at about 2600 m (Muses and Bara plateaus) that could effectively increase the snow accumulation and formation of ice. This is also obvious on the present geomorphology of the uplands of Mt Olympus that bares traces of very extensive past glaciations (Figure 25).

3.2.1 Advanced studies on Mt Olympus

The first radiometric data came soon after the study of Smith et al. (1997) by Manz (1998) who tried to improve the age control of the glacial deposits by dating boulder surfaces from the lower units applying the cosmogenic ^{36}Cl exposure dating method. This was one of the earliest attempts to apply cosmogenic exposure dating in the Mediterranean. The sampled boulders yielded ages ranging from 32 to 56 ka that appear to disagree with the findings from Northern Greece and Montenegro, which suggest that the most extensive glaciation phase took place during Middle Pleistone (Skamnellian Stage/MIS 12 and Vlasian Stage/MIS 6 - Hughes et al., 2006a, 2010, 2011). However, the geomorphological context of the boulders sampled by Manz (1998) is unclear and similar ages have been found from moraines on Mount Chelmos (Pope et al., 2017) where it has been argued that these deposits identify with a phase of glaciation belonging to MIS 3. The absence of a reliable and internally consistent chronology for the Mount Olympus glacial record presented in these first studies limited its value as a basis for information retrieval in the palaeoclimatic context and prevented accurate correlations with other sites (Woodward and Hughes, 2011; Hughes and Woodward, 2017; Pavlopoulos et al., 2018).

Interestingly, study of Styllas et al. (2018) on Mt Olympus brought up new evidence supporting several glaciation episodes during the Late-glacial and Holocene. In particular, a chronology of glacial phases of Mt Olympus was proposed based on cosmogenic ^{36}Cl exposure dating of moraine boulders. Samples were taken from boulders within two high altitude cirques just below Olympus' highest peaks: the northeast facing and steeply inclined Throne of Zeus (TZ) cirque at 2580 m a.s.l. and the deeper, longer and more enclosed northwest oriented Megala Kazania (MK) cirque at 2200 m a.s.l. (Figure 26, Figure 27). Notably, the chronological order of the obtained ages is in good agreement with the stratigraphy of glacial landforms (Styllas et al., 2018).

A first phase (LG1) of glacial advance/stabilization is recorded in both cirques at 15.6 ± 2.0 -14.2 ± 1.0 ka [revised timing after Leontaritis et al. (2020) based on Styllas et al. (2018)]. These glaciers started retreating by 14.09 ± 1.74 ka (Styllas et al., 2018) as dating of exposed bedrock within one of the dated moraines in the TZ cirque indicated. This phase tentatively correlates with the Oldest Dryas (17.5-14.7 ka; Rasmussen et al., 2006) and is characterized by cold and arid climate (Styllas et al., 2018). A set of clearly shaped moraines (MK-A) was mapped in the MK cirque below the LG-1 moraine complexes at an altitude of 2150 m a.s.l. and was ascribed to a glacial advance phase predating LG-1 and presumably near or before the LGM. Since this study was focused on the Late-glacial to Holocene glaciations this moraine was not sampled. However, this morphostratigraphic unit can be correlated with Unit 1 deposits of Smith et al. (1997) and the Tymphian Stage of the Pindus Chronostratigraphy (Leontaritis et al., 2020) as also shown in Table 5. A second glacial phase (LG2) was attributed to 13.2 ± 2.0 - 13.5 ± 2.3 ka, taking the mean of moraine boulders ages ranging from 14.6 to 12.5 ka . However, considering that taking a mean of scattered ages is not the best choice (Ivy-Ochs et al., 2007) and combined with the lack of any other evidence from palaeoclimate proxies or other glacial studies in the western Balkans for this period, Leontaritis et al. (2020) did not consider this phase and instead suggested that the respective boulder ages are attributed to LG1 and LG3 phases (Table 6). The LG3, was characterized as a glacial retreat phase at 12.6 ± 1.6 - 12.0 ± 1.5 ka and is tentatively correlated to the Younger Dryas (12.9-11.7 ka ; Rasmussen et al., 2014) under cold and dry climatic conditions (Styllas et al., 2018).

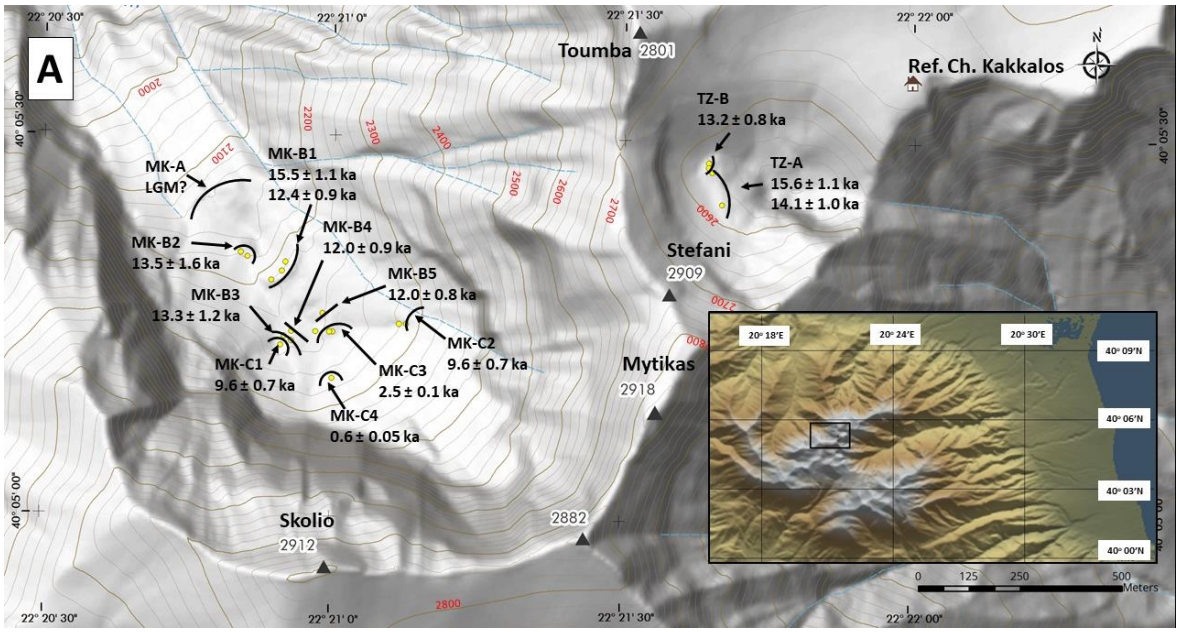

Figure 26. Mean cosmogenic ^{36}Cl surface exposure ages of moraines in the Megala Kazania (MK) and Throne of Zeus (TZ) cirques on Mt Olympus (from Styllas et al., 2018).

As regards the Holocene, three distinct phases were recorded within the MK cirque. The first phase of glacial stagnation or re-advance is placed at 9.6 ± 1.2 ka (HOL1) is strongly supported by identical ages of boulders coming from distinct moraines of the same morphostratigraphic order while the second phase is placed at 2.6 ± 0.3 - 2.3 ± 0.3 ka (HOL2). Finally, the most recent glacier advance (HOL3) is dated to 0.64 ± 0.08 ka, at the beginning of the Little Ice Age, constrained by only one dated sample. However, glacier of snow/ice patch expansion would be expected during the Little Ice Age since evidence for this has been identified at multiple sites further north in Montenegro (Hughes, 2007, 2010b).

Table 6. Late-glacial to Holocene glacial phases of Mt Olympus (after Leontaritis et al., 2020 with data from Styllas et al., 2018)

Phase	Glacier behaviour	Age
Little Ice Age (HOL3)	Advance	0.64 ± 0.08 ka
Late Holocene (HOL2)	Advance	2.6 ± 0.3 - 2.3 ± 0.3 ka
Early Holocene (HOL1)	Stagnation/ Re-advance	9.6 ± 1.2 ka
Younger Dryas (LG3)	Retreat	12.6 ± 1.6 - 12.0 ± 1.5 ka
Oldest Dryas (LG1)	Advance/Stabilisation	15.6 ± 2.0 -14.2 ± 1.0 ka

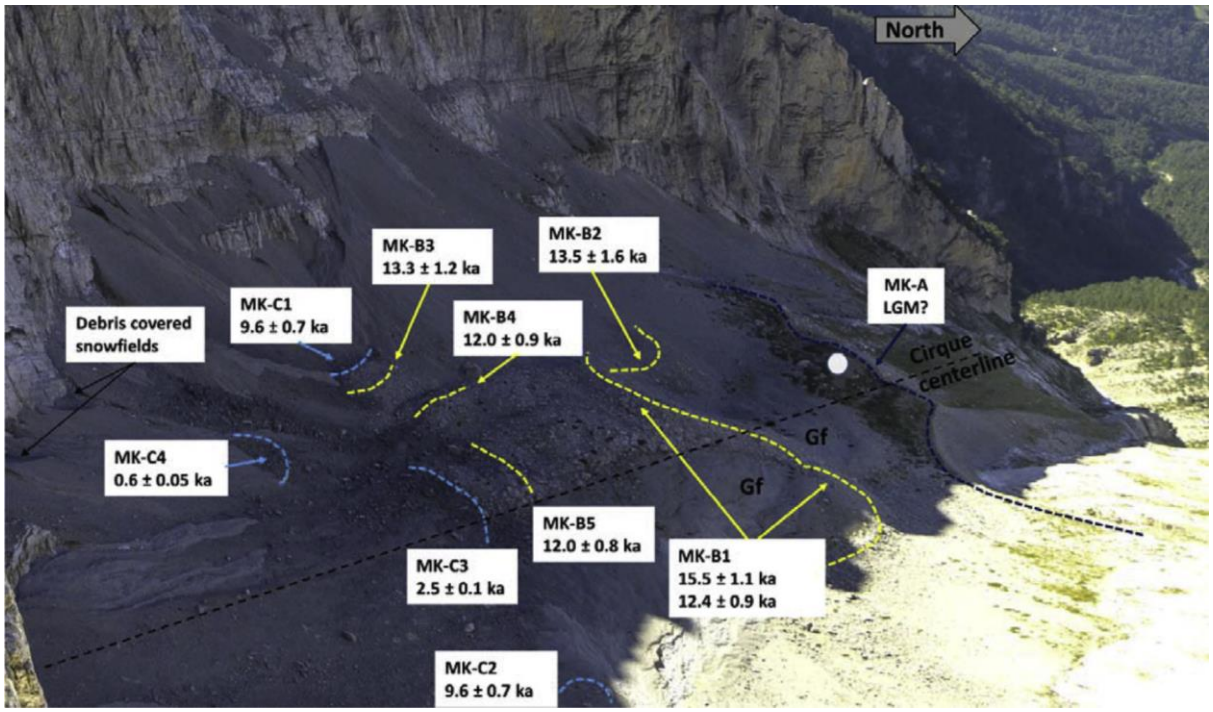

Figure 27. The view of Megala Kazania (MK) cirque from the summit of Mount Olympus, Mytikas (2918m). Moraine complexes MK-A (dark blue dashed line), MK-B (yellow dashed lines) and MK-C (light blue dashed lines) and sampled moraine crests (MK-B1 to B5, MK-C1 to C4) are shown with their respective ^{36}Cl ages (from Styllas et al., 2018).

It should be noted that due to the uncertainties in the cosmogenic exposure dating techniques that are related to the assumed production rates and the correction coefficients for erosion/snow cover, the age control of these glacial deposits is to a certain extent limited (Leontaritis et al., 2020). Indicatively, for the reported ages of Styllas et al. (2018) the combined effect of the erosion/snow cover correction coefficients shifts backwards the raw calculated age of a sample by 8-15% whilst the analytical and production rate errors are within ± 10-15% of the final calculated age (Leontaritis et al., 2020). Therefore, even though the above-mentioned glacial phases of Mt Olympus can be placed with confidence within the Late-glacial and the Holocene respectively, the reported ages should be viewed with caution and the precise timing of the glacier phases is likely to be subject to revision (Leontaritis et al., 2020). The same is true of the earlier ages obtained by Manz (1998).

3.3 Peloponnese (south Greece) and the complex glaciations during the Tymphian Stage

The highest mountains in the Peloponnese (Figure 1), Mt Taygetos (2407 m a.s.l.), Mt Chelmos (2355 m a.s.l.), Mt Ziria (2375 m a.s.l.) and Mt Erymanthos (2224 m a.s.l.), are dominated by limestone lithologies and hold abundant glacial evidence like cirques, glacial valleys, and moraines suggesting their multiple glaciations during the Quaternary. However, the geochronology and the palaeoclimatic context of this glacial record have been only explored partly so far (Pavlopoulos et al., 2018; Pope et al., 2017). In particular, Mt Chelmos is the only mountain of the Peloponnese that has to a certain extent been studied to an advanced level. The first pioneering studies on Mt Chelmos report cirques, moraines, glacial boulders and ice-moulded bedrock which are generally attributed to Quaternary glaciers (Philippson, 1892; Maull, 1921; Mistardis, 1937a, 1937b, 1937c, 1946). Later on, Mastronuzzi et al. (1994) presented glacial features on Mt Chelmos that were attributed a Late Pleistocene age, although no ages were obtained. The first advanced studies on Mt Chelmos were conducted only years later by Pope et al. (2017) followed by a part of this research that was dedicated to Mt Chelmos. The former study is summarised in the next section while the results of the latter one have been published by Pavlopoulos et al. (2018) and are presented in detail in Chapter 5.

Further south in the Peloponnese, glacial features are reported on Mt Taygetos by Maull (1921), Mistardis (1937a), Mastronuzzi et al. (1994), Pope (2010) and Kleman et al. (2016). On the eastern slopes of the massif there is an impressive set of moraines and glacial boulders within a steep cirque at an altitude of only 1850 m a.s.l. (Leontaritis et al., 2020; Figure 28). Pope (2010) argued that glacial meltwater is likely to have been closely related to alluvial fan

development in the Sparta fans situated downslope and luminescence dating suggests that proximal fan sediments were deposited between 250 and 130 ka (MIS 8–6) (Pope and Wilkinson, 2006). However, the moraine and proximal fan soils differ significantly in terms of magnetic and iron properties, which are proxies for weathering (Pope and Millington, 2000), and this may reflect a large age difference.

Even though in the study of Mastronuzzi et al. (1994) it is claimed that Chelmos and Taygetos are the only mountains in the Peloponnese where glacial traces can be recognized, Mistardis (1937a) reports glacial cirques and moraines on Mt Erymanthos while recent observations from Mt Ziria, just a few km to the east of Mt Chelmos, suggest that this massif has also been glaciated in the past (Pope et al., 2017).

Figure 28. The set of terminal moraines at Gouves (alt. 1850 m a.s.l.) on Mt Taygetos (Photo: June 2017).

3.3.1 Advanced studies on Mt Chelmos

The first advanced systematic study on Mt Chelmos was conducted by Pope et al. (2017), and included detailed geomorphologic mapping of glacial evidence and a dating program of the younger moraine deposits with cosmogenic ^{36}Cl (Figure 29).

The most extensive glacial phase along with its unequivocal glacial traces (morphotratigraphic unit 1) remains undated but has been correlated with the Skamnellian/Vlasian Stages of northern Greece (MIS 12/MIS 6) on the basis of its morphostratigraphic position. This unit could represent more than one glaciation episodes but

it was not possible to distinguish multiple moraine units that correspond to both stages. During this glacial phase Mt Chelmos was glaciated by a plateau ice field with valley glaciers characterised by a mean ELA of 1967 m a.s.l. radiating out of it (Pope et al., 2017). Deposits from these glaciers were found down to 1180 m a.s.l. in the northeast.

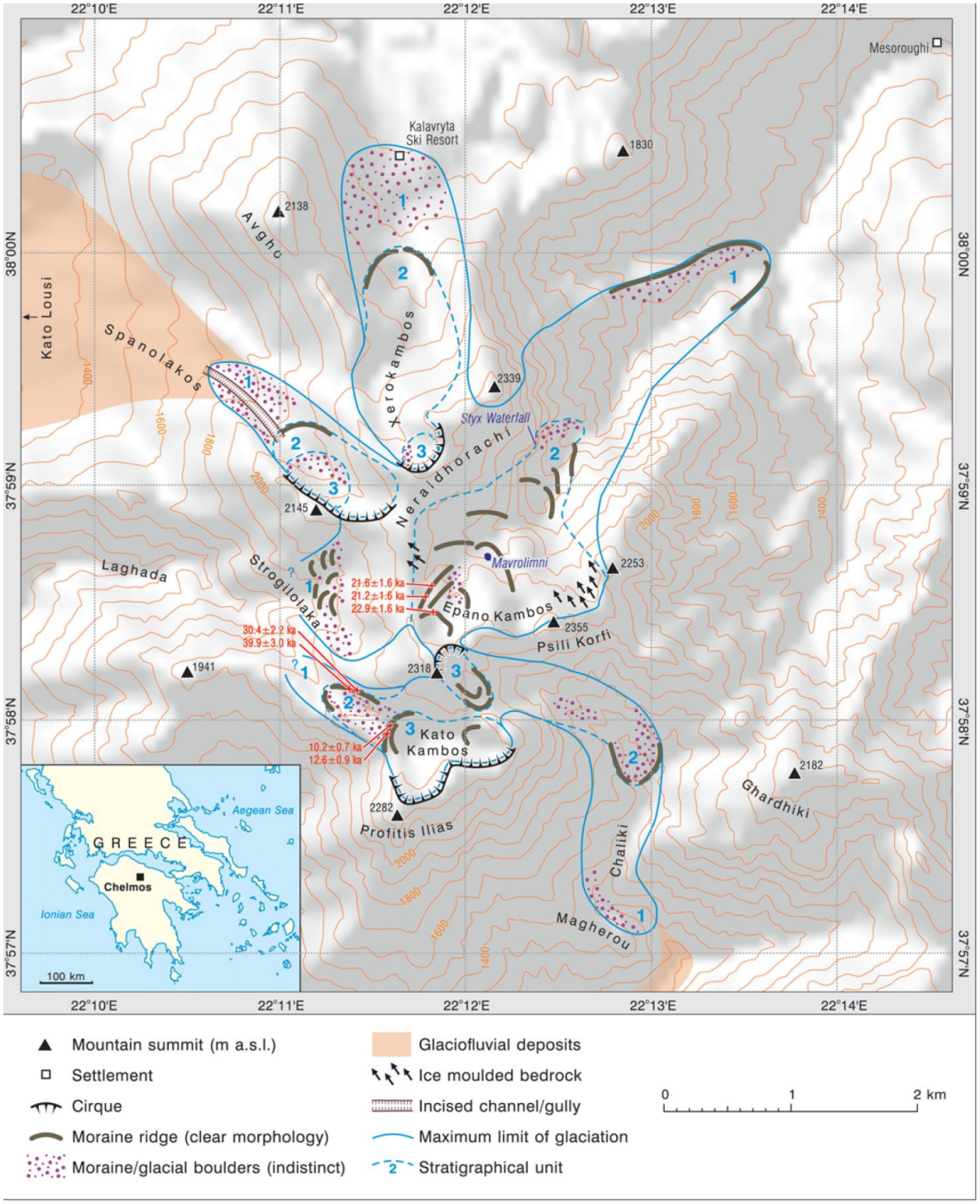

Figure 29. Glacial Geomorphological map of Mt Chelmos showing sample locations and exposure ages (from Pope et al., 2017).

The younger high-altitude moraines at the head of the valleys were formed during Late Pleistocene glacial phases by smaller valley and cirque glaciers. Glacial boulders from these moraines were dated using cosmogenic ^{36}Cl exposure dating (Pope et al., 2017). The yielded ages suggest that these moraines are the result of glacier advance/stabilization during two phases in Late Pleistocene at 39.9 ± 3.0 - 30.4 ± 2.2 ka (morphostratigraphic unit 2 – mean ELA 2046 m a.s.l.) characterized by cirque and valley glaciers and at 12.6 ± 0.9 - 10.2 ± 0.7 ka (morphostratigraphic unit 3- mean ELA 2174 m a.s.l.) during which small glaciers were confined within the existing cirques.

Table 7. Glacial Morphostratigraphic units of Mt Chelmos according to the study of Pope et al. (2017)

Morphostratigraphic Unit	Altitude Range mean ELA	Age (^{36}Cl dating)	Glacial Stage (corresponding MIS)
3	2100 m a.s.l. ELA – 2174 m a.s.l.	12.6 ± 0.9 to 10.2 ± 0.7 ka	MIS 2 - Younger Dryas
Retreat Phase	2200 m a.s.l. ELA >2200 m a.s.l.	22.9 ± 1.6 to 21.2 ± 1.6 ka	MIS 2 – Global LGM - Tymphian Stage
2	1600-2100 m a.s.l. ELA – 2046 m a.s.l.	39.9 ± 3.0 to 30.4 ± 2.2 ka	MIS 3 - Tymphian Stage
1	950-1450 m a.s.l. ELA – 1967 m a.s.l.	correlation with Middle Pleistocene glacial phases	MIS 12 – Skamnellian Stage MIS 6 – Vlasian Stage

At the global LGM glaciers were present but exposure ages of 22.9 ± 1.6 - 21.2 ± 1.6 ka from a suite of recessional moraines (Retreat phase – mean ELA 2046 m a.s.l.) in the highest parts of the Epano Kambos valley in the central part of the massif is assumed to indicate glacier retreat at this time. The ages from these moraines combined with the older ages from unit 2 moraines suggest that ice is likely to have occupied the cirques of Mount Chelmos from MIS 3 to 2 and oscillated in response to varying climatic conditions (Pope et al., 2017). The most recent phase of glaciation associated with morphostratigraphic Unit 3 (mean ELA – 2174 m a.s.l.) is recorded by clear cirque moraines that are present in the highest parts of some, though not all, of the glaciated valleys (see Figure 29). This last phase probably correlates with the Younger Dryas (12.9-11.7 ka; Rasmussen et al., 2014).

3.4 Central Greece (The Mountains of Sterea Hellas and the Agrafa mountains)

Traces of former glaciers on the mountains of central Greece that are dominated by limestone lithologies were already identified by the first pioneer researchers in the beginning of the 20th century. In Sterea Hellas just 70 km north of Mt Chelmos, traces of extensive glacial valleys and till as well as high altitude well-preserved moraines within numerous typical cirques were reported on Mt Parnassos (2457 m a.s.l. – Renz, 1910; Maull, 1921; Mistardis, 1937a; Pechoux, 1970) and Mt Vardousia (2495 m a.s.l. - Maull 1921; Mistardis 1937a) and to a lesser extent on Mt Gkiona (2504m a.s.l – Mistardis, 1937a; Pechoux, 1970) and Mt Tymphrestos (2312m a.s.l – Klebelsberg, 1932). Indeed, these observations of glacial evidence in the mountains of central Greece can be confirmed both on the field and on satellite imagery (Leontaritis et al., 2020).

It has been claimed that evidence of glaciation in Greece is present only in mountains that exceed 2200 m a.s.l. in altitude (Boenzi and Palmentola, 1997) but the mountains of central Greece hold abundant evidence that the geographical and altitudinal extent of former glaciers in Greece has been underestimated. This is suggested both by early studies and by recent field observations by the author in the mountains of southern Pindos (Figure 30), in the Agrafa Mountains (1900-2184 m a.s.l. – Hunt and Sugden, 1964) and further south in the mountains of Evritania (Mt Chelidona 1974 m a.s.l. - Figure 31, Mt Kaliakouda 2099 m a.s.l. – Mistardis, 1937a). It should be recognised that while the glacial sedimentary records in the mountains of central Greece constitute a potentially important archive of former glacial episodes, it has not yet been systematically studied (Leontaritis et al., 2020).

Moreover, the dating of the glacial landforms found in the above-mentioned mountains is of great importance for understanding the missing links between Northern Greece and the Peloponnese (Pavlopoulos et al., 2018). As the glacial studies for Mt Olympus (Styllas et al., 2018) in the northeast and for Mt Chelmos (Pope et al., 2017) that were published in the course of this research raised further questions in terms of moisture supply in these areas, the importance of creating a key geographical link for Late Pleistocene glaciations between the well-studied Pindus mountains/Mt Olympus in northern Greece and Mt Chelmos in the south was further highlighted. Such a link would allow for the comparison and interpretation of the results from these studies and the reconstruction of the palaeoclimatic conditions across Greece at these times.

Figure 30. The geomorphology of several mountains in the southern Pindus range bare numerous glacial and periglacial features like this characteristic glacially scoured U-shaped valley under the Hatzi peak (2038 m a.s.l.) with evident glacial sediments (Photo: July 2018).

Figure 31. Moraines below the summit of Mt Chelidona (1974 m a.s.l.) in Evritania, southcentral Greece (Photo: June 2015)

Initial studying of satellite imagery as well as field observations, showed that between the glacial sedimentary records in the mountains of Sterea Hellas in central Greece (Mt Parnassus, Mt Gkiona, and Mt Vardousia - Figure 1) high-altitude and thus stratigraphically younger glacial deposits are present in all three mountains but the uppermost glacial deposits (>2000 m a.s.l.) within north-oriented cirques on Mt Parnassus are best preserved. Therefore, in this effort to create a key-link between Late Pleistocene glaciations in northern and southern Greece, it is here argued that research should primarily focus on the Parnassus massif and as a next step the results should be confirmed in the nearby Giona and Vardousia mountains. For this reason, the characteristics of Mt Parnassus and the results of a preliminary geomorphological study are presented next as an outline of future glacial/geochronological research focusing on its uppermost glacial deposits.

Chapter 4. Mt Mavrovouni: Geomorphological evidence, geochronology and glacial reconstructions

The glacial geomorphologic study and cosmogenic ^{36}Cl dating work presented here is part of a journal article that is in preparation for publication (Leontaritis et al., 2021).

4.1 Setting of Mt Mavrovouni

Mt Mavrovouni is located in the north Pindus Mountains in NW Greece, only 20km to the east/southeast of Mt Tymphi (2497 m a.s.l.) and 30km to the southeast of Mt Smolikas (2637 m a.s.l.) (Figure 1; Figure 32). Its highest peak (Flega) reaches an altitude of 2157 m a.s.l.; considerably lower than the neighbouring mountains. Its lithology is similar to Mt Smolikas and Mt Vasilitsa (2248 m a.s.l.). All three belong to the Northern Pindus ophiolitic complex, part of a nappe which is tectonically overthrust onto the Eocene flysch of the Pindus Zone (Dupuy et al., 1984).

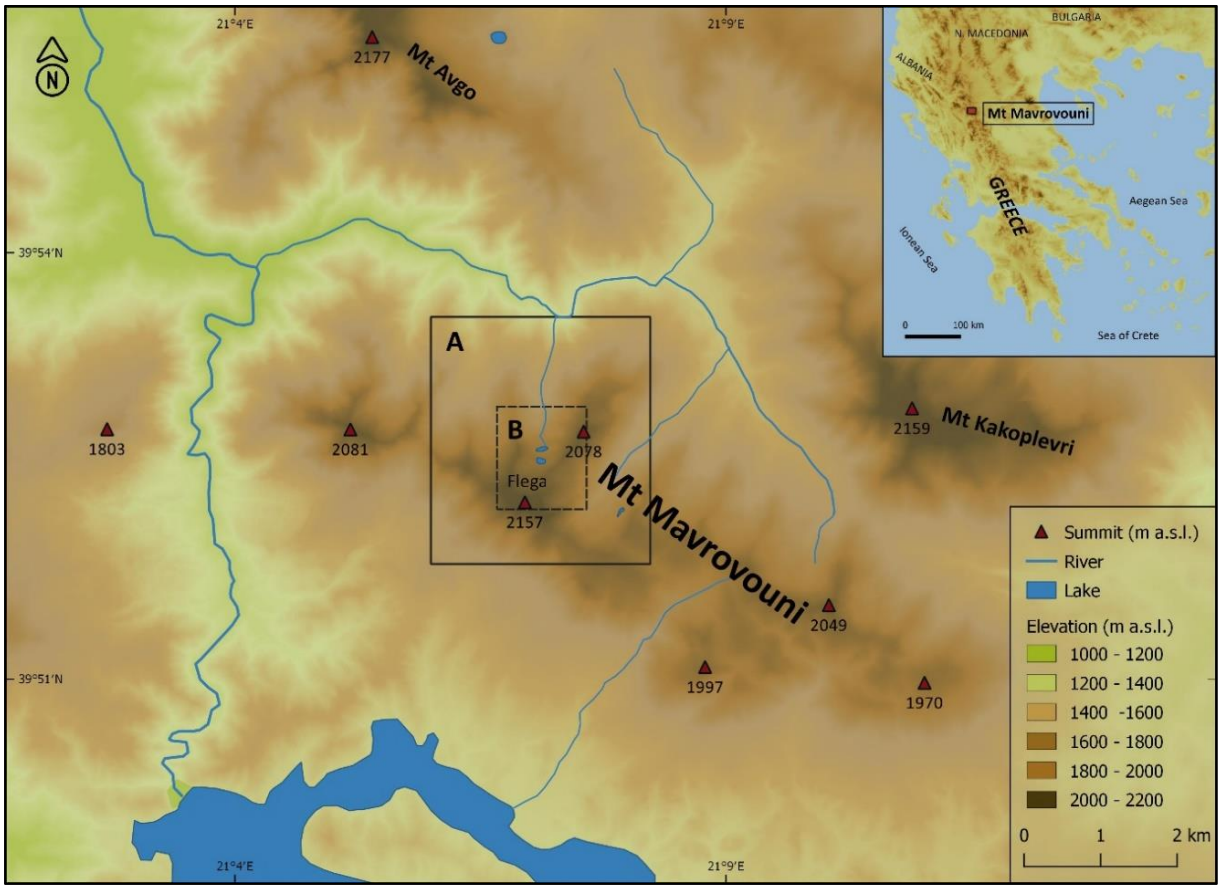

Figure 32. Map of the study area on Mt Mavrovouni. Detailed glacial geomorphologic maps of the areas denoted by boxes A and B are given in Figure 39 and Figure 45 respectively.

The Pindos ophiolite is one of several ophiolites within the Hellenides in Greece and Albania (Figure 33) that likely correspond to an originally magmatic, layered oceanic crust with remnants of a clear dyke complex and an overlying lava section that formed in the Jurassic Tethyan basin and was subsequently obducted (Robertson, 2002; Rassios and Dilek, 2009). The thickness of the complex ranges between 3 and 5 km (Robertson, 2002; Saccani and Photiades, 2004; Rassios and Moores, 2006).

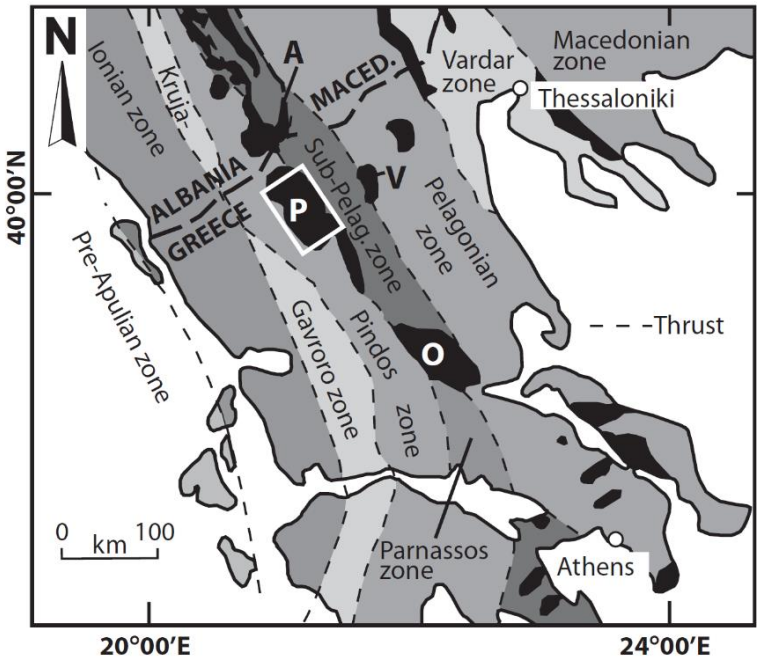

Figure 33. The Pindos ophiolite within the Hellenides. P, Pindos ophiolite;V,Vourinos ophiolite; O, Othris ophiolite;A, Albanian ophiolites (from Pelletier et al., 2008).

In particular, Mt Mavrovouni belongs to the Dramala Complex subunit which represents oceanic mantle and part of its crustal sequence (Pelletier et al., 2008). It primarily consists of locally serpentinized, harzburgite-tectonite restite (i.e. depleted mantle harzburgite) of Mid-Jurassic age while subordinate lithologies include dunite, pyroxenite and a range of ultramafic cumulate rocks (Jones and Robertson, 1991). All these ultramafic rocks have slightly to highly serpentinized equivalents (Pelletier et al., 2008). Mesozoic limestones and Palaeozoic crystalline schists are also present locally, at the overthrust nappe of the ophiolitic complex (IGME, 1959). Similarly to its ophiolitic neighbours, Mt Mavrovouni is less complex in form compared with the limestone dominated Mt Tymphi (see section 3.1), as it is a generally rounded mountain with many steep V-shaped valleys cut in to it and only a few and relatively short crags. The slopes of the massif are densely forested up to 1800 m, with subalpine terrain, open grasslands and scattered *Pinus heldreichii* (Bosnian pines) dominating its uplandsn(Leontaritis, 2019). The vegetation of the lower altitude zone (900-1600 m a.s.l.) is

generally dominated by *Pinus nigra* (black pine), while *Fagus moesiaca* (Balkan beech) grows only in north oriented slopes between 1200 and 1600 m a.s.l. (Leontaritis, 2019). From this point on takes over the resilient Bosnian pine with some smaller trees surviving the harsh environment up to almost 2100 m a.s.l. (Leontaritis, 2019).

As regards its glacial geomorphology, cirque-valley systems seem to be present only on its northern slopes and the glacial sequence in them is typically more fragmented compared with the nearby Mt Tymphi (see section 3.1.1). Still, well-preserved evidence of a complete high altitude glacial/periglacial sequence is present within a well-developed cirque in the typically U-shaped Mnimata valley (Figure 34). Based on the altitude, extent and geomorphological context, this sequence is expected to be Late Pleistocene in age. As the aim of this part of the research is the completion of the Late Pleistocene part of the Pindus chronostratigraphy, special focus was given on constraining the timing of glacial/periglacial processes that formed these deposits. Moraines at lower altitudes are present in neighbouring valleys implying older and much more extensive glaciation phase(s) which is in consistence with evidence from elsewhere in the mountains of Greece (e.g. Mt Tymphi, Mt Chelmos, Mt Smolikas, Mt Olympus; Leontaritis et al. 2020 and references therein). As it will be discussed later, the formation of these moraines could be ascribed to Middle Pleistocene (MIS 12/ MIS 6) according to the evidence from the nearby Mt Tymphi (see section 3.1.1).

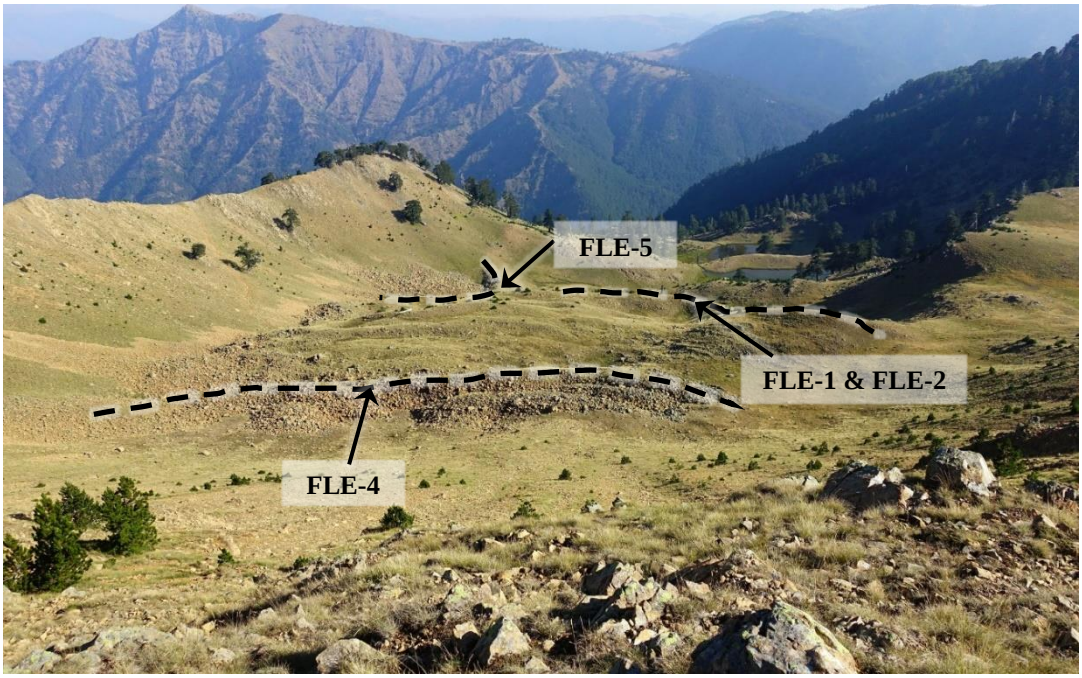

Figure 34. The Mnimata U-Shaped valley and the glacial/periglacial sequence within a well-developed cirque. Sample locations on terminal moraine/pronival rampart ridges (dashed black lines) are denoted. Photo from the Flegka Peak at 2157 m a.s.l. (Photo: August 2016)

No glaciers, permafrost or permanent snow fields are present today. The present-day precipitation and annual temperature range at the nearby villages of Vovousa, Greveniti, Elatochori and Metsovo are summarized in Table 8. When mean temperatures for these four weather stations are extrapolated using a lapse rate of 0.6ºC per 100 m of altitude, the mean annual temperature at 2000 m a.s.l. is about 4.5ºC while the mean monthly temperatures for July and January are 13.8ºC and -3.0ºC respectively. With a mean annual precipitation of 1520 mm for the four stations at an average altitude of 1037 m a.s.l. the mean annual precipitation at 2000 m is expected to exceed 2000 mm (Furlan 1977). Snow cover on the northern slopes above 1800 m a.s.l. lasts from early December to late May.

Table 8. Precipitation and temperature data from weather stations near Mt Mavrovouni (precipitation data from Fotiadi et al. 1999; temperature data from Gouvas and Sakellariou, 2011; reference period >20yr).

Meteorological Station	Altitude (m a.s.l.)	Annual Precipitation (mm)	Mean Temperature (ºC)		
			Annual	Jan	Jul
Vovousa	1000	1439	9.8	0.4	19
Elatochori	1014	1626	10.4	1.1	20.3
Greveniti	976	1512	10.9	1.4	20.2
Metsovo	1160	1514	10.5	1.0	19.6
Mean	1037.5	1523	10.4	0.98	19.8
Mt Mavrovouni (Extrapolation)	2000	>2000 mm	4.5	-3.0	13.8

4.2 Methods applied

4.2.1 Geomorphological mapping

Geomorphological mapping on Mt Mavrovouni was initiated with the use of available topographic maps (1:50,000, Anavasi,2016; Open Street Maps), the regional 1:50,000 Geological Sheet of the Greek Institute for Geological and Mineral Exploration (IGME, 1959), high-resolution standard satellite imagery (Google Earth, Bing Maps) and orthophotos from the Hellenic Cadastre. After identifying possible glacial and periglacial features from this material, detailed fieldwork was conducted in summer 2016, 2017 and 2018 in order to confirm the morphology and origin of these features, record their characteristics and map them using a standard GPS/Glonass device (Garmin 64s). At the lower densely forested northern slopes of

Mt Mavrovouni (below 1700-1800 m a.s.l.), fieldwork revealed features that could not be recognised by aerial or satellite imagery. Additionally, drone aerial photos and videos were taken from the upper Mnimata valley within the well-developed cirque under the Flega Peak (Figure 34). This material was of great use in interpretating the recorded glacial/periglacial deposits and processes that resulted in their formation. The geomorphological maps were finally produced using the Digital Elevation Model provided by the National Cadastre at a resolution of 5 m.

4.2.2 Sample collection

Sampling for ^{36}Cl cosmogenic dating was focused on the glacial/periglacial deposits sequence in the upper Mnimata valley (Figure 34). As regards the lower in the valley, matrix supported and well-consolidated terminal moraine, 2 samples (FLE-1 and FLE-2 in Figure 34) were taken from the largest (up to 1m diameter) and partly embedded glacial boulders along the moraine ridge (Figure 35). The pronival deposits are less consolidated and are characterised by larger (1-5m diameter) and more angular boulders which in places are only partially supported by matrix. Two boulders (FLE-4 and FLE-5 in Figure 34) along the most consolidated part of the pronival deposits were chosen for sampling (Figure 36). All sampled boulders are of ophiolitic lithology. Samples were obtained with the use of a hammer and chisel from the upper 2-3cm of a flat rock surface as far away as possible from the boulder's edges.

Figure 35. Sampled boulder on the well-consolidated terminal moraine (samples FLE-1 & FLE -2) (Photo: October 2016)

Figure 36. Sampled boulder on the crest of the less-consolidated pronival deposits (sample FLE-4) (Photo: October 2016)

Topographic shielding for the four sample was determined with the use of a well-established and open access DEM-based GIS toolbox dedicated to the calculation of cosmogenic nuclide topographic shielding for discrete sample points (Li, 2018; available online at https://web.utk.edu/~yli32/programs.html). Moreover, rocks in the study area generally show very limited signs of weathering, like for example exposed ice-polished bedrock that still bears clearly its glacial striations, indicating negligible erosion. Therefore, an erosion correction factor for the calculation of the final ages was not considered. Also, information about contemporary and Late Pleistocene snow cover is not available so this was not considered. Still, if these factors were considered, the final ages are likely to be only some hundred years younger. In the framework of this research and taking into consideration the calculated age uncertainties, such deviations are practically negligible and the calculated ages can be correlated with the age of moraine deposition. The location and characteristics of the collected samples are summarised in Table 9.

Table 9. Location and characteristics of collected ^{36}Cl samples. Snow correction and erosion corrections factors are neglected for all samples.

Sample ID	Latitude (N°)	Longitude (E°)	Elevation (m a.s.l.)	Sample thickness (cm)	Sample Density (g cm^{-3})	Topographic Shielding
FLE-1	39.8737	21.1204	2017	2	2.7	0.978
FLE-2	39.8735	21.1205	2017	2.5	2.7	0.985
FLE-4	39.8725	21.119	2038	3	2.7	0.978
FLE-5	39.8749	21.1193	1978	3	2.7	0.989

4.2.3 Samples preparation and processing and AMS measurements

Rock samples were first processed at the National Technical University of Athens where they were crushed and sieved. Subsequently the 250-500 μm fraction underwent a chemical processing stage at the Purdue Rare Isotope Measurement Laboratory (PRIMElab) at Purdue University. About 130g of the 250-500μm fraction of each sample was leached in 5% HNO_3 (nitric acid) to remove any bulk carbonates. Samples were then leached in 5% HNO_3 in an ultrasonic tank for at least eight hours, acid was decanted and the samples were rinsed in deionized water, and then leached in 5% HNO_3 in an ultrasonic tank for at least eight hours again to remove meteoric ^{36}Cl. After triple-rinsing in deionized water, samples were oven-dried. About 30 g of the dried sample, including an addition of approximately 1 mg of chloride with a $^{35}Cl/^{37}Cl$ ratio of 273 (dilution spike), were dissolved in a mixture of 90 g of deionized water, 150 g of concentrated HF (hydrofluoric acid), and 2 g of concentrated HNO_3. After acid addition, sample was placed in a 60ºC water bath for at least four hours. After this initial period of heating, 15 g of concentrated nitric acid were added to make sure all species were oxidized and the sample was placed back into the bath for at least eight hours. Upon full dissolution the fluoride dissolution products were removed by centrifugation and chloride recovered by the addition of $AgNO_3$ (silver nitrate) to produce the target AgCl (silver chloride). Chloride was purified by dissolution in concentrated NH_4OH (ammonium hydroxide) with the addition of $Ba(NO_3)_2$ (barium nitrate) to precipitate any sulphates in the form of $BaSO_4$ (barium sulphate). After the removal of sulphates through centrifugation, the silver ammoniac chloride complex was loaded onto anion exchange columns to facilitate the quantitative separation of any residual sulphate and the chloride was eluted and then isolated by precipitation with $AgNO_3$, centrifugation, and drying. The AgCl targets were pressed into a AgBr (silver bromide) bed within copper target holders. The ^{36}Cl to total stable chloride ratio and the stable $^{35}Cl/^{37}Cl$ ratio were measured by Accelerator Mass Spectrometry (AMS) on the tandem accelerator at PRIMElab. The AMS analytical data for the 4 samples are summarised in Table 10.

Table 10. AMS analytical data for ^{36}Cl samples

Sample ID	Mass (g)	Dilution Spike (mg Cl)	$^{36}Cl/Cl$ Ratio ($x10^{-15}$)	$^{35}Cl/^{37}Cl$ Stable Ratio	Cl content (ppm)	Measured ^{36}Cl (atoms / g of rock)
FLE-1	30.242	1.0805	108.5	5.48	58.89	177,513 ± 7,113
FLE-2	30.188	1.0864	186.7	5.51	58.57	307,692 ± 10,891
FLE-4	30.213	1.0841	161.7	3.90	188.59	622,774 ± 27,000
FLE-5	30.221	1.0676	368.0	8.50	23.43	386,192 ± 8,942

4.2.4 Geochemistry

Major/minor element and trace element concentrations were determined using ICP-ES (Inductively Coupled Plasma Emission Spectrometry) and ICP-MS (ICP Mass Spectrometry) respectively at the Acme labs in Canada (Bureau Veritas Mineral Laboratories). The same elemental analysis in the processed target fraction was determined using Lithium Borate ($LiBO_2/Li_2B_4O_7$) fusion coupled with ICP-ES analysis at the same laboratory. Prior to the analyses, samples were pulverized to 85%, passing 200 mesh. The geochemistry of the 4 rock samples is presented in Table 11. Please notice that the Cl content of rock samples has been measured by AMS and the respective results are included in Table 10.

Table 11. Geochemistry of the serpentinized peridotite samples for ^{36}Cl dating. For major and minor elements, results are given for both bulk rock and target (processed) rock samples.

Major and minor element mass fraction (wt %)											
Sample ID	SiO_2	Al_2O_3	Fe_2O_3	MgO	CaO	Na_2O	K_2O	TiO_2	MnO	L.O.I.	$C0_2$
Bulk rock samples											
FLE-1	43.44	0.43	8.21	41.22	0.36	0.02	0.01	<0.01	0.11	4.6	0.6
FLE-2	44.17	0.22	8.48	42.33	0.24	0.01	<0.01	<0.01	0.12	2.9	0.6
FLE-4	41.48	0.21	8.35	40.38	0.21	0.01	<0.01	<0.01	0.11	7.5	0.6
FLE-5	45.03	1.61	8.35	39.45	1.42	0.03	<0.01	0.02	0.12	2.5	0.6
Target rock samples											
FLE-1	45.98	0.43	8.63	39.36	0.39	0.01	<0.01	<0.01	0.11	-	-
FLE-2	46.3	0.22	8.88	41.26	0.24	<0.01	<0.01	<0.01	0.12	-	-
FLE-4	44.16	0.24	8.58	39.16	0.2	<0.01	<0.01	<0.01	0.1	-	-
FLE-5	46.21	1.8	8.64	38.62	1.61	0.03	<0.01	0.02	0.12	-	-

Trace element concentrations (ppm)											
Sample ID	B	Sm	Gd	U	Th	Li	V	Ba	Ni	Sc	Co
Bulk rock											
FLE-1	<3	<0.05	<0.05	<0.1	<0.2	<0.001	22	8	2388	6	123.6
FLE-2	<3	<0.05	<0.05	<0.1	<0.2	<0.001	16	10	2473	5	126.5
FLE-4	<3	<0.05	<0.05	<0.1	<0.2	<0.001	23	4	2470	4	123.6
FLE-5	<3	<0.05	0.06	<0.1	<0.2	<0.001	51	6	2214	11	113.3

Bulk rock compositions primarily reflect the proportions of minerals present. The sample rocks are mainly composed of silica (SiO_2: 41-45 wt%) and magnesium (MgO: 39-42 wt%) while they are characterised by high Fe concentrations (8-8.5 wt%), as expected for this rock

type. Moreover, all samples are highly depleted in TiO_2 (<0.02 wt%). Based on these compositions, these rock samples are peridotites/harzburgites with predominant serpentine alteration (Kelemen et al., 2004). Notably, three of the sampled rocks are strongly depleted in CaO (relative to Al_2O_3 which is also absent in the composition of these samples), suggesting that serpentinization removed almost all of the calcium that was originally present in the peridotite protolith (Kelemen et al., 2004). These compositions correspond to compositions of serpentinized harzburgites and serpentinites from the Othrys ophiolites (Figure 33; Magganas and Koutsovitis, 2015), of serpentines from mantle Harzburgites and serpentinized peridotites (Economou-Eliopoulos and Vacondios, 1995; Pelletier et al., 2008; Kapsiotis, 2014) from the Dramala unit of the Pindos ophiolitic complex and finally of serpentinites from the southern Atlantic oceanic crust (Dilek et al., 1997a). The fourth sample (FLE-5) has slightly higher CaO and Al_2O_3 contents at 1.42 wt% and 1.61 wt% respectively, correlating with the composition of serpentinized lherzolites from the Othrys ophiolites according to the petrological analyses of Magganas and Koutsovitis (2015). A rock density of 2.7 g cm^{-3} was considered for all samples (Table 9), in accordance to the respective values for ultramafic peridotites with medium to high serpentinization degree (>70%) from the Pindos ophiolitic complex (Bonnemains et al., 2016).

In the present research, the Loss On Ignition (LOI) was assumed to represent inherent water content for all samples (Table 11) as suggested by the study of Kelemen et al. (2004) on ultramafic rocks with predominant serpentine alteration from oceanic crust in the Mid-Atlantic Ridge. In the latter study, XRD results showed high water content (12.6–15.2 wt%) and limited CO_2 concentration (0.05–0.20 wt%) whereas LOI (11.8–13.1 wt%) slightly underestimated the total volatile content because of the conversion of FeO to Fe_2O_3 during heating of the sample powders to ~1000°C. As regards CO_2 content, it was assumed at 0.6 wt% in accordance with the average content of CO_2 in hydrothermally altered peridotites from oceanic crust (Kelemen et al., 2011).

4.2.5 Cosmogenic ^{36}Cl exposure age calculations

This study represents the first documented use of ^{36}Cl dating on ophiolitic rocks. Despite this, the theory and method should be equally applicable to samples of this lithology with no major issues. Due to low Ca and K concentrations, the samples are dominated by production from Cl, with a non-negligible contribution from Fe making these production rates more important than in other samples. The calculated ages (discussed below) were consistent with local and regional moraine morphostratigraphy, further supporting use of the technique.

The exposure ages of the samples were calculated using the Online Cronus ^{36}Cl Exposure Age Calculator v2.1 (http://cronus.cosmogenicnuclides.rocks/2.1/html/cl/; Marrero et al., 2016a). The time-dependent and nuclide-dependent Lifton-Sato-Dunai scaling (LSDn) scaling framework (Lifton et al., 2014) was selected as the best-fitting model when compared to all the datasets of the CRONUS project (Phillips et al., 2016). This model is based on equations from a nuclear physics model and incorporates dipole and non-dipole magnetic field fluctuations and solar modulation (Lifton et al., 2014; Marrero et al., 2016a). The LSDn scaling framework includes separate scaling factors for spallation reactions with Ca, K, Fe and Ti, and also for low energy reactions (Borchers et al., 2016; Marrero et al., 2016b). The production rates used in the calculator and the respective results are shown in Table 12. A fast neutron attenuation length of 156 g/cm2 was calculated by the model in CRONUScalc for the samples' location (latitude, longitude, elevation; Marrero et al., 2016a), which is based on atmospheric attenuation lengths calculated from the PARMA model of Sato et al. (2008).

Table 12. Spallation and thermal neutron [$P_f(0)$] - production rates for LSDN scaling framework used in the calculator (data from Marrero et al.,2016b; 2020 and S. Marrero pers. comm. 07/10/2020)

Ca atoms ^{36}Cl (g Ca)$^{-1}$ yr^{-1}	K atoms ^{36}Cl (g K)$^{-1}$ yr^{-1}	$P_f(0)$ neutrons (g air)$^{-1}$ yr^{-1}	Fe ^{36}Cl (g Fe)$^{-1}$ yr^{-1}	Ti ^{36}Cl (g Ti)$^{-1}$ yr^{-}
55.6 ± 4.2	156 ± 12	714 ± 191	1.86	3.8

The results of the Online Cronus ^{36}Cl Exposure Age Calculator v2.1 for the four considered samples are summarised in Table 13.

Table 13. Exposure ages, share of total ^{36}Cl production and total production rates of ^{36}Cl per element as calculated by the online Cronus ^{36}Cl Exposure Age Calculator (v2.1) for the considered samples. Reported total production rates correspond to production from spallation and slow muons for Ca and K, low energy neutrons for Cl and spallation only for Fe and Ti.

Results obtained with Online Cronus ^{36}Cl Exposure Age Calculator (v2.1)											
Sample ID	Age (ka)	Production rate (atoms ^{36}Cl g^{-1} y^{-1})					Percentage of total ^{36}Cl production (%)				
		Cl	Ca	K	Fe	Ti	Cl	Ca	K	Fe	Ti
FLE-1	17.0 ± 4.2	7.894	0.547	0	0.506	0	88.23	6.11	0	5.65	0
FLE-2	26.6 ± 6.6	8.714	0.337	0	0.522	0	91.02	3.52	0	5.45	0
FLE-4	20.0 ± 5.0	25.214	0.282	0	0.507	0	96.97	1.08	0	1.95	0
FLE-5	54.2 ± 9.9	3.316	2.051	0	0.454	0.002	56.94	35.22	0	7.80	0.04

Observing the calculated ^{36}Cl production rates (atoms g^{-1} y^{-1}) and percentages of the total production from Ca, K, and Cl (Table 13; Figure 37), it can easily be concluded that ^{36}Cl production takes place mainly from Cl (57-97%). This can be explained by the almost-zero concentrations of calcium (CaO) and potassium (K_2O) in most samples. However, the effect of the higher production rates from Ca spallation are clear in one case (sample FLE-5). Although the sample contains only 1.42% of CaO (Table 11), the production from Ca accounts for 35.2% of the total ^{36}Cl production.

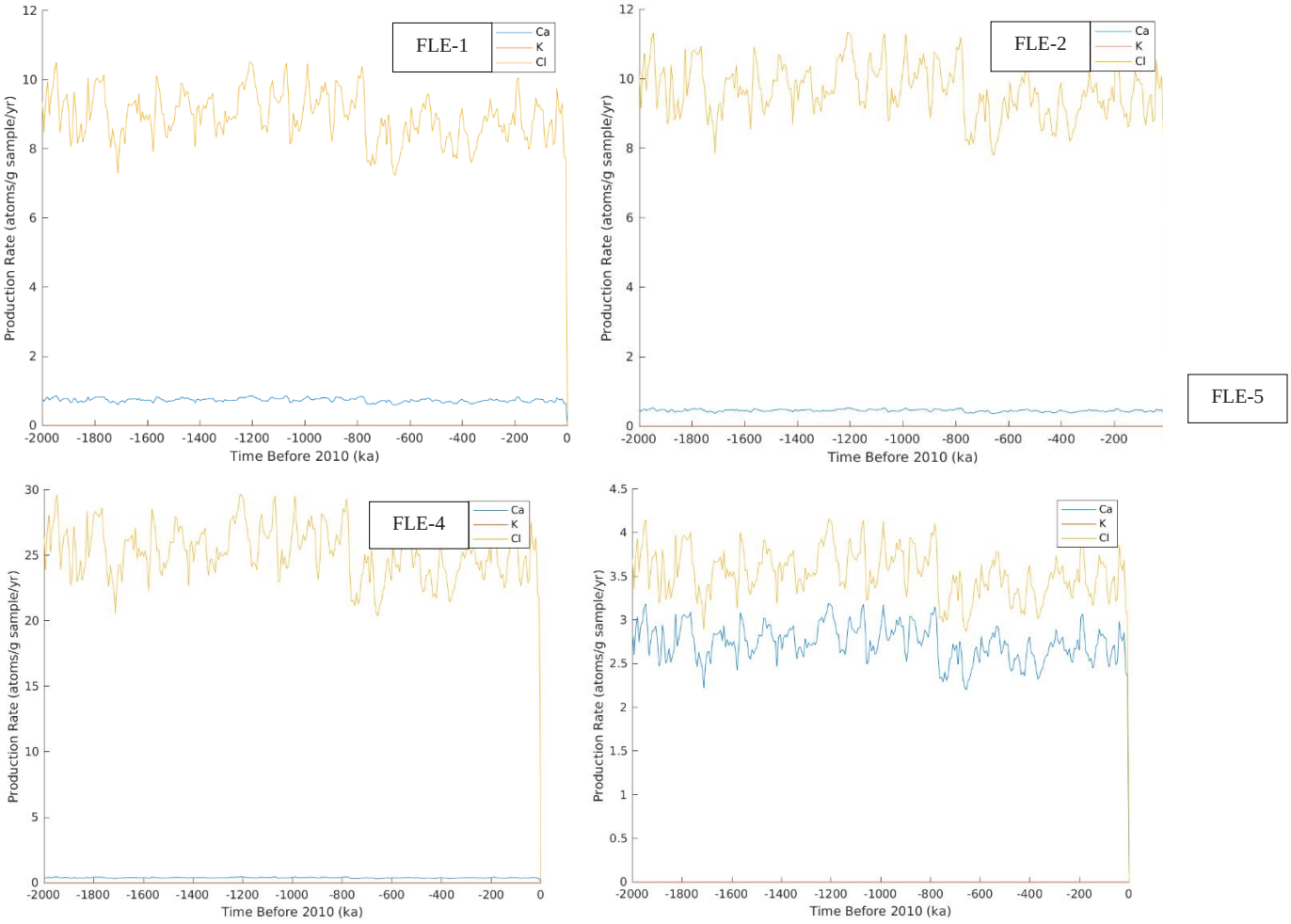

Figure 37. Calculated ^{36}Cl production rates through time from Ca, K and Cl for the considered samples as plotted by the Online Cronus ^{36}Cl Exposure Age Calculator (v2.1)

The production rate of ^{36}Cl from Fe ranges between 0.454 and 0.522 atoms g^{-1} y^{-1}, accounting for 1.95-7.8% of the total ^{36}Cl production (Table 13). For most common rock types, the combined contributions from Ti and Fe are typically less than 1-2% of the total ^{36}Cl production, but for oxide mineral separates it could be much larger (Marrero et al., 2016b). In our case, as the composition analysis showed (Table 11), the rock samples are characterised by

very high concentrations of Fe_2O_3 (8-8.5%). As the current version of the calculator is suspected to miscalculate the ^{36}Cl production rate from Fe due to insufficient calibration of the model, the calculated ^{36}Cl production from Fe and therefore the resulting ages could be subject to revision. In order to test this issue, further runs with a beta version of the Cronus ^{36}Cl Exposure Age Calculator Calculator v2.2 were conducted by S. Marrero (pers. comm. 08/10/2020). In this version, new Fe production rates of 1.29 ± 0.11 atoms ^{36}Cl $(g\ Fe)^{-1}$ yr^{-1} as reported from Moore and Granger (2019) are incorporated in the LSDn scaling model (S. Marrero pers. comm. 09/11/2020). The results obtained with the beta version (v2.2) of the calculator are summarised in Table 14 and show negligible differences in the resulting ages and production rates compared with the respective results obtained with the latest online version (v2.1) of the calculator. As Moore and Granger (2019) underline that additional data are needed to confirm the scaling behaviour described in their work, the above-described results are a significant outcome of this research.

Table 14. Exposure ages as calculated by the beta version of the Cronus ^{36}Cl Exposure Age Calculator Calculator v2.2 against the results calculated by the online Cronus ^{36}Cl Exposure Age Calculator v2.1

Sample ID	Age (ka) - Cronus ^{36}Cl Exposure Age Calculator v2.2(beta)	Age (ka) - Cronus ^{36}Cl Exposure Age Calculator v2.1
FLE-1	17.2 ± 4.2	17.0 ± 4.2
FLE-2	26.7 ± 6.5	26.6 ± 6.6
FLE-4	20.2 ± 4.8	20.0 ± 5.0
FLE-5	55.1 ± 9.8	54.2 ± 9.9

4.3 Results

4.3.1 Glacial Geomorphology

Detailed mapping was performed in three north-oriented major glacial valleys on Mt Mavrovouni (Figure 39). All valleys extend between the main NW-SE watershed at c. 2100 m a.s.l. and the floor of the Valia Calda Valley at c. 1300-1200m a.s.l. This research primarily focused on the Mnimata valley where geochronological control of the uppermost glacial/periglacial sequence was attempted. The neighbouring Arkoudolakos and Flega valleys to the west and to the east respectively were studied mainly for their older low-altitude moraines. It should be noted that traces of glaciation were also observed in other north-oriented valleys but the glacial sequence was fragmentary, incompletely shaped or less well-preserved compared with the studied valleys. No traces of glaciation were identified in the southern slopes.

4.3.1.1 Flega Valley

The Flega glacial valley is generally U-shaped and has a N-NE orientation. However, along the main axis of the valley runs the homonymous Flega river which has caused deep cut-off erosion creating a steep, V-shaped bank-riverbed profile. The head of the valley is ice steepened, forming a wide and not very well-developed cirque. The edges of this main cirque stand between 1950 and 2050 m a.s.l.

On the western side of the valley there is a sharper and poorly developed proto-cirque just below Flega peak (2157 m a.s.l.) with E-NE orientation (Figure 38). Unlike the main cirque, it is characterised by extensive talus cones, frost-shattered debris and large angular boulders. As regards glacial deposits elsewhere in the upper valley, glacial evidence is generally fragmented and limited to sub-rounded glacial boulders with quite indistinct depositional limits (Figure 39). The formation of these deposits could be synchronous with the high-altitude glacial/periglacial sequence in the adjacent Mnimata valley to the W (morphostratigraphic unit 2 in Figure 39) but they could also be synchronous to the older and more extensive deposits lower in the valley that belong to morphostratigraphic unit 1. However, a moraine (or prnivar rampart?) dammed swamp/seasonal lake (Figure 40 and Figure 41) is present on the eastern flank of the valley, at an altitude of 1880 m a.s.l. It has been correlated with unit 2 deposits in the Mnimata valley on grounds of altitude and has therefore been ascribed to morphostratigraphic unit 2 (Figure 39).

Figure 38. The E-NE looking and debris-filled proto-cirque below the Flega Peak. (Photo: August 2016)

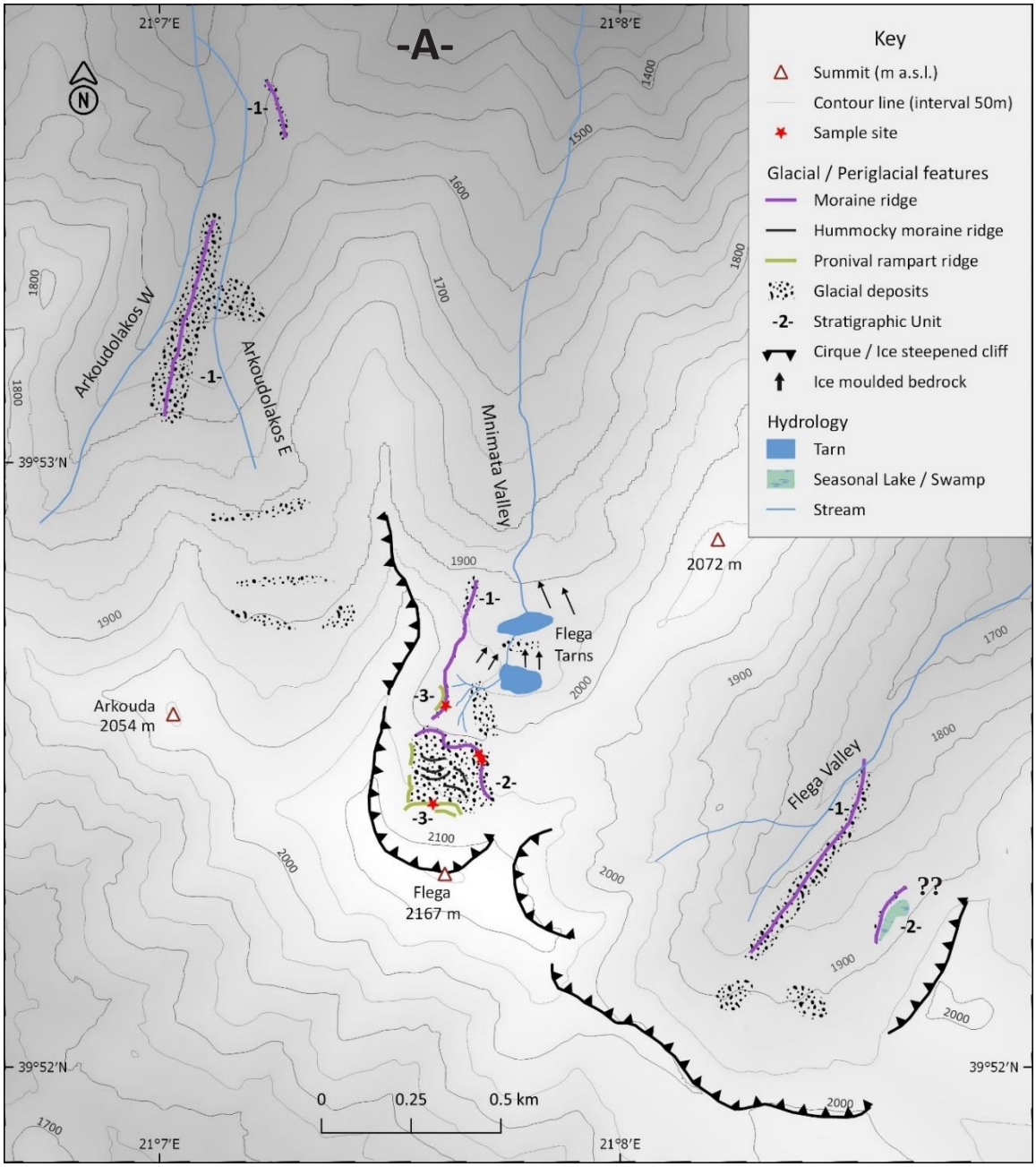

Figure 39. Glacial geomorphologic map of the study area on Mt Mavrovouni. This is panel A in Figure 32.

In the lower part of the valley (below 1900 m a.s.l.), a continuous lateral/termino-lateral moraine extending from 1740 to 1840m a.s.l. in altitude and 600m in length has been identified (Figure 39). The moraine converges to the modern river channel, indicating the position of the former glacier's snout, although the terminal frontal moraine must have been eroded from run-off water. This moraine has most probably been formed by a glacier originating from the central-western part of the NE Flega main cirque and the NE Flega sub-cirque but a source from the western section of the cirque cannot be excluded. The inner and steeper (western) flank of the moraine shows signs of considerable creep as the base of the trunks of the pine

trees growing there are downslope bended, typically indicative of creeping unstable soils (Figure 42). Moreover, a cross-section of this moraine has been exposed (Figure 43) where the morainic deposits haven been incised by a lateral tributary stream of the main Flega river. The small size of the stream and the relatively big incision it has caused to the moraine is an indication of how susceptible are these ophiolite-derived moraines to water erosion.

Figure 40. The moraine dammed seasonal lake/swamp on the eastern part of the upper Flega valley. (Photo: August 2016)

Figure 41. Glacially transported boulder within the glacial deposits damming the seasonal lake/swamp at the upper Flega valley. Notice the cracks in the boulder that upon further glacial working would have decomposed this 1.5m in diameter boulder into smaller clasts. (GPS device for scale) (Photo: July 2018)

Figure 42. The creeping inner flank of the Flega formation moraine (Photo: July 2018).

Observing the revealed exposure of the deposits, these ophiolite-derived glacial sediments are characterized by clast-rich lithology with sandy to muddy matrix which ares partly consolidated (Figure 43a and b). The clasts are striated and subrounded. Larger boulders do not exceed 1.5m in diameter and are mostly evident along the moraine crest (Figure 43c). Notably glacier boulders are smaller in size compared to limestone-derived moraines (e.g. in Mt Tymphi or in Mt Chelmos) and large blocks (>5m in diameter), more typical of granite/gneiss lithologies but also present in limestones, are absent probably due to the several cracks and joints present in the parent ophiolitic bedrock (e.g. Figure 41). These characteristics are in consistence with Middle Pleistocene glacial deposits of ophiolitic lithology from Mt Smolikas (Hughes et al., 2006d) and Mt Vasilitsa (Hughes, 2004). As it will be discussed later, the Flega formation could be correlated with the most extensive Middle Pleistocene Skamnellian/Vlasian Stages of northern Greece (MIS 12/MIS 6) on grounds of geomorphological context and altitude range of the deposits. This unit could represent more than one glaciation episodes but it was not possible to distinguish multiple moraine units that correspond to both stages.

Figure 43. The Flega formation moraine; a) ***(Top left):*** *the sandy to muddy matrix and unsorted gravels at the lowermost part of the exposure;* ***b) (Top right):*** *subrounded clasts supported by sandy matrix at the uppermost part of the exposure;* ***c) (Bottom):*** *larger subrounded and striated glacial boulders along the moraine crest (Photo: July 2018).*

4.3.1.2 Mnimata (Flega Lakes) valley

The Mnimata glacial valley extends below the summit of Mt Mavrovouni (Flega Peak at 2157 m a.s.l.) with a N orientation. It is typically U-shaped and headed by an ice-steepened, and well-developed cirque (Figure 44a). A detailed glacial geomorphological map of the valley is shown in Figure 45. The upper valley is characterised by a clearly shaped and well-preserved glacial/periglacial sequence of thick glacial deposits between 2050 and 2000 m a.s.l. which is the focal point of this research (Figure 44). The lower limit of the sequence is defined by a well-shaped terminal moraine. Two samples for ^{36}Cl exposure dating were taken from the moraine crest at 2017 m a.sl. (FLE-1 and FLE-2 in Figure 44a, Figure 45). The middle part of the sequence can be described as a hummocky moraine with scattered subrounded glacial boulders that must have formed upon the retreat of the former glacier that created the above-mentioned moraine. These deposits most probably have undergone further periglacial creep, without though any typical rock-glacial features as lobes.

Above these deposits, there is a sharp and continuous ridge mainly composed of large angular boulders that have been deposited at the centre of the cirque-floor. These boulders are considerably different in shape compared to the glacially worked and therefore subrounded boulders found lower in the main sediment unit. For this reason, these deposits are ascribed to a distinct younger stratigraphic unit (Unit 3 in Figure 39 and Figure 45). A sample was taken from a well-stabilised boulder on the crest of these deposits at 2038 m a.s.l. (FLE-4 in Figure 44b, Figure 45). Two minor crests of similar deposits are nested in the eastern part of the main ridge (Figure 44b). The main ridge along with the two minor crests of the angular deposits are interpreted as pronival ramparts that formed after the formation of the main sediment unit during persisting cold conditions that were sufficiently cold and humid for the formation of a permanent snow filed but unfavourable for the development of a dynamic icefield. Local topography and shading from the cirque-walls must have favoured the formation of this nevé field as it is absent elsewhere in the mountain. Further up-valley no boulders or clasts can be found, supporting the hypothesis of the formation of a pronival rampart during prevailing cold conditions with increased debris supply due to freeze-thaw weathering of the cirque walls.

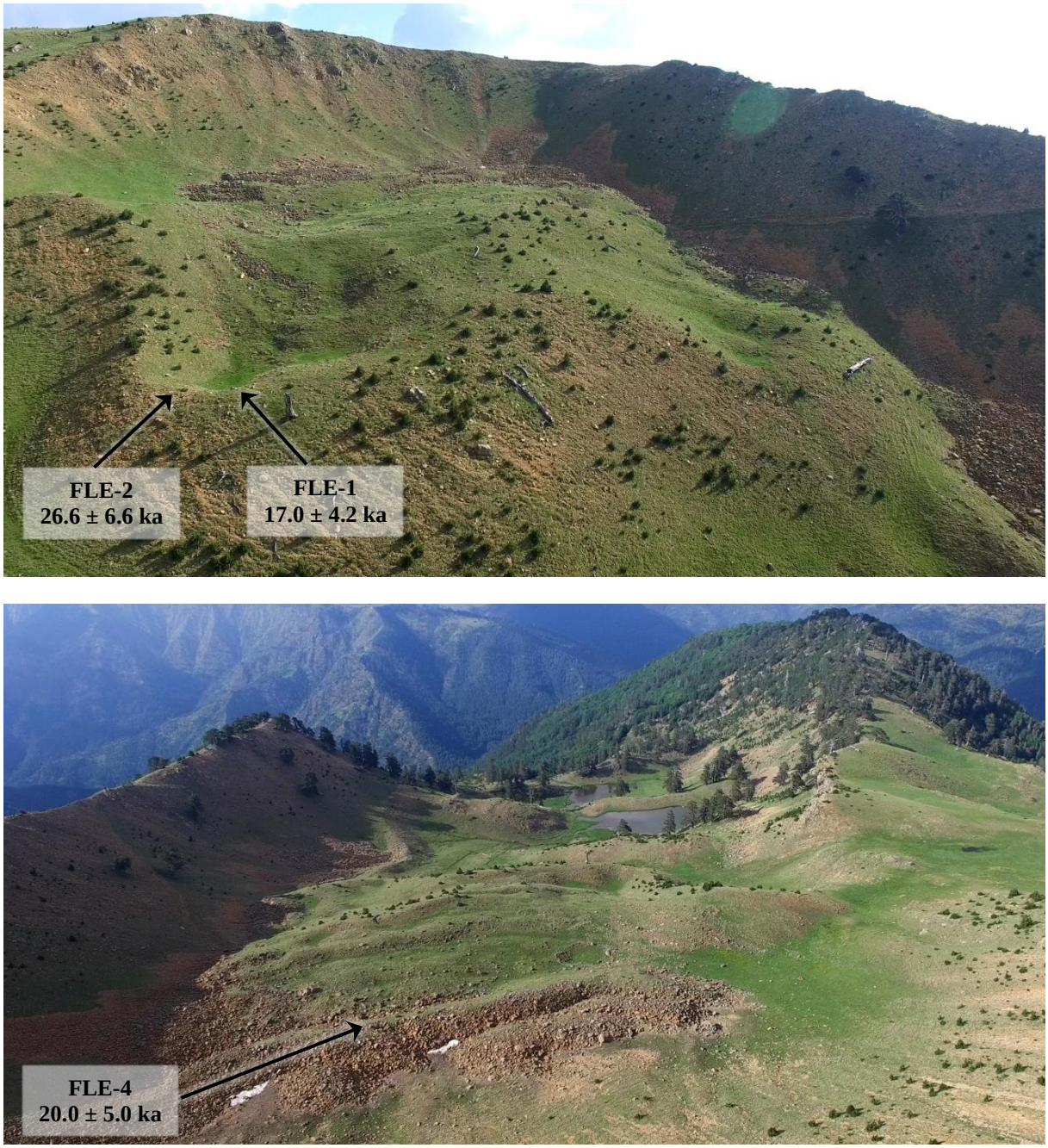

Figure 44. The upper Mnimata valley and the glacial/periglacial sequence along with sample locations for ^{36}Cl dating: ***a) (Top):*** *Looking up valley (S). Notice the terminal moraine delimiting this set of deposits in the foreground and the well-developed cirque;* ***b) (Bottom):*** *Looking down valley (N). Pronival deposits can be seen in the foreground along with the denoted sample location. In the background there are the Flega tarns sitting in ice-scoured hollows on the impermeable bedrock. Notice also the lateral moraine and trimline in the base of the western (left) flank of the valley (Aerial Photos: George Panayiotopoulos, June 2019)*

The middle part of the valley, extending between 2000 m a.s.l. and the treeline at 1850 m a.s.l. is characterised by two glacial lakes known as the upper and lower Flega lakes. The valley along this part is spilled with glacial boulders (Figure 45, Figure 46). Furthermore, a lateral moraine that in places is visible as a trimline extends between 2010 and 1880 m a.s.l. along the

western flank of the valley. It can also be clearly distinguished in the aerial photos that were captured with the drone (Figure 44b), although its down-valley extent is impossible to be established due to dense tree cover. This feature is correlated with glacial activity that predates the glacial/periglacial sequence in the upper valley that is described above and in particular it could be correlated with morphostratigraphic unit 1 deposits in the two adjacent valleys (Figure 39).

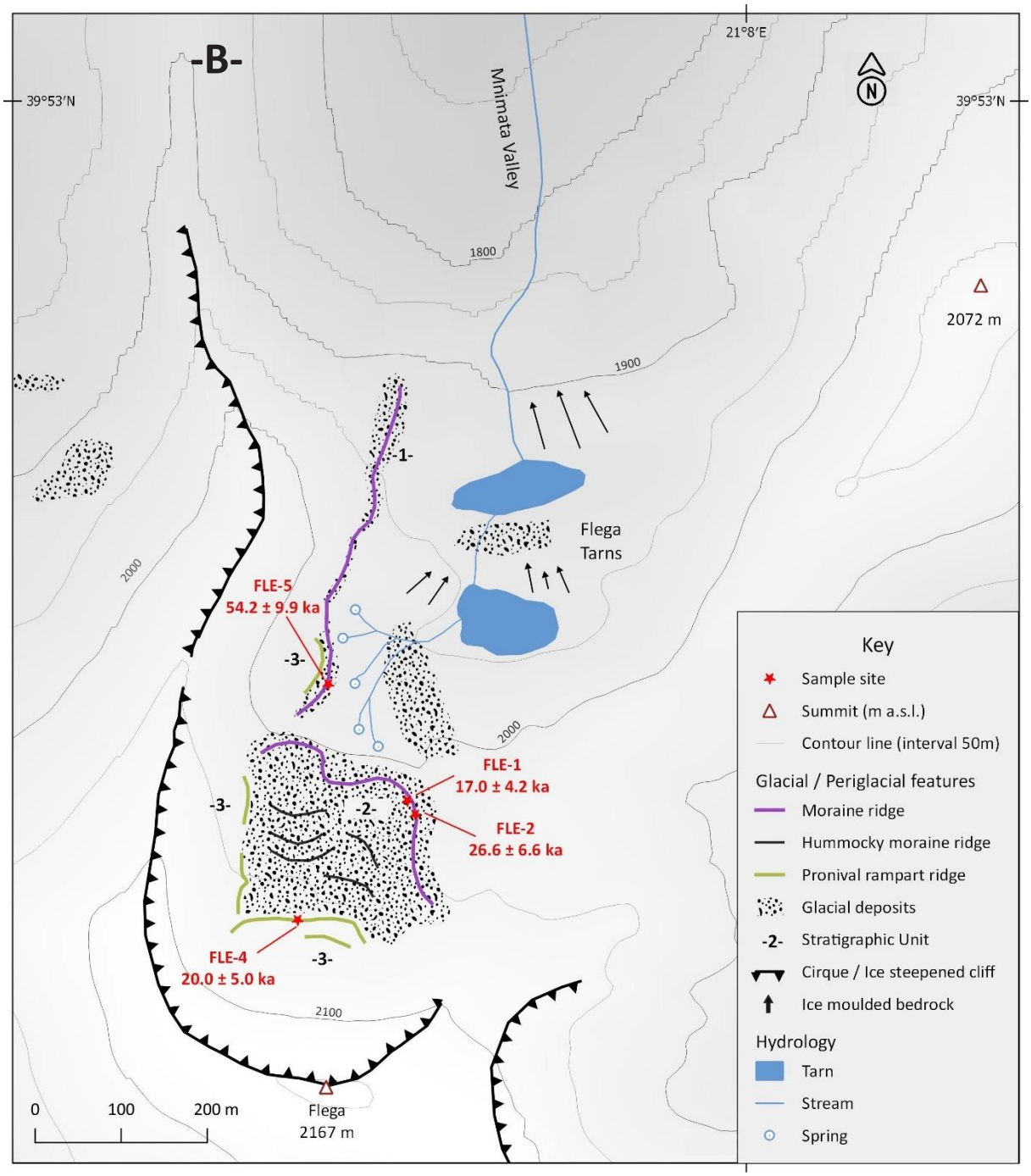

Figure 45. Detailed glacial geomorphologic map of the Mnimata Valley. This is panel B in Figure 32.

.

Figure 46. Glacially transported and sub-rounded boulders between the two tarns (Photo August 2016).

The upper part of this moraine has been overridden by pronival deposits (Figure 47) with similar characteristics to the pronival rampart that has been sampled at the upper part of the valley and therefore they have been ascribed to the same morphostratigraphic unit (Unit 3 in Figure 39 and Figure 45). A sample for ^{36}Cl dating has been taken from the crest of these deposits at 1980 m a.s.l. (FLE-5 in Figure 45 and Figure 47). Behind the crest there are angular debris that were most probably deposited after the disappearance of the nevé field.

Figure 47. The upper part of the lateral moraine at the W flank of the valley that has been partially buried under pronival rampart deposits. Sample location FLE-5 is also denoted. Notice the streams nourishing the upper Flega tarn that spring below the deposits and onto the ice-scoured exposed impermeable bedrock that also host the two tarns (Photo August 2016).

As regards the two lakes, notably, they are indeed glacial in origin but are not moraine-dammed as initially expected from the analysis of satellite imagery. Actually, they sit on ice scoured hollows on the impermeable bedrock (Figure 46). It is indicative that there are at least five springs just above the upper lake where the aquifer meets the exposed impermeable bedrock (Figure 45, Figure 47). These springs nourish the two lakes. More importantly though, ice-scoured and polished bed-rock has been identified just below the lower tarn at 1900 m a.s.l. that still bares clear striations in the direction of the paleaoglacier ice-flow on its surface (Figure 48). This indicates minimum erosion of the rock surface (Gosse and Philips, 2001) and confirms the neglection of erosion in the calculation of exposure ages of glacial boulders described in section 4.2.5. Moreover, if the paleo-glacier that scoured the bedrock and also formed the two tarns is correlated with the above-mentioned lateral moraine/trimline and the lowermost glacial deposits from the two adjacent valleys that have been attributed to morphostratigraphic unit 1, the surface exposure dating of this bedrock could be used for the first time to independently test the Middle Pleistocene chronology in the Balkans that until now is based on U-series of secondary calcites from limestone-derived moraines. Finally, the lower part of the valley that extends below the treeline is difficult to reach and the down-valley limit of the conducted fieldwork was limited to some tens of meters below the lower of the two tarns.

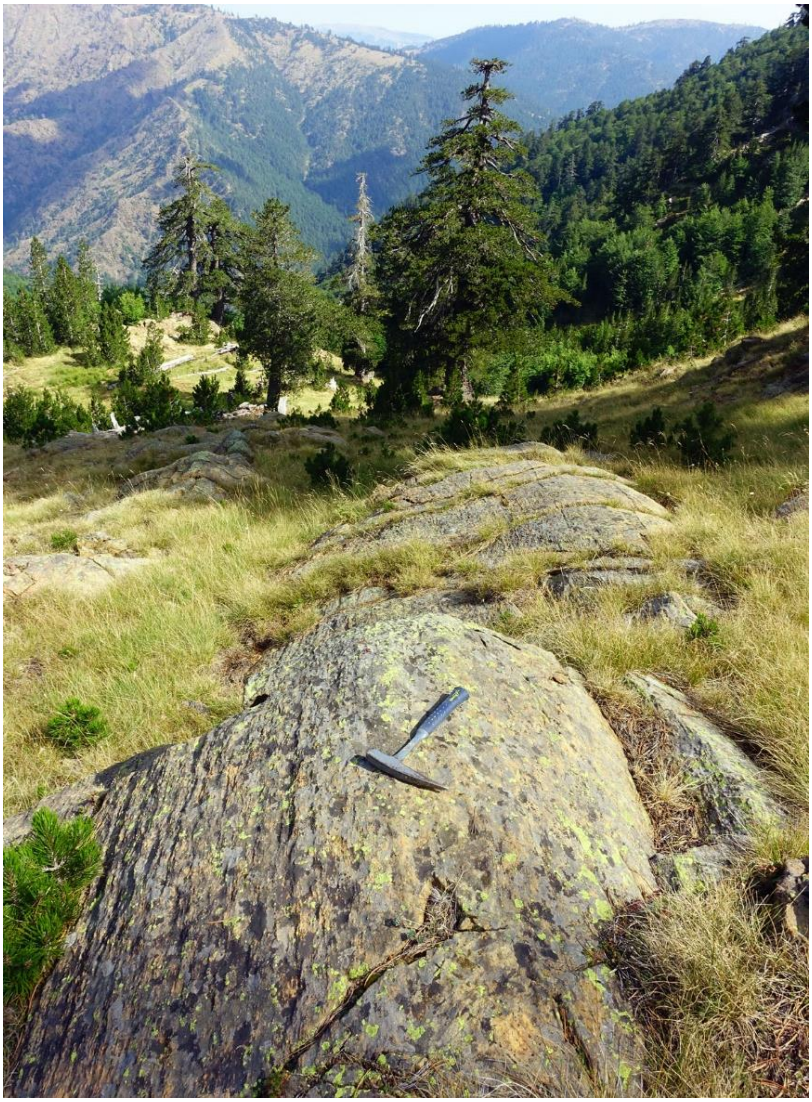

Figure 48. Ice-polished bedrock with well-preserved striations below the lower Flega tarn indicative of very low erosion rates (Photo August 2016).

4.3.1.3 Arkoudolakos (Bear) valley

The upper part of the Arkoudolakos glacial valley includes two converging valleys with similar characteristics (Figure 39). The western branch has a NE orientation and is quite steep and inaccessible so it was excluded from field work. Moreover, the identification of glacial geomorphologic features from satellite imagery is also difficult due to the pine-forest cover. The eastern branch (N orientation) though has been studied in detail. This branch is a U-shaped and wide valley but its head is really smooth and does not bear typical glacial geomorphological features like a cirque or ice-steepened headwalls (Figure 49).

Figure 49. The U-shaped E branch of the upper Arkoudolakos valley. The red dashed line denotes the lateral moraine that extends below the confluence of the two upper valley branches. (Photo August 2016)

However, scattered glacial boulders and remnants of sub-glacial till are evident throughout the upper part of the valley (e.g. Figure 50). Similarly, to the Flega valley the depositional limits are indistinct and although these deposits could be correlated on terms of altitude with morphostratigraphic unit 2 deposits from the two adjacent valleys they could also be synchronous to the older and more extensive deposits lower in the valley that belong to morphostratigraphic unit 1 (Figure 39).

Figure 50. Sub-rounded glacier boulder right on the treeline of the upper Arkoudolakos valley. (Photo August 2017)

The main valley has a N orientation, is densely forested and along its central axis has undergone - typical for ophiolites - V-shaped erosion by run-off water. Two moraines have been identified in the lower part of the main valley that are ascribed to the Bear formation. The first is a clear and well-shaped lateral moraine that extends right from the point where the two upper branches of the valley converge at 1660 m. a.s.l. (Figure 49) and down to 1500m a.s.l. where it has been washed away by the river that runs along the valley (Figure 51). Its total length is about 800 m. The second moraine is a termino-lateral moraine extending from 1510 to 1470 m a.s.l. and only 300 m in length, but most importantly it defines the down-valley extent of the glacier that formed these two moraines. Both moraines are covered by dense beech forests and thus are unrecognisable from satellite imagery and difficult to capture with a handheld camera as well. Finally, it should be noted, that no exposures of the moraines were discovered. The Bear formation is correlated with the Flega formation and is ascribed to morphostratigraphic unit 1 (Figure 39). This unit is in turn correlated with the most extensive Middle Pleistocene Skamnellian/Vlasian Stages of northern Greece (MIS 12/MIS 6). Similarly to the Flega valley, although this unit could represent more than one glaciation phases it was not possible to distinguish multiple moraine units that correspond to both stages.

Figure 51. The Bear formation moraine; ***a) (Top left)****: large glacial boulder (d~2 m) along the densely forested moraine,* ***b) (Top right):*** *subrounded and striated boulders and clasts along the well-shaped moraine crest and;* ***c) (Bottom):*** *another glacially transported large boulder next to the path that runs along the moraine ridge (backpack length ~0.6 m for scale) (Photos July 2018).*

4.3.2 Chronology

As described above, sampling was limited to the stratigraphically youngest set of glacial deposits in the Mnimata valley. The yielded ^{36}Cl exposure ages for the main terminal moraine samples FLE-1 and FLE-2 were 17 ± 4.2 ka and 26.6 ± 6.6 ka respectively. The older age is considered to be the most representative for moraine deposition (Ivy-Ochs and Kober, 2008; Ivy-Ochs and Briner, 2014), whilst the younger one may represent a period of moraine

degradation and boulder exhumation as also argued by Allard et al. (2020) in their study on glacial chronology of moraines of similar age in the nearby Mt Tymphi with the application of ^{36}Cl exposure dating on glacial boulders. The alternative interpretation of taking a mean value of the landform ages is susceptible to inaccuracies (Ivy-Ochs et al., 2007) especially if incomplete exposure and moraine dismantling are suspected (Applegate et al., 2010; D'Arcy et al., 2019). Moreover, sample FLE-1 was taken from the inner side of the moraine which is more susceptible to degradation and mass wasting processes while FLE-2 was taken from one of the highest points on the moraine ridge making it less likely to have undergone significant exhumation. This moraine is thus considered to have been formed by an advancing cirque glacier when it reached its maximum extent close in time to the global LGM (27.5-23.3 ka; Hughes and Gibbard, 2015) as the yielded age of sample FLE-2 at 26.6 ± 6.6 ka falls within this interval.

As regards the pronival ramparts at the uppermost part of this set of deposits (FLE-4) and at the western flank of the upper valley (FLE-5) that were expected to have formed synchronously, the samples yielded ages of 20.0 ± 5.0 ka and 54.2 ± 9.9 ka respectively. The most representative age for the formation of these periglacial features is considered to be the younger one as the pronival ramparts in question are stratigraphically younger than the terminal moraine ridge that was dated to 26.6 ± 6.6 ka. Moreover, the FLE-4 sample was taken from a large and well stabilised boulder on the highest point of the pronival rampart within a section of angular deposits lacking finer material and therefore minimising the probability of exhumation or other mass wasting processes. On the other hand, the FLE-5 age could have been affected by inheritance of ^{36}Cl atoms from previous exposure, for example when it was still attached to the cirque wall. However, marked inheritance in moraine boulders is rare (Heyman et al. 2011) and incomplete exposure is more likely to be an issue (Ivy-Ochs and Briner, 2014). Therefore, a more probable interpretation is that this boulder was actually deposited alongside the lateral moraine that has been ascribed to glacial activity during Middle Pleistocene and correlated with Unit 1 deposits in this and the two adjacent valleys. In this case, the boulder was part of this moraine that has been deformed by a nevé field and partly buried under pronival rock slope failure deposits. The age of this sample could then represent a period of boulder exhumation.

4.4 Reconstructing the glacial history of Mt Mavrovouni

Mt Mavrovouni has clear evidence of glaciation, such as moraines, glacially transported boulders, ice-steepened cirques, U-shaped valleys, tarns and ice-polished and striated bedrock.

A reconstruction of the glacial history of Mt Mavrovouni using the presented evidence is summarised in Table 15. The reconstruction of the palaeoglaciers and the calculationof the respective ELAs were conducted with the use of the GIS toolbox and the methodology described in section 2.3. Only the palaeoglaciers in the Aroudolakos valley and in the Mnimata valley corresponding to morphostratigraphic units 1 and 2 respectively (Figure 39) were reconstructed as elsewhere the definition of the glacial limits based on the identified geomorphological evidence is subject to excessive uncertainties.

The most extensive glaciation(s) was characterised by valley glaciers in northern slopes that reached down to 1500 m a.s.l. The most representative reconstructed glacier for this phase was the Arkoudolakos valley glacier which had an ELA of 1785 m a.s.l., covered an area of ~0.63 km^2 and was ~1.98. km long. This phase remains undated but is likely to be Middle Pleistocene in age as they could be correlated with the stratigraphically oldest moraines identified in the studied glacial valleys on Mt Tymphi and dated with uranium-series (Hughes et al. 2006a; section 3.1.1). On Mt Tymphi there have been identified two Middle Pleistocene phases, the Skamnellian (MIS12) and the Vlasian Stages (MIS6). However, on Mt Mavrovouni the largest glaciation is represented by a single morphostratigraphic unit (Unit 1 in Figure 39) Nevertheless, similarly to Mt Chelmos, where multiple moraine units that could correspond to both Skamnellian and Vlasian Stage glaciations could not be identified (Pope et al., 2017), it is possible that more than one glaciation is represented by the morphostratigraphically older unit.

Table 15 Glacial morphostratigraphic units on Mt Mavrovouni

Morphostratigraphic Unit	Altitude Range mean ELA	Age (*^{36}Cl dating)*	Glacial Stage and corresponding MIS
3	1950-2050 m a.s.l. ELA n.a.	20.0 ± 5.0 ka	MIS 2 -LGM to Late-glacial
2	1950-2040 m a.s.l. ELA –1785 m a.s.l.	26.6 ± 6.6 ka	MIS 2 - LGM
1	1470 -1840 m a.s.l. ELA – 2090 m a.s.l.	correlation with Middle Pleistocene glacial phases	MIS 12 – Skamnellian Stage MIS 6 – Vlasian Stage

The morphostratigraphic analysis and the ^{36}Cl ages from the glacial/periglacial sequence in the upper Mnimata valley provides further insight into the Late Pleistocene glaciation on Mt Mavrovouni. The older of the ^{36}Cl exposure ages obtained from the terminal moraine of

morphostratigraphic unit 2 (Figure 45) suggests that the local glacial maximum during Late Pleistocene took place at 26.6 ± 6.6 ka within the LGM (27.5-23.3 ka ; Hughes and Gibbard, 2015). The age uncertainty suggests that this glacial phase could predate or postdate the LGM by 5 ka and 3 ka respectively. However ^{36}Cl Ages from Mt Tymphi (section 3.1.1.2) and Mt Chelmos (section 5.5) calculated with similar production rates as the ones used in this research suggest a pre-LGM Late Pleistocene glacier maximum at 29.0 ± 3.0 - 25.7 ± 2.6 ka and 36.5 ± 0.9 - 28.6 ± 0.6 ka respectively. Therefore, a pre-LGM to LGM local glacier maximum on Mt Mavrovouni is more likely. The glacier in the Mnimata valley at this stage had an ELA of 2090 m a.s.l., covered an area of ~0.1 km^2 and was ~0.35 km long. There is no evidence for the timing of glacier retreat after this pre-LGM to LGM local glacier maximum but evidence from Mt Tymphi (section 3.1.1.2) and Mt Chelmos (section 5.5) suggest that LGM glaciers had retreated by 24.5 ± 2.4 ka and by 22.2 ± 0.3 - 19.6 ± 0.5 ka (section 5.5) respectively.

As regards the peroglacial pronival rampart deposits of the same sequence which were ascribed to morphostratigraphic unit 3 (Figure 39 and Figure 45), the most representative ^{36}Cl age has placed their formation at 20.0 ± 5.0 ka. The interpretation argued here is that after the local Late Pleistocene maximum around the LGM at 26.6 ± 6.6 ka and the subsequent glaciers retreat, cold conditions persisted until 20.0 ± 5.0 ka when the presence of perennial snow/ nevé fields along the topographically shaded cirque slopes and the increased debris supply due to freeze-thaw weathering of the cirque walls combined with rock slope failures led to the deposition of these pronival ramparts. The evidence of periglacial features during this transitional phase from the LGM to the Late-glacial suggests that unfavourable conditions for the formation of glaciers prevailed but were cold/humid enough to preserve perennial snow fields in topographically favourable positions close to the cirque walls. This is further supported by initial results on Mt Tymphi, suggesting that small glaciers (<0.6 km^2) persisted in the northeast cirques at 18.0 ± 1.9 ka perhaps sustained by avalanching snow and topographic shading from the Goura cliffs (Allard et al., 2020).

4.4.1 Application of cosmogenic ^{36}Cl exposure dating on ophiolitic lithologies

One of the main novelties of the geochronological study of glacial deposits on Mt Mavrovouni is the application of cosmogenic ^{36}Cl exposure dating on ophiolitic boulders for the first time. Although small in number, the presented ^{36}Cl ages are in consistence with the chronology of Late Pleistocene glaciations on the limestone-dominated Mt Tymphi and Mt Chelmos as it has been shown. This is of great importance from a methodological point of view as it proves in practice that the application of cosmogenic ^{36}Cl dating on ophiolites, which

was in principle possible, is indeed applicable. This conclusion opens up the perspective of dating the only complete glacial sequence identified in Greece which has been mapped on the ophiolitic Mt Smolikas (see section 3.1.2). Moreover, the ^{36}Cl dating of ophiolite samples with high Fe_2O_3 content (8-8.5 wt %) contributes on the validation of current scaling behaviour and ^{36}Cl production rates from Fe spallation for which further data from high Fe-content samples is needed (Moore and Granger, 2019).

As regards the wider framework of Quaternary glaciations in Greece, this record constitutes the only chronology of Late Pleistocene glaciations on the mountains of Greece that is independent from inherent issues in surface exposure dating of limestones such as the erosion rate of rock surfaces. The importance of independent age constraints is also stressed by Ivy-Ochs and Kober (2008)

Chapter 5. Mt Chelmos: Geomorphological evidence, geochronology and update of glacial reconstructions

A part of the glacial morphological study and OSL dating work that is presented in this chapter has been included in the journal publication of Pavlopoulos et al. (2018).

5.1 Setting of Mt Chelmos

Mt Chelmos forms part of the mountain chain of the External Hellenides and rises to 2355 m a.s.l., favouring the accumulation of snow which does not melt until late summer. Its distance from the coastline is only 25km, reflecting the intense tectonic uplift rates in the region. In particular, although plate movements and orogenesis are still active far to the west, the Gulf of Corinth, immediately to the north of Mt Chelmos, is a very active fault-controlled rift, with contemporary uplift of the Peloponnese leading to new faulting (Figure 52; Pope et al. 2017 and references therein). On the basis of geologic data and uplifted topography the estimated vertical uplift rates range from 0.3 mm/yr (Collier et al., 1992) to 1.1 mm/yr since at least 0.5 Ma (De Martini et al., 2004; McNeill and Collier, 2004) and 1.55 mm/yr over the last 350ka (Armijo et al.,1996). During the Holocene rates are increasing to 1.3–2.2 mm/yr (Stewart, 1996; Stewart and Vita-Finzi, 1996) and up to 3-3.5 mm/yr (Pirazzoli et al., 2004).

Mt Chelmos is formed by a geological sequence of three distinct tectonic units. The first (upper unit) corresponds to the Olonos-Pindos Unit, which consists of pelagic limestones and radiolarites of Mesozoic age which are overlain by Tertiary flysch (Pope et al., 2017). The second intermediate unit corresponds to the Gavrovo-Tripolis Unit, mainly composed of Upper Triassic-Upper Eocene carbonate formations (Pavlopoulos et al., 2018). These two geological zones bear similar geological/lithological properties but differ as to the geological age. The presence of carbonate formations (highly soluble in water), the supply of water from melting ice, and the precipitation and the influence of tectonism have led to significant karstic processes on Chelmos. As a result, notable karstic landforms can be observed in the study area in the western part of the massif (Figure 53), such as a polje, karstic sinkholes, dolines, caves, karstic springs etc (Pavlopoulos et al., 2018). The northeastern lower slopes of the mountain are composed of high-pressure/low-temperature metamorphic rocks of the lowest Phyllites–Quartzites Unit that formed during the main alpine orogenesis, which culminated in the Oligocene and Miocene,while subsequent orogenic processes resulted in the exhumation of these metamorphic rocks (Skourtsos and Kranis, 2009; Skourtsos and Lekkas, 2011).

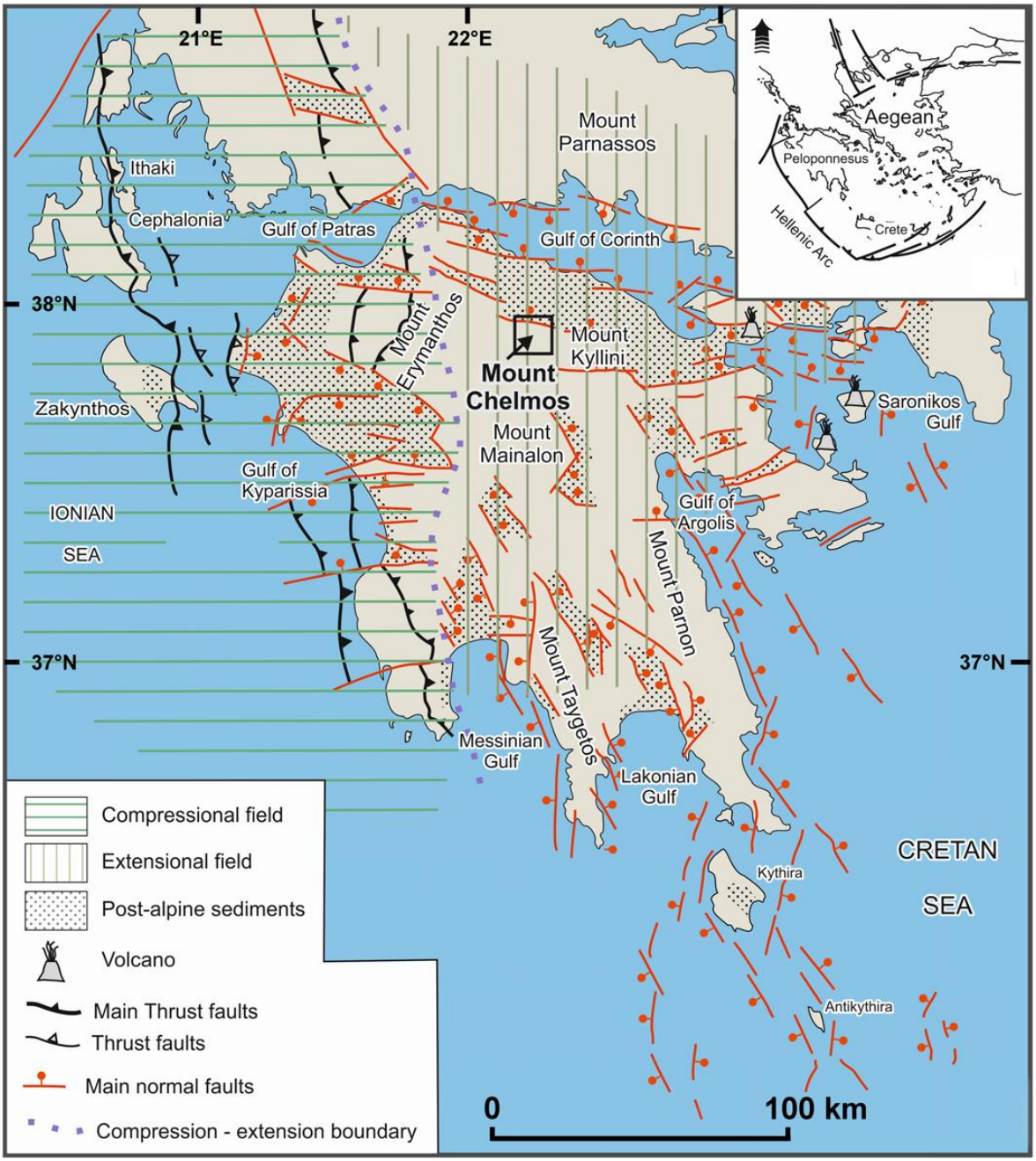

Figure 52. Location of Mt Chelmos in Greece showing the major tectonic features of the area. (From Pope et al., 2017)

The study area of this research includes the southwestern part of Mt Chelmos, which includes the Loussoi polje (Figure 53). Likewise, sedimentary formations (northern part) of later age can be seen. The most recently deposited sediments (Pleistocene-Holocene age) can be found in the north-western part (gravels) and in the central part of the area depicted in Figure 53. These types of sediments are mainly transported and deposited by surface runoff along with gravitational processes.

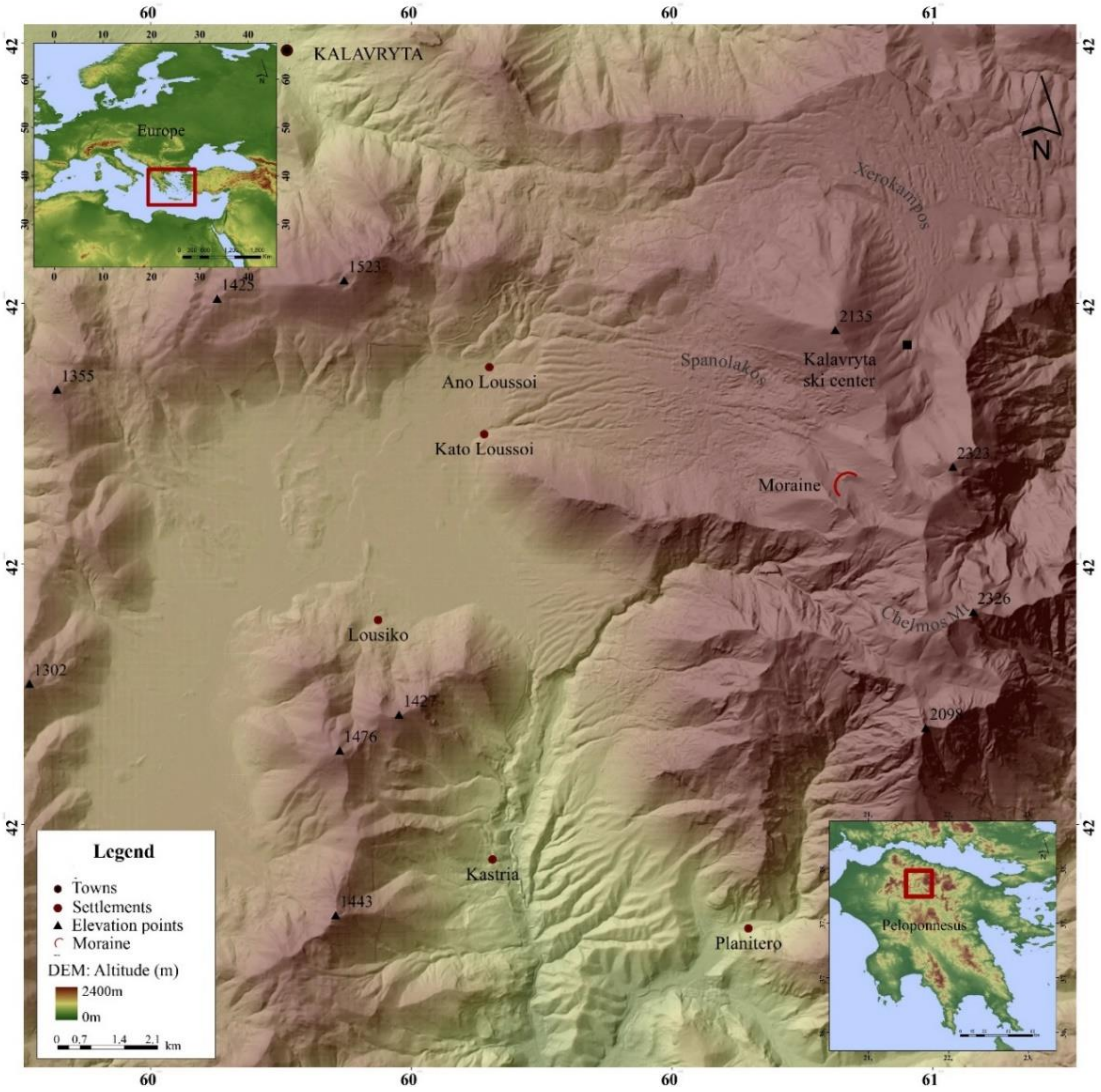

Figure 53. Location map of the study area on Mt Chelmos (from Pavlopoulos et al., 2018)

Several glacial landforms can be distinguished within the study area (e.g. Figure 54). A full review of all glacial studies on the massif is given in section 3.3. As the aim of this study was to provide further evidence and timing constraints on the glaciation history of Mt Chelmos, a moraine within the Spanolakos glacial valley, which drains the north-western flank of the mountain to the polje of Ano Loussoi, was selected as the most representative high-altitude glacial feature to be dated. The location of the moraine can be seen in Figure 1. This clear arcuate termino-lateral moraine has also been identified by Mastronuzzi et al. (1994) and Pope et al. (2017) and, although it has never been dated, it has been correlated by Pope et al. (2017) with other dated units based upon their morphostratigraphy. Its formation has therefore been attributed to a glacial advance/stabilization phase during 40-30 ka. In the framework of this study, it was decided to collect samples from this moraine and date them in 2014 before the

first version of the study of Pope et al. (2017) which was published in 2016. Still, the yielded ages of the samples are useful in order to test the above-mentioned assumptions.

Figure 54. Glacial cirque at the uplands of Mt Chelmos (Photo: February 2015)

The nearest climatic data are available from the Akrata, Ano Loussoi and Kalavryta weather stations (Table 16). When mean temperatures for these two stations are extrapolated using a lapse rate of 0.6º C per 100 m of altitude, the mean annual temperature at 2000 m a.s.l. is about 5.3º C while the mean monthly temperatures for July and January are 13.8 ºC and -3.0ºC respectively. It is notable that these mean temperatures are similar to the ones calculated for Mt Mavrovouni in Nortwestern Greece regardless a difference of more than one degree in latitude (λ=22.1º and 21.05º for Mt Chelmos and Mt Mavorvouni respectively). With a mean annual precipitation of 933mm for the four stations at an average altitude of 647 m a.s.l. the mean annual precipitation at 2000 m a.s.l. is expected to exceed 1500 mm based on a linear interpolation of the precipitation in Akrata (160 m a.s.l.) and Kalavryta (731 m a.s.l.). Snow cover on the northern slopes above 1800 m a.s.l. lasts from late December to early May. The precipitation is strongly seasonal, with a wet winter season and arid summers typical of a Mediterranean climate (Koutsopoulos and Sarlis, 2003). No glacier permafrost or permanent snow field survives on Mt Chelmos today.

Table 16. Precipitation and temperature data from weather stations near Mt Chelmos (data from Gouvas and Sakellariou, 2011; reference period>20yr)

Meteorological Station	Altitude (m a.s.l.)	Annual Precipitation (mm)	Mean Temperature (°C)		
			Annual	Jan	Jul
Akrata	160	867	17	8.5	26.1
Ano Loussoi	1050	-	10.5	2.4	18.9
Kalavryta	731	999	12.8	4.5	21.7
Mean	647	933	13.4	5.1	22.2
Mt Chelmos (Extrapolation)	2000	>1500 mm	5.3	-3	14.1

5.2 Geomorphological mapping

Geomorphological mapping was conducted following the principles described in section 2.1. Research was initiated by collecting maps and satellite imagery. The second stage of the geomorphological mapping involved the *in-situ* collection of data. During fieldwork many landforms, as well as a number of topographical and geological features, which were not apparent or recognizable on the maps and images of the study area, were documented. Finally, during the fieldwork four (4) samples from a glacial moraine were collected and dated by the OSL method. The obtained results were proved to be very useful for further defining the glaciation phases of Mt Chelmos during the Tymphian Stage (MIS 5d-2).

5.2.1 Topographic data

The topographic maps that were used in this study included the large scale (1/5,000) topographic sheets of Loussoi and the surrounding area, by the Hellenic Military Geographical Service, as well as the medium scale (1/50,000) geological map from the Institute of Geology and Mineral Exploration (IGME, 1977; 1978). The topographic maps provided the 4-meter contours. In the areas where the slope was less than 15° the 4 m and the 2 m contours were digitized in order to enrich the Digital Elevation Model (DEM) provided by the National Cadastre (cell size 5 m). Cirques, moraines and glacial valleys have first been detected from the observation of the high-accuracy orthophoto (see following section) and the DEM. During fieldwork these landforms have been spotted, recorded and mapped with a GPS device.

5.2.2 Remote sensing data

Remote sensing data included large scale aerial photos by the National Cadastre, Quickbird satellite images, ALOS imagery and Google Earth imagery, which were used to enhance the DEM. These combined with orthophotos provided significant information on the glacial, periglacial and karstic features within the study area and contributed towards creating a representative geomorphological map.

5.2.2.1 Advanced Land Observing Satellite (ALOS)

Almost all environmental and geological studies need quite accurate elevation data with global coverage. The increased need for elevation data has simultaneously accelerated the development of algorithms for automatic Digital Surface Model (DSM) extraction (Toutin 2001, 2004). As described in Nikolakopoulos et al. (2006) the along-track stereo-data acquisition is superior as it reduces radiometric image variations (refractive effects, sun illumination, temporal changes) and thus increases the correlation success rate in any image matching. The vertical accuracy of ALOS PRISM DSM created with photogrammetric techniques has been assessed in many studies worldwide (Takaku et al., 2007, 2008; Maruya and Ohyama, 2007, 2008; Gruen and Wolff, 2007; Lamsal et al., 2011) and for the Greek territory especially (Nikolakopoulos and Vaiopoulos, 2011; Nikolakopoulos, 2013). In general, the vertical accuracy of ALOS DSM ranges between 2 and 3 m and thus ALOS DSM is characterized as one of the most accurate sources for elevation data.

5.2.2.2 PRISM data Processing

The automatic DSM creation from ALOS PRISM stereopair is described in detail in Nikolakopoulos et al. (2010). A PRISM data set acquired in 2008 over Chelmos Mountain (provided freely by The European Space Agency) was used in this study. A stereo pair (Nadir and Forward) with a base to height ratios (B/H) of 0.45 was processed using Leica Photogrammetry Suite (LPS). Twenty-five ground control points and more than forty tie points were used. A DSM with a pixel size of 7.5 m was created and no further processing (editing) was performed. The vertical accuracy of the DSM from PRISM data was controlled using 145 ground control points very well spread around the study area. The RMS error was calculated at 7.7 m an acceptable according to the sensor specifications and the steep relief. A final orthophoto with 2.5 m spatial resolution was created and used in the suite of this study with the respective DSM.

5.2.3 Semi-automated geomorphological mapping

Basic criteria for the identification of the landforms were slope and lithology. Specifically, according to Van Asselen et al. (2006) topographic gradients greater than 35 degrees were treated as cliffs (alpine formations) while in case these gradients were within a buffer zone of 20 m from streams they were treated as down-cut erosion. Finally, topographic gradients between 5 and 35 degrees were treated as deposit cones and debris (post alpine deposits). The areas that were marked by the automated process were verified by remote sensing images (ALOS orthophoto, Google Earth) and fieldwork. The shapes of the valleys, down-cutting erosion and gorges were identified by the combined study of the topographic maps, the slope map and fieldwork, while landforms like caves, were mainly identified through literature and fieldwork.

5.2.4 Geomorphological map composition

The geographical entities were classified according to their characteristics following the rules of cartographic generalization, abstraction and simplification (Gustavsson, 2006). Specifically, discrete levels of information were generated concerning topographical, hydrographical, geological and geomorphological features. Lithology, tectonics, and geomorphology is generally in accordance with most geological and geomorphological maps (Pavlopoulos et al. 2009). In general, the aim was to create a final geomorphological map, which along with its legend is self-explanatory (Figure 55). Since the contours are displayed with light shades of grey, indication of the relief inclinations was essential as an additional feature of the morphology, in order to improve the map clarity.

5.3 Geomorphology of study area

The landscape of the study area is characterized by karstic, fluvial and glacial landforms. The most significant karstic landform is situated at the center of the map and can be described as a smooth relief (low inclination) area. It has been formed by the dissolution of limestone, and it is characterized as a polje (Tsoflias, 1973; Koutsi and Stournaras, 2011). The Ano-Loussoi polje is mainly infilled by alluvial deposits-sediments transported by the fluvial and glacio-fluvial processes. These torrents are nourished by the melting of the seasonal ice and snow during spring/summer, as well as by rainwater during winter, to form the main stream of the polje known by the toponym "Mana Stream" (Koutsi and Stournaras, 2011).

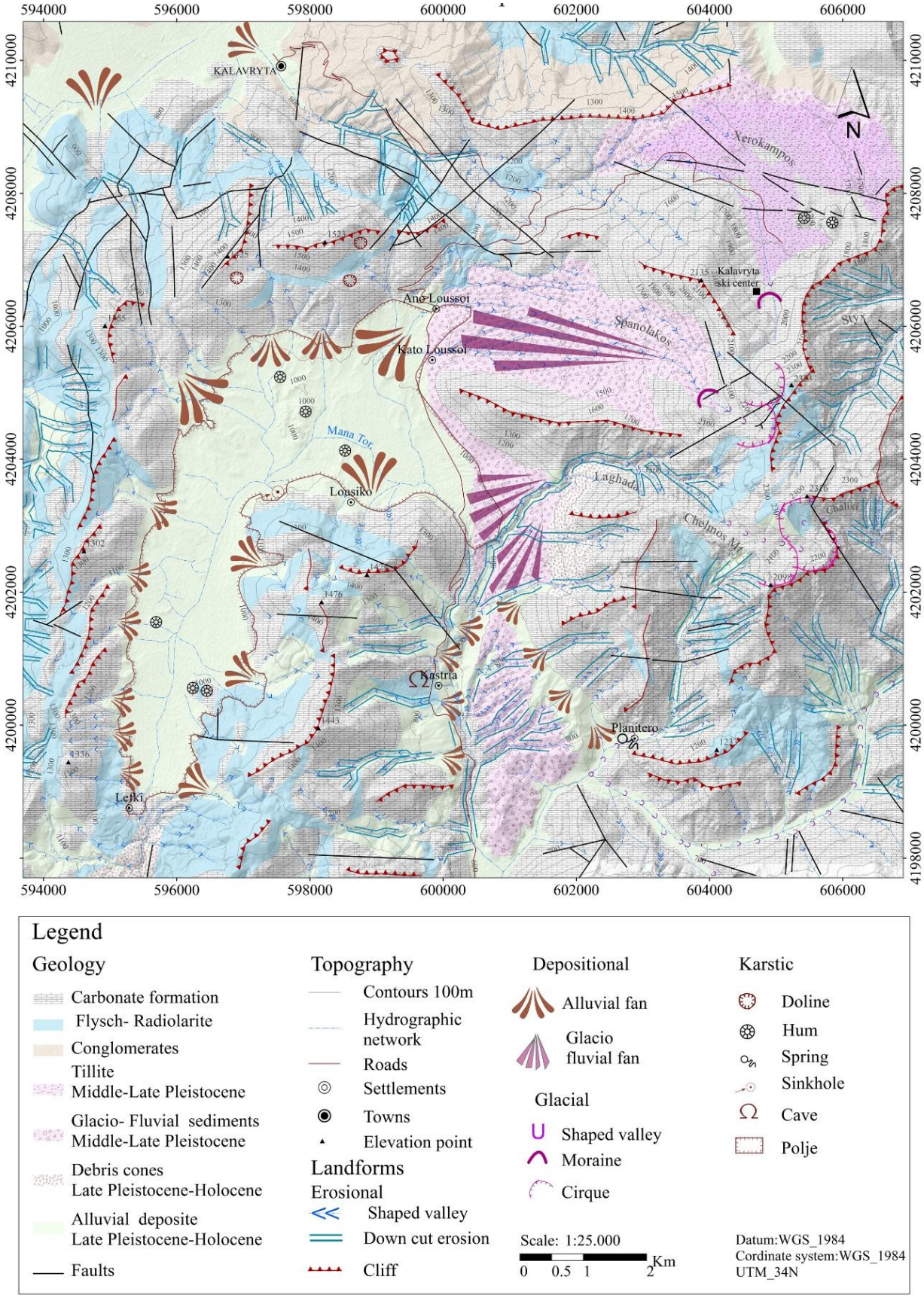

Figure 55. Geomorphological map of the study area: geology and landforms (from Pavlopoulos et al., 2018)

This stream actually drains the whole area through two karstic sinkholes within the polje. Moreoever, the presence of the karstic springs in Planitero village and the presence of sinkholes in the western part of Loussiko village (located in the centre of the map) provide additional indications about the intensity of karstic processes.

5.3.1 Glacial and glacio-fluvial features

Glacial landforms can be found mainly in the northern-eastern part of the study area in altitudes between 1500-2200 m a.s.l. Cirques are situated on the higher part of Mt Chelmos, in the eastern part of the geomorphological map (Figure 55, Figure 56), at altitudes between 2000 and 2200 m a.s.l. and have also been reported by Mastronuzzi et al. (1994) and Pope et al. (2017). Most interestingly, on Mt Chelmos there is a number of glacial valleys reported also in the studies of other researchers (Philippson 1892; Maull 1921; Mistardis 1937b,c, 1946; Mastronuzzi et al. 1994; Pope et al. 2017). Within the study area of the present thesis the most interesting examples are the valleys of Spanolakos, the valley of Xerokambos where the Kalavryta ski resort is located and the valley of Laghada in the central part of the study area (Figure 55). For reasons of consistency, the three morphostratigraphic units defined by Pope et al. (2017) have been used to correlate the different glacial features, deposits and sedimentary units. These morphostratigraphic units along with the ^{36}Cl exposure ages are summarized in Table 17 and Figure 56.

Table 17. Glacial morphostratigraphic units of Mt Chelmos according to the study of Pope et al. (2017)

Morphostratigraphic Unit	Altitude Range mean ELA	Age (^{36}Cl dating)	Glacial Stage (corresponding MIS)
3	2100 m a.s.l. ELA – 2174m a.s.l.	12.6 ± 0.9 - 10.2 ± 0.7 ka	MIS 2 - Younger Dryas
2 (Retreat Phase)	2200 m a.s.l. ELA – 2046m a.s.l.	22.9 ± 1.6 - 21.2 ± 1.6 ka	MIS 2 – Global LGM - Tymphian Stage
2	1600-2100 m a.s.l. ELA – 2046m a.s.l.	39.9 ± 3.0 - 30.4 ± 2.2 ka	MIS 3 - Tymphian Stage
1	950-1450 m a.s.l. ELA – 1967 m a.s.l.	correlation with Middle Pleistocene glacial phases	MIS 12 – Skamnellian Stage MIS 6 – Vlasian Stage

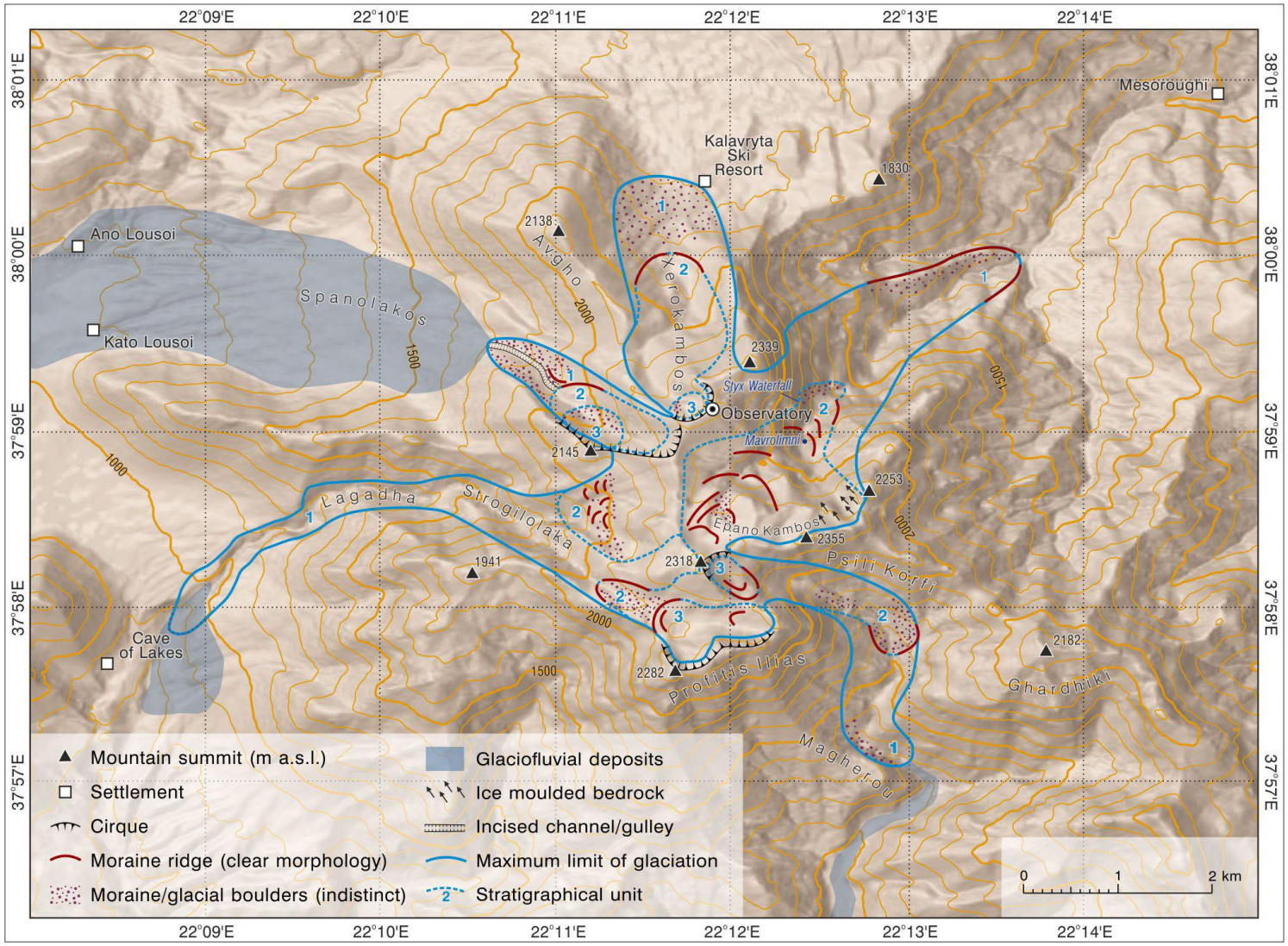

Figure 56. Glacial Geomorphological map of Mt Chelmos (from Leontaritis et al., 2020 based on the map of Pope et al., 2017). Some morphostratigraphic units are diachronous, like for example unit 2 moraines that differ in age in different valleys (see Table 18)

5.3.1.1 Spanolakos Valley

The glacial origin of the Spanolakos valley (2145-1300 m a.s.l.) has also been recognized by Pope et al. (2017), distinguishing three main glacial features attributed to three distinct morphostratigraphic units. A well-preserved cirque at 2145 m a.s.l. marks the head of the valley (Figure 55 and Figure 56) along with large boulders and an indistinct moraine (morphostratigraphic unit 3). The most interesting glacial feature however is a very clear arcuate termino-lateral moraine (Mastronuzzi et al., 1994; Pope et al., 2017) at an altitude of 1900-2050 m a.s.l. Although it has never been dated, this moraine has correlated by Pope et al. (2017) with the Kato Kambos formation and morphostratigraphic Unit 2 (Table 17) on grounds of altitude and morphostratigraphy. Its formation has therefore been attributed to a glacial advance/stabilisation phase at 40-30 ka. However, the samples collected from the same moraine were dated with the OSL method and yielded an age of 89-86 ka (Pavlopoulos et al., 2018; see section 5.4).

The lower part of the Spanolakos valley (1900-1200 m a.s.l.) lies within the area below the sampled glacial moraine and is characterized by thick accumulations of gravels and sand interbeds. This sediment unit was firstly identified by Pope et al. (2017) and has been associated with glacial activity in the Middle Pleistocene (morphostratigraphic unit 1 in Table 17), based on the vast expanse of glaciation and the respective geochronological framework of North Pindus in Greece (Hughes et al., 2006a). Between 1700 and 1900 m a.s.l. cemented gravels and sands are topped by numerous large perched boulders and this range of heights has been noted as the approximate down-valley extent of the largest former glacier limit in this valley (Pope et al., 2017). In the same study, the range between 1700-1200 m a.s.l. where larger boulders are absent was interpreted as a stacked sequence of glacio-fluvial fans. This formation of glaciofluvial sediments can be seen in Figure 55 and Figure 56. These units are clearly distinguished from those derived from erosional and depositional processes. Due to erosional processes V-shaped valleys and down cut erosion are formed by the action of the hydrographic network. The alluvial fans are present mainly in the western part of the study area, where most of the torrents deriving from the neighbouring mountains end up in the polje of Loussoi, forming a continuous line of alluvial fans. A direct result of the above alluvial and glacial sediment flows was the extensive deposition inside, and in the boundaries, of the polje, filling it with sediments. These sediments are cohesive and they are reported in the geological maps as "Kato Soudena" formation.

5.3.1.2 Xerokambos Valley

This valley drains the northern flanks of Mt Chelmos. Its glacial origin is easily distinguishable and several glacier landforms, like a glacial cirque (Figure 55 and Figure 56) and scattered perched boulders at the head of the valley at ca. 2200 m a.s.l. (morphostratigraphic unit 3 in Table 17) as well as a terminal moraine at ca. 1850 m a.s.l., have been identified (Philippson, 1892; Mistardis, 1937b, 1937c, 1946; Mastronuzzi et al., 1994; Pope et al., 2017). The moraine has not been dated but it has been correlated by Pope et al. (2017) with the Kato Kambos formation and morphostratigraphic Unit 2 (Table 17) on grounds of altitude. Its formation has therefore been attributed to a glacial advance/stabilisation phase during 40-30 ka. However, given the new evidence from the dating of a termino-lateral moraine in the Spanolakos valley at a similar altitude (1900-2050 m a.s.l.) this moraine could also be correlated with a newly defined glacial advance/stabilization phase at 89-86 ka. The central part of the moraine at 1850 m a.s.l. has been destroyed by ski-resort earthworks in 1985. However, Mistardis (1937b, 1946) describes it as a quite high and very clear arcuate terminal moraine, blocking entirely the valley. Mistardis names it “Loutsa”, which means seasonal lake in Greek, and indeed Philippson (1892) states that a seasonal lake was present there. Later on, in 1937, Mistardis (1937b; 1946) observed that the modern river channel at that time incised the moraine and as a result it was draining the hollow area behind the moraine, preventing the accumulation of water. Downstream from the moraine there was found a fluvial fan of fine, well-sorted deposits (Mistardis, 1937b; 1946). Moreover, Mistardis in the same studies remarked that the flat bottom of the hollow implied a lacustrine origin. The former lake bottom was plane and rich in fine sediments while scattered large-size perched boulders were found. The breakage of this moraine-dammed lake in Xerokambos valley between years 1896 and 1937 could be linked with tremendous floods in Peloponnesus at the beginning of the 20th century (Diakakis et al., 2011). Indicative of the scale of the storms and floods of this period is the creation of the nearby Tsivlos lake by a huge landslide on 24th March 1913 (Stavropoulou et al., 2003). Finally, Mistardis (1937b, 1946) reports another smaller moraine at ca. 2000 m a.s.l., partly blocking the valley and although it has not been confirmed by any other researchers, some remnants of these glacial deposits can indeed be observed, flanking the ski run above the upper building of the ski resort.

At the lower part of the valley (1650-1700 m a.s.l.), the construction of the ski resort runs, buildings and car park has destroyed much of the evidence. The scattered surviving glacial features (mainly sub-rounded boulders and thin diamicton deposits) have been interpreted by

Pope et al. (2017) as the probable furthest extent of former glaciers during Middle Pleistocene (morphostratigraphic unit 1 in Table 17).

However, further evidence at lower altitudes within the valley indicates further glacial/periglacial processes. Specifically, there has been identified a well-preserved cemented diamicton tillite unit (Figure 55 and Figure 56), just below the car park at ca. 1650 m a.s.l. (Figure 57). The upper-altitude tillites consist of poorly sorted cemented sub-rounded rocks, boulders and gravels and can be spotted on the ground surface. The unit's downvalley depositional limits are not clear but the cemented gravels, probably of glacio-fluvial origin extend down to 1200 m a.s.l. at the western part of the Xerokambos valley. This unit has also been reported by Tsoflias (1973), and was characterized as cemented conglomerates. At lower altitudes (<1500 m a.s.l.), it mainly consists of gravels which are also exposed by the main road from Kalavryta to the ski resort. However, at this stage, the absence of clear evidence for the glacial limits makes rather difficult the determination of the extent of the largest former glacier in Xerokambos valley.

Figure 57. Detail of the diamicton tillite unit below the ski resort car park at ca. 1650 m a.s.l. (Figure from Pavlopoulos et al., 2018; Photo: Aris Leontaritis, March 2016)

5.3.1.3 Lagadha valley

This valley neighbours the Spanolakkos valley in the south and drains the western flanks of Mt Chelmos, including the basins of Strogilolaka (northern branch of Lagadha valley) and Kato Kambos (southern branch of Lagadha valley) (Figure 55, Figure 56) .

The Kato Kambos valley (2280-2250 m a.s.l.) has clearly glacial origins and is headed by a well-developed cirque at 2280 m a.s.l. (Maull 1921; Mistardis 1937c; Pope et al. 2017). Its upper part is a glacio-karst cirque basin where cirque moraines have been identified at ca. 2140 m a.s.l. and perched boulders have been dated with cosmogenic ^{36}Cl by Pope et al. (2017). The results indicate a glacial advance/stabilisation phase at 13-10 ka characterizing morphostratigraphic unit 3 (Table 17). Further down the valley, between 2050 and 2140 m a.s.l. another latero-frontal moraine has similarly been identified and perched boulders at ca. 2120 m a.s.l. have been dated with cosmogenic ^{36}Cl by (Pope et al. 2017). The results indicate a glacial advance/stabilisation phase at 40-30 ka characterizing morphostratigraphic unit 2 (Table 17). Glacial boulders can be found down to 2050 m a.s.l. perched just above the steep and steeply incised upper Laghada valley which has been interpreted as the down-valley glacial limit of this unit (Pope et al., 2017). Occasional boulders can also be seen further down until the point where Kato Kambos valley converges on the southern branch of the Stogilolaka valley, but no further deposits have been preserved due to the steepness of the valley.

Similarly, within the Strogilolaka valley (2100-1900 m a.s.l.) there is abundant glacial evidence, like glacial boulders lying on top of diamicton ridges, but deposits have been poorly preserved due to modern stream activity (Pope et al. 2017). In any case, the limits of morphostratigraphic unit 1 have not been yet identified within the Lagadha valley, which ends up right on the southern edge of the Loussoi polje.

The lower part of the Lagadha valley, stretching from 1000 to 2000 m a.s.l., is very steep at middle altitudes (1400-2000 m a.s.l.) and deeply eroded by surface runoff for its entire stretch (V shaped - Figure 55 and Figure 56). At around 1000 m a.s.l. it reaches the polje of Loussoi where extended alluvial deposits similar to the ones found in the lower Spanolakos valley above the settlement of Loussoi can be seen (Figure 55 and Figure 56).

This area is characterized by thick accumulations of gravels and sands, superficially (<5 m in thickness) cemented in places (zone a in Figure 58). Interestingly, this sedimentary formation expands over the southern edge of the polje, where it has been exposed both by the modern Lagadha river channel on its eastern side and by the modern river channel draining the polje on its western side. The latter vertical section is about 40 m deep and can be seen in Figure 58.

As it can be observed in this picture, the material at the upper part (zones a and b in Figure 58) is stratified forming a stacked sequence of gravel and sand accumulations, resembling the Spanolakos formation. It could therefore be characterized as a sequence of glacio-fluvial fans. The large sub-rounded boulders (>2 m in diameter) present in stratified sands (zones a and b) are consistent with a glacio-fluvial origin. However, the lower part of the unit (zone c in Figure 58) is a non-stratified diamicton with gravels, rocks and sub-rounded rocks (ca. 0.5–1 m in diameter). A more detailed picture of the unsorted material in zone c can be seen in Figure 59. These lower parts of the Laghada sedimentary formation could be interpreted as a former moraine which has then been eroded and subsequently mixed-with/covered-by later glacio-fluvial fans during more recent glaciation-deglaciation phases. Alternatively, they could be high-energy glaciofluvial deposits emanating from a glacier front that was a short distance up-valley at the apex of the fan in the Lagadha gorge (Figure 56).

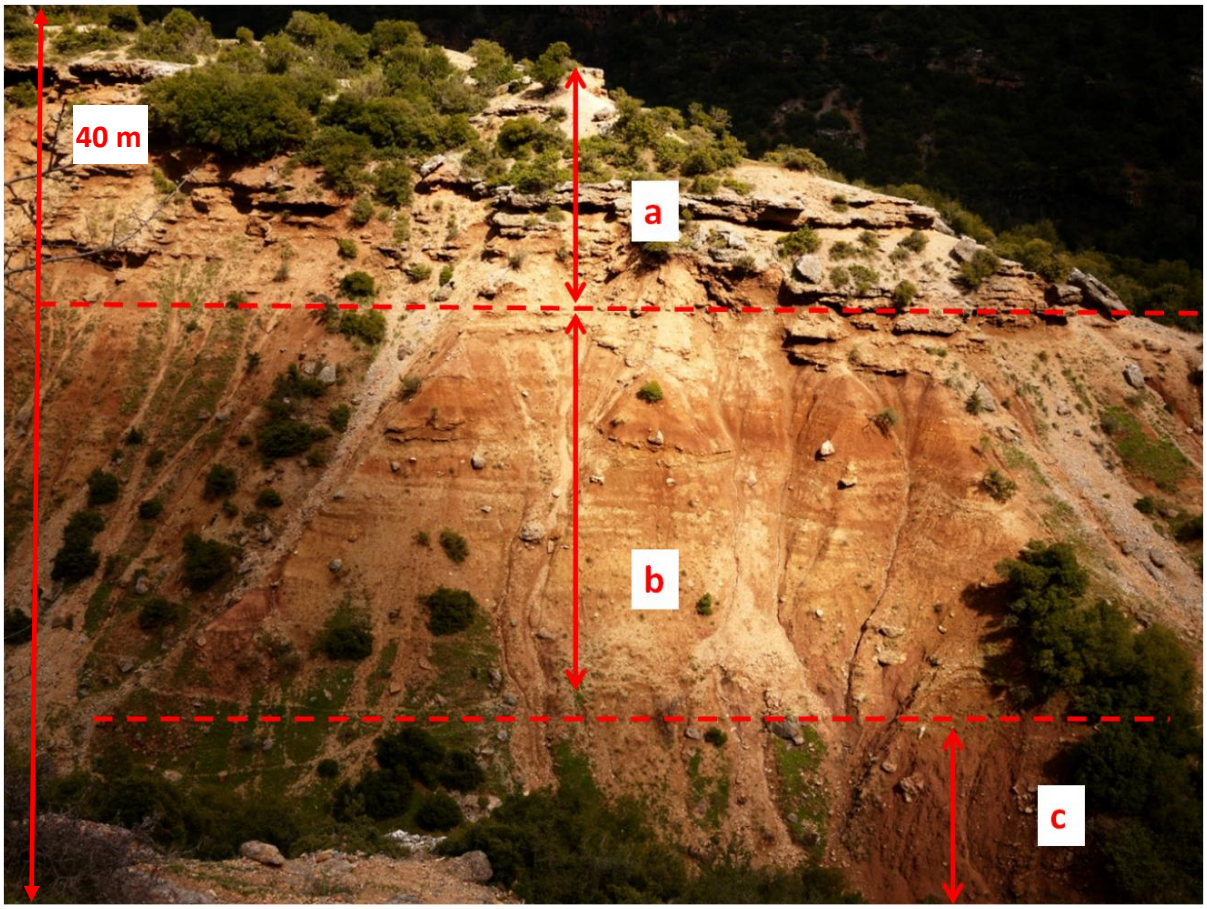

Figure 58. The Lagadha alluvial fan at ca. 950 m a.s.l. The lower part of this fan (zone c) is characterised by sub-rounded rock and boulder deposits. These are likely to be glacial in origin, either moraines or high-energy glaciofluvial deposits emanating from a glacier front that was a short distance up-valley. The boulders present in stratified sands (zones a and b) are consistent with a glacio-fluvial origin. (Figure from Pavlopoulos et al. 2018; Photo: Aris Leontaritis, March 2016)

Figure 59. The diamicton lower part of the Lagadha sedimentary formation (zone c in Figure 58) topped by clearly stratified sand layers (zone b in Figure 58). Possibly a glacial moraine eroded and buried by later glacio-fluvial deposits. (Figure from Pavlopoulos et al. 2018; Photos: Aris Leontaritis, May 2017)

Moreover, the southern part of the Laghada sedimentary formation remains exhumed by the later glacio-fluvial sequences, forming a ridge (Figure 60). As it can be seen from the photo, there are large limestone sub-rounded boulders exposed on its surface, similar to the ones found in the buried diamicton zone describe above. From a morphostratigraphic point of view, the buried diamicton zone is in the same position as the ridge. This evidence indicates that this ridge could be a former moraine created by the most extensive glacier in the Laghada valley. This sedimentary unit could thus be interpreted as the approximate down-valley extent of the largest glacier in this valley. In this case, it can be correlated with the diamicton deposits identified by Pope et al. (2017) at the lower parts of Chaliki valley (1300 m a.s.l.) and the Styx valley (1200 m a.s.l.) in the Neraidorachi area at the southern and eastern flanks of Mt Chelmos respectively. Conclusively these deposits could be correlated with morphostratigraphic unit 1 (Table 17) and hence could be attributed a Middle-Pleistocene age. However, considering the alternative interpretation that the lower zone of the sediments represents high-energy glaciofluvial deposits, this sedimentary formation could be associated with a glacier front that existed nearby in the valley and these have since been buried by later alluvial fan deposits.

Figure 60. The southern un-buried part of the moraine(?) ridge. ***Top:*** *looking north.* ***Middle:*** *Detail of top picture* ***Bottom:*** *looking southeast. The large sub-rounded boulders exposed on the ridge surface are solid limestone boulders rather than blocks of cemented gravels that are found elsewhere on the surface of the northern part of the Lagadha sedimentary formation. These ridges are in terms of strata position in consistence with the respective diamicton deposits shown in zone c of Figure 58. (Figure from Pavlopoulos et al., 2018; Photos: Aris Leontaritis, May 2017)*

5.4 Optically stimulated luminescence (OSL) dating of moraine deposits

As already discussed, several glacial landforms can be distinguished within the study area. However, this research focuses the Spanolakkos glacial valley which drains the north-western flank of Mt Chelmos to the Polje of Ano Loussoi. The Spanolakkos valley has also been identified by Pope et al. (2017), distinguishing three main glacial features attributed to three distinct morphostratigraphic units. The most interesting glacial feature is a very clear and well-developed arcuate termino-lateral moraine at an altitude of 1900-2050 m a.s.l. (Figure 61). Although it has never been dated, this moraine has correlated by Pope et al. (2017) with the Kato Kambos formation and morphostratigraphic Unit 2 (Table 17) on grounds of altitude and morphostratigraphy. Its formation has therefore been attributed to a glacial advance/stabilisation phase at 40-30 ka. In the framework of this study, it was decided to collect samples from this moraine and date them in 2009, well before the first version of the study of Pope et al. (2017) was published in 2016. Still, the yielded ages of the samples are useful in order to test the above-mentioned assumptions.

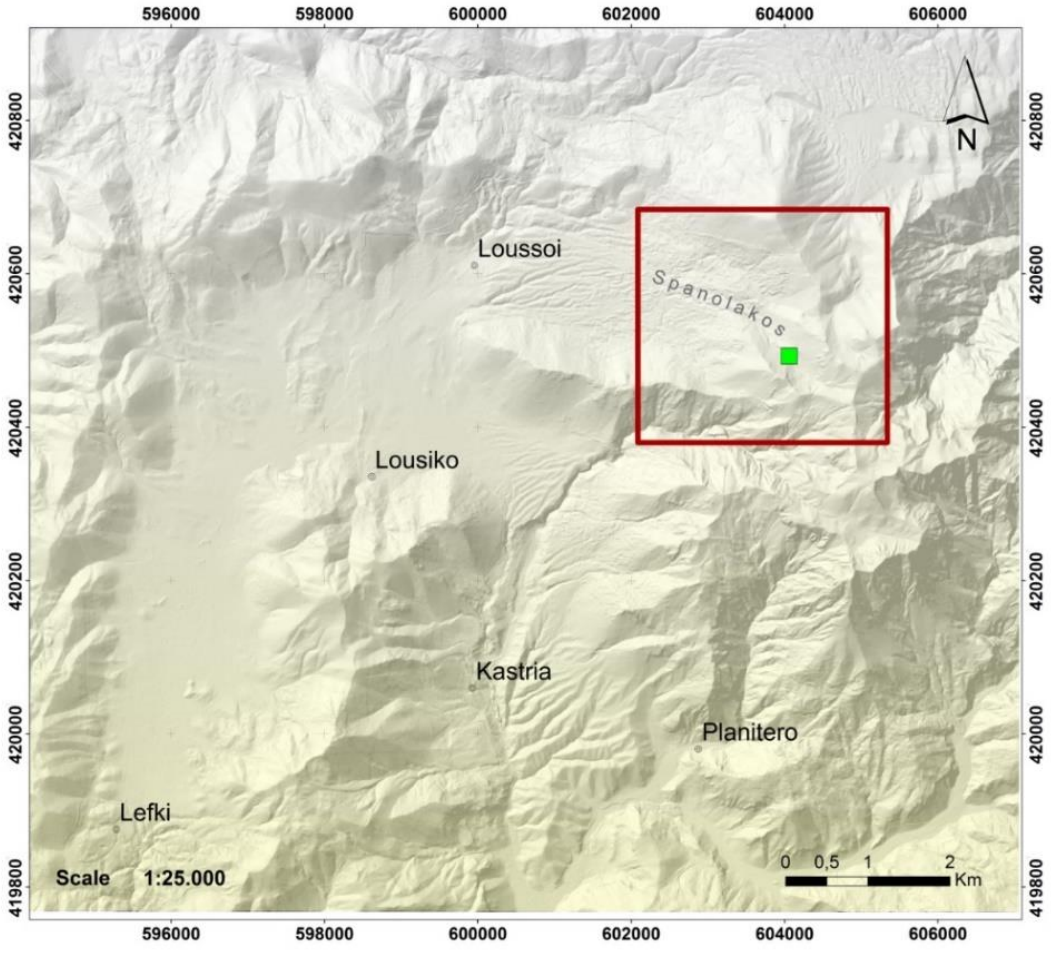

Figure 61. The sampling site for OSL dating.

Four glacial sediment samples (LOUS1, LOUS3, LOUS4, LOUS6) were collected from the lower part of the moraine (Figure 62). Two of the samples (LOUS1, LOUS3,) were taken in aluminium tubes from cohesive sands and fine gravels at a depth of 50cm from the exposed surface in order to ensure they were undisturbed while the other two (LOUS4, LOUS6) were collected as blocks from cemented material (tillites). The two latter samples had to be carved under controlled illumination conditions (subdued ~580 nm light) in order to extract their light-safe interior prior to chemical treatments. All samples were subsequently submitted for OSL dating at 'Demokritos' OSL dating laboratory (Athens, Greece).

Figure 62. ***Left:*** *The dated arcuate termino-lateral moraine in the Spanolakos valley (1900-2050 m a.s.l.).* ***Right:*** *Arrow points at the sample spot in the lower part of Spanolakos moraine. (Figure from Pavlopoulos et al. 2018; Photos: Kosmas Pavlopoulos – 2009)*

All samples underwent standard chemical and mechanical treatment (e.g. Athanassas et al. 2012) to isolate quartz grains. Initial steps involved treatment with HCl (10% concentration) and H_2O_2 (20% concentration). Remaining sediment residue was found to be fine-grained and clay-rich and, therefore, a fine-grain (or slit-grain) dating approach was followed (see Rhodes, 2011). The material underwent grain-size fractionation through suspension, isolating the 4-11μm particle-size fraction. The isolated fine fraction was then submitted to hexafluorosilicic acid (H_2SiF_6, 40% concentration) for several days to dissolve the feldspathic content and purify the fine-grained quartz. Retained fine-grain quartz was then divided into sub-samples (aliquots) and was mounted on stainless disks (1 cm in diameter) to produce large aliquots.

Luminescence measurements were carried out using a RISØ-TL/OSL-15 reader. Equivalent dose measurements were carried out running the post-infrared OSL (pIR-OSL) protocol by Banerjee et al. (2001) on multiple aliquots (~20 aliquots/sample), generating in this way a number of individual equivalent doses per sample. Specifically, measurement of natural

infrared stimulated luminescence (IRSL) and OSL signals were succeeded by the measurement of the IRSL and OSL responses to a series of regenerated laboratory irradiations, all normalized by the IRSL and OSL response to a constant laboratory dose respectively, known as the test dose (Murray and Wintle, 2000).

OSL stimulation induced explicit decay curves for samples LOUS1, LOUS3 (Figure 63a) but poor signal-to-noise ratios for LOUS4, LOUS6, quite untypical of quartz. This observation implies the dominance, and therefore the suitability, of quartz in samples LOUS1, LOUS3 but absence of it in samples LOUS4, LOUS6. Therefore, only samples LOUS1, LOUS3 were considered for further analysis. A typical regenerated growth curve is illustrated in Figure 63b. Moreover, both LOUS1, LOUS3 yielded normal and relatively tight equivalent dose distributions, endorsing the reliability of the calculated equivalent dose and hence, of the OSL ages. A typical equivalent dose distribution is shown in (Figure 63c).

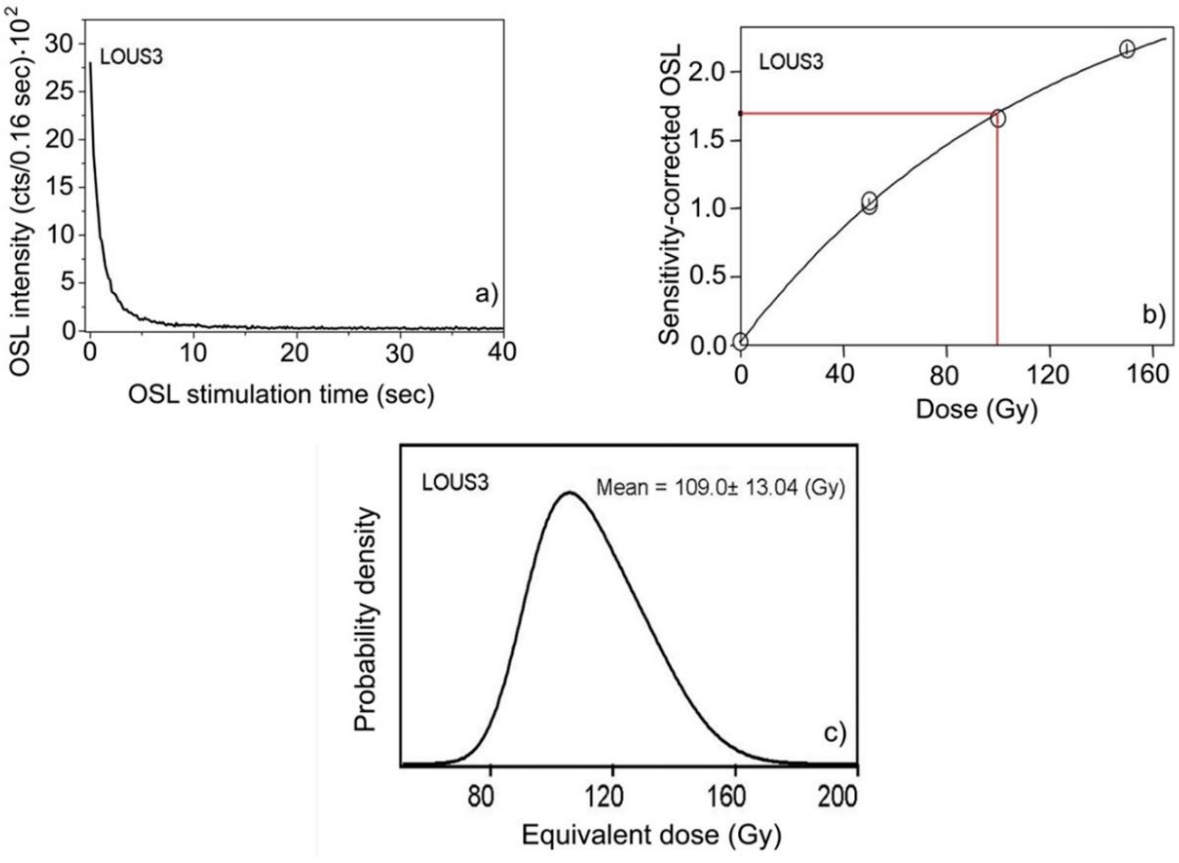

Figure 63. ***a) (Top left)****: Typical OSL decay curve. Top Right* ***b) (Top right)****: growth curve - interpolation of the natural signal onto the growth curve defines the equivalent dose on X-axis.* ***c)(Bottom)****: equivalent dose distribution. All figures for the LOUS3 moraine sample (from Pavlopoulos et al., 2018).*

Dose rate estimation involved measurements of the sample's radioelement content in U, Th and K by means of ICP-MS (Inductively Coupled Plasma– Mass Spectrometry) combined with in situ γ-spectrometry. Concentrations of U and Th (in ppm) and K (in % by weight) were then converted to dose rate units by taking into account conversion factors published by Adamiec and Aitken (1998). The dose rate values were further corrected for moisture content, grain-size attenuation and cosmic-ray contribution. The dose rate for samples LOUS1 and LOUS3 was finally estimated to be 0.79 ±0.1 Gy/ka. OSL ages were subsequently calculated (see section 2.2.3.2) at 89±9 ka and 86±7 ka respectively.

5.5 Summary and overview of the glacial and glacio-fluvial features on Mt Chelmos

In this section, the glacial features that were identified and presented in this research are summarized along with the findings of other researchers in an effort to correlate them with each other and lead to a better understanding of the glaciation history of Mt Chelmos. The different morphostratigraphic units and the correlated glacial stages are summarized in Table 18. The respective geomorphological map is presented in Figure 56.

Table 18. Updated glacial morphostratigraphic units on Mt Chelmos according to data from Pope et al. (2017) and Pavlopoulos et al. (2018). The ^{36}Cl exposure ages are reported according to the recalculations of Allard et al. (2020) with the updated production rates of Marrero et al. (2006b) as presented in Table 19

Morphostratigraphic Unit	Altitude Range mean ELA	Age (*[1] OSL Dating, [2] ^{36}Cl dating)*	Glacial Stage and corresponding MIS
3	2100 m a.s.l. ELA – 2174m a.s.l.	13.1 ± 0.2 - 10.5 ± 0.3 ka [2]	MIS 2 - Younger Dryas
2c Retreat Phase	2200 m a.s.l. ELA >2200m a.s.l.	22.2 ± 0.3 - 19.6 ± 0.5 ka [2]	MIS 2 – Global LGM - Tymphian Stage
2b	1600-2100 m a.s.l. ELA – 2046 m a.s.l.	36.5 ± 0.6 - 30.4 ± 2.2 ka [2]	MIS 3 - Tymphian Stage
2a	1850-2050 m a.s.l. n/a	89 ± 9 - 86 ± 7 ka [1]	MIS 5b - Tymphian Stage
1	950-1450 m a.s.l. ELA – 1967 m a.s.l.	correlation with Middle Pleistocene glacial phases	MIS 12 – Skamnellian Stage MIS 6 – Vlasian Stage

The lowest glacial sediments/deposits identified are the eroded/buried moraines at the lower Laghada valley (down to ca. 950 m a.s.l.). They have been interpreted as the down-valley limits of these glaciers and correlated with the respective sediments of morphotratigraphic unit 1, identified by Pope et al. (2017) in the Chaliki valley in the south (down to ca. 1300 m a.s.l.) and the lower Styx valley in the north-east (down to ca. 1150 m a.s.l.). These new findings, complement our knowledge of the most extensive glaciation on Mt Chelmos. Based on correlations with evidence from northern Greece and Montenegro this glaciation took place during the Middle Pleistocene, most probably during the Skamnellian Stage (MIS 12) and/or the Vlasian Stage (MIS 6) (Pope et al., 2017).

The next morphostratigraphic unit (unit 2 in Table 18) is correlated to the Tymphian Stage (MIS 5d-2) and is subdivided into three sub-units. The most significant evidence for this period came from the OSL dating of the termino-lateral moraine at an altitude of 1900-2050 m a.s.l. in the Spanolakos valley. This moraine had initially been ascribed an age of 40-30 ka based on a morphostratigraphic correlation with the dated Kato Kambos formation (Pope et al., 2017) but the new OSL dating of samples from the foot of the moraine yielded ages of 89-86 ka, indicating that this could be another glacier advance/stabilization phase. This moraine has been classified in the morphostratigraphic subunit 2a. Given the morphostratigraphic similarity, in-valley position headed by a clear cirque of quasi-identical orientation (N-NW) and altitude, the Xerokambos moraine at 1850 m a.s.l. could also be correlated with this unit.

The formerly defined morphostratigraphic unit 2 (Pope et al. 2017), correlated with the Kato Kambos unit and a glacier advance/stabilization phase is redefined as subunit 2b in Table 18. Similarly, the glacial retreat phase that was also classified in morphostratigraphic unit 2 by Pope et al. (2017) is here ascribed to a distinct sub-unit (2c).

The upper moraine in the Xerokambos valley, identified by Mistardis (1937b; 1946) at 2000 m a.s.l. has been almost completely destroyed by ski-run earthworks but could either be correlated with morphotratigraphic unit 2b or interpreted as a recessional moraine and could be ascribed to sub-unit 2c. Finally, morphostratigraphic unit 3 remains as defined by Pope et al. (2017).

As regards the timing constraint of these stratigraphically younger deposits units (unit 2b, 2c and 3) the original comsmogenic ^{36}Cl exposure ages reported by Pope et al. (2017) were calculated using the Excel spreadsheet and the production rates of Schimmelpfennig et al.

(2009; 2011) and the authors argue that due to the continual refinements to the understanding of ^{36}Cl systematics, especially with regard to production rates, these ages are very likely to be subject to revision. Indeed, Allard et al. (2020) recalculated these ages with the updated and more reliable production rates of Marrero et al. (2016a) using the CRONUS Online Calculator v2.0 (http://cronus.cosmogenicnuclides.rocks/2.0/html/cl/) and these ages have been adopted in this research (Table 18). The differences in final ages due to the two different calculation models are reported in Table 19.

Table 19. Original and recalculated ^{36}Cl ages for the different stratigraphic units in Mt Chelmos. Ages reported by Pope et al. (2017) have been calculated with the Excel spreadsheet and the production rates of Schimmelpfennig et al. (2009; 2011), whilst the ages reported by Allard et al. (2020) have been recalculated with the updated and more reliable production rates of Marrero et al. (2016a) using the CRONUS Online Calculator v2.0

Stratigraphic Unit	^{36}Cl Age (Pope et al., 2017)	^{36}Cl age (Allard et al. 2020)
3	12.6 ± 0.9 - 10.2 ± 0.7 ka	13.1. ± 0.2 - 10.5 ± 0.3 ka
2c	22.9 ± 1.6 - 21.2 ± 1.6 ka	22.2 ± 0.3 - 19.6 ± 0.5 ka
2b	39.9 ± 3.0 - 30.4 ± 2.2 ka	36.5 ± 0.9 - 28.6 ± 0.6 ka

Chapter 6. Preliminary glacial geomorphological study of Mt Parnassus

The latest glacial studies on Mt Olympus (Styllas et al., 2018) in northeastern Greece Mt Tymphi in the northwest (Allard et al., 2020) and Mt Chelmos (Pope et al., 2017) in the south which were published in the course of this research were partly controversial as regards Late Pleistocene glaciation (see 2.3). This highlighted the importance of a key geographical link between the well-studied Pindus mountains/Mt Olympus in northern Greece and Mt Chelmos in the south. Such a link would allow for the comparison and interpretation of the results from these studies and the reconstruction of the palaeoclimatic conditions across Greece at these times. As in central Greece the high-altitude glacial deposits are best preserved on Mt Parnassus (see section 3.4), it is argued that this massif is the most appropriate for creating this link.

In this context, the geomorphological evidence presented here give an account of field sedimentological observations on Mt Parnassus in comparison with the work of the first systematic mapping and geomorphological interpretation of glacial and periglacial features of Pechoux (1970). This work forms the basis of a future glacial/geochronological project focusing on the uppermost and thus stratigraphically younger glacial deposits.

6.1 Setting of Mt Parnassus

Mt Parnassus is located in Sterea Hellas in central Greece (Figure 64) and is one of the ten tallest mountains in Greece with its highest peak, Liakoura, reaching an altitude of 2457 m a.s.l. Its characterised by a broad and slightly inclined high-altitude plateau drained by steep valleys and surrounded by several peaks exceeding 2300 m in altitude.

Central-eastern mainland Greece is a strip of land between two actively deforming gulfs (Jolivet et al., 1994): Korinthos to the south and Evoia to the north (Figure 64). The Gulf of Corinth is characterized by particularly high rates of deformation that reach an average rate of about 10 mm/yr (Ambraseys and Jackson, 1990; Billiris et al., 1991), which are among the highest in the Mediterranean area. The Delphi fault bounds the Mount Parnassus massif to the south and it is the most prominent of the active antithetic structures of the Gulf of Corinth Rift (Péchoux, 1977; Armijo et al., 1996; Piccardi, 2000 and references therein). Geologic and geomorphic features indicate that the fault is active with an average slip rate between 0.5 and 0.7 mm/yr during the last 1 Ma (Piccardi, 2000).

The region of central-eastern mainland Greece is characterized by an alpine nappe-pile structure, overprinted by neotectonic features (Kranis and Papanikolaou, 2001). The lowermost nappe is the Pindos Unit while the Parnassos Unit, which occupies the greatest part of central-eastern mainland Greece is placed between the underlying Pindos and the overlying Sub-Pelagonian Units. The Parnassos unit is a 1.5-2 km thick Upper Triassic to Paleocene neretic carbonate sequence, terminating with a typical Paleocene clastic sequence (flysch) (Kranis and Papanikolaou, 2001). The Sub-Pelagonian unit on the other hand is an Upper Triassic - Middle Jurassic carbonate platform that evolves into a Middle to Late Jurassic clastic sequence followed by Upper Cretaceous carbonate sediments and flysch deposition in the Danian (Richter et al., 1994; 1996). Mt Parnassus is mainly built by the Parnassos Unit while only relics/klippen of the Sub-Pelagonian unit can be found within the massif. The trace of the surface that separates these two units marks the foot of Mt Parnassos northern front, an impressive physiogeographic feature more than 2000 m high (Kranis and Papanikolaou, 2001).

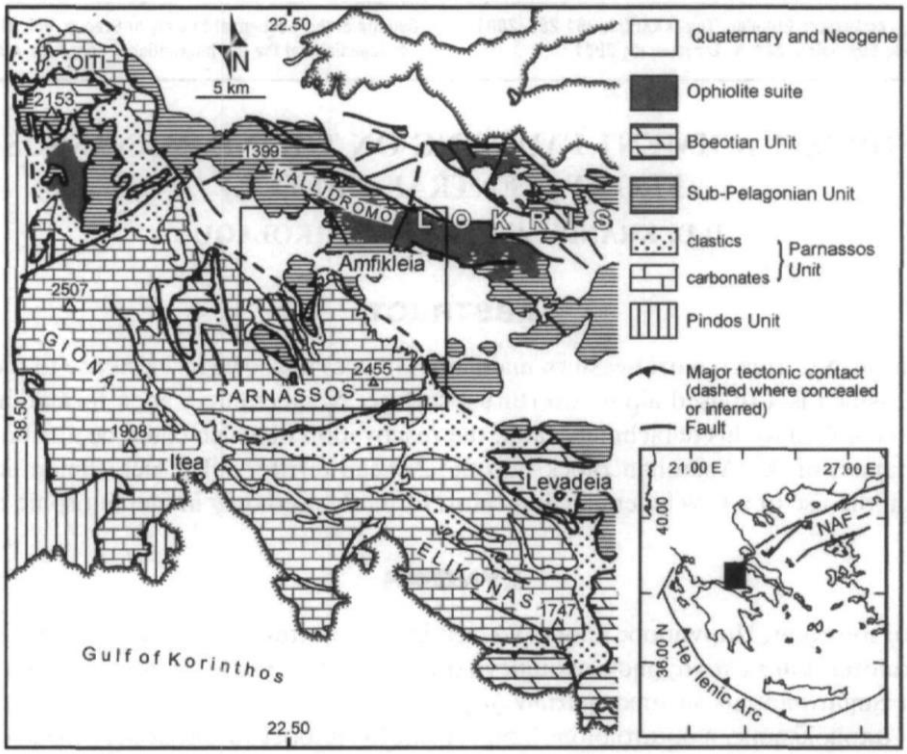

Figure 64. Summary geological map of Mt Parnassus within central-eastern mainland Greece (Sterea Hellas). NAF: North Anatolian Fault. (from Kranis and Papanikolaou, 2001)

As regards the glacial geomorphology of the Parnassus massif, U-shaped valleys headed by deep glacial cirques indicate its extensive glaciation, even though glacial deposits other than erratic boulders have not been preserved (or discovered yet) within these valleys probably due the steepness of its slopes in all orientations. In any case this extensive phase(s) must have

occurred during the Middle Pleistocene (MIS 12/ MIS 6) according to the Pindus Chronostratigraphy in Northern Greece (see section 3.1). Within the high altitude (>2000 m) north-oriented cirques, younger glacial deposits are evident and most importantly, some clear and well-preserved moraines are evident in many cirques (Pechoux, 1970; see also next section). Given their morphostratigraphy, altitude and orientation and according to the glacial-research background in the mountains of Greece presented in 2.3, these younger deposits are expected to be Late-Pleistocene in age. Therefore, the dating of these moraines is in principle ideal for the purpose of a future dating project.

No glaciers, permafrost or permanent snow fields are present today. The present-day precipitation and annual temperature range at the nearby villages of Ano Souvala, Gravia, Grammeni Oxia, and Itea are summarized in Table 20. When mean temperatures for these four weather stations are extrapolated using a lapse rate of 0.6 ^{o}C per 100 m of altitude, the mean annual temperature at 2000 m a.s.l. is about 5.6 ^{o}C while the mean monthly temperatures for July and January are 14.7 ^{o}C and -3.1 ^{o}C respectively. With a mean annual precipitation of 936 mm for the four stations at an average altitude of 583 m a.s.l. the mean annual precipitation at 2000 m as.s.l. is expected to exceed 2000 mm based on a linear interpolation of the precipitation in Itea (20 m a.s.l.), Ano Souvala (700 m a.s.l.), and Grammeni Oxia (1160 m a.s.l.). Snow cover on the northern slopes above 1800 m a.s.l. lasts from late December to early May.

Table 20. Precipitation and temperature data from weather stations near Mt Parnassus (data from Gouvas and Sakellariou, 2011; reference period>20yr)

Meteorological Station	Altitude (m a.s.l.)	Annual Precipitation (mm)	Mean Temperature (^{o}C)		
			Annual	Jan	Jul
Ano Souvala	700	1141	13.2	4.3	22.5
Gravia	450	889	14.3	5.4	23.7
Grammeni Oxia	1160	1245	11.5	2.9	20.4
Itea	20	470	17.2	9.1	26.1
Mean	583	936	14.1	5.4	23.2
Mt Parnassus (Extrapolation)	2000	>2000 mm	5.6	-3.1	14.7

6.2 Geomorphological evidence

Through this preliminary geomorphological field study a few clear and well preserved, moraines within at least five high altitude (>2000 m a.s.l.), north-facing cirques have been identified (Figure 65). All cirque moraines are confined to positions close to the cirque walls. They bare no characteristics of pronival ramparts or other nival or periglacial features, while their overall morphological characteristics indicate a glacial origin as Pechoux (1970) also argued. Given the extent of the glaciers, the moraines are surprisingly high above the ground (10-25 m), most likely an effect of karstic processes where glaciers tend to burrow into dolines (Pechoux, 1970). According to the morphostratigraphy, altitude and relative position within the valleys as well as the lack of soil development and according to the glacial-research background in the mountains of Greece presented in the previous sections, these deposits are expected to be close to the LGM or Late-glacial in age. It should be noted that whilst Holocene glaciers are unlikely at this altitude/latitude (Hughes et al., 2006c), the presence of snow patches within the cirques until late September reported by Pechoux (1970) which has been confirmed on the field, strengthen the hypothesis that the stratigraphically younger moraines are likely to be Late-glacial in age.

The glacial origin of these deposits is confirmed by the exposure of a cross section through the moraine of the Arnovrisi cirque due to earthworks for the development of a ski resort in the area. The outcrop shows that the moraine is made of a typical till deposit (Figure 66). There are two nested moraine crests at 2100 m a.sl. in Arnovrisi cirque (Figure 66a) that could be ascribed to two distinct glacial phases. Similarly to the Yerontovrahos moraine at 2200 m a.s.l. (Figure 65), these deposits are unsuitable for exposure dating with cosmogenic ^{36}Cl as they are very close to the ski runs and lifts and glacial boulders that could be sampled may have been moved in the course of the earthworks.

In the Liakoura cirque (Figure 65) there have been identified two nested moraines at 2250 m a.s.l. (Figure 67; Pechoux, 1970). These moraines are ideal for sampling as their shape is well defined with a height of 20 m (Figure 67a) and there are plenty of large boulders (d >1 m) lying on their crests that are suitable for surface exposure ^{36}Cl dating. This site is also isolated and far from the ski-runs, thus minimising the risk of human intervention. It should be noted that evidence suggests that the two moraines might belong to two distinct glacial phases as the outer moraine is considerably more dismantled compared to the inner moraine, and glacial boulders on its surface are also more weathered (Figure 67a). Therefore, it would be worth dating both.

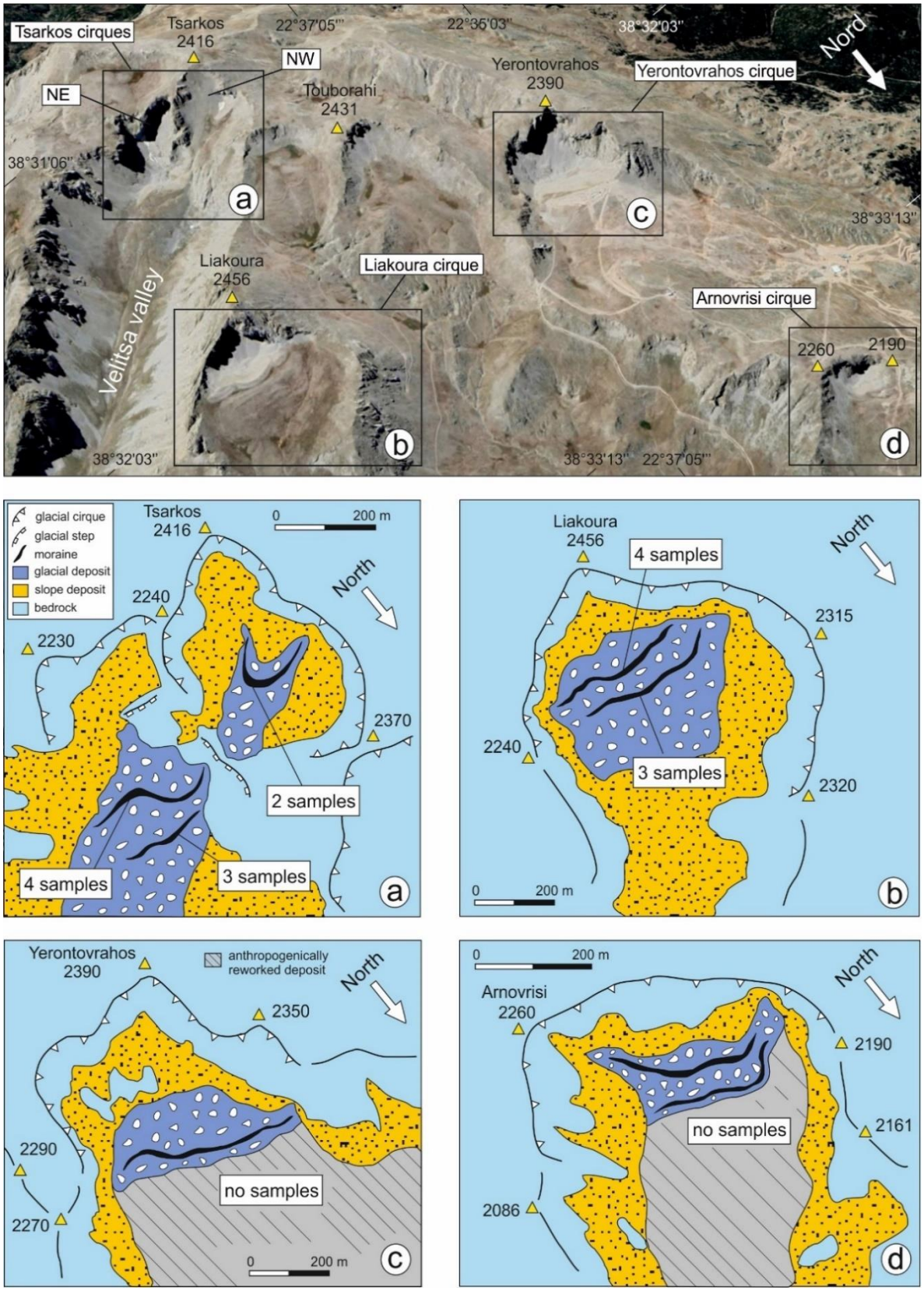

Figure 65. Geomorphological maps of key sites mentioned in the main text including, in panel a and b, the specific location of the moraines that would be aimed to be sampled in this project. Sites in panel c and d were ultimately not considered for sampling because of a lack of large boulders and the proximity to the ski runs and lifts (anthropogenically-reworked deposit refers to work done for the ski resort).

Figure 66. ***a) (Top)****: The Arnovrisi moraines seen from the peak above the cirque;* ***b) (Bottom)****: The glacial deposits exposed by ski resort earthworks* ***(left)*** *are characterized by clast-rich lithology with sandy to muddy matrix* ***(right)****. The fine-grained material is unconsolidated and the clasts consist of various sizes of sub-rounded limestone boulders (1m long hiking pole for scale) (Photos: September 2019).*

The glacial deposits in the Tsarkos NW and NE cirques were next studied (Figure 65). The Tsarkos NW deposits comprise of a single, clear moraine within a cirque at 2250-2300 m a.s.l. (Figure 68) that was also identified by Pechoux (1970). Its shape is well-developed and the moraine reaches 10 m in height. As regards its suitability for ^{36}Cl dating, although it is generally composed of small rock fragments and sands there are at least two large boulders on its crest that are suitable for sampling. This moraine can be correlated with the moraines in the other

cirques and is expected to be Late-Pleistocene in age. This hypothesis is further strengthened by the presence of snow in late September (Figure 68).

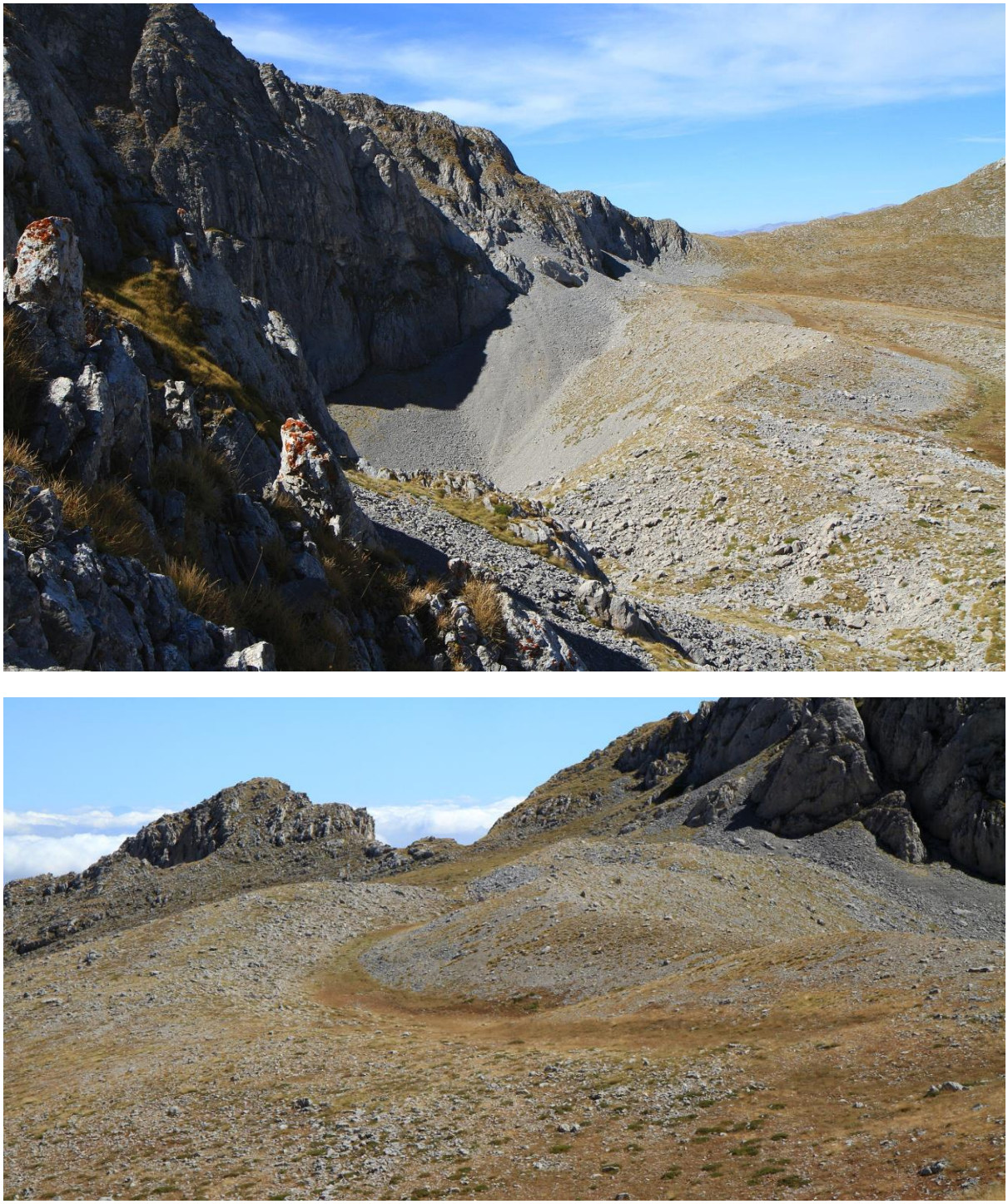

Figure 67. ***a) (Top)****: Frontal moraine and glacio-karst depression within the glacial cirque at 2250 m a.s.l. below the peak of Liakoura (2474m a.s.l.);* ***b) (Bottom)****: The clearly shaped inner Liakoura moraine (right) nested into the more dismantled outer moraine.*

Figure 68. The NW Tsarkos small cirque and related moraine at 2250-2300 m a.s.l. Notice the presence of snow in September, which strengthens the hypothesis that this is a Late Pleistocene moraine.

The Tsarkos NW is part of the deeply ice-scoured Velitsa glacial valley (Figure 65; Figure 69b) but the main head of the valley is actually marked by the Tsarkos NE cirque. The upper Velitsa valley is characterised by thick accumulations of unshaped glacial deposits spilled with very large glacial boulders. This sediment unit was described by Pechoux (1970) as a rock-glacier but although it has undoubtedly undergone some periglacial creep it lacks the distinct characteristics of rock glaciers such as lobes. Therefore, it is here considered as a sedimentary unit of glacial deposits. A well developed and clearly shaped moraine with a height of 25 m is nested into the older deposits near the cirque walls, at an altitude of 2140 m a.s.l. (Figure 69). The moraine is double-crested like the Liakoura moraine, with an abundance of large boulders that are suitable for ^{36}Cl dating and it would be worth dating both the inner and the outer moraine crests. It should be noted that a snow patch behind this highest moraine is still present in September 2019, giving strength to the hypothesis that the most recent phase of moraine-building is likely to be Late-glacial in age.

Finally, it should be noted that the cirques mentioned here are well-developed and their creation cannot be ascribed to the very restricted – probably Late Pleistocene - glacial phase(s) during which the above-described cirque moraines formed. The cirques have been inherited by previous glaciations of the massif that are indicated by the presence of ice-scoured and deepened U-shaped valleys (Pechoux, 1970). Specific evidence of an older more extensive glaciation phase has been identified only in the Velitsa valley and are shortly presented next.

Figure 69. ***a) (Top)****: The thick glacial deposits at the head of the Velitsa glacial valley and the clearly shaped moraine near the walls of the Tsarkos NE cirque. Notice the greenish patch below the moraine at the cirque floor: that is a flat surface filled with clay deposits that could have been the bottom of a former moraine- dammed lake. The outer moraine crest lays just below and left of the clear inner ridge;* ***b) (Bottom):*** *The glacial deposits unit as seen from the saddle north of the Liakoura peak. The two moraine ridges are easily distinguishable. The shaded crags of the NE Tsarkos cirque can be seen behind with a snow patch still lingering at the end of September. At the upper right corner is the lower basin of the Tsarkos NW cirque.*

6.2.1 Morphostratigraphically older mid-altitude deposits

The valley of Velitsa (Figure 65) is the only valley where morphostratigraphically older glacial deposits have been preserved. In particular, a well-shaped, 950-metre in length terminolateral moraine has been preserved in the southeastern flank of the valley between 1860 and 1470 m a.s.l. (Figure 70; Figure 71). The lower Velitsa valley below this point becomes narrow and very steep. Elsewhere on Mt Parnassus, stratigraphically older deposits remain elusive and this could be attributed on the one hand to the fact that some glacial valleys such as the Liakoura valley are very steep below 2000m a.s.l. and any deposits are impossible to be preserved there whilst on the other hand the extensive earthworks in the less-inclined valleys below Arnovrisi and Yerontovrahos cirques for the construction of the ski-resort have destroyed any possible evidence (Figure 65). Pechoux (1970) also argues that moraines might have been eroded by excessive run-off water during a rapid glacial melt-out or during the successive interglacial period(s). Unfortunately, there are also no reports on low-altitude glacial evidence by early researchers.

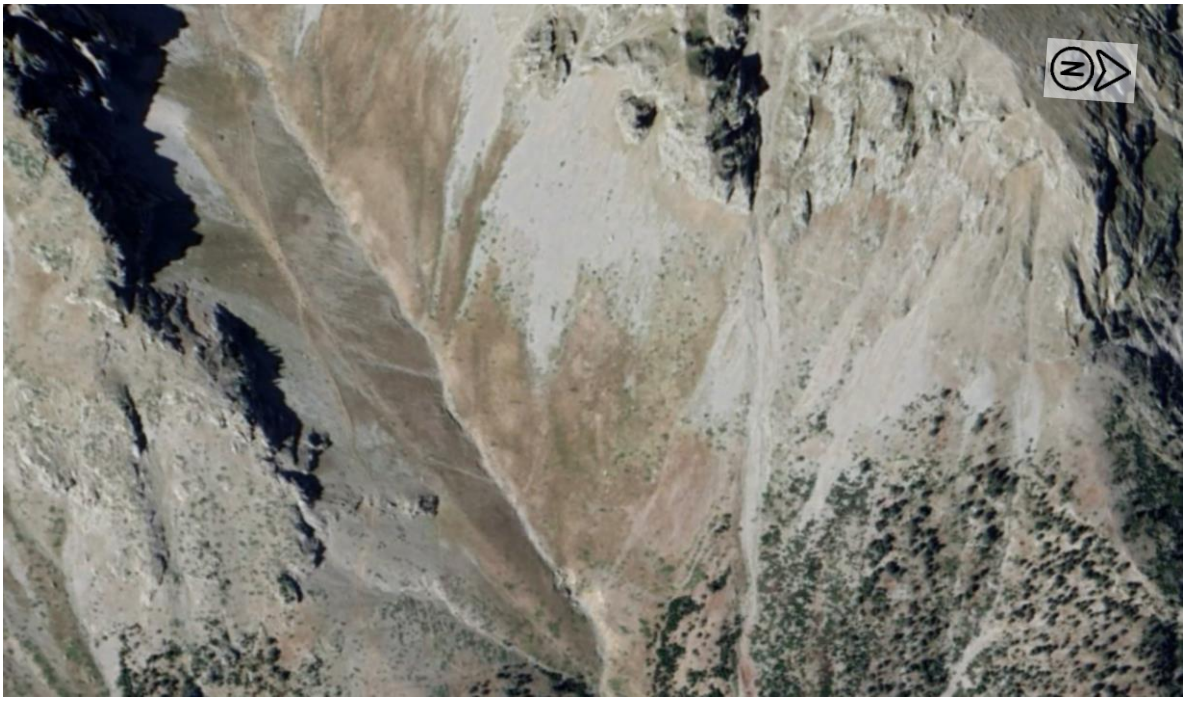

Figure 70. The Velitsa valley as depicted in virtual globe imagery (Google Earth). Notice the clear terminolateral moraine starting at the shade of the craggy southeastern valley walls at the upper left corner and converges to the thalweg (valley path) at the bottom of the picture following the shape of the former glacier's snout

Figure 71. The Velitsa valley as seen from the Liakoura peak looking SE. Notice the lateral moraine highlighted by the sunny patch at the center of the picture. The lower terminolateral part of the moraine can be faintly seen converging towards the Thalweg of the valley between the clouds.

Chapter 7. Discussion of results and correlation with other proxies

7.1 Towards a robust geochronological framework for Quaternary glaciations in Greece

The main purpose of this doctoral research is to contribute to the addressing of temporal gaps in the glacial history of the Pindus Mountains with new insights from the glacial record of Mt Mavrovouni and its connection with the glacial record of southern mountainous Greece towards a geographical expansion of this framework.

The work presented in this thesis along with the important glacial studies on different mountains of Greece (Mt Chelmos - Pope et al., 2017; Mt Olympus - Styllas et al., 2018; Mt Tymphi – Allard et al., 2020) which have been published in the course of this research have crucially contributed to great progress towards the achievement of these goals. In particular, the main issue of the complete absence of geochronological data from Late Pleistocene onwards has been addressed and we now have a quite well-established Late Pleistocene glacial maximum around and little bit prior to the LGM with cold conditions probably persisting through the Late-glacial. Glacier development during the Holocene was very limited and restricted only to Mt Olympus due to strong local topographic and climatic factors. As regards the Middle Pleistocene Stages, although they were already well-established by radiometric data in N. Greece and in Montenegro, the glacial extent has been revised as it is greater than previous thought with some massifs throughout Greece showing evidence of the occupation of their upland by former ice caps during these periods of extensive glaciation.

An updated and robust geochronological framework of Quaternary glaciations in Greece is presented here along with a detailed analysis and discussion of the results that were produced from this doctoral research. Moreover, the different glacial phases are placed within the regional palaeoglaciological and palaeoclimatological context of the Balkans and the Mediterranean in general and correlations are attempted. As it can be concluded from the following discussion, the more we understand about the glacial history of Greece and the Mediterranean the more research questions are raised. Therefore, further research is needed to clarify important aspects of Quaternary glaciations such as a possible revision and expansion of the Middle Pleistocene glaciation extent and the deeper understanding of the local climate response in the mountains of Greece to major global and regional Late Pleistocene to Holocene climatic events such as the LGM, Heinrich Events and the Younger Dryas. Particular suggestions for further research are included in the discussion that follows.

7.1.1 The importance of the study on the ophiolitic Mt Mavrovouni for glacial research in Greece

The glacial study of Mt Mavrovouni presented in Chapter 4 has been of great importance for glacial research in Greece. Firstly, alongside the study of Allard et al. (2020) in the limestone-dominated Mt Tymphi nearby it addresses an important geographical and temporal gap in the glacial geochronological framework of Greece and the Mediterranean in general. At the same time, the application of cosmogenic ^{36}Cl exposure dating on ophiolitic boulders for the first time, constitutes the only chronology of Late Pleistocene glaciations on the mountains of Greece that is independent from inherent issues in surface exposure dating of limestones such as the erosion rate of rock surfaces. The importance of independent age constraints is also stressed by Ivy-Ochs and Kober (2008)

From a methodological point of view, the ^{36}Cl dating of ophiolite samples with high Fe_2O_3 content (8-8.5 wt %) is of great importance as it contributes to the validation of current scaling behaviour and ^{36}Cl production rates from Fe spallation for which further data from high Fe-content samples is needed (Moore and Granger, 2019). Moreover, the validation of the theoretical suitability of ^{36}Cl dating on ophiolites based on the consistency of the yielded ages with ^{36}Cl ages from limestones on Mt Tymphi and Mt Chelmos opens up the perspective of dating the only complete glacial sequence identified in Greece which has been mapped on the ophiolitic Mt Smolikas (see section 3.1.2)

7.2 Discussing the Quaternary glacial history of Greece

The geomorphological and geochronological data and the respective glacial phases are summarised chronologically into different time periods composing the first organised database for glacial studies in Greece (Table 21). Each period is discussed in detail next, based on the study of Leontaritis et al. (2020), which has been published in the framework of this research, focusing on the results from Mt Mavrovouni (Chapter 4) and Mt Chelmos (Chapter 5) as well as to the new evidence from other mountains in Greece (2.3).

It should be noted that due to the uncertainties in the cosmogenic exposure dating techniques, the age control of younger glacial deposits is to a certain extent limited. Therefore, even though certain glacial phases can be placed with confidence within the Late-glacial or Holocene, the reported ages should be viewed with caution and the precise timing of the glacial phases is likely to be subject to revision (Leontaritis et al., 2020).

Table 21. Overview table of the glacial history of Greece (modified from Leontaritis et al., 2020).

Glacial Evidence on the mountains of Greece					
Glacial Stage	Geographical Position	Dating avg. ELA	Period (Age)	Type of Evidence	Reference Study
Holocene	Mt Olympus HOL3	^{36}Cl n/a	MIS 1 (0.64 ka)	glacial boulder	Styllas et al., 2018
	Mt Olympus HOL2	^{36}Cl n/a	MIS 1 (2.6 - 2.3 ka)	moraines and glacial boulders	Styllas et al., 2018
	Mt Olympus HOL1	^{36}Cl n/a	MIS 1 (9.6 ka)	moraines and glacial boulders	Styllas et al., 2018
Late-glacial	Mt Olympus LG3	^{36}Cl >2300 m	Younger Dryas (12.6 - 12.0 ka)	Retreat moraines	Styllas et al., 2018
	Mt Chelmos	^{36}Cl 2174 m	Younger Dryas (13.1 - 10.5 ka)	moraines and glacial boulders	Pope et al., 2017
	Mt Smolikas	n/a 2372 m	Late-lacial (-)	moraines	Hughes et al., 2006c
	Mt Olympus LG1	^{36}Cl >2200 m	Oldest Dryas (15.6 - 14.2 ka)	moraines and glacial boulders	Styllas et al., 2018
Tymphian Stage	Mt Tymphi	^{36}Cl -	Post – LGM (18 ka)	Cirque moraine	Allard et al., 2020
	Mt Mavrovouni	^{36}Cl -	Post-LGM (20.0 ka)	Pronival rampart ridge	Present thesis & Leontaritis et al., 2021
	Mt Chelmos	^{36}Cl >2200m	LGM (22.2 – 19.6 ka) *	Retreat moraines	Pope et al., 2017
	Mt Tymphi	^{36}C 2231 m	LGM (24.5 ka)	cirque moraines retreat positions	Allard et al., 2020
	Mt Mavrovouni	^{36}Cl 2090 m	LGM (26.6 ka)	Terminal moraine	This study & Leontaritis et al., 2021
	Mt Tymphi	^{36}Cl 2016 m	Pre-LGM 29.0 - 25.7	moraines and glacial boulders	Allard et al., 2020
	Mt Smolikas	n/a 2241m	Pre-LGM (29.0 - 25.7 correl.)	moraines	Hughes, 2006c
	Mt Chelmos	^{36}Cl 2046 m	Pre-LGM (36.5 – 28.6 ka) *	moraines and glacial boulders	Pope et al., 2017
	Mt Olympus	n/a >2150 m	Pre-LGM	moraine ridge	Styllas et al., 2018
	Mt Chelmos	OSL n/a	MIS 5b (89 - 86 ka)	Terminolateral moraine ridge	This sudy & Pavlopoulos et al., 2018
Vlasian Stage	Mt Tymphi	U-series 1862 m	MIS6 (190 - 126 ka)	moraines, till, calcites	Hughes et al., 2006a
	Mt Smolikas	n/a 1997m		moraines, till	Hughes, 2004
Skamnellian Stage	Mt Tymphi	U-series 1741 m	MIS 12 (480 - 430 ka)	moraines, till calcites	Hughes et al., 2006a
	Mt Smolikas	n/a 1680 m		moraines, till	Hughes, 2004
	Mt Chelmos	n/a 1967 m		moraines, till	Pope et al., 2017
	Mt Mavrovouni	n/a 1785 m		moraines, till	This study & Leontaritis et al., 2021

* ^{36}Cl ages recalculated by Allard et al. (2020) with updated production rates of Marrero et al. (2006b)

7.2.1 Middle Pleistocene glaciations (Skamnellian – Vlasian Stages)

The most extensive glacial phases in the mountains of Greece most probably took place during Middle Pleistocene and particularly during MIS 12 (Skamnellian Stage) and MIS 6 (Vlasian Stage). This has been well established by radiometric data (uranium series from secondary calcites in limestone-derived moraines/till) from Mt Tymphi in north-western Greece (Woodward et al., 2004; Hughes, 2004; Hughes et al., 2006a). Later studies in the mountains of Montenegro and more specifically in the Orjen, Durmitor, Sinjajevina, and Moraća massifs confirmed that the largest glaciations there also date from the Middle Pleistocene and at least two distinct glacial advance phases were identified (Hughes et al., 2010; 2011). Furthermore, evidence in the Gran Sasso massif of the Apennines in central Italy suggests that during Middle Pleistocene there were two glacial advances during which glaciers reached further down-valley positions compared to the LGM and in particular it was estimated that glacial extent exceeded that of the local LGM by about 5–10% (Giraudi and Giaccio, 2015). In the Alps, there is also evidence that glaciers were more extensive during the Middle Pleistocene Stages compared to the LGM (Ivy-Ochs et al., 2006a; Gianotti et al., 2015)

At this point it should be noted that the stratigraphically older moraines on Mt Tymphi (and similarly in the mountains of Montenegro) have been ascribed to MIS 12 based on maximum uranium series ages from secondary calcites that are beyond the upper limit of U-series dating which is 350 ka (Woodward et al., 2004; Hughes et al., 2006a). It is important to recognise that as U/Th ages denote the age of secondary calcites formation sometime after deposition and in this case during the more favourable warm interglacial periods, the oldest ages for a particular deposit can be used to infer glacial activity during a previous cold stage (Woodward et al., 2004). For this reason, the yielded ages of the older moraines (>350ka) indicate that calcites formation was associated with MIS 11 (or older) although the precise ages are unknown (Woodward et al., 2004; Hughes et al., 2006a). Taking also into account that the next glacial period preceding 350ka (MIS11) is MIS 12 which is considered to be the most extreme climatic glacial interval of the last ~500 ka (Tzedakis et al., 2003) the deposition of these moraines was ascribed to this interval (Hughes et al., 2006a). Most interestingly, detailed sedimentological analyses of the diamicton sequences within these stratigraphically older moraines on Mt Tymphi, indicated that stacked diamicts facies separated by gravels related to meltout and glacial retreat record at least three phases of former glacial advance and retreat within the same glacial episode (Hughes et al., 2006e).

Great insight into sequential deposition of glacial sediments separated by 100 ka cycles during Pleistocene is inferred by the detailed stratigraphic study of the Ivrea morainic ampitheatre, a vast end moraine system (505 km^2) at the outlet of the Aosta Valley (Italy) in the southern Alps (Gianotti et al., 2015). In this study the glacigenic succession was divided into 9 distinct stratigraphic units on the basis of buried stratigraphic of interglacial/interstadial markers such as embedded palaeosols and palustrine deposits along with the pedostratigraphic analysis (Figure 72). Each unit has been ascribed to distinct glacial advance phases that have been correlated with the global isotopic curve from Lisieki & Raymo (2005). The age of the oldest (outermost) deposits (first stratigraphic unit –MGD synthem) has been constrained to a minimum age of 780 ka (MIS 19) on palaeomagnetic basis, according to both reverse and normal magnetization of two glaciolacustrine sequences resting below and above the subglacial till (Gianotti et al., 2015 and references therein). Therefore, its formation has been attributed to glacial activity during MIS 20 or 22 (Gianotti et al., 2015). The next unit directly constrained by dating of its overlying and buried palaeosol cap to MIS5 is the eighth unit (SER synthem) that has been attributed to glacial activity during the penultimate glaciation (MIS 6). Notably, the most extensive glaciation is correlated with the seventh unit (MAG synthem) on the basis of its marginal ice extent in the amphitheatre. According to tentative correlations of the stratigraphically older and younger units in relation to the MIS 6 and MIS 20/22 chronostratigraphic marks, its formation has been ascribed to MIS 8 (Figure 72; Gianotti et al., 2015). However, these correlations are subject to revision when more geochronological data become available and this age could be shifted to MIS 10 or 12. The innermost and thus stratigraphically younger sediment unit (Ivrea Synthem) dates to the LGM and several LGM retreat stadials have been recorded within the amphitheatre and upvalley prior to the final rapid recession of glaciers after 20 ka.

Unlikely morainic amphitheatres formed by large ice lobes where successive very big accumulations of glacial and glaciofluvial deposits are nested into each other preserving the sequence order (Figure 72), in mountain valleys younger glaciers are expected to override and rework remaining glacial sediments from previous glacial phases, incorporating them to their own deposits and thus destroying the evidence of a distinct glaciogenic sediments sequence. Based on the above analysis, it can be concluded that within the stratigraphically older deposits in Mt Tymphi and in the mountains of Greece in general, there could be incorporated deposits from older glacial phases. Therefore, MIS 6 glaciers for example may have overridden MIS8 or MIS 10 glacial sediments incorporating them to these younger sediment groups as also

pointed by Hughes et al. (2006a). This is the case also for the more extensive MIS 12 glaciers that could have incorporated glacial sediments from preceding Middle or even Upper Pleistocene glaciations. Conclusively, based on the evidence on Mt Tymphi, the MIS 6 glaciation (Vlasian Stage) was the most extensive of the MIS 10-MIS 2 period and the MIS 12 glaciation (Skamnellian Stage) was the most extensive glaciation up to the Early-Middle Pleistocene boundary (MIS 20).

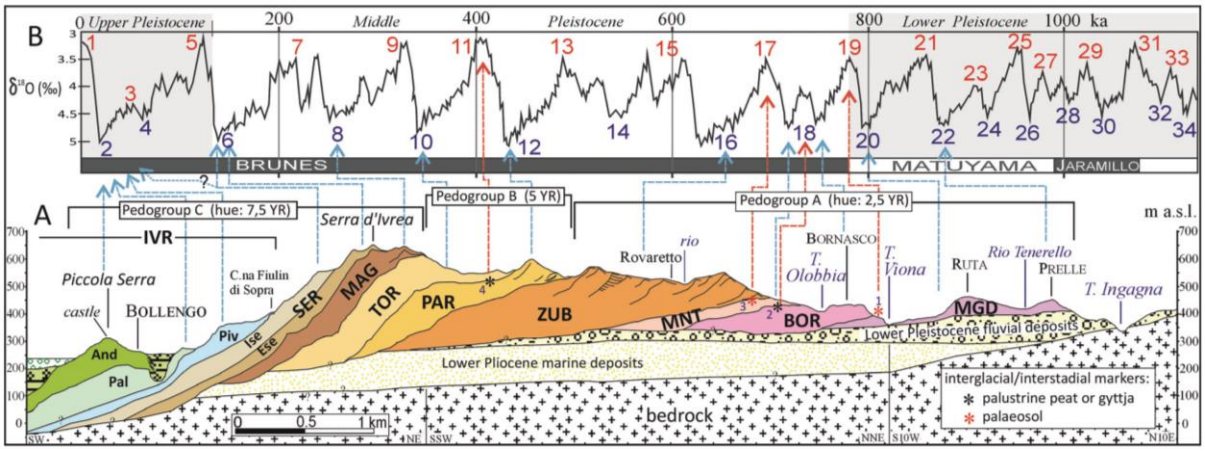

Figure 72. ***A)*** *Geological cross-section of the lateral north-eastern sector of Ivrea Morainic Amphitheatre, where all the stratigraphic units have been recognized. Interstadial or interglacial markers are indicated with asterisks (1-4);* ***B)*** *The glacigenic sequence is tentatively correlated with the subsequent Pleistocene glaciations on the global isotopic curve of Lisieki and Raymo (2005) (From Gianotti et al., 2015).*

Similar glacial deposits in terms of extent and altitude reach with those recorded on Mt Tymphi were also mapped on Mt Chelmos (Pope et al., 2017) and Mt Smolikas (Hughes, 2004; Hughes et al., 2006c) and have been attributed to the Middle Pleistocene, although without obtaining any radiometric dates. It should be noted that on Mt Chelmos multiple moraine units that could correspond to both Skamnellian and Vlasian Stage glaciations could not be identified, although it is possible that more than one glaciation is represented by the stratigraphically older unit (Pope et al., 2017). This also the case in Mt Mavrovouni (Chapter 4), where the most extensive glaciation(s) was characterised by valley glaciers in northern slopes that reached down to 1500 m a.s.l. as indicated by the stratigraphically older moraines identified in lower positions within the studied glacial valleys. The altitudinal reach is higher compared to Mt Tymphi (2497 m a.s.l.) and Mt Chelmos (2355 m a.s.l.,) but it should be taken into consideration that Mt Mavrovouni reaches an altitude of only 2157 m a.s.l. whereas most importantly, unlikely these two massifs with the extended high-altitude plateaus, it is characterised by limited high altitude areas that favour the accumulation of snow and the formation of extensive glaciers. This glacial phase remains undated but is likely to be Middle

Pleistocene in age as indicated by the stratigraphically older moraines identified in lower positions within the studied glacial valleys that have been correlated with Mt Tymphi and Mt Chelmos. Moreover, during the research on Mt Chelmos, there were also recorded the Laghada deposits presented in Chapter 5. These heavily eroded diamicton deposits are buried within the Lagadha alluvial fan at an altitude of 950 m a.s.l. and could be interpreted as till deposited by a former thin and long glacier draining the central ice field, and notably reaching similar altitudes with the respective Middle Pleistocene glaciers on Mt Tymphi. Elsewhere in mainland Greece, evidence of vast glacier formation is evident in numerous mountains higher than 1900 m a.s.l. which can rather safely be ascribed to these Middle Pleistocene glacial phases (Leontaritis et al., 2020).

7.2.1.1 Ice configuration during Middle Pleistocene glaciation

A very interesting conclusion regarding the glacial extent and ice configuration during Middle Pleistocene glaciations in Greece can be drawn by the inclusion of the new evidence from Mt Tymphi and Mt Smolikas (2.3) in the bigger picture we have for these glacial phases in Greece and W. Balkans. The evidence from Mt Chelmos implies that during the Skamnellian Stage the massif was glaciated by a plateau ice field with valley glaciers radiating from a central ice dome (Pope et al., 2017). The same ice configuration is very likely to have occurred over the mountains of Montenegro (Hughes et al., 2010, 2011) as well as over Mt Tymphi and Mt Smoilkas in NW Greece as it is argued here. The new evidence from W. Tymphi presented in indicate that ice breached the watershed of a W oriented valley and the till identified at lower altitudes (down to 800 m a.s.l.) was an outlet lobe of a larger plateau ice-field rather than a stand-alone valley glacier (section 3.1.1.1). If this was the case, the extent of glaciation during the most extensive Middle Pleistocene glacial phase have so far been underestimated. Thus, it is very likely that during the Skamnellian Stage Mt Tymphi was glaciated by a plateau ice field with valley glaciers radiating from a central ice dome centred over the plateau among its highest peaks.

As regards Mt Smolikas, the so far published evidence from Mt Smolikas is controversial since it suggests that only its northern slopes were glaciated during Middle Pleistocene (Hughes et al. 2006c), a fact that has been attributed to its ophiolitic lithology (Hughes et al. 2007). However, based on the new sedimentological observations presented in section 3.1.3, glaciers on Mt Smolikas also formed on its southern slopes and not only on its northern slopes as it was up to now believed. This implies that as was the case on nearby Mt Tymphi, slope orientation does not seem to have played a significant role on the formation of glaciers during the most

extensive Middle Pleistocene glacial phase. Moreover, new evidence of vast Skamnellian Stage glaciers in another N. oriented valley (section 3.1.3.1), indicates that a plateau ice field with valley glaciers radiating from a central ice dome centred over the tallest peaks of the massif is likely. However, further evidence is needed in order to confirm this hypothesis. A detailed geomorphological study focusing also in the eastern part of the massif where the glacial sequence is fragmentary is needed in order to eventually clear out the Middle Pleistocene ice limits on Mt Smolikas.

Finally, there is still an open question regarding the extent of Middle Pleistocene glacial phases on Mt Olympus (Leontaritis et al., 2020) as it has also been underlined by the presentation of some new low-altitude evidence from the eastern piedomont of the massif in section 3.2.

Overall, this discussion shows that new perspectives have been opened up in our understanding of Middle Pleistocene glaciation in the mountains of Greece and in particular that plateau ice fields dominated the palaeoglacier geometry of the most extensive glacial phases, such as during the Skamnellian Stage, resulting in outlet glaciers forming on all slope orientations.

7.2.1.2 Evidence from regional pollen and other palaeoenvironmental records

In the palaeovegetation/palaeoclimatic record from Tenaghi Philippon (see Figure 2 for location) a close correspondence between abundances of tree populations and ice volume has been suggested, as the subsequent aridity and cooling of ice accumulation would lead to tree population reductions (Tzedakis et al., 2003). Based on the extremely low abundance of arboreal pollen (AP), MIS 12 is considered to be the most extreme climatic glacial interval of the last ~500 ka (Tzedakis et al., 2003), followed by MIS 6 and MIS 2.

Pollen assemblages from Lake Ohrid (see Figure 2 for location), indicate a not so dry (compared to other glacial intervals) glacial period in the Balkan peninsula (Sadori et al., 2016; Koutsodendris et al., 2019). In between 487-424 ka BP a two-step reduction of AP abundance implies that the MIS 12 glacial phase has been cold but not very dry (Sadori et al., 2016). Centennial-scale-resolution of the pollen record, shows on the one hand that the forest cover around Lake Ohrid decreased substantially over the course of MIS 12 but at the same time a persisting presence and abrupt changes in tree populations is also recorded despite the severe character of the glacial conditions indicating a pronounced millennial-scale climate variability (Koutsodendris et al., 2019). This bears strong resemblance to the interstadial and stadial events

of the Last Glacial (Koutsodendris et al., 2019) and a similar trend has also been identified in the pollen record of Tenaghi Philippon for MIS 8 (Fletcher et al., 2013) Most importantly, the repeated forest expansion/contraction events are also characterised by differences in moisture availability with annual precipitations values ranging from 25% higher to 10-35% lower than today (Koutsodendris et al., 2019). These conditions would have been very favourable for the development of very extensive glaciers similarly to the LGM glaciers in the Alps which is consistent with the glacial record and the geochronology from Mt Tymphi (Hughes et al., 2006a)

Similarly, during the long glacial phase corresponding to MIS 6, low AP abundances, but also interesting vegetation variability in the palaeoarchives of the southern Balkans is evidenced (Tzedakis et al., 2003; Roucoux et al., 2011; Sadori et al., 2016). Arboreal pollen abundance of the early part of MIS 6 in Lake Ioannina is high, in relation to the late part, and shows pronounced oscillations, implying cool and wet conditions (Roucoux et al., 2011). In Lake Ohrid, the second part of MIS 6 appears to be the driest phase of the last 500 ka (Sadori et al., 2016), while pollen-based palaeoclimatic reconstructions point to cold and dry conditions in the area (Sinopoli et al. 2019).

The analysis of the time proxy series of Lake Ohrid for the last 1.36 Ma and model data has shown that winter precipitation appears increased during periods of low Northern Hemisphere winter insolation due to orbital forcing on changes in precipitation variability (Wagner et al., 2019). Therefore, during periods like MIS 12 and MIS 6, favourable climatic conditions for the formation of glaciers must have prevailed. However, this correlation does not apply during colder and drier glacial periods with increased global ice volume (Wagner et al., 2019) such as the later parts of these two severe stages. The extensive MIS 12 and MIS 6 glaciers were therefore most probably formed during the early and relatively wet parts of these severe cold stages (Leontaritis et al., 2020), as reduced precipitation during the later arid parts would have inhibited glacier build-up (Hughes et al. 2003). Hughes et al. (2006d) also argued that the maximum extent of glaciers during the Vlasian Stage (MIS6 / 190-130 ka) might have occurred in an interval of cold, yet more moist conditions, prior to limit of the pollen record of Lake Ioannina at 133 ka that indicates very arid climatic conditions at the end of MIS 6 (Tzedakis et al. 2002). This evidence underlines that winter precipitation is a crucial factor for the glaciers expansion as precipitation strongly controls the mass balance of glaciers (Ohmura et al. 1992).

Finally, it should be mentioned that the study of the rift basin in the Gulf of Corinth to the north of Mt Chelmos (Figure 52) based on analysis of syn-rift sediment thicknesses from

integration of seismic profiles around the rift showed changes in the sedimentation regime (volume and character of sediments) over the last ~550ka corresponding to orbital-timescale cycles of 100ka (McNeill et al. 2019). In particular, it was concluded that during glacial intervals (MIS 12, 8, 6 and 5d-2), the basin was isolated from the ocean, and sedimentation rates due to enhanced fluvial input into the basin were ~2–7 times higher than those during the interglacials (excepting the Holocene) when the basin was marine (McNeill et al. 2019). Moreover, as increased sediment fluxes during glacial periods reflect increased sediment production and supply (McNeill et al. 2019) and pollen-based precipitation reconstructions from the region (Tzedakis et al., 2006; Sadori et al., 2016) indicate a decrease in precipitation during glacials rather than an increase (also discussed above), it has been inferred that reduced vegetation cover during glacials drove increased erosion and higher sediment flux from the rift flanks (McNeill et al. 2019). Nevertheless, it is here argued that an additional factor for the increased sediment supply during glacial intervals can be associated with the glacial erosion induced by the extensive glacial activity on Mt Chelmos both during Middle Pleistocene as the above-presented evidence suggests and during the Last Glacial Cycle as it is discussed next.

7.2.2 The Last Glacial Cycle (Tymphian Stage: MIS 5d-2)

The Tymphian Stage in Greece (Hughes et al. 2006a) corresponds to the Last Glacial Cycle corresponds to the period MIS 5d-2 following the Eemian interglacial (MIS 5e) that ended at ~115 ka (Dahl-Jensen et al., 2013). The Last Glacial Cycle is characterised by pronounced climatic oscillations and major global and regional climatic events such as the Last Glacial Maximum (LGM), the Heinrich Stadials (HS 1-10) and the Younger Dryas. The LGM in particular is the timing between 26.5 and 19 ka, when the accumulation of ice in large ice sheets of the Northern Hemisphere between 33.0 and 26.5 ka reached their maximum position (Clark et al., 2009; Hughes et al., 2016). Hughes and Gibbard (2015) suggest a timing of 27.5−23.3 ka for the LGM based on the global dust record in polar ice cores and this is adopted here.

The later part of the Last Glacial Cycle is known as the Late-glacial and was characterized by two cold periods that favoured glacial advance: the Oldest and the Younger Dryas (YD) at 17.5-14.7 ka (Rasmussen et al., 2006) and 12.9-11.7 ka (Rasmussen et al., 2014) respectively. These two cold periods have long been recognised to form the beginning and end of the Late-glacial interval and are recognized in the oxygen isotope record of Greenland cores and correlate with GS-2.1a and GS-1 stadials in the GRIP ice core (Björck et al., 1998; Rasmussen et al., 2006). It is noted that the Oldest Dryas, although it is a pollen assemblage zone well-

recognised in northern Europe, in the Mediterranean it is not so clearly recorded and therefore for this time interval it is preferrable to refer to Heinrich Stadial -1 (HS1: 18.0-15.6 ka; Sanchez Goñi and Harrison, 2010).

In this section a full account of the local climate response to these climatic events as it has been imprinted in the glacial record in the mountains of Greece is given. Generally, evidence throughout the mountains of Greece suggests that the Tymphian Stage – the last cold stage in Greece – saw much more restricted glacier development compared with the Middle Pleistocene glaciations.

7.2.2.1 Early Tymphian Stage (MIS 5d-5a)

The issue of glacial activity in the Mediterranean during the cold sub-stages of MIS 5 (5d and 5b) has been characterized by Woodward et al. (2004) as an intriguing one and it was acknowledged that further work was required to confirm this.

Evidence for a possible glaciation phase in Mt Chelmos during the early Tymphian Stage, was presented in Chapter 5 and has also been published by Pavlopoulos et al. (2018). The OSL dating of samples from morainic deposits at an altitude of 1900-2050 m a.s.l. in the Spanolakos valley yielded burial ages of 89-86 ka that could indicate another phase in glacial evolution in the Peloponnese during MIS5b.

A very similar glacial sequence to the one recorded in Mt Chelmos has been identified in the Pyrenees (Pavlopoulos et al., 2018). Peña et al. (2004) applied OSL to date glacio-fluvial deposits in the Gallego Valley in the western part of the mountain range. They were able to differentiate between three phases of glacier advance/stabilization, at ca. 155.8 ka (Sabiñánigo phase – MIS 6), 85 ka (Aurín phase – MIS 5b) and 35.7 ka (Senegüe phase – MIS 3) which correlate very well with glacier Phases I, IIa and IIb (see Table 18 and section 5.5)

However, the OSL moraine burial ages from Mt Chelmos constitute the only glacial evidence in Greece and the Western Balkans for MIS 5b and further geochronological data is needed to further test this hypothesis. Specifically, although different evidence has indicated a possible glaciation phase in the mountains of Greece during this period, this is the first time that evidence is supported by direct glacial geochronology. In particular, the extensive dating program on Mt Tymphi in northern Greece provided some unclear evidence for the glaciation phases during the Tymphian Stage (Late Pleistocene - MIS 5d- MIS 2). The separation of Late and Middle Pleistocene glacial units was achieved by detailed mapping and by applying U-series dating methods to date secondary calcite cements in glacial deposits on Mount Tymphi

(Woodward et al. 2004; Hughes et al. 2006a). However, radiometric ages have only been obtained from the Middle Pleistocene moraines because no secondary calcites were found in younger moraines. There was just one case, in Vrichos member, where a single calcrete sample from a lateral moraine at 1750 m a.s.l. yielded a uranium series age of 80.45±15.10 ka, indicating that this moraine system had a minimum age of creation during MIS 5b-4 (Woodward et al. 2004). Evidence from morphologically similar nearby moraines showed two generations of calcite growth (131.25 ± 19.25 ka and 81.70 ± 12.90 ka). In this case, the older of the two ages provided the minimum age of the latter moraine complex, suggesting a related glacial phase during MIS 6. Accordingly, the moraine of Vrichos member has also been correlated with this unit. Tymphian stage deposits on the other hand, are clearly younger than those of the Vlasian stage based on stratigraphic position and soil PDI data (Hughes et al. 2006a) as well as on the ^{36}Cl-based geochronology (Allard et al., 2020), and are limited to rock glaciers and small moraines in high altitudes (>1700 m a.s.l.). It is therefore possible, that multiple episodes of glacial activity had occurred during the Tymphian stage, with only the last of these being recorded in the glacial stratigraphic record (Hughes et al. 2006a; 2006d).

As it is more thoroughly discussed in section 7.2.2.5, indirect evidence of a glacial advance phase during MIS 5b came with the development of a chronostratigraphic framework for fluvial glacially-derived sediments deposited by the Voidomatis River, which drains the southern slopes of Mount Tymphi (Lewin et al., 1991; Macklin et al., 1998). Four separate alluvial units were recognised correlating with deposition during MIS 6, MIS 5b and MIS 2 respectively. As regards the MIS 5b unit in particular, maximum uranium-series ages were calculated at 80 ± 7 ka (Lewin et al., 1991; Macklin et al., 1998, Hamlin et al., 2000). However, on Mt Tymphi no evidence of ^{36}Cl ages from moraine boulders that correspond with earlier phases of glaciation during the Late Pleistocene, i.e. at 80 ka, was found (Allard et al., 2020). The suggested interpretation is that glaciers at these times were probably much smaller than those dated to the local Late Pleistocene glacial maximum at 29.0-25.7 ka and any older moraines, deposited inside of these limits, were very likely reworked by later and more extensive glacier advances (Allard et al., 2020). These fluvial units could suggest that glaciers oscillated within the upper valleys and cirques of Mount Tymphi throughout the Late Pleistocene (Allard et al., 2020) but they could also represent fluvial reworking of the limestone-rich outwash that was deposited during the Middle Pleistocene (Woodward et al., 2008).

At a global level, the time interval 89-84 ka is representative of stadial conditions of the early part of the MIS-5 interglacial (at the end of cold stadial MIS 5b). This is shortly after both

global temperatures and atmospheric concentrations of CO_2 have fallen significantly and the Laurentide ice sheet has expanded to a significant size, but before the Fennoscandian ice sheet could have a major influence on climate (Hoogakker et al. 2016). The pollen-based biomization for 84 ka (MIS 5b) clearly reflects the warmer and wetter conditions with more CO_2 available than at the LGM (21 ka), especially in Europe, with the majority of sites showing highest affinity scores for the temperate forest biomes (Hoogakker et al. 2016). Sites in other parts of the world show similar affinity scores to those at the LGM, although there are not many sites and it is less clear whether they reflect widespread climatic conditions (Hoogakker et al. 2016). On the other hand, according to the evaluation of the GISP2 ice core as to the variability in the North Atlantic at the millennial-scale, the ages of cooling events during MIS-5 were dated to 85.20–86.00 and 103.55– 103.80 ka respectively (Rohling et al. 2003), which are in agreement with moraine deposition OSL ages from Mt Chelmos (Pavlopoulos et al., 2018).

7.2.2.2 Around the Last Glacial Maximum (MIS 4 – start of the Late-glacial at 17.5ka)

The geochronological data that have been produced in the last five years for the interval between MIS 4 and the Late-glacial (Table 21) have been crucial for the address of the most important temporal gap in the geochronological framework of the glacial history of Greece (Leontaritis et al., 2020) by targeting the previously undated Late Pleistocene record.

The geochronological framework of Late Pleistocene glaciations in the Pindus mountains in NW Greece is the best dated in Greece. The consistent 36Cl dates from ophiolite-derived moraines from Mt Mavrovouni that was presented in Chapter 4 and the 36Cl dates from limestone moraines (Allard et al., 2020) suggest a Late Pleistocene local glacial maximum prior to but close to the LGM (27.5-23.3 ka) within the errors of the calculated ages. In particular, the largest glaciers on Mt Tymphi during Late Pleistocene reached their terminal positions no later than 25.7 ± 2.6 - 29.0 ± 3.0 ka (Allard et al., 2020) while glaciers had retreated to the high cirques by 24.5 ± 2.4 ka during Heinrich Stadial 2 (Allard et al., 2020). Most importantly, this timing of a near-LGM late Pleistocene glacier maximum was confirmed by the 36Cl geochronology of ophiolitic glacial boulders from an end moraine of a cirque glacier in Mt Mavrovouni, indicating stabilisation of the most extensive Late Pleistocene glaciers at 26.6 ± 6.6 ka (Chapter 4; Leontaritis et al., 2021). The application of cosmogenic 36Cl exposure dating on ophiolitic boulders for the first time, constitutes the only chronology of Late Pleistocene glaciations on the mountains of Greece that is independent from inherent issues in surface exposure dating of limestones such as weathering rates of rock surfaces. Most importantly the obtained exposure ages in the Pindus mountains have been carefully scrutinized in the

framework of detailed field studies, including local moraine stratigraphy and regional morphostratigraphic relationships as well as in light of independent age constraints as urged by (Ivy-Ochs and Kober, 2008).

The timing constraint of a local Late Pleistocene glacial maximum in the Pindus mountains in NW Greece near the LGM is in good agreement with well-preserved outwash sediments dating to 28-24 ka in the Voidomatis River record downstream of the Mt Tymphi dated moraines (Lewin et al., 1991; Macklin and Woodward, 2009) and is consistent with the Ioaninna basin pollen record (Tzedakis et al., 2002) indicating cool and wet conditions, most favourable for glacier growth, at 30-25 ka (Allard et al., 2020; see also section 7.2.2.4).

It should be noted that the age uncertainty of the terminal moraines' deposition on Mt Mavrovouni (26.6 ± 6.6 ka) suggests that this glacial phase could predate or postdate the LGM by 3 and 6 ka respectively. However, the ^{36}Cl ages from Mt Tymphi and Mt Chelmos (Table 21; see also next paragraphs) suggest a pre-LGM Late Pleistocene glacier maximum. Therefore, a pre-LGM to LGM local glacier maximum on Mt Mavrovouni is more likely although more data is needed to build a robust age model. On this basis and according to the geomorphological studies on Mt Smolikas (Hughes et al., 2006c) and Mt Olympus (Styllas et al., 2018) in NW and N Greece respectively (see Figure 1 for locations) the well-formed moraines of Stratigraphic Unit 3 at 2000-2200 m a.s.l. on Smolikas (Hughes et al., 2006c; see section 3.1.2; and the moraine MK-A at 2150 m a.s.l. on Olympus (Styllas et al., 2018; see section 3.2.1) which lack any cosmogenic dating data can be ascribed to a glacial advance phase prior or within the LGM. As regards Mt Smolikas in particular, taking into account its proximity to Mt Tymphi and Mt Mavrovouni and under the light of the above-discussed ^{36}Cl chronologies from Tymphian Stage moraines on these mountains, this stratigraphic group could be correlated with a glacial phase close to the LGM between ~29.0 and 25.7 ka.

In the Peloponnese, the study of Pope et al. (2017) on Mt Chelmos showed that Pleistocene glaciers reached their maximum extent at 36.5 ± 0.9 - 28.6 ± 0.6 ka (Pope et al., 2017 - recalculated ages by Allard et al., 2020; see Table 18 and Table 19) implying that ice is likely to have occupied the cirques of Mount Chelmos from MIS 3 to 2 and oscillated in response to varying climatic conditions, especially in response to millennial-scale shifts between cold/dry and cool/wet conditions in Greece (see discussion in Hughes et al., 2006d).

The shift of the recorded local Late Pleistocene glacier maximum on the Pindus mountains (Mt Tymphi, Mt Mavrovouni) and Mt Chelmos prior to the global LGM, is in accordance with evidence from other mountains across the Mediterranean like the Pyrenness (García-Ruiz et

al., 2010) northern Spain (^{10}Be ages: 33ka; Rodriguez-Rodriguez et al., 2011), Southern Spain (^{36}Cl ages: 30-35ka; Gómez-Ortiz et al., 2012; Palacios et al. 2016) and the Italian Apennines (33-27 ka; Giraudi, 2012). Interestingly, cosmogenic dates from the western and central Taurus Range in Turkey suggest similar pre-LGM glacier advance phases: at 35 ± 2.5 - 28.1 ± 2.6 ka (^{36}Cl) on Mt Akdağ (Sarıkaya et al. 2014) at 46.0 ± 7 - 29.8 ± 2.3 ka (^{36}Cl) on Mount Bolkar (Çiner and Sarıkaya, 2017) and at 29.7 ± 2.9 ka (^{10}Be, ^{26}Al) on the nearby Dedegöl Mountains (Köse et al., 2019). Glacial advance during MIS3/early MIS2 in these areas has been associated with the prevalence of optimal cold and wet conditions (Oliva et al., 2019).

As regards part of the LGM after 25 ka, glaciers were present in the mountains of Greece but exposure ages of glacial retreat by 24.5 ± 2.4 ka in Mt Tymphi (Allard et al., 2020) and by 22.2 ± 0.3 - 19.6 ± 0.5 ka from Mt Chelmos (Pope et al., 2017 recalculated by Allard et al., 2020; see Table 18 in section 5.5119) are assumed to indicate glacier retreat at this time, earlier than the retreat of Northern Hemisphere mountain glaciers at ~19 ka (Clark et al., 2009). Kuhlemann et al. (2013) have also argued that arid climatic conditions in Western Balkans prevailed during the LGM. This is consistent with climatic deterioration during Heinrich Stadial 2 ([HS 2: 26.5 -24.3 ka - Sanchez Goñi and Harrison, 2010] Macklin et al., 1997) and a marked regional temperature depression between 25.6 and 23.2 ka (Galanidou et al., 2000; Hughes, 2004) when cold and drier conditions prevailed, reducing regional moisture supply and therefore inducing glacial retreat (Allard et al., 2020).

This is further supported by evidence from Mt Tymphi where the presence of debris rock glaciers -which are stratigraphically younger than the moraines deposited by the most extensive glaciers that occupied the cirques at 25.7 ± 2.6 ka (Allard et al., 2020) - below small cirque glaciers, has been interpreted as the result of arid and cold climate conditions (Hughes et al., 2003). Palmentola and Stamatopoulos (2006) identified a number of rock glaciers on Mt Peristeri and the adjacent Tzoumerka massif (Figure 1) and although no dating data are available, they have ascribed their formation to the LGM. However, they recognise a possibility that these rock glaciers might date to the Late-glacial (Palmentola and Stamatopoulos, 2006; Leontaritis et al., 2020).

At a global level, the LGM is succeeded an interval associated with changes on the northern summer insolation induced by orbital forcing that resulted in the onset of Termination I at high latitudes and mountain regions at 19−20 ka, as well as an abrupt rise in sea level (Clark et al., 2009; Shakun et al., 2015).

In Greece, evidence from periglacial features on Mt Mavrovouni suggest that after the retreat of LGM glaciers, cold conditions persisted until 20.0 ± 5.0 ka but were unable to sustain dynamic glaciers (Chapter 4; Leontaritis et al., 2021). This is supported by a ^{36}Cl age from a pronival rampart ridge. The deposition of pronival ramparts has been attributed to the presence of perennial snow/nevé fields within the topographically shaded glacial cirque slopes and the increased debris supply due to freeze-thaw weathering of the cirque walls combined with rock slope failures. Furthermore, on Mt Tymphi, initial results suggest that small glaciers (<0.6 km^2) persisted in the northeast cirques at 18.0 ± 1.9 ka, perhaps sustained by avalanching snow and topographic shading from the Goura cliffs (Allard et al., 2020). The evidence from Mt Mavrovouni and Mt Tymphi, thus suggest unfavourable conditions for glacier development during this transitional phase from the LGM to the late-glacial and the Holocene but cold/humid enough to preserve perennial snow fields (i.e. nevé fields) and small glaciers in topographically favourable positions. This is consistent with other proxies from the Ioannina Lake that indicate locally cold and drier climate persisting during this period that would have inhibited glacier development (Allard et al., 2020), such as low lake levels between 20 and 22 ka (Frogley, 1998) and a drop of temperatures by 7-10^{o}C with annual rainfall around 600 mm as it has been estimated by the analysis of the lacustrine pollen record in Ioannina (Tzedakis et al., 2002). Finally, a decline in limestone derived fine sediment input from 24.3 ± 2.6 to 19.6 ± 3.0 ka in the Voidomatis River record implies the presence of smaller glaciers in the in the Voidomatis headwaters (i.e. in the high altitude S-oriented cirques of Mt Tymphi) than earlier within the LGM (Macklin et al.,1997). The young limiting age of the Vikos unit is consistent with the deposition of pronival ramparts on Mt Mavrovouni and overlaps within uncertainty with a possible moraine deposition in the Laccos cirque on Mt Tymphi discussed above, thus giving some support to this initial evidence for small cirque glaciers on the massif at 18ka (Allard et al., 2020). Nonetheless, more data are needed from this period in the Pindus mountains in order to build a more robust age model.

7.2.2.3 The Late-glacial (17.5-11.7 ka)

In Greece, glacial deposits from the Late-glacial are rare have so far been dated only on Mt Chelmos and Mt Olympus at 2100 m a.s.l. and 2200-2250 m a.s.l. respectively (Table 21). In particular a limited glacial advance phase has been dated on Mt Chelmos at 13.1 ± 0.2 - 10.5 ± 0.3 ka (Pope et al., 2017 recalculated by Allard et al., 2020; see Table 18 in section 5.5119) that can be correlated with YD (Leontaritis et al., 2020), whereas in Olympus a similar advance/stabilization of glaciers dated at 15.6 ± 2.0 -14.2 ± 1.0 ka (Phase LG1; Styllas et al.,

2018) has been ascribed by Leontaritis et al. (2020) to HS1 (18.0-15.6 ka). The morphological features of glacial deposits on Mt Olympus that were dated to YD though, suggest a glacial retreat phase and unfavourable conditions for glacial advance (Phase LG3 at 12.6 ± 1.6 - 12.0 ± 1.5 ka; Styllas et al., 2018). These findings further support the assumptions of Hughes et al. (2006c) that have correlated the high-altitude (2300-2400 m a.s.l.) glacial deposits mapped on Mt Smolikas (Hughes 2004) to the moraine complexes found above 2200 m a.s.l. in the Megala Kazania cirque in Mt Olympus, ascribing their formation to the Late-glacial.

Notably, both on Mt Tymphi (Allard et al., 2020) and on Mt Mavrovouni (Chapter 4; Leontaritis et al., 2021) in the Pindus mountains no evidence of glacial activity during the Late-glacial has been identified. This is supported by the fact that there is no glacially-derived outwash sediment detected in the slackwater flood deposits dating to 17.5 ± 0.3 and 17.2 ± 0.4 ka from the Voidomatis catchment (Woodward et al., 2001; 2008) , implying the absence of glaciers in the Voidomatis headwaters (i.e. in the high altitude S-oriented cirques of Mt Tymphi) during this period (Allard et al., 2020). The paucity of Late-glacial moraines on Mt Tymphi possibly indicates that relatively unfavourable climatic conditions for glaciers formation continued throughout most of the Late-glacial.

Further insights for the formation of glaciers in the Pindus mountains during the Late-glacial can be inferred by a future dating program targeting the undated Late Pleistocene record on Mt Smolikas in northwest Greece. As it was analysed in section 3.1.2 there have been recorded four discrete phases of Pleistocene glacial activity on Mt Smolikas implying that there is one even younger stage of glaciation here compared to Mt Tymphi (Hughes et al., 2006c). In particular, these glacial landforms exceed in altitude the floors of the highest cirques on Mt Tymphi by 200 m and therefore could postdate the youngest moraines on Mount Tymphi (~24.5 ka – Allard et al., 2020) as advocated by Hughes et al. (2006c). It has been argued that they could have been formed after the local glacier maximum and the last cold stage - during the Late-glacial (17.5-11.7 ka; Rasmussen et al., 2006; 2014) - and in particular that they might be Younger Dryas in age (Hughes, 2004; Hughes et al., 2006c). This hypothesis is further supported by the pollen record of the near-by Lake Prespa as it is analysed in detail in the next section. It is here noted that the pollen record of Lake Prespa might be more representative for the climate conditions prevailing on Mt Smolikas compared with Lake Ioannina due to their proximity as well as the absence of intervening tall mountain massifs between them (Figure 1 and Figure 2).

Thus, the glacial sequence on Mt Smolikas is the most complete recorded glacial sequence in the Pindus mountains and NW Greece in general. The potential of this important sequence has only been partially explored, as the ophiolitic lithology of Mt Smolikas posed some difficulties in the dating of glacial deposits (Woodward and Hughes, 2011). However, as it has been proven by this research, the cosmogenic ^{36}Cl exposure dating method is applicable in ophiolites, opening up the perspective of a future ^{36}Cl dating program on Mt Smolikas (see discussion in section 7.1.1; Leontaritis et al., 2021). Moreover, the importance of dating this glacial sequence for building a robust age model for the Late Pleistocene glacial history of Greece is further highlighted by the fact that it would constitute the only complete Late Pleistocene chronology in Greece that is independent from inherent issues in surface exposure dating of limestones such as the weathering rate of rock surfaces.

The need for focused research on the Late Pleistocene and especially Late-glacial deposits on Mt Smolikas is crucial in order to compare the studies in the Peloponnese, Mt Olympus and northwest Greece and draw some conclusions upon the timing and ELAs of the recorded glacial advance/retreat phases is also underlined by Leontaritis et al. (2020). Furthermore, such a study would allow to confirm the (close to) LGM timing of the local Late Pleistocene glacier maximum, the late-LGM glacier retreat as well as the cold and dry conditions during the transition interval to the Late-glacial as analysed in the previous section.

A number of studies in southern Balkans provide further evidence for these Late-glacial phases. A similar glaciation to the LG1 glacial phase in Olympus occurred in Mt Pelister, situated immediately east of Lake Prespa in The Republic of North Macedonia, at 15.24 ± 0.85 ka (^{10}Be Ages; Ribolini at el., 2017) that can also be correlated with the Gschnitz stadial of the Alps (Ivy-Ochs et al., 2006b) and the Fontari Stadial at 15 ka in the Italian Apennines (Giraudi and Frezzotti, 1997). Similarly, glacial advance has been dated to 17-14 ka in the south Carpathians (Retezat Mountains; Reuther et al., 2017) and to 19-14 ka in the Rila Mountains in Bulgaria, although the latter has been interpreted as a late LGM phase (Kuhleman et al., 2013). In the Šara Range in Kosovo two phases of glacial advance have been dated with ^{10}Be to 19.4-14.0 ka and 14-12 ka whereas rock glaciers developed within cirques between 12.4 ± 1.0 and 11.7 ± 0.6 ka indicating the increasing seasonal aridity (Kuhleman et al., 2009). As regards the former glacial phase, the oldest age points to a moraine formation in the course of the LGM, whereas the others could potentially represent recessional moraines (Hughes et al., 2013). On the other hand, the stratigraphically younger high-altitude moraines (2020-2300 m a.s.l.) were ascribed to the YD (Kuhleman et al., 2009). On Mount Orjen, Montenegro,

uranium-series dating of secondary carbonates within a terminal moraine in the Reovci valley provides a minimum age glacial advance of 17.3 ± 0.6 ka (Hughes et al., 2010). Evidence for glacier advance phases early in the Late-glacial has also been identified in the Maritime Alps in Italy (Federici et al., 2012; Federici et al., 2017 and references there in) and on several mountains in Turkey (Sarıkaya and Çiner, 2017 and references there in).

The YD phase is strongly supported by the cosmogenic ^{36}Cl ages from the Galicica Mountains between Lakes Ohrid and Prespa in The Republic of North Macedonia, where five limestone boulders from an end moraine were dated with ^{10}Be to 12.8-11.3 ka (Gromig et al., 2018). Uranium-series dating of secondary calcites within moraines in Montenegro also attests to moraine formation prior to 13.4 ± 0.4 ka, 10.6 ± 0.2 ka and 9.6 ± 0.8 ka in the Durmitor Massif (Hughes et al., 2011), and before 9.6 ± 0.8 ka at Mount Orjen (Hughes et al., 2010).

Further northwest, in Bosnia and Herzegovina, Žebre et al. (2019) dated 20 moraine boulders that yielded ages spanning from Oldest Dryas in Velež Mountain (14.9 ± 1.1 ka) to YD in Crvanj Mountain (11.9 ± 0.9 ka) while Çiner et al. (2019) report YD ages (within error) from the Svinjača (13.2 ± 1.8 ka) and Glavice (13.5 ± 1.8 ka) areas. A YD glacial advance phase is also consistent with evidence from the Italian Maritime Alps (Federici et al., 2017 and references therein), the Italian Apennines (Giraudi and Frezzotti, 1997) and western Taurus range in Turkey (Sarıkaya and Çiner, 2017).

7.2.2.4 Late Pleistocene pollen records

In an effort to examine possible correlations between the glacial record and other regional palaeoclimatic proxies, selected regional pollen records plotted against age (ka), in correlation to the recorded glacial phases in the mountains of Greece and the planktonic foraminiferal $\delta^{18}O$ in the LC21 marine sediment core from the Aegean Sea are presented in Figure 73.

A regards Late Pleistocene in general a close examination of arboreal pollen (AP) and AP excluding *Pinus* frequencies from existing archives (Figure 73) shows that the duration and independent characteristics of vegetation patterns vary significantly implying differences connected with local microclimates, topography and elevation (Leontaritis et al., 2020). For example, the comparison of the Tenaghi Philippon record at low elevation (Müller et al., 2011; Milner et al., 2016 Wulf et al., 2016) with the intermediate to higher altitude ones of Lakes Ioannina, Prespa and Ohrid (Tzedakis et al., 2003; Panagiotopoulos et al., 2014; Sadori et al., 2016; Wagner et al., 2019) showcases the variability of trees response to Last Glacial climatic oscillations like the Heinrich Stadials.

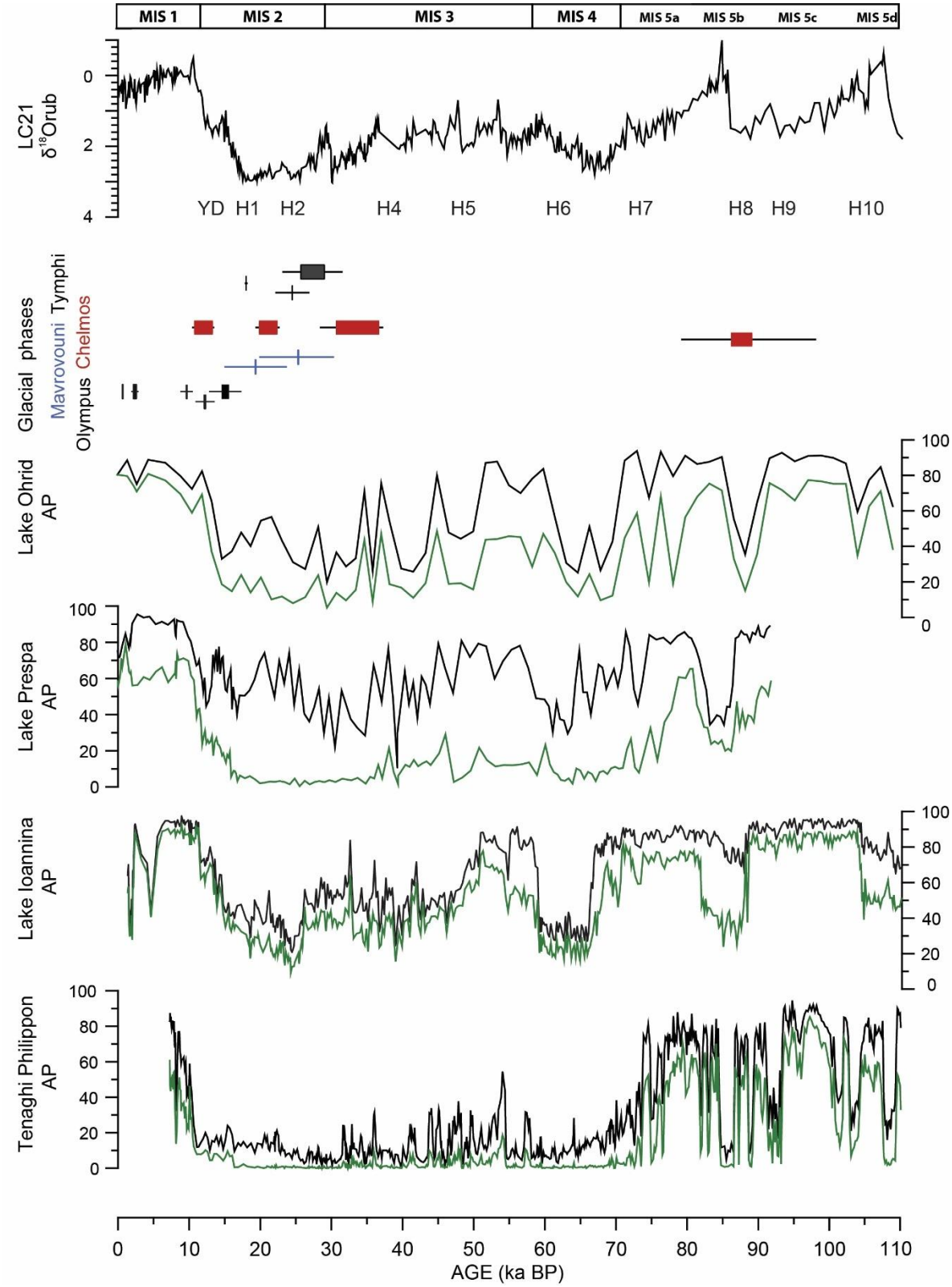

Figure 73. Selected regional pollen records plotted against age (ka), in correlation to planktonic foraminiferal $\delta^{18}O$ in the LC21 marine sediment core from the Aegean Sea (Grant et al., 2012). Arboreal Pollen (AP) in black and AP excluding Pinus in green from: Tenaghi Philippon (data from Wulf et al., 2018), Lake Ioannina (AP excluding Pinus and Juniperus: Tzedakis et al., 2002), Lake Ohrid (Sadori et al., 2016; Wagner et al., 2019) and Lake Prespa (Panagiotopoulos et al., 2014). See Figure 2 for location of sites. (modified from Leontaritis et al., 2020).

The palaeovegetation and palaeoclimatic records from Lake Ioannina, Lake Ohrid and Lake Prespa are in agreement with the onset of the recorded glacial episodes just before the onset of AP percentages reduction (Leontaritis et al., 2020). The catchments of these lakes include mountainous areas with significant glacial deposits like the Pindus Mountain ridge, Mt Pelister and the Galicia Mountains respectively, adding up into their value as independent palaeoarchieve for discussion. The diversification of the planktonic foraminiferal $\delta^{18}O$ palaeoclimatic records in LC21 and the Arboreal Pollen (AP) excluding *Pinus* in Tenaghi Philippon compared with the other pollen records, can be attributed both to the low altitude of the latter and to the fact that they are open systems and in direct correlation with the Aegean atmospheric and sea circulation. This particular climatic system influences the local climate by increasing precipitation and modifying the wind regime with prevailing southern winds (Leontaritis et al., 2020).

Further examining the pollen records of the southern Balkan Peninsula, several abrupt vegetation successions indicating major changes in moisture availability and temperature correlated to the succession of Greenland cold events have been identified during the Early Last Glacial, corresponding to the later facies of the MIS 5 (Tzedakis, 1999, 2003; Panagiotopoulos et al., 2014; Milner et al., 2016; Sinopoli et al., 2018), while this vegetation pattern of rapid expansion and reduction of forest populations continues throughout the Last Glacial (Figure 73). A scheme connecting the tree population abundance with climatic favourable conditions for glacier formation has been proposed by Hughes et al. (2006d) based on the pollen record of Lake Ioannina (Tzedakis et al. 2002). Taking into consideration that that precipitation strongly controls the mass balance of glaciers (Ohmura et al. 1992), even during major stadials that are characterized by low total AP frequencies related with arid and cold climatic conditions, reduced precipitation would have inhibited glacier build-up and would have forced the retreat of pre-existing glaciers (Hughes et al. 2003). Therefore, there are two types of intervals with the most favourable conditions for glacier formation. The first are intermediate phases between the most pronounced peaks and troughs of major stadials and interstadials while the second type is characterised by large differences between total AP frequencies and AP frequencies excluding the tolerant of cold conditions *Pinus* and *Juniperus* species, reflecting to moist yet cold conditions (Hughes et al. 2006d). Such intervals are recognized at 30-25 ka, 35-31 ka and 88-83 ka. The former period could be correlated with a possible local pre-LGM to LGM Late-Pleistocene Glacial Maximum whilst the period between 88-83ka could be correlated with a glacial phase during the MIS 5b stadial (Leontaritis et al.,

2020). It should be noted that the MIS 5b stadial is clearly recorded in the presented pollen records (Figure 73) whereas the pre-LGM period shows considerable variability in AP abundances among the different sites (Leontaritis et al., 2020).

Allard et al. (2020) used the pollen record of Lake Ioannina (Tzedakis et al. 2002) along with this scheme to further support their ^{36}Cl geochronology for Late Pleistocene glaciation in the nearby Mt Tymphi (35 km to the N; see Figure 2 for locations). In particular they argue that a local last glacier maximum on Mt Tymphi no later than 29-25.7 ka (Table 21) is consistent with the Ioannina basin pollen record which indicates cool and wet conditions, most favourable for glacier growth between 25 and 30 ka (Allard et al., 2020). This is also in consistence with the ^{36}Cl geochronology on Mt Mavrovouni (30 km to the NE of Lake Ioannina; see Figure 2 for locations) that suggests a glacier advance phase at 26.6 ka (Chapter 5; Table 21). Unfortunately, such a high resolution and independently-dated archive is not appealable yet in southern Greece in order be used as a comparison for Mt Chelmos, as the Kopais record immediately east of Mt Parnassus in southcentral Greece (see Figure 1 for location) suffers several dating uncertainties (Tzedakis, 1999).

In the pollen record of Lake Prespa (Figure 73) during the intervals corresponding to HS1 (18.0-15.6 ka) and the YD (17.5-14.7 ka) large differences between total AP frequencies and AP frequencies excluding the *Pinus* species are evidenced (Panagiotopoulos et al., 2014). The expansion of montane coniferous forest over the mesophilous one might reflect to moist yet cold local climate conditions that would have favoured the expansion of glaciers during these intervals in near-by mountains, such as Mt Smolikas, according to the scheme described above.

7.2.2.5 The Fluvial Record in the Voidomatis catchment

Some further insights into the timing of Late Pleistocene glaciations were inferred from radiometric dates obtained from fluvial sediments deposited downstream of the glaciated headwaters of the Voidomatis catchment on Mt Tymphi which provide some constraint on the upstream glacial chronology (Hughes and Woodward, 2008). The uranium-series method was used successfully to develop a chronostratigraphic framework for the coarse-grained alluvial units at lower elevations in the Voidomatis River basin (Macklin et al., 1998; Hamlin et al., 2000) providing ages that were in good agreement with other methods such as ESR, TL (Lewin et al.,1991) and radiocarbon (Woodward et al., 2001). Hamlin et al. (2000) recognized at least four separate alluvial units. Secondary carbonates within three of them, yielded maximum uranium-series ages of 113 ± 6 ka, 80 ± 7 ka and 28.2 ± 7 ka–24.3 ± 2.0 ka (Lewin et al., 1991; Hamlin et al., 2000; Woodward et al., 2008) correlating with deposition during MIS 6, MIS 5b

and MIS 2 respectively. The sand and silt matrix of these alluvial units is dominated by limestone-rich fines, which are derived from glacial erosion in the catchment headwaters (Lewin et al., 1991; Woodward et al., 1992; 1995). The uranium-series ages thus suggest that large glaciers and active moraine complexes were present in the headwaters of this river system.

7.2.3 Holocene glaciations

As regards the Holocene, Mt Olympus is the only mountain to hold such evidence in Greece. Cosmogenic 36 Cl exposuse dating of glacial deposits suggests three discrete phases of glacial advance (Styllas et al., 2018). Local topography seems to have played a crucial role for the viability of these late glaciers as the deposits are found in a high-altitude cirque with NW aspect and high walls (up to 600 m) that provide extended shading, while windblown snow from the surrounding ridges (2900 m a.s.l.) is another factor that could have contributed in the formation of glaciers during climatically unfavourable conditions (Styllas et al., 2018).

The first phase of glacial stagnation (HOL1 in Table 21) or short re-advance is placed at 9.6 ± 1.2 ka (^{36}Cl ages - Styllas et al., 2018) during a general early Holocene phase of warming and glacier retreat just before the onset of very humid and warm conditions in the north Aegean Sea (Styllas et al., 2018). The second Late Holocene phase (HOL2 in Table 21) of glacial advance at 2.6 ± 0.3 - 2.3 ± 0.3 ka (^{36}Cl ages - Styllas et al., 2018) under wet conditions and solar insolation minima is correlated with North Atlantic's Bond 2 event (Bond et al., 2001) and the Homeric solar Minimum (Wirth and Sessions, 2016). The most recent glacier advance (HOL3 in Table 21) is dated to 0.64 ± 0.08 ka (^{36}Cl ages - Styllas et al., 2018), at the beginning of the Little Ice Age. Whilst this is constrained by only one age, glacier or snow/ice patch expansion would be expected during the Little Ice Age since evidence for this has been identified at multiple sites further north in the Pirin and Rila mountains in Bulgaria (Gachev, 2020), Montenegro (Hughes, 2007, 2010b).

Unlike on Mount Olympus, historical satellite imagery from late summer (Hughes, 2018) appears to confirm that there are no permanent snowfields on Smolikas. Based on this evidence and snow melt modelling, it has been argued that on Mt Smolikas there are no glacial or nival features dating to the Holocene (Hughes, 2018).

7.3 ELAs, Palaeoatmospheric circulation and precipitation patterns

A comparison of ELAs throughout Greece is attempted here in an effort to deduce some conclusions regarding the moisture supply patterns in the different massifs and the regional palaeoatmospheric circulation during different Pleistocene intervals. In reality, dedicated research with meticulous modelling and a great number of data is needed for approaching this issue which is out of the scope of this research. Still, some interesting conclusions can be drawn from the existing glacial geochronological database of the mountains of Greece (Table 21) as it is discussed next.

7.3.1 Considerations for interregional ELA comparisons

7.3.1.1 Tectonic Uplift

A crucial issue when attempting ELA comparisons is the consideration of the tectonic uplift history of the different massifs. Tectonic activity has, in some places, significantly influenced the altitude of the glacial cirques and the terminal moraines (Giraudi and Giaccio, 2015; Bathrellos et al., 2015) so that comparing ELAs between different areas is problematic given the uncertainties in knowing the uplift history of each area (Pope et al., 2017). Attempts of ELA comparisons in the mountains of Greece will mainly focus on the Pindus Mountains (Mt Tymphi, Mt Mavrovouni, Mt Smolikas) in northwest Greece, on Mt Olympus in north Greece and Mt Chelmos in the Peloponnese in south Greece so it is important to summarise estimations of the tectonic uplift in these regions.

The Pindus mountains are characterised by estimated tectonic uplift rates of 0.4 – 0.8 mm/yr for the Epirus region although rates might be greater (King and Bailey, 1985). This is a rough assumption for the Pindus mountains that includes many uncertainties but at the same time it is the best available estimation of uplift rates in the region. The estimated rates regard the whole region with many active local faults in the different massifs that are present in Epirus (section 3.1). It is therefore likely that uplift rates may vary for each mountain discussed here and especially between the limestone-dominated Mt Tymphi and the ophiolitic Mt Smolikas and Mt Mavrovouni. Tectonic movements are more active in the northern Peloponnesus area, where uplift rates have been estimated at 1.1-1.3 mm/yr over the last 350-500ka (Armijo et al.,1996; De Martini et al., 2004; McNeill and Collier, 2004) increasing to 1.3–2.2 mm/yr (Stewart, 1996; Stewart and Vita-Finzi, 1996) during the Holocene. Here, a rate of 1.1-1.3 mm/yr is considered for the Middle and Late Pleistocene and 2 mm/yr for Holocene as the more representative values for the area of Mt Chelmos. On Mt Olympus the tectonic uplift rate

has been estimated between 1.3mm/yr over the last 250ka (Smith et al., 1997) and 1.6mm/yr over Pleistocene (Nance, 2010). Indicative total uplifts for different glacial phases at these two regions based on the presented estimated uplift rates are summarised in. Table 22

Table 22. Estimated total uplift of the Pindus mountains and Mt Chelmos for the different glacial phases of the recorded glacial history of Greece (Table 21). See text for uplift rates and references.

Glacial Phase	Total Uplift		
	Pindus Mountains	Mt Chelmos	Mt Olympus
Younger Dryas (11ka)	4.4 - 8.8 m	22-25 m	14.3 - 17.6 m
LGM (25ka)	10 - 20 m	37-40 m	32.5 - 40 m
Pre-LGM (30ka)	12 - 24 m	43-47 m	39 – 48 m
MIS 6	60 - 120 m	175-203 m	195 – 240 m
MIS 12	180 - 360 m	505-593 m	585 – 720 m

7.3.1.2 Impact of Lithospheric Glacial Isostatic Adjustment and denundation on mountain topographic evolution

Apart from uncertainties in the estimation of tectonic uplift rates, other major geological uncertainties which affect the ELA comparisons between mountains in different areas and of different lithologies include the estimation of the impact of isostatic response to lithospheric loading/unloading caused by glaciation/deglaciation and glacial/postglacial erosion during major glaciations/deglaciations (e.g. Delacou et al., 2004; Sue et al., 2007; Nocquet et al., 2016; Mey et al., 2016) and the impact of post-glacial denudation on mountain topographic evolution (e.g. Whipple, 2009; Champagnac et al., 2012).

Constraints for estimating the contribution of glacial isostatic adjustment (i.e. postglacial crustal rebound) to present-day uplift rates in the Alps (Sternai et al., 2019) showed that the isostatic adjustment to the last deglaciation and postglacial erosion accounts for the entire current rock uplift rate in the Eastern Alps and roughly half of the respective rate in Central and Western Alps. It should be noted that even small ice caps, such as those that formed in the mountains of Greece and the Balkans during Middle Pleistocene, can long-term effect the elevation of massifs, as shown by evidence of small LGM ice caps dominating present-day rock uplift in tectonically active regions in the Alps (Mey et al., 2016).

As regards denundation, functional relationships between erosion and topography have remained elusive for most mountain ranges (Delunel et al., 2020). However, it has been

recognised that glacial erosion may cause isostatic uplift of rocks (e.g., Champagnac et al., 2007) and accelerate post-glacial mountain erosion (e.g., Herman et al., 2013) influencing the evolution of the relief for tens of thousands of years after glacial retreat (Salcher et al., 2014). An insight of post-glacial topographic forcing on erosion rates is provided by the quantitative study of erosion rates in the Austrian Alps (Dixon et al., 2016) which are 2 to 4 times higher in previously glaciated catchments compared with non-glaciated ones, reflecting the erosional response to local topographic preconditioning by repeated glaciations. Moreover, rock strength is another decisive parameter of the intensity of post-glacial erosion (e.g. DiBiase et al., 2010; Salcher et al., 2014) that could lead to measurable differences in the relief evolution of mountains with significantly different lithologies in terms of rock strength such as the carbonic Mt Tymphi and Mt Chelmos and the ophiolitic Mt Smolikas and Mt Mavrovouni in Greece.

Although the importance of these mechanisms has been highlighted, they remain largely unknown in the mountains of Greece and the Balkans. Thus, cirque or valley-floors elevations at different glacial or interglacial intervals might have been different than those suggested by estimated average long-term tectonic uplift rates presented above. Still, for the scope of this research, and especially regarding the conclusions derived from major regional differences in ELAs during Late Pleistocene glacial phases are unlikely to be significantly affected.

7.3.1.3 Air temperature and palaeosea-level

As the Peloponnese (Mt Chelmos) and northern Greece (Pindus Mountains/Mt Olympus) are separated by more than 1^{o} of latitude (λ=22.1^{o} and ~21.05^{o} for Mt Chelmos and the Pindus Mountains respectively). a warmer climate is expected for the Peloponnese. However, data from weather stations representative for the Pindus Mountains (Table 8) and for Mt Chelmos in the Peloponnese (Table 16) show that modern temperatures extrapolated to 2000m a.s.l. in these two regions show negligible differences. Mean annual temperatures have been estimated at 4.5 and 5.3 ^{o}C for the Pindus mountains and Mt Chelmos respectively, mean month temperatures at -3 ^{o}C for January in both areas and at 13.8 and 14.1 ^{o}C respectively for July. The dependence of air temperatures mainly on altitude within the short latitudinal range that corresponds to Greece has also been advocated by Papada and Kaliampakos (2016). Additionally, Katsoulakos and Kaliampakos (2014) showed that in mountainous areas of little but not insignificant latitudinal variation, such as a country level (Greece/ Austria in their study) or a region within a larger country (Italy in their study), heating demand in buildings - which is a direct function of air-temperature - can be predicted based only on altitude with over 90% accuracy. Thus, any ELA differences at similar palaeoaltitudes should be attributed to

differences in precipitation rather than to lower temperature differences at higher latitudes (and vice versa).

Finally, it should be noted that the reconstructed ELAs, presented below as above modern sea-level, may be lower than if presented as above palaeosea-level as eustatic sealevels were 120 m lower around Greece (Lambeck, 1995) as it has also been underlined in other glacial studies in Greece (Hughes, 2004; Pope et al., 2017; Allard et al., 2020). However, as comparisons between different areas are not diachronous but refer to the same periods, this factor is not considered in this analysis.

7.3.2 ELAs of glaciers in the mountains of Greece

The Skamnellian stage glaciers (MIS 12) in the Pindus Mountains in northwest Greece had a mean ELA of 1741m a.s.l. on Mt Tymphi and 1680 m a.s.l. on Mt Smolikas (Hughes, 2004; Hughes et al., 2006a), whilst on Mt Mavrovouni glaciers were slightly higher at 1785 m a.s.l. (Chapter 4; Leontaritis et al., 2021), probably reflecting drier climate conditions on Mt Mavrovouni due to its more inland location to the southeast of Mt Tymphi (Figure 1). On Mt Chelmos in the Peloponnese the largest Middle Pleistocene glaciation was characterized by ELAs of 1967m a.sl. (Pope et al., 2017). This difference of 180-280 m could be attributed to the difference in tectonic uplift during this long period (Table 22) and thus ELAs can be considered to have been at comparable palaeoaltitudes of ~1350-1450 m (above modern sea level) which implies consistent climate conditions throughout Greece during this severe cold stage which has been recognised as the most extreme climatic glacial interval of the last ~500 ka (Tzedakis et al., 2003).

For the pre-LGM to LGM period the available data from dated glacial deposits comes from Mt Tymphi where the glaciers during the local Late Pleistocene Glacier Maximum at 25.7-29.0 ka had an ELA of 2016 m a.s.l. (Allard et al., 2020), whereas on Mt Chelmos the glaciers at 36.5 – 28.6 ka (Pope et al., 2017 recalculated by Allard et al., 2020; see Table 21) had a mean ELA of 2046 m a.s.l. (Pope et al., 2017). Taking into account the tectonic uplift of these massifs since the last 30ka it appears that glaciers were characterised by similar ELAs at ~1990-2000 m (above modern sea level) implying that glaciers during this period formed under similar climate conditions. On Mt Mavrovouni, glaciers at 26.6 ka had an ELA of 2090 m a.s.l. (Chapter 4; Leontaritis et al., 2021), slightly higher than on Mt Tymphi as for the Middle Pleistocene glaciation. The glaciers that have been attributed to the same period on Mt Smolikas based on morphostratigraphic correlations of the respective glacial deposits between

Mt Tymphi and Mt Smolikas, had a higher mean ELA of 2241 m a.s.l. (Hughes, 2004). However, these deposits remain undated and no conclusions can be drawn.

As regards the Late-glacial, although glacial deposits in the mountains of Greece are rare and have so far been dated only on Mt Olympus (HS1: Phase LG1 at 15.6-14.2 ka, YD: Phase LG3 at 12.6 - 12.0 ka; Styllas et al., 2018) and Mt Chelmos (YD; 12.6-10.2 ka; Pope et al., 2017 recalculated by Allard et al., 2020; see Table 21), the ELAs for the Late-glacial glaciers show an interesting and unexpected trend (Leontaritis et al., 2020). Whilst in northern Greece Late-glacial glaciers were absent on Mt Tymphi (Allard et al., 2020), the assumed YD glaciers on Mt Smolikas had a mean ELA of 2372 m a.s.l. (Hughes, 2004; no cosmogenic dating data and therefore likely to be subject to revision) and on Mt Olympus the Late-glacial moraines had an ELA higher than 2300 m a.s.l. (the lowest moraines lying at 2250 m a.s.l. and the cirque walls at 2500 m a.s.l.; Styllas et al., 2018), on Mt Chelmos the YD palaeoglaciers appear to have been considerably lower at a mean ELA 2174 m a.s.l. (Pope et al., 2017). Some 70km north of Mt Smolikas, on Mt Pelister, Oldest Dryas glaciers had an ELA of 2250 m a.s.l. (Ribolini et al., 2017) which is still higher compared with Mt Chelmos, while in above the nearby Lake Ohrid, the YD glaciers had a slightly lower ELA of 2130 m a.s.l. (Gromig et al., 2018). It should be noted that no information on the uplift history of these massifs is known and climate is considerably colder both on Mt Pelister: (mean annual temperature is 2.7°C, with January and July being the coldest [−5.8°C] and warmest [11.5°C] months respectively at ~2100m a.s.l.; Ribolini et al., 2017) and in the Galicica mountains (mean annual temperature of ca. 3.4 ^{o}C at 2010 - 2050 m a.s.l.; Gromig et al., 2018).

These differences in Late-glacial reconstructed glacier ELAs between those massifs, points toward more conducive for glaciation conditions in the Peloponnesus than in the northern Pindus Mountains and Mt Olympus (Pope et al., 2017). Furthermore, taking into account that air temperatures are not dependent on latitude in the mountainous regions of Greece, a considerably wetter climate in southern Greece than in northern Greece during this interval is suggested (Leontaritis et al., 2020).

Examining the precipitation map of Greece today (Figure 74) it is evident that moisture supply is strongly associated with westerlies and hints at a west–east track of atmospheric depressions through the Mediterranean (Leontaritis et al., 2020). A good indication of the impact of westerlies on the western Balkans climate is the fact that the Pleistocene glaciers on Mt Orjen in Montenegro were ~500-600 m lower than in the Peloponnese and in the Republic of North Macedonia (Leontaritis et al., 2020), a situation that could have been forced only by

considerably higher precipitation in Montenegro which today on average exceeds 5000 mm per year (Gromig et al. 2018). The Pindus Mountains extend from the NW to the SE causing orographic precipitation to the westerly depressions and as a result rain shadow to eastern mainland Greece where Mt Olympus is located. Indeed, the source of moisture and snow supply on Mt Olympus generally occurs from southeast moisture-laden fronts from the Aegean Sea but the same time it is also associated with large-scale atmospheric circulation patterns primarily related to enhanced westerlies over the eastern North Atlantic (Styllas et al., 2019). This is reflected on the fact that the eastern (marine) side of Mount Olympus receives on average 200mm more precipitation than the western (continental) side (period of observations 1960-2000; Styllas et al., 2016).

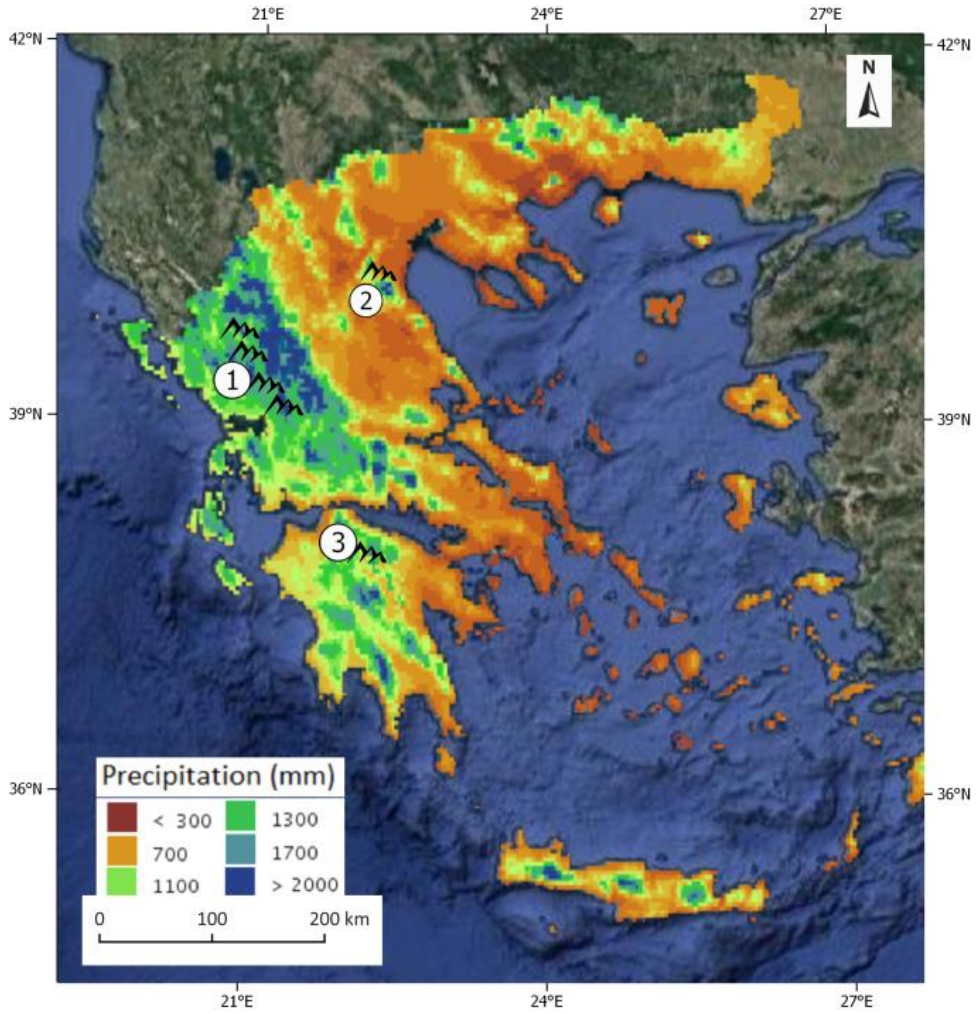

Figure 74. Annual precipitation in Greece (source: Climatic Atlas of Greece - climatlas.hnms.gr). 1. Pindus Mountains, 2. Mt Olympus, 3. Mt Chelmos (from Leontaritis et al., 2020)

As regards Mt Chelmos, today it receives less moisture than northwest Greece (Figure 74) as in contrast to western Balkans where moisture and snow supply is strongly associated with

westerlies (e.g. Hughes et al., 2010; Gromig et al., 2018) on Mt Chelmos most of the snow is precipitated by south-west atmospheric systems. It should be noted that although southerly air masses are generally characterised by high air temperatures, even today they are sufficiently cold during winter to deliver snow at high altitudes (>1800m a.s.l.) on Mt Chelmos as modern observations indicate (personal observations; dedicated work is needed to confirm this), and this phenomenon would be even stronger during a Pleistocene cold stage winter (Pope et al., 2017).

As a conclusion, the similar ELAs of LGM glaciers in southern and northern Greece and the supressed ELAs of Late-glacial glaciers in southern Greece suggest equally wet climate during the LGM and wetter climate in southern Greece during the Late-glacial which in turn implies that given the different patterns in moisture/snow supply in each massif, the prevailing moisture-bearing atmospheric systems that delivered winter snow to the mountains of Greece had a more southerly track than today as also suggested by Pope et al. (2017) and Leontaritis et al. (2020).

Further insights into the Late Pleistocene precipitation regime of this region that provide support to this conclusion can be inferred by palaeoatmospheric circulation patterns reconstruction for the Mediterranean basin based on the recent analysis of the time proxy series from Lake Ohrid for the last 1.36 Ma and model data by Wagner et al. (2019). More specifically, the reconstruction of the geographical expansion of geopotential height anomalies associated with precipitation maxima in Lake Ohrid (Figure 75) showed pronounced troughs in the central Mediterranean area and an increase in rainfall during the winter half-year in western Balkans (Wagner et al. 2019), which is crucial for glaciers formation in this area. Enhanced winter precipitation in the Mediterranean mid-latitudes is a result of local cyclogenesis combined with the southward shift in the atmospheric circulation cells in the Northern Hemisphere during winter (Wagner et al. 2019) which in turn favours a more southerly trajectory for storm tracks across the North Atlantic and into the Mediterranean (Kutzbach et al., 2014). Moreover, the local cyclogenesis in central Mediterranean during precipitation maxima (Figure 75) forces moisture supply to the mountains of Greece into a SW-NE track which implies significantly enhanced precipitation in the Peloponnese compared to northern Greece and the Republic of North Macedonia as it can also be observed in similar cyclogenesis events today (Leontaritis et al., 2020). On the other hand, the precipitation regime in the coastal mountains of Montenegro would not be affected. This is also consistent with oxygen isotope data from speleothems in the Central Alps (Luetscher et al., 2015) which

indicate that major glacier advances during the LGM had a primary moisture source from southerly advection, pointing to the Mediterranean Sea and the subtropical area as source regions for high precipitation rates in the Alps (Monegato et al., 2017).

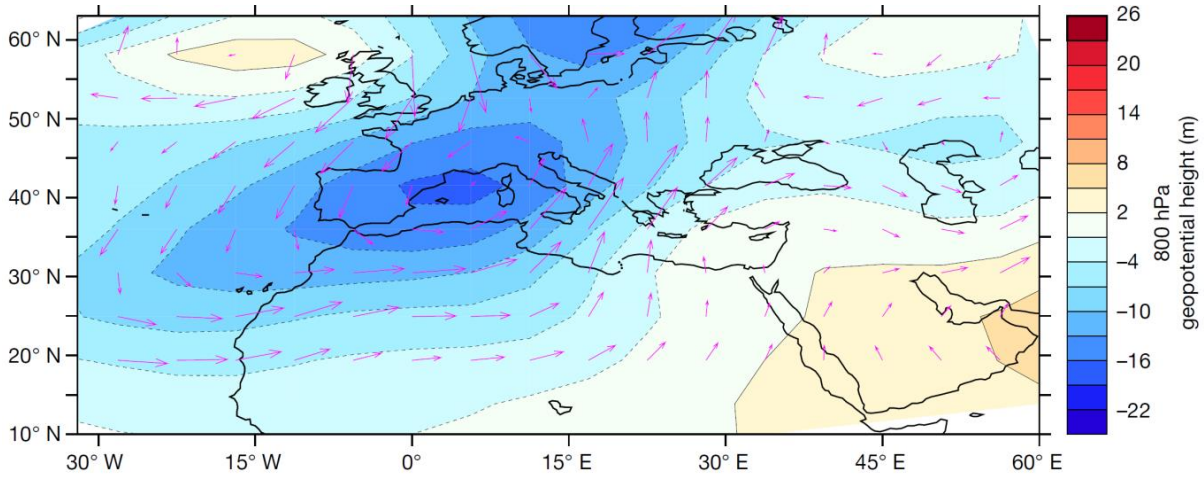

Figure 75. Composite anomalies of September–November, 800 hPa geopotential height (m, shading) and wind (m s^{-1}, vectors) associated with precipitation maxima in Lake Ohrid. (from Wagner et al. 2019)

Overall, the presented glacial evidence and the respective ELAs are in accordance with this hypothesis while at the same time it underlines the significance of precipitation in the formation of glaciers. Therefore, as the moisture supply of the atmospheric systems in Greek mountains is one of the main driving forces along with air-temperature depressions for the different glaciation cycles, it can be concluded that the development of glaciers must have been more prominent at the climatic transition onsets between (wet) interglacial and (arid) glacial intervals or between interstadial and stadial intervals when more humid climate conditions prevailed .

Chapter 8. Conclusions

The main objective of this doctoral research was to contribute to the addressing of temporal gaps in the glacial chrono-stratigraphy of the Pindus Mountains with new insights from the glacial record of Mt Mavrovouni and its connection with the glacial record of southern mountainous Greece towards a geographical expansion of this framework. To a great extent these goals have been achieved.

Specific conclusions that can be from this research are summarised in the following points:

- The consistency of the yielded ^{36}Cl ages from the ophiolitic samples on Mt Mavrovouni with ^{36}Cl ages from morphostratigraphically similar limestone-derived glacial deposits on Mt Tymphi has validated the suitability of cosmogenic ^{36}Cl exposure dating on ophiolites. At the same time these ages address the most important temporal gap in the glacial geochronological framework of Greece

- The application of cosmogenic ^{36}Cl exposure dating on ophiolitic boulders for the first time, constitutes the only chronology of Late Pleistocene glaciations on the mountains of Greece that is independent from inherent issues in surface exposure dating of limestones such as the erosion rate of rock surfaces.

- The ^{36}Cl dating of ophiolite samples with high Fe_2O_3 content (8-8.5 wt %) contributes to the validation of current scaling behaviour and ^{36}Cl production rates from Fe spallation for which further data from high Fe-content samples is needed.

- The perspective of dating the most complete recorded glacial sequence in Greece on the ophiolitic Mt. Smolikas, where four distinct stratigraphic units have been correlated with glacial phases spanning from the Middle Pleistocene to the Late-glacial has been opened.

- As the Peloponnese (Mt Chelmos) and northern Greece (Pindus Mountains/Mt Olympus) are separated by 2^o of latitude a warmer climate is expected for the Peloponnese but data from weather stations show that modern temperatures in these two mountain regions show negligible differences and mainly depend on altitude. Thus, any ELA differences at similar palaeoaltitudes in the mountains of Greece should be attributed to differences in precipitation rather temperature differences.

The geomorphological and geochronological data from all the available glacial studies in Greece and the respective glacial phases have been summarised chronologically into different time periods composing the first organised database for glacial studies in Greece (Table 21). The analysis and discussion of this database provides further insights into our current understanding of glaciations in the mountains of Greece. A synopsis of the main points for each period is given next.

A. Middle Pleistocene

- The most extensive glacial phases in the mountains of Greece most probably took place during Middle Pleistocene and particularly during MIS 12 (Skamnellian Stage) and MIS 6 (Vlasian Stage).

- In mountain valleys younger glaciers are expected to override remaining glacial sediments from previous glacial phases. Therefore, based on the evidence from the mountains of Greece, it can be concluded that the MIS 6 glaciation was the most extensive of the MIS 10-MIS 2 period and the MIS 12 glaciation was probably the most extensive glaciation up to the Early-Middle Pleistocene boundary (MIS 20).

- The glacial extent during the Middle Pleistocene Stages, has been revised as it is greater than previous thought. New evidence presented from Mt Tymphi and Mt Smolikas in NW Greece and some observations from Mt Olympus in northern Greece alongside published studies on Mt Chelmos in the Peloponnese as well as in Montenegro suggest that their uplands were occupied by former extensive ice field/ice caps with outlet glaciers forming on all slope orientations.

- The palaeovegetation/palaeoclimatic record of the southern Balkans indicate cold but wet climate conditions during the early parts of MIS 12 and MIS 6 followed by cold and arid conditions, indicating glacier build-up during the early and relatively humid parts of these severe cold stages. Moreover, the recently published analysis of time proxy series for the last 1.36 Ma showed that increased winter precipitation, corresponds with periods of low Northern Hemisphere winter insolation providing very favourable conditions for the formation of extensive ice-fields.

- Differences 220-280 m between ELAs of Skamnellian Stage (MIS 12) glaciers on Mt Tymphi/Mt Smolikas and Mt Chelmos have been attributed to the calculated differences in tectonic uplift since this long period. Thus ELAs are likely to have

been at comparable palaeoaltitudes (~1350-1450 m above modern sea level) which implies consistent climate conditions throughout Greece during this severe cold stage.

B. Last Glacial Cycle (Tymphian Stage MIS 5d-2)

- On Mt Chelmos, the OSL dating of samples from morainic deposits at an altitude of 1900-2050 m a.s.l. in the Spanolakos valley yielded burial ages of 89-86 ka that could indicate another phase in glacial evolution in the Peloponnese during MIS5b. However, the OSL moraine burial ages from Mt Chelmos constitute the only glacial evidence in Greece and the western Balkans for MIS 5b and further geochronological data is needed to further test this hypothesis.

- The geochronological framework of Late Pleistocene glaciations in the Pindus mountains in NW Greece is the best dated in Greece. A Late Pleistocene local glacial close in timing to the Last Glacial Maximum (27.5-23.3 ka) is suggested by the consistent ^{36}Cl dates from ophiolite-derived moraines from Mt Mavrovouni, where the stabilisation of the most extensive Late Pleistocene glaciers took place at 26.6 ± 6.6 ka, and the recently publishes ^{36}Cl dates from limestone moraines on Mt Tymphi, where the largest glaciers during Late Pleistocene reached their terminal positions no later than 29.0 ± 3.0 - 25.7 ± 2.6 ka and retreated to the high cirques by 24.5 ± 2.4 ka. The timing constraint of a local Late Pleistocene glacial maximum in the Pindus mountains in NW Greece near the LGM is in good agreement with well-preserved outwash sediments in the Voidomatis River record downstream of Mt Tymphi and is consistent with the Ioaninna basin pollen record indicating cool and wet conditions, most favourable for glacier growth, at 30-25 ka.

- On Mt Chelmos in southern Greece, recent studies showed that Pleistocene glaciers reached their maximum extent at 36.5 ± 0.9 - 28.6 ± 0.6 ka while a glacier retreat phase was dated at 22.2 ± 0.3 - 19.6 ± 0.5 ka implying that ice is likely to have occupied the cirques of Mount Chelmos from MIS 3 to 2 and oscillated in response to varying climatic conditions, especially in response to millennial-scale shifts between cold/dry and cool/wet conditions in Greece.

- Taking into consideration tectonic uplift over the last 30ka, ELAs of glaciers during the pre-LGM to LGM period on Mt Tymphi and Mt Chelmos appears to have been

at ~1990-2000 m above modern sea level, implying that glaciers during this period formed under similar climate conditions. On Mt Mavrovouni, glaciers at 26.6 ka had an ELA of 2090 m a.s.l. which can be attributted to slightly drier climate condition on Mt Mavrovouni due to its more inland location to the southeast of Mt Tymphi.

- The evidence from Mt Mavrovouni (pronival rampart dated with ^{36}Cl at 20.0 ± 5.0 ka) and Mt Tymphi (terminal moraines in the northeast cirques recently dated with ^{36}Cl at 18.0 ± 1.9 ka), suggest unfavourable conditions for glacier development during the transitional phase from the LGM to the Late-glacial and the Holocene but cold/humid enough to preserve nevé fields and small glaciers in topographically favourable positions.

- Examining regional pollen archives showed that the duration and independent characteristics of vegetation patterns vary significantly during the Last Glacial Cycle implying differences connected with local microclimates, topography and elevation. Still, the palaeovegetation and palaeoclimatic records from Lake Ioannina, Lake Ohrid and Lake Prespa are in agreement with the onset of the recorded glacial episodes just before the onset of Arboreal Pollen percentages reduction. Unfortunately, such a high resolution and independently-dated archive is not appealable yet in southern Greece in order be used as a comparison for Mt Chelmos.

- As regards the Late-glacial, although glacial deposits in the mountains of Greece are rare and have so far been dated with ^{36}Cl only on Mt Olympus (HS1: 15.6-14.2 ka, YD: 12.6 - 12.0 ka) and Mt Chelmos (YD: 12.6-10.2 ka). The ELAs for the Late-glacial glaciers show an interesting trend. Whilst in northern Greece Late-glacial glaciers were absent on Mt Tymphi (Allard et al., 2020), the assumed YD glaciers on Mt Smolikas had a mean ELA of 2372 m a.s.l. and on Mt Olympus the Late-glacial moraines had an ELA higher than 2300 m a.s.l., on Mt Chelmos the YD palaeoglaciers had a considerably lower ELA at 2174 m a.s.l. (Pope et al., 2017). These differences in Late-glacial ELAs, points towards a considerably wetter climate in southern Greece than in northern Greece during this interval.

- The analysis of modern precipitation data underlined the different moisture supply regime in different mountain regions across Greece. In the Pindus Mountains

(northwest Greece) moisture and snow supply is strongly associated with westerlies whereas Mt Chelmos (south Greece) and Mt Olympus (northeast Greece) today receive less moisture than northwest Greece and most of the snow is precipitated by south-west atmospheric systems and southeast moisture-laden fronts from the Aegean Sea respectively.

- The similar ELAs of LGM glaciers in southern and northern Greece and the supressed ELAs of Late-glacial glaciers in southern Greece indicates equally wet climate during the LGM and wetter climate in southern Greece during the Late-glacial. This can be attributed to the palaeoatmospheric circulation mechanisms and precipitation regime during this period. Enhanced winter precipitation in southern Greece is a result of a more southerly trajectory for storm tracks across the Mediterranean while at the same time the local cyclogenesis in central Mediterranean forced moisture supply into a SW-NE track.
- As regards the Holocene, very small glaciers formed in some north-oriented deep cirques on Mt Olympus where they survived because of strong local topographic and climatic controls.

Finally, a general conclusion is that even though important information has been added in the last two decades, there is need for further research in Greece and the wider Balkans to establish the timing and extent of glaciations. Important aspects of Quaternary glaciations in Greece that remain open include a possible revision and expansion of the Middle Pleistocene glaciation extent based on dedicated glacial studies in southern, central and Northeastern Greece, and the deeper understanding of the local climate response in the mountains of Greece to major global and regional Late Pleistocene to Holocene climatic events.

References

Adamiec, G. and Aitken, M.J. (1998). Dose-rate conversion factors: update. *Ancient TL 16*, 37-50.

Agassiz, L. (1840). *Études sur les glaciers.* Neuchâtel, Switzerland: Jent and Gaßmann, pp. 346.

Allard, L.J., Hughes, P.D., Woodward, J.C., Fink, D., Simon, K., Wilcken, K.M. (2020). Late Pleistocene glaciers in Greece: A new ^{36}Cl chronology. *Quaternary Science Reviews 245*, 1-27. https://doi.org/10.1016/j.quascirev.2020.106528

Ambraseys, N. and Jackson, J. (1990). Seismicity and associated strain of central Greece between 1890 and 1988. *Geophysical Journal International 101*, 663–708.

Anavasi (2016). *Valia Kalda -Vasilitsa 1:50,000 hiking map [Topo 50, 6.4]*. Anavasi Maps & Guides, Athens, Greece.

Angelier, J. (1978). Tectonic evolution of the Hellenic arc since the Late Miocene. *Tectonophysics* 49, 23-36. https://doi.org/10.1016/0040-1951(78)90096-3

Applegate, P.J., Urban, N.M., Laabs, B.J.C., Keller, K., Alley, R.B. (2010). Modeling the statistical distributions of cosmogenic exposure dates from moraines. *Geoscientific Model Development (GMD) 3*, 293-307. https://doi.org/10.5194/gmd-3-293-2010

Armijo, R., Meyer, B.G., King. G.P., Rigo, A., Papanastassiou, D. (1996). Quaternary evolution of the Corinth Rift and its implications for the Late Cenozoic evolution of the Aegean. *Geophysical Journal International 126*, 11-53. https://doi.org/10.1111/j.1365-246X.1996.tb05264.x

Athanassas. C., Bassiakos, Y., Wagner, G.A., Timpson, M.E. (2012). Exploring palaeogeographic conditions at two palaeolithic sites in Navarino, southwest Greece, dated by optically stimulated luminescence. *Geoarchaeology 27*, 237-258. https://doi.org/10.1002/gea.21406

Aubouin, J. (1959) Contribution à l' étude géologique de la Grèce septentrionale: Le confins de l' Epire et de la Thessalie. *Annales Géologiques des Pays Helléniques 10*, 525.

Bailey, R.M., Smith, B.W., Rhodes, E.J. (1997). Partial bleaching and the decay form characteristics of quartz OSL. *Radiation Measurements 27*, 123–136. https://doi.org/10.1016/S1350-4487(96)00157-6

Balco, G. (2020). Glacier Change and Paleoclimate Applications of Cosmogenic-Nuclide Exposure Dating. *Annual Review of Earth and Planetary Sciences 48*, 21-48. https://doi.org/10.1146/annurev-earth-081619-052609

Balco, G. and Schaeffer, J.M. (2006). Cosmogenic nuclide and varve chronologies for the deglaciation of southern New England. *Quaternary Geochronology 1*, 15-28. https://doi.org/10.1016/j.quageo.2006.06.014

Balco, G., Rovey, C.W. II, Stone, J.O.H. (2005). The first glacial maximum in North America. *Science 307*, 222. https://doi.org/10.1126/science.1103406

Banerjee, D., Murray, A.S., Bøtter-Jensen, L., Lang, A. (2001). Equivalent dose estimation using a single aliquot of polymineral fine grains. *Radiation Measurements 33*, 73- 94. https://doi.org/10.1016/S1350-4487(00)00101-3

Barrows, T.T., Stone, J.O., Fifield, L.K. & Creswell, R.G. (2002). The timing of the Last Glacial Maximum in Australia. *Quaternary Science Reviews 21*, 159-173. https://doi.org/10.1016/S0277-3791(01)00109-3

Bassiouka, A. (2011). The demographic identity of mountainous areas of Greece. *Master thesis in Environment and Development of Mountainous Areas*. National Technical University of Athens, Athens, Greece.

Bathrellos, G. D., Skilodimou, H. D. Maroukian, H. (2015). The significance of tectonism in the glaciations of Greece. IN: Hughes, P. D. & Woodward J. C. (Eds.). *Quaternary Glaciation in the Mediterranean Mountains.* London: Geological Society of London Special Publications 433, 237-250. https://doi.org/10.1144/SP433.5

Bavec, M., Tulaczyk, S. M.,Mahan, S. A., Stock, G. M. (2004). Late Quaternary glaciation of the Upper Soca River Region (Southern Julian Alps, NW Slovenia). *Sedimentary Geology 165*, 265−283. https://doi.org/10.1016/j.sedgeo.2003.11.011

Benn, D.I. and Ballantyne, C.K. (2005). Palaeoclimatic reconstruction from Loch Lomond Readvance glaciers in the West Drumochter Hills, Scotland. *Journal of Quaternary Science 20*, 577–592. https://doi.org/10.1002/jqs.925

Benn, D.I. and Hulton, N.R.J. (2010). An Excel (TM) spreadsheet program for reconstructing the surface profile of former mountain glaciers and ice caps. *Computers and Geosciences 36*, 605–610. https://doi.org/10.1016/j.cageo.2009.09.016

Billiris, H., Paradissis, D.,Veis, G., England, P., Featherstone,W., Parsons, B., Cross, P., Rands, P., Rayson, M., Sellers, P., Ashkenazi, V., Davison, M., Jackson, J., Ambraseys, N. (1991). Geodetic determination of tectonic deformation in central Greece from 1900 to 1988. *Nature 350*, 124–129. https://doi.org/10.1038/350124a0

Boenzi, F. and Palmentola, G. (1997). Glacial features and snow-line trend during the last glacial age in the Southern Apennines (Italy) and on Albanian and Greek mountains. *Zeitschrift für Geomorphologie, 41*, 21–29.

Boenzi, F., Palmentola, G., Sanso, P. and Tromba, F. (1992). Le Tracce Glaciali Del Massiccio Dello Smolikas (Catena Del Pindo – Grecia). *Rivista Geografica Italiana 99*, 379-393.

Bond, G., Kromer, B., Beer, J., Muscheler, R., Evans, M.N., Showers, W., Hoffmann, S., Lotti-Bond, R., Hajdas, I., Bonani, G. (2001). Persistent solar influence on North Atlantic climate during the Holocene. *Science 294*, 2130-2136. https://doi.org/10.1126/science.1065680

Bonnemains, D., Carlut, J., Escartın, J., Mevel, C., Andreani, M., Debret, B. (2016). Magnetic signatures of serpentinization at ophiolite complexes. *Geochemistry Geophysics Geosystems 17*, 2969–2986. https://doi.org/10.1002/2016GC006321

Borchers, B., Marrero, S., Balco, G., Caffee, M., Goehring, B., Lifton, N., Nishiizumi, K., Phillips, F., Schaefer, J., Stone, J. (2016). Geological calibration of spallation production rates in the CRONUS-Earth project. *Quaternary Geochronology 31*, 188-198. https://doi.org/10.1016/j.quageo.2015.01.009

Bourcart J. (1922). *Les Confins Albanais Administrés Par La France (1916-1920): Contribution a la Géographie Et a la Géologie de l'Albanie Moyenne*. Paris, France: Librairie Delagrave, pp. 104.

Bowen, D.Q. (1978). *Quaternary Geology: a Stratigraphic Framework for Multidisciplinary Work*. New York: Pergamon Press, pp. 94.

Brigham-Grette, J. (1996). Geochronology of glacial deposits. IN: Menzies, J. and van der Meer, J. (Eds.). *Past Glacial Environments: Sediments, Forms and Techniques*. Chichester: Wiley, pp. 377−410. https://doi.org/10.1016/C2014-0-04002-6

Briner, J.P., Kaufmann, D.S., Manley, W.F., Finkel, R.C., Caffee, M.W. (2005). Cosmogenic exposure dating of late Pleistocene moraine stabilization in Alaska. *Geological Society of America Bulletin 117*, 1108-1120. https://doi.org/10.1130/B25649.1

Brynjólfsson, S., Schomacker, A., Ingólfsson, Ó. (2014). Geomorphology and the Little Ice Age extent of the Drangajökull ice cap, NW Iceland, with focus on its three surge-type outlets. *Geomorphology 213*, 292–304. https://doi.org/10.1016/j.geomorph.2014.01.019

Cacho, I., Grimalt, J.O., Pelejero, C., Canals, M., Sierro, F.J., Flores, J. A., Shackleton, N.J. (1999). Dansgaard–Oeschger and Heinrich event imprints in Alboran Sea palaeotemperatures. *Paleoceanography 14*, 698–705. https://doi.org/10.1029/1999PA900044

Cerling, T.E., Poreda, R.J., Rathburn, S.L.(1994). Cosmogenic ^{3}He and ^{21}Ne age of the Big Lost River flood, Snake River plain, Idaho. *Geology 22*, 227-230. https://doi.org/10.1130/0091-7613(1994)022<0227:CHANAO>2.3.CO;2

Chadwick, O.A., Hall, R.D., Phillips, F.M. (1997). Chronology of glacial advances in the central Rocky Mountains. *Geological Society of America Bulletin 109*, 1443–52. https://doi.org/10.1130/0016-7606(1997)109<1443:COPGAI>2.3.CO;2

Champagnac, J., Molnar, P., Anderson, R., Sue, C., Delacou,B. (2007). Quaternary erosion-induced isostatic rebound in the western Alps. *Geology 35*, 195–198. https://doi.org/10.1130/G23053A.1

Champagnac, J.-D., Molnar, P., Sue, C., Herman, F. (2012). Tectonics, climate, and mountain topography. *Journal of Geophysical Research 117*, B02403. https://doi.org/10.1029/2011JB008348

Chandler, B.M.P., Lovell, H., Boston, C.M., Lukas, S., Barr, I.D., Benediktsson, Í.Ö., Benn, D.I.,Clark, C.D., Darvill, C.M., Evans, D.J.A., Ewertowski, M.W., Loibl, D., Margold, M., Otto,J.-C., Roberts, D.H., Stokes, C.R., Storrar, R.D., Stroeven, A.P. (2018). Glacial geomorphological mapping: A review of approaches and frameworks for best practice. *Earth Science Reviews 185*, 806-846. https://doi.org/10.1016/j.earscirev.2018.07.015

Çiner, A. and Sarıkaya, M.A. (2017). Cosmogenic ^{36}Cl Geochronology of late Quaternary glaciers on the Bolkar Mountains, south central Turkey. IN: P., Hughes & J., Woodward (Eds.). *Quaternary Glaciation in the Mediterranean Mountains*. London: Geological Society of London Special Publications 433, pp. 271-287. https://doi.org/10.1144/SP433.3

Çiner, A., Stepišnik, U., Sarıkaya M.A., Žebre, M., Yıldırım, C. (2019). Last Glacial Maximum and Younger Dryas piedmont glaciations in Blidinje, the Dinaric Mountains

(Bosnia and Herzegovina): insights from ^{36}Cl cosmogenic dating. *Mediterranean Geoscience Reviews 1*, 25-43. https://doi.org/10.1007/s42990-019-0003-4

Clark ,P.U., Dyke, A.S., Shakun, J.D., Carlson, A.E., Clark, J., Wohlfarth, B., Mitrovica, J.X., Hostetler, S.W., McCabe. A.M. (2009). The Last Glacial Maximum. *Science 325*, 710-714. https://doi.org/10.1126/science.1172873

Colhoun, E.A. (1988). Recent morphostratigraphic studies of the Australian Quaternary. *Progress in Physical Geography 12*, 264–81. https://doi.org/10.1177/030913338801200207

Collier, R. E. L., Leeder, M. R., Rowe, P. J., Atkinson, T. C. (1992). Rates of tectonic uplift in the Corinth and Megara Basins, central Greece. Tectonics 11, 1159–1167. https://doi.org/10.1029/92TC01565

Cvijic, J. (1898). Das Rilagebirge und seine ehemalige Vergletscherung. *Zeitschrift der Gesellschaft für Erdkunde zu Berlin 33*, 200-253.

Cvijic, J. (1917). L'epoque glaciaire dans la peninsule balkanique. *Annales de Geographie 26*, 189–218.

Dahl-Jensen, D., NEEM Community (2013). Eemian interglacial reconstructed from a Greenland folded ice core. *Nature 493*, 489−494. https://doi.org/10.1038/nature11789

D'Arcy, M., Schildgen, T.F., Strecker, M.R., Wittmann, H., Duesing, W., Mey, J., Tofelde, S., Weissmann, P., Alonso, R.N. (2019). Timing of past glaciation at the Sierra de Aconquija, northwestern Argentina, and throughout the Central Andes. *Quaternary Science Reviews 204*, 37-57. https://doi.org/10.1016/j.quascirev.2018.11.022

Davis, N. K., Locke, W.W., Pierce, K.L., Finkel, R.C. (2006). Glacial Lake Musselshell: Late Wisconsin slackwater on the Laurentide ice margin in central Montana, USA. *Geomorphology 75*, 330-345. https://doi.org/10.1016/j.geomorph.2005.07.021

De Martini, P.M., Pantosti, D., Palyvos, N., Lemeille, F., McNeill, L.C., Collier, R.E.L. (2004). Slip rates of the Aigion and Eliki Faults from uplifted marine terraces, Corinth Gulf, Greece. *Comptes Rendus Geoscience 336*, 325–334. http://doi.org/10.1016/j.crte.2003.12.006

Demek, J. (1972). *Manual of detailed geomorphological mapping*. Prague: IUG, pp. 344.

Delacou, B., Sue, C., Champagnac, J.D., Burkhard, M. (2005). Origin of the current stress field in the Western/Central Alps: role of gravitational reequilibration constrained by numerical modelling. *Geological Society of London Special Publications 243*, 295−310. https://doi.org/10.1144/GSL.SP.2005.243.01.19

Delunel, R., Schlunegger, F., Valla, P.G., Dixon, J., Glotzbach, C., Hippe, K., Kober, F., Molliex, S., Norton, K.P., Salcher, B., Wittmann, H., Akçar, N., Christl, M. (2020). Late-Pleistocene catchment-wide denudation patterns across the European Alps. *Earth-Science Reviews 211*, 103407. https://doi.org/10.1016/j.earscirev.2020.103407

Desilets, D., Zreda, M., Pradu, T. (2006). Extended scaling factors for in situ cosmogenic

nuclides: New measurements at low latitude. *Earth and Planetary Science Letters 246*, 265-276. https://doi.org/10.1016/j.epsl.2006.03.051

Diakakis M, Deligiannakis G, Mavroulis S, 2011. Flooding in Peloponnese, Greece: A contribution to flood hazard assessment. IN: N., Lambrakis, G., Stournaras, K. Katsanou (Eds.). *Advances in the Research of Aquatic Environment*. Berlin: Springer, pp. 199-206. https://doi.org/10.1007/978-3-642-19902-8

DiBiase, R.A., Whipple, K.X., Heimsath, A.M., Ouimet, W.B. (2010). Landscape form and millennial erosion rates in the San Gabriel Mountains, CA. *Earth and Planetary Science Letters 289*, 134–144. https://doi.org/10.1016/j.epsl.2009.10.036

Diener, C. (1886). *Libanon. Grundlinien der physischen Geographie und Geologie von Mittel-Syrien.* Wien: A. Hölde. pp. 412.

Dilek, Y., Kempton, P.D., Thy, P., Hurst, S.D., Whitney, D., and Kelley, D.S. (1997). Structure and petrology of hydrothermal veins in gabbroic rocks from Sites 921 to 924, MARK area (Leg 153): alteration history of slow-spread lower oceanic crust. IN: Karson, J.A., Cannat, M., Miller, D.J., and Elthon, D. (Eds.). *Proc. ODP, Sci. Results,153: College Station, TX (Ocean Drilling Program).* doi:10.2973/odp.proc.ir.153.1995

Dixon, J. L., von Blanckenburg, F., Stüwe, K., Christl, M. (2016). Glaciation's topographic control on Holocene erosion at the eastern edge of the Alps. *Earth Surface Dynamics 4*, 895–909. https://doi.org/10.5194/esurf-4-895-2016

Duller, G.A.T. (2008). *Luminescence Dating: Guidelines in Using Luminescence Dating in Archaeology*. Swindon: English Heritage. https://doi.org/10.1002/jqs.1328

Duller, G. A. T., Wintle, A. G., Hall, A. M. (1995). Luminescence dating and its application to key pre-Late Devensian sites in Scotland. *Quaternary Science Reviews 14*, 495−519. https://doi.org/10.1016/0277-3791(95)00017-J

Dunai, T.J., Lifton, N.A. (2014). The nuts and bolts of cosmogenic nuclide production. *Elements 10*, 347-350. https://doi.org/10.2113/gselements.10.5.347

Dunne, J., Elmore, D., Muzikar, P. (1999). Scaling factors for the rates of production of cosmogenic nuclides for geometric shielding and attenuation at depth on sloped surfaces. *Geomorphology 27*, 3–11. https://doi.org/10.1016/S0169-555X(98)00086-5

Dupuy, C., Dostal, J., Capedri, S., Venturelli, G. (1984). Geochemistry and petrogenesis of ophiolites from Northern Pindos (Greece). *Bulletin of Volcanology 47*, 39-46. https://doi.org/10.1007/BF01960539

Economou-Eliopoulos, M., Vacondios, I. (1995). Geochemistry of chromitites and host rocks from the Pindos ophiolite complex, northwestern Greece. *Chemical Geology 122*, 99-108. https://doi.org/10.1016/0009-2541(94)00154-Z

Ehlers, J. and Gibbard, P. L. (2003). Extent and chronology of glaciations. *Quaternary Science Reviews 22*, 1561−1568. https://doi.org/10.1016/S0277-3791(03)00130-6

Elmore, D. and Phillips, F.M. (1987). Accelerator mass spectrometry for measurement of long-lived radioisotopes. *Science 236*, 543-550. https://doi.org/10.1126/science.236.4801.543

Elmore, D., Ma, X., Miller, T., Mueller, K., Perry, M., Rickey, F., Sharma, P., Simms, P., Lipschutz, M., Vogt, S. (1997). Status and plans for the PRIME Lab AMS facility. *Nuclear*

Instruments & Methods in Physics Research 123, 69-72. https://doi.org/10.1016/S0168-583X(96)00621-0

Fabryka-Martin, J.T., (1988). *Production of radionuclides in the earth and their hydrogeologic significance, with emphasis on chlorine-36 and iodine-129.* Ph.D. Thesis. Tucson: University of Arizona, pp. 400.

Faugeres, L. (1969). Problems created by the geomorphology of Olympus, Greece: Relief, formation, and traces of Quaternary cold periods with discussion. *Association Francaise pour l'Etude du Quaternaire 6*, 105–127.

Federici, P.R., Granger, D.E., Ribolini, A., Spagnolo M., Pappalardo, M., Cyr, A.J. (2012). Last Glacial Maximum and the Gschnitz stadial in the Maritime Alps according to ^{10}Be cosmogenic dating. *Boreas 41*, 277-291. https://doi.org/10.1111/j.1502-3885.2011.00233.x

Finkel, R. C., Owen, L. A., Barnard, P. L., Caffee, M. W. (2003). Beryllium-10 dating of Mount Everest moraines indicates a strong monsoonal influence and glacial synchroneity throughout the Himalaya. Geology 31, 561−564. https://doi.org/10.1130/0091-7613(2003)031<0561:BDOMEM>2.0.CO;2

Fletcher, W.J., Müller, U.C., Koutsodendris, A., Christanis, K., Pross, J. (2013). A centennial-scale record of vegetation and climate variability from 312 to 240ka (Marine Isotope Stages 9c-a, 8 and 7e) from Tenaghi Philippon, NE Greece. *Quaternary Science Reviews 78*, 108–125. https://doi.org/10.1016/j.quascirev.2013.08.005

Florineth, D. and Schlüchter, C. (2000). Alpine evidence for atmospheric circulation patterns in Europe during the Last Glacial Maximum. *Quaternary Research 54*, 295–308. https://doi.org/10.1006/qres.2000.2169

Fotiadi, A.K., Metaxas, D.A. and Bartzokas, A. (1999). A statistical study of precipitation in northwest Greece. *International Journal of Climatology 19*, 1221-1232. https://doi.org/10.1002/(SICI)1097-0088(199909)19:11<1221::AID-JOC436>3.0.CO;2-H

Frye, J.C. and Willman, H.B. (1962). Morphostratigraphic units in Pleistocene stratigraphy. *American Association of Petroleum Petrologists Bulletin 46*, 112–113. https://doi.org/10.1306/BC743763-16BE-11D7-8645000102C1865D

Frogley, M.R., 1998. *The Biostratigraphy, Palaeoecology and Geochemistry of a Long Lacustrine Sequence from NWGreece* (Thesis). Cambridge: University of Cambridge. https://doi.org/10.17863/CAM.16400

Fuchs, M. and Owen, L. A. (2008). Luminescence dating of glacial and associated sediments: review, recommendations and future directions. *Boreas 37*, 636−659. https://doi.org/10.1111/j.1502-3885.2008.00052.x

Furlan, D. (1977). The Climate of Southeast Europe. IN: Wallen, C.C. (Ed.). *Climates of Central and Southern Europe.* Amsterdam: Elsevier, *(*pp. 185-223*).*

Gachev, E. (2020). Holocene glaciation in the mountains of Bulgaria. *Mediterranean Geoscience Reviews 2*, 103–117. https://doi.org/10.1007/s42990-020-00028-3

Galanidou, N., Tzedakis, P.C., Lawson, I.T., Frogley, M.R., 2000. A revised chronological and paleoenvironmental framework for the Kastritsa rockshelter, northwest Greece. Antiquity 74, 349-355. https://doi.org/10.1017/S0003598X00059421

García-Ruiz, J.M., Moreno, A., González-Sampériz, P., Valero-Garcés, B., Martí-Bono, C. (2010). La cronología del último ciclo glaciar en las montañas del sur de Europa. Una revision. *Revista Cuaternario y Geomorfología 24*, 35-46.

Gianotti, F., Forno, M.G., Ivy-Ochs, S., Monegato, G., Pini, R., Ravazzi, C. (2015). Stratigraphy of the Ivrea morainic amphitheatre (NW Italy): an updated synthesis. *Alpine and Mediterranean Quaternary* 28, 29 – 58.

Giraudi, C. (2012). The Campo Felice Late Pleistocene glaciation (Apennines, central Italy). *Journal of Quaternary Science 27*, 432-440. https://doi.org/10.1002/jqs.1569.

Giraudi, C. and Frezzotti, M. (1997). Late Pleistocene glacial events in the Central Apennines, Italy. *Quaternary Research 48*, 280–290. https://doi.org/10.1006/qres.1997.1928

Giraudi, C. amd Giaccio, B. (2015). Middle Pleistocene glaciations in the Apennines, Italy: new chronological data and preservation of the glacial record. IN: Hughes, P.D. and Woodward, J.C. (eds), *Quaternary Glaciation in the Mediterranean Mountains.* London: Geological Society of London Special Publications 433, pp. 161-178. https://doi.org/10.1144/SP433.1

Gómez-Ortiz, A., Palacios, D., Palade, B., Vazquez-Selem, L., Salvador-Franch, F. (2012). The deglaciation of the Sierra Nevada (Southern Spain). *Geomorphology 159-160*, 93-105. https://doi.org/10.1016/j.geomorph.2012.03.008

Gosse, J.C. and Phillips, F.M. (2001) Terrestrial in situ cosmogenic nuclides: theory and application. *Quaternary Science Reviews 20*, 1475-1560. https://doi.org/10.1016/S0277-3791(00)00171-2

Gosse, J.C., Klein, J., Evenson, E.B., Lawn, B., Middleton, R. (1995) Beryllium-10 dating of the duration and retreat of the last Pinedale glacial sequence. *Science 268*, 1329-1333 https://doi.org/10.1126/science.268.5215.1329

Gouvas, M. and Sakellariou, N. (2011). Climate and forest vegetation of Greece. National Observatory of Athens, Institute of Environmental Research and Sustainable Development, Technical Library Report Nr: 01/2011 (in Greek).

Grant, K.M., Rohling, E.J., Bar-Matthews, M., Ayalon, A., Medina-Elizalde, M., Bronk Ramsey, C., Satow, C., Roberts, A.P. (2012). Rapid coupling between ice volume and polar temperature over the past 150,000 years. *Nature 491*, 744-747. https://doi.org/10.1038/nature11593

Gromig, R., Mechernich, S., Ribolini, A., Wagner, B., Zanchetta, G., Isola, I., Bini, M., Dunai, T. J. (2018). Evidence for a Younger Dryas deglaciation in the Galicica Mountains (FYROM) from cosmogenic ^{36}Cl. *Quaternary International 464*, 352-363. https://doi.org/10.1016/j.quaint.2017.07.013

Gruen, A. and Wolff, K. (2007). DSM generation with ALOS/PRISM data using SAT- PP. *International Geoscience and Remote Sensing Symposium (IGARSS)*, 3606-3609.

Guido, Z.S., Ward, D.J., Anderson, R.S. (2007). Pacing the post-Last Glacial Maximum demise of the Animas Valley glacier and the San Juan Mountain ice cap, Colorado. *Geology 35*, 739-742. https://doi.org/10.1130/G23596A.1

Gustavsson, M., Kolstrup, E., Seijmonsbergen, A.C. (2006). A new symbol-and-GIS based detailed geomorphological mapping system: Renewal of a scientific discipline for understanding landscape development. *Geomorphology 77*, 90 - 111. https://doi.org/10.1016/j.geomorph.2006.01.026

Hallet, B. and Putkonen, J. (1994.) Surface dating of dynamic landforms: Young boulders on aging moraines. *Science 265*, 937–940.

Hamlin, R.H.B., Woodward, J.C., Black, S., Macklin, M.G. (2000). Sediment fingerprinting as a tool for interpreting long-term river activity: the Voidomatis basin, Northwest Greece In: Foster, I.D.L. (Eds.), *Tracers in Geomorphology*. Chichester, UK: Wiley, pp. 473–501.

Harden, J.W. (1982). A quantitative index of soil development from field descriptions: Examples from a chronosequence in central California. *Geoderma 28*, 1-28. https://doi.org/10.1016/0016-7061(82)90037-4

Hays, J. D., Imbrie, J., Shackleton, N. J. (1976). Variations in the Earth's orbit: pacemaker of the ice ages. *Science 194*, 1121–1132. https://doi.org/10.1126/science.194.4270.1121

Herman, F., Seward, D., Valla, P. G., Carter, A., Kohn, B., Willett,S. D., Ehlers, T. A. (2013). Worldwide acceleration of mountain erosion under a cooling climate. *Nature 504*, 423–426. https://doi.org/10.1038/nature12877

Heyman, J., Stroeven A.P., Harbor, J.M., Caffee, M.W. (2011). Too young or too old: Evaluating cosmogenic exposure dating based on an analysis of compiled boulder exposure ages. *Earth and Planetary Science Letters 302*, 71-80. https://doi.org/10.1016/j.epsl.2010.11.040

Hippe, K., Ivy-Ochs, S., Kober, F., Zasadni, J., Wieler, R. Wacker, L., Kubik, P.W., Schlüchter, C. (2014). Chronology of Lateglacial ice flow reorganization and deglaciation in the Gotthard Pass area, Central Swiss Alps, based on cosmogenic ^{10}Be and in situ ^{14}C. *Quaternary Geochronology 19*, 14-26. https://doi.org/10.1016/j.quageo.2013.03.003

Hoogakker, B. A. A., Smith, R. S., Singarayer, J. S., Marchant, R., Prentice, I. C., Allen, J. R. M. ,Anderson, R. S., Bhagwat, S. A., Behling, H., Borisova, O., Bush, M., Correa-Metrio, A., de Vernal, A., Finch, J. M., Frechette, B., Lozano-Garcia, S., Gosling, W. D., Granoszewski, W., Grimm, E. C., Grüger, E., Hanselman, J., Harrison, S. P., Hill, T. R., Huntley, B., Jimenez-Moreno, G., Kershaw, P., Ledru, M.-P., Magri, D., McKenzie, M., Müller, U., Nakagawa, T., Novenko, E., Penny, D., Sadori, L., Scott, L., Stevenson, J., Valdes, P. J., Vandergoes, M., Velichko, A., Whitlock, C., Tzedakis, C.et al. (2016) Terrestrial biosphere changes over the last 120 kyr. *Climate of the Past 12*, 51-73. https://doi.org/10.5194/cp-12-51-2016

Hughes, A.L.C., Gyllencreutz, R., Lohne, O.S., Mangerud, J., Svendsen, J.I. (2016). The last Eurasian ice sheets - a chronological database and time-slice reconstruction, DATED-1. Boreas. 45, 1−45. https://doi.org/10.1111/bor.12142

Hughes P.D. (2004). Quaternary glaciation in the Pindus Mountains, northwest Greece. PhD thesis, University of Cambridge.

Hughes, P.D. (2007). Recent behaviour of the Debeli Namet glacier, Durmitor, Montenegro. *Earth Surface Processes and Landforms 10*, 1593-1602. https://doi.org/10.1002/esp.1537

Hughes, P.D. (2010a). Geomorphology and Quaternary stratigraphy: The roles of morpho-, litho-, and allostratigraphy. *Geomorphology 123*, 189-199. https://doi.org/10.1016/j.geomorph.2010.07.025

Hughes, P.D. (2010b). Little Ice Age glaciers in Balkans: low altitude glaciation enabled by cooler temperatures and local topoclimatic controls. *Earth Surface Processes and Landforms 35*, 229–241. https://doi.org/10.1002/esp.1916

Hughes, P.D. (2018). Little Ice Age Glaciers and Climate in the Mediterranean Mountains: A New Analysis. *Cuadernos de Investigación Geográfica 44*, 15-46. https://doi.org/10.18172/cig.3362

Hughes, P.D., and Woodward, J.C. (2008). Timing of glaciation in the Mediterranean mountains during the last cold stage. *Journal of Quaternary Science 23*, 575–588.https://doi.org/10.1002/jqs.1212

Hughes, P. D. and Gibbard, P. L. (2015). A stratigraphical basis for the Last Glacial Maximum (LGM). *Quaternary International 383*, 174-185. https://doi.org/10.1016/j.quaint.2014.06.006

Hughes, P.D. and Woodward, J.C. (2017). Quaternary Glaciation in the Mediterranean Mountains: A New Synthesis. In: Hughes ,P.D., Woodward, J.C. (Eds.), *Quaternary glaciation in the Mediterranean Mountains.* London: Geological Society of London Special Publications 433, pp. 1-23. https://doi.org/10.1144/SP433.14

Hughes, P.D., Gibbard, P.L., Woodward, J.C. (2003). Relict rock glaciers as indicators of Mediterranean palaeoclimate during the Last Glacial Maximum (Late Würmian) of northwest Greece. *Journal of Quaternary Science 18*, 431-40. https://doi.org/10.1002/jqs.764

Hughes, P.D., Gibbard, P.L., Woodward, J.C. (2005). Quaternary glacial records in mountain regions: A formal stratigraphical approach. *Episodes 28*, 85-92.

Hughes, P.D., Woodward, J.C., Gibbard, P.L., Macklin, M.G., Gilmour, M.A., Smith, G.R. (2006a). The glacial history of the Pindus Mountains, Greece. *The Journal of Geology 114*, 413-434. https://doi.org/10.1086/504177

Hughes, P.D., Woodward, J.C., Gibbard, P.L. (2006b). Quaternary glacial history of the Mediterranean mountains. *Progress in Physical Geography 30*, 334-364. https://doi.org/10.1191/0309133306pp481ra

Hughes P.D., Woodward, J.C., Gibbard, P.L. (2006c). The last glaciers of Greece. *Zeitscrift fuer Geomorphologie 50*, 37-46.

Hughes, P.D., Woodward J.C., Gibbard, P.L. (2006d). Late Pleistocene glaciers and climate in the Mediterranean, *Global and Planetary Change 50*, 83-98. https://doi.org/10.1016/j.gloplacha.2005.07.005

Hughes, P.D., Gibbard, P.L., Woodward, J.C. (2006e). Middle Pleistocene glacier behaviour in the Mediterranean: sedimentological evidence from the Pindus Mountains, Greece. *Journal of the Geological Society of London 163*, 857–867. https://doi.org/10.1144/0016-76492005-131

Hughes P.D., Gibbard, P.L., Woodward, J.C. (2007). Geological controls on Pleistocene glaciations and cirque form in Greece. *Geomorphology 88*, 242–253. https://doi.org/10.1016/j.geomorph.2006.11.008

Hughes, P.D., Woodward, J.C., van Calsteren, P.C., Thomas, L.E., Adamson, K.R. (2010). Pleistocene ice caps on the coastal mountains of the Adriatic Sea: palaeoclimatic and wider palaeoenvironmental implications. *Quaternary Science Reviews 29*, 3690–3708. https://doi.org/10.1016/j.quascirev.2010.06.032

Hughes, P.D., Woodward, J.C., van Calsteren, P.C., Thomas, L.E. (2011). The glacial history of the Dinaric Alps, Montenegro. *Quaternary Science Reviews 30*, 3393–3412. https://doi.org/10.1016/j.quascirev.2011.08.016

Hughes, P.D., Gibbard, P.L., Ehlers, J. (2013). Timing of glaciation during the last glacial cycle: evaluating the concept of a global 'Last Glacial Maximum' (LGM). *Earth-Science Reviews 125*, 171-198. https://doi.org/10.1016/j.earscirev.2013.07.003

IGME (Institute of Geology and Mineral Exploration) (1959) 1:50,000 Geological map of Greece. Metsovon Sheet (No. 94). Institute of Geological and Mineral Exploration, Athens.

IGME (Institute of Geology and Mineral Exploration) (1970). 1:50,000 Geological map of Greece. Tsepelovon Sheet (93). Institute of Geological and Mineral Exploration, Athens.

IGME (Institute of Geology and Mineral Exploration) (1977) 1:50,000 Geological map of Greece. Aeghion Sheet (No. 201). Institute of Geological and Mineral Exploration, Athens.

IGME (Institute of Geology and Mineral Exploration) (1978) 1:50,000 Geological map of Greece. Dafni Sheet (No. 216). Institute of Geological and Mineral Exploration, Athens.

IGME (Institute of Geology and Mineral Exploration) (1987). 1:50,000 Geological map of Greece. Konitsa Sheet (No. 82). Institute of Geological and Mineral Exploration, Athens.

Ivy-Ochs, S. and Briner, J. (2014). Dating disappearing ice with cosmogenic nuclides. *Elements 10*, 351–356. https://doi.org/10.2113/gselements.10.5.351

Ivy-Ochs, S. and Kober, F. (2008). Surface exposure dating with cosmogenic nuclides. E&G Quaternary Science Journal 57, 179–209. https://doi.org/10.3285/eg.57.1-2.7

Ivy-Ochs, S., Kerschner, H., Reuther, A., Maisch, M., Sailer, R., Schaefer, J., Kubik, P.W., Synal, H.-A., Schlüchter, C. (2006a). The timing of glacier advances in the northern European Alps based on surface exposure dating with cosmogenic ^{10}Be, ^{26}Al, ^{36}Cl, and ^{21}Ne. IN: Alonso-Zarza, A.M., Tanner, L.H. (Eds.). *In Situ-Produced Cosmogenic Nuclides and Quantification of Geological Processes.* Geological Society of America, Special Paper 415. https://doi.org/10.1130/2006.2415(04)

Ivy-Ochs, S., Kerschner, H., Kubik, P.W., Schlüchter, C. (2006b). Glacier response in the European Alps to Heinrich Event 1 cooling: the Gschnitz stadial. *Journal of Quaternary Science 21*, 115–130. https://doi.org/10.1002/jqs.955

Ivy-Ochs, S., Kerschner, H., Schlüchter, C. (2007). Cosmogenic nuclides and the dating of Lateglacial and Early Holocene glacier variations: The Alpine perspective. *Quaternary International 164-165*, 53-63. https://doi.org/10.1016/j.quaint.2006.12.008

Jolivet, L. and Faccenna, C. (2000). Mediterranean extension and the Africa-Eurasia collision. *Tectonics 19*, 1095– 1106. https://doi.org/10.1029/2000TC900018

Jolivet, L., Brun, J.P, Gautier, P., Lallemant S., and Patriae M. (1994). 3-D kinematics of extension in the Aegean region from the early Miocene to the Present, insights from the ductile crust. *Bulletin Société Géologique de France 165*, 195-209.

Jones, G. and Robertson, A.H.F. (1991). Tectono-stratigraphy and evolution of the Mezozoic Pindus ophiolite and related units, northwestern Greece. *Journal of the Geological Society, London 148*, 267–288. https://doi.org/10.1144/gsjgs.148.2.0267

Kaplan, M.R., Ackert, R.P., Singer, B.S., Douglass, D.C., Kurz, M.D. (2004). Cosmogenic nuclide chronology of millennial-scale glacial advances during O-isotope stage 2 in Patagonia. *Geological Society of America Bulletin 116*, 308-321. https://doi.org/10.1130/B25178.1

Kaplan, M.R., Douglass, D.C., Singer, B.S., Caffee, M.W. (2005). Cosmogenic nuclide chronology of pre-last glacial maximum moraines at Lago Buenos Aires, 46 degrees S, Argentina. Quaternary Research 63, 301-315. https://doi.org/10.1016/j.yqres.2004.12.003

Kapsiotis, A. (2014). Composition and alteration of Cr-spinels from Milia and Pefki serpentinized mantle peridotites (Pindos Ophiolite Complex, Greece). *Geologica Carpathica 65*, 83-95. https://doi.org/10.2478/geoca-2013-0006

Katsoulakos, N.M. and Kaliampakos, D.C. (2014). What is the impact of altitude on energy demand? A step towards developing specialized energy policy for mountainous areas. *Energy Policy 71*, 130-138. https://doi.org/10.1016/j.enpol.2014.04.003

Kelemen, P., Kikawa, E., Miller, J., Abe, N., Bach, W., Carlson, R.L., Casey, J.F., Chambers, L.M., Cheadle, M., Cipriani, A., Dick, H.J.B., Faul, U., Garces, M., Garrido, C., Gee, J.S.,Godard, M., Griffin, D.W., Harvey, J., Ildefonse, B., Iturrino, G.J., Josef, J., Meurer, W.P.,Paulick, H., Rosner, M., Schroeder, T., Seyler, M., Takazawa, E. (2004). Site 1268. IN: Kelemen, P.B., Kikawa, E., Miller, D.J., et al., *Proc. ODP, Init. Repts., 209: College Station, TX (Ocean Drilling Program)*, 1–171. doi:10.2973/odp.proc.ir.209.103.2004

Kelemen, P., Matter, J., Streit, E., Rudge, J., Curry, W.B., Blusztajn, J. (2011). Rates and Mechanisms of Mineral Carbonation in Peridotite: Natural Processes and Recipes for Enhanced, in situ CO_2 Capture and Storage. *Annual Review of Earth and Planetary Sciences 39*, 545-576. https://doi.org/10.1146/annurev-earth-092010-152509

King, G. and Bailey, G. (1985). The palaeoenvironment of some archaeological sites in Greece: the influence of accumulated uplift in a seismically active region. *Proceedings of the Prehistoric Society 51*, 273–282. https://doi.org/10.1017/S0079497X0000712X

King, G., Sturdy, D., Bailey, G. (1997). The tectonic background to the Epirus Landscape. In: Bailey, G.N. (Ed.), *Klithi: Palaeolithic settlement and Quaternary landscapes in northwest Greece. Klithi in its local and regional setting* (vol. 2). Cambridge: MacDonald Institute for Archaeological Research, pp. 541–558.

Klasen, N., Fiebig, M., Preusser, F., Reitner, J.M., Radtke, U. (2007). Luminescence dating of proglacial sediments from the Eastern Alps. *Quaternary International 164/165*, 21–32. https://doi.org/10.1016/j.quaint.2006.12.003

Klebelsberg, R.V. (1932). Der Tymphrestos im Aetolischen Pindos. *Jahrbuch der Geologischen Bundesanstalt 82*, 17–30.

Kleman, J., Borgström, I., Skelton, A., Hall, A. (2016). Landscape evolution and landform inheritance in tectonically active regions: The case of the Southwestern Peloponnese, Greece. *Zeitschrift für Geomorphologie 60*, 171-193. https://dx.doi.org/10.1127/zfg/2016/0283

Koutsi, R. and Stournaras, G. (2011). Groundwater vulnerability assessment in the Loussi polje area, N Peloponessus: the PRESK method. IN: N., Lambrakis, G., Stournaras, K. Katsanou (Eds.). *Advances in the Research of Aquatic Environment*. Berlin: Springer, pp. 335-342. https://doi.org/10.1007/978-3-642-24076-8_39

Koutsodendris, A., Kousis, I., Peyron, O., Wagner, B. (2019). The Marine Isotope Stage 12 pollen record from Lake Ohrid (SE Europe): Investigating short-term climate change under extreme glacial conditions. *Quaternary Science Reviews 221*, 105873. https://doi.org/10.1016/j.quascirev.2019.105873

Koutsopoulos, K. and Sarlis, G. (2003). Contribution to the study of the flora of Vouraikos gorge (Peloponnesos, Greece). *Flora Mediterranea 12*, 299–314.

Köse, O., Sarıkaya, M.A., Çiner, A., Candaş, A. (2019). Late Quaternary glaciations and cosmogenic 36Cl geochronology of Mount Dedegöl, south-west Turkey. *Journal of Quaternary Science 34*, 51-63. https://doi.org/10.1002/jqs.3080

Kraak, M.J., Oremling, F.J. (2010). *Cartography: visualization of spatial data (3rd Edition).* London: Routledge.

Kranis, H. and Papanikolaou, D. (2001). Evidence for detachment faulting on the NE Parnassos mountain front (Central Greece). *Bulletin of the Geological Society of Greece 34*, 281-287. https://doi.org/10.12681/bgsg.17024

Kuhlemann, J., Rohling, E.J., Krumrei, I., Kubik, P., Ivy-Ochs, S., Kucera, M. (2008). Regional synthesis of Mediterranean atmospheric circulation during the last glacial maximum. *Science 321*, 1338–1340. https://doi.org/10.1126/science.1157638

Kuhlemann, J., Milivojevic, M., Krumrei, I., Kubik, P.W. (2009). Last glaciations of the Sara range (Balkan peninsula): Increasing dryness from the LGM to the Holocene. *Austrian Journal of Earth Science 102*, 146–158.

Kuhlemann, J., Gachev, E., Gikov, A., Nedkov, S., Krumrei, I., Kubik, P. (2013). Glaciation in the Rila mountains (Bulgaria) during the Last Glacial Maximum. *Quaternary International 293*, 51–62. https://doi.org/10.1016/j.quaint.2012.06.027

Kutzbach, J. E., Chen, G., Cheng, H., Edwards, R., Liu, Z., (2014). Potential role of winter rainfall in explaining increased moisture in the Mediterranean and Middle East during periods of maximum orbitally-forced insolation seasonality. *Climate Dynamics 42*, 1079–1095. https://doi.org/10.1007/s00382-013-1692-1

Lal, D. (1988). In situ-produced cosmogenic isotopes in terrestrial rocks. *Annual Review of Earth and Planetary Sciences 16*, 355-388. https://doi.org/10.1146/annurev.ea.16.050188.002035

Lal, D. (1991). Cosmic ray labeling of erosion surfaces: in-situ nuclide production rates and erosion models. *Earth and Planetary Science Letters 104*, 424-439. https://doi.org/10.1016/0012-821X(91)90220-C

Lal, D. and Peters, B. (1967). Cosmic ray produced radioactivity on the Earth. IN: Sitte K. (Ed.). *Kosmische Strahlung II / Cosmic Rays II. Handbuch der Physik / Encyclopedia of Physics* vol 9. Berlin, Heidelberg: Springer, pp. 551-612. https://doi.org/10.1007/978-3-642-46079-1_7

Lambeck, K. (1995). Late Pleistocene and Holocene sealevel change in Greece and south-western Turkey: a separation of eustatic, isostatic and tectonic contributions. *Geophysical Journal International 122*, 1022–1044. https://doi.org/10.1111/j.1365-246X.1995.tb06853.x

Lamsal, D., Sawagaki, T., Watanabe, T. (2011). Digital terrain modelling using Corona and ALOS PRISM data to investigate the distal part of Imja Glacier, Khumbu Himal, Nepal. *Journal of Mountain Science 8*, 390-402. https://doi.org/10.1007/s11629-011-2064-0

Lehmkuhl, F. (1998). Quaternary glaciations in central and western Mongolia. *Quaternary Proceedings 6*, 153–67. https://doi.org/10.1016/S1571-0866(04)80130-1

Lemmen, D.S. and England, J. (1992). Multiple glaciations and sea level changes, northern Ellesmere Island, high arctic Canada. *Boreas 21*, 137–52. https://doi.org/10.1111/j.1502-3885.1992.tb00021.x

Leontaritis, A.D. (2019). *Walking and Trekking in Zagori*. Kendal, UK: Cicerone Press.

Leontaritis, A.D., Kouli, K., Pavlopoulos, K. (2020). The glacial history of Greece: a comprehensive review. Mediterranean Geoscience Reviews 2: 65–90. https://doi.org/10.1007/s42990-020-00021-w

Leontaritis A.D., Pavlopoulos, K., Ribolini, A., Marrero, S., Spagnolo, M., Hughes, P.D. (2021). Timing of Late Pleistocene glaciations in the North Pindus mountains, Greece: ^{36}Cl exposure ages from Mt Mavrovouni. *Quaternary Science Reviews – in preparation for publication.*

Lewin, J., Macklin, M. G., Woodward, J.C. (1991). Late Quaternary fluvial sedimentation in the Voidomatis Basin, Epirus, northwest Greece. *Quaternary Research 35*, 103–115. https://doi.org/10.1016/0033-5894(91)90098-P

Li, Y., 2018. Determining topographic shielding from digital elevation models for cosmogenic nuclide analysis: a GIS model for discrete sample sites. *Journal of Mountain Science 15*, 939–947. https://doi.org/10.1007/s11629-018-4895-4

Lian, O. B. and Roberts, R. G. (2006) Dating the Quaternary: Progress in luminescence dating of sediments. *Quaternary Science Reviews 25*, 2449−2468. https://doi.org/10.1016/j.quascirev.2005.11.013

Lifton, N., Sato, T., Dunai, T.J. (2014). Scaling in situ cosmogenic nuclide production rates using analytical approximations to atmospheric cosmic-ray fluxes. *Earth and Planetary Science Letters 386*, 149-160. https://doi.org/10.1016/j.epsl.2013.10.052

Lionello, P., Malanotte-Rizzoli, P., Boscolo, R. (2006). *Mediterranean Climate Variability*. Amsterdam: Elsevier.

Lisiecki, L.E. and Raymo, M..E. (2005). A Pliocene- Pleistocene stack of 57 globally distributed benthic $\delta^{18}O$ records. *Paleoceanography, 20*, 1003-1020. https://doi.org/10.1029/2004PA001071

Louis, H., 1926. Glazialmorphologishche Beobachtungen im albanischen Epirus. *Zeitschrift der Gesellschaft für Erdkunde 1926*, 398–409.

Lowe, J.J. and Walker, M.J.C. (1997). *Reconstructing Quaternary environments.* London: Longman, pp. 446.

Luetscher, M., Boch, R., Sodemann, H., Spötl, C., Cheng, H., Edwards, R.L., Friscia, S., Hof, F., Müller, W. (2015). North Atlantic storm track changes during the Last Glacial Maximum recorded by Alpine speleothems. *Nature Communications 6*, 6344, 1-6. https://doi.org/10.1038/ncomms7344

Lukas, S. (2006). Morphostratigraphic principles in glacier reconstruction – a perspective from the British Younger Dryas. *Progress in Physical Geography 30*, 719–736. https://doi.org/10.1177/0309133306071955

Macklin, M.G. and Woodward, J.C. (2009). Rivers and environmental change. In: Woodward, J.C. (Ed.). *The Physical Geography of the Mediterranean*. Oxford: Oxford University Press, pp. 319-252.

Magganas, A. and Koutsovitis, P (2015). Composition, melting and evolution of the upper mantle beneath the Jurassic Pindos ocean inferred by ophiolitic ultramafic rocks in East Othris, Greece. International Journal of Earth Sciences 104, 1185–1207. https://doi.org/10.1007/s00531-014-1137-z

Manz, L.A. (1998). Cosmogenic ^{36}Cl chronology for deposits of presumed Pleistocene age on the Eastern Piedmont of Mount Olympus, Pieria, Greece. Unpublished MSc thesis, Ohio University, USA.

Marrero, S.M., Phillips, F.M., Borchers, B., Lifton, N., Aumer, R., Balco, G. (2016a). Cosmogenic nuclide systematics and the CRONUScalc program. *Quaternary Geochronology 31*, 160-187. https://doi.org/10.1016/j.quageo.2015.09.005

Marrero, S.M., Phillips, F.M., Caffee, M.W., Gosse, J.C. (2016b). CRONUS-Earth cosmogenic ^{36}Cl calibration. *Quaternary Geochronology 31*, 199-219. https://doi.org/10.1016/j.quageo.2015.10.002

Marrero, S.M., Phillips, F.M., Caffee, M.W., Gosse, J.C. (2020). Corrigendum to 'CRONUS-Earth cosmogenic ^{36}Cl calibration. Quaternary Geochronology 31 (2016) 199–219]'. In press.

Maruya, M. and Ohyama, H. (2007). Estimation of height measurement accuracy for ALOS PRISM triplet images. *International Geoscience and Remote Sensing Symposium (IGARSS)*, 2869-2872.

Maruya, M. and Ohyama, H. (2008). Accurate dem and ortho-rectified image production from alos/prism. *International Geoscience and Remote Sensing Symposium (IGARSS)*, 2869-2872.

Mastronuzzi G., Sanso, P., Stamatopoloulos, L. (1994). Glacial landforms of the Peloponnisos (Greece). *Rivista Geografica Italiana 101*, 77-86.

Maull, O. (1921). Beiträge zur Morphologie des Peloponnes und des sdlichen Mittelgriechenlands. *Geographische Abhandlungen 10*, 179-302.

McNeill, L.C. and Collier, R.E.L. (2004). Uplift and slip rates of the eastern Eliki fault segment, Gulf of Corinth, Greece, inferred from Holocene and Pleistocene terraces 1. *Journal of the Geological Society London 161*, 81–92. http://doi.org/10.1144/0016-764903-029

McNeill, L.C., Shillington, D.J., Carter, G.D.O. Everest, J. D., Gawthorpe, R. L., Miller, C., … Green, S.et al. (2019). High-resolution record reveals climate-driven environmental and sedimentary changes in an active rift. *Scientific Reports 9*, 3116 (2019). https://doi.org/10.1038/s41598-019-40022-w

Messerli, B. (1967). Die Eiszeitliche und die gegenwartige Vergletscherung im Mittelmeeraum. *Geographica Helvetica 22*, 105–228.

Mey, J., Scherler, D., Wickert, A., Egholm, D., Tesauro, M., Schildgen, T., Strecker, M. (2016). lacial isostatic uplift of the European Alps. *Nature Communications 7*, 13382. https://doi.org/10.1038/ncomms13382

Milankovic, M. (1941). *Kanon der Erdbestrahlung und seine Anwendung auf das Eiszeitenproblem.* Royal Serbian Academy special publications, Section of Mathematical and Natural Sciences v. 132. Belgrade : Mihaila Ćurčića.

Milner, A.M., Roucoux, K.H., Collier, R.E.L., Müller, U.C., Pross, J., Tzedakis, P.C. (2016). Vegetation responses to abrupt climatic changes during the Last Interglacial Complex (Marine Isotope Stage 5) at Tenaghi Philippon, NE Greece. *Quaternary Science Reviews 154*, 169-181. https://doi.org/10.1016/j.quascirev.2016.10.016

Mistardis, G. (1935). *Geomorphological research in northeastern Epirus* (In Greek). Athens, Greece: Hellenic Geographical Society

Mistardis, G. (1937a). *Sur la morphologie des parties superieures des hautes montagnes de la Grece.* Reprinted from the bulletin of the first Panhellenic mountaineering Conference in Athens, pp. 35-41. Athens, Greece: Hellenic Geographical Society

Mistardis. G. (1937b). Traces de glaciation dans la partie montagneuse du nord du Peloponese. Zeitschrift für Gletscher Kunde XXV, 122-129.

Mistardis. G. (1937c). *Recherche geomorphologique dans la partie superieure des monts Aroania (Chelmos).* Reprinted from the bulletin of the first Panhellenic mountaineering Conference in Athens, pp. 94-103. Athens, Greece: Hellenic Geographical Society

Mistardis. G. (1946). *Aroania (Chelmos*). "To Vouno"- Greek Mountaineering Club edition (in Greek), pp 37-64. Athens, Greece: Hellenic Geographical Society

Monegato, G., Ravazzi, C., Donegana, M., Pini, R., Calderoni, G., Wick, L. (2007). Evidence of two-fold glacial advance during the last glacial maximum in the Tagliamento end moraine system (Eastern Alps). *Quaternary Research 68*, 284–302. https://doi.org/10.1016/j.yqres.2007.07.002

Monegato, G., Scardia, G., Hajdas, I., Rizzini, F., Piccin, A. (2017). The Alpine LGM in the boreal ice-sheets game. *Scientific Reports 7*, 2078. https://doi.org/10.1038/s41598-017-02148-7

Moore, A.K. and Granger, D.E. (2019). Calibration of the production rate of cosmogenic ^{36}Cl from Fe. *Quaternary Geochronology 51*, 87-98. https://doi.org/10.1016/j.quageo.2019.02.002

Murray, A.S. and Wintle, A.G. (2000). Luminescence dating of quartz using an improved single - aliquot regenerative - dose protocol. *Radiation Measurements 32*, 57-73. https://doi.org/10.1016/S1350-4487(99)00253-X

Müller, U.C., Pross, J., Tzedakis, P.C., Gamble, C., Kotthoff, U., Schmiedl, G., Wulf, S., Christanis, K. (2011). The role of climate in the spread of modern humans into Europe. *Quaternary Science Reviews 30*, 273-279. https://doi.org/10.1016/j.quascirev.2010.11.016

Nance, R.D. (2010). Neogene–Recent extension on the eastern flank of Mount Olympus, Greece. *Tectonophysics 488*, 282–292. https://doi.org/10.1016/j.tecto.2009.05.011

Niculescu, C. (1915). Sur les traces de glaciation dans le massif Smolica chaıne du Pinde meridional. *Bulletin de la Section Scientifique de l'Academie Roumaine 3*, 146–151.

Nikolakopoulos, K.G. (2013). Comparison of different along the track high resolution satellite stereopair for DSM extraction. *Proceedings of SPIE 8893*, 1-10.

Nikolakopoulos, K.G. and Vaiopoulos, D. (2011). Validation of ALOS DSM. *Proceedings of SPIE 8181*, 1031-11.

Nikolakopoulos, K.G., Kamaratakis, E., Chrysoulakis, N. (2006). SRTM vs ASTER Elevation Products. Comparison for two Regions in Crete, Greece. *International Journal of Remote Sensing 27*, 4819-4838. https://doi.org/10.1080/01431160600835853

Nikolakopoulos, K.G., Vaiopoulos, D., Tsombos, P. (2010). DSM from ALOS data: the case of Andritsena, Greece. *Proceedings of SPIE 7831*,1-10.

Nocquet, J.M., Sue, C., Walsperdorf, A., Tran, T., Lenotre, N., Vernant, P., Cushing, M., Jouanne, F., Masson, F., Baize, S., Chery, J. (2016). Present-day uplift of the western Alps. *Scientific Reports 6*, 28404. https://doi.org/10.1038/srep28404

Oerlemans, J. (2005). Extracting a climate signal from 169 glacier records. *Science 308*, 675–677. https://doi.org/10.1126/science.1107046

Ohmura A., Kasser, P., Funk, M. (1992). Climate at the equilibrium line of glaciers. *Journal of Glaciology 38*, 397-411. https://doi.org/10.3189/S0022143000002276

Ohmura A. and Boetcher, M. (2018). Climate on the equilibrium line altitudes of glaciers: Theoretical background behind Ahlmann's P/T diagram. *Journal of Glaciology 64*, 489-505.

Oliva, M., Palacios, D., Fernández-Fernández, J. M., Rodríguez-Rodríguez, L., Garcia Ruiz, J-M., Andrés, N., Carrasco, R. M., Pedrazza, J., Perez Alberti, A., Valcarel, M., Hughes, P.D. (2019). Late Quaternary glacial phases in the Iberian Peninsula. *Earth Science Reviews 192*, 564-600. https://doi.org/10.1016/j.earscirev.2019.03.015

Osmaston, H.A. (2005). Estimates of glacier equilibrium line altitudes by the Area×Altitude, theArea×Altitude Balance Ratio and the Area×Altitude Balance Index methods and their validation. *Quaternary International 138–139*, 22–31. https://doi.org/10.1016/j.quaint.2005.02.004

Owen, L. A., Finkel, R. C., Caffee, M. W. (2002). A note on the extent of glaciation throughout the Himalaya during the global Last Glacial Maximum. *Quaternary Science Reviews 21*, 147−157. https://doi.org/10.1016/S0277-3791(01)00104-4

Palacios, D., Gomez-Ortiz, A., Andres, N., Salvador, F., Oliva, M., 2016a. Timing and ne geomorphologic evidence of the Last Deglaciation stages in Sierra Nevada (southern Spain). Quaternary Science Reviews 150, 110−129. https://doi.org/10.1016/j.quascirev.2016.08.012

Palmentola, G., Boenzi, F., Mastronuzzi, G., Tromba, F. (1990). Osservazioni sulle trace glaciali del M. Timfi, Catena del Pindo (Grecia). Geografia Fisica e Dinamica Quaternaria 13, 165–170.

Palmentola, G. and Stamatopoulos, L. (2006). Preliminary data about sporadic permafrost on Peristeri and Tzoumerka massifs (Pindos chain, Northwestern Greece). *Revista de geomorhologie 8*, 17-23.

Panagiotopoulos K., Böhm A., Leng M.J., Wagner B., Schäbitz F. (2014). Climate variability over the last 92 ka in SW Balkans from analysis of sediments from Lake Prespa. *Climate of the Past 10*, 643-660. https://doi.org/10.5194/cp-10-643-2014

Papada, L. and Kaliampakos, D. (2016). Developing the energy profile of mountainous areas. *Energy 107*, 205-214. https://doi.org/10.1016/j.energy.2016.04.011

Paterson, W.S.B. (1994). *The Physics of Glaciers*. London: Pergamon/Elsevier.

Pavlopoulos, K., Evelpidou, N., Vassilopoulos, A. (2009). *Mapping geomorphological environments*. Berlin: Springer Science & Business Media, pp 5-47.

Pavlopoulos, K., Leontaritis, A., Athanassas, C.D., Petrakou C., Vandarakis D., Nikolakopoulos K., Stamatopoulos L., Theodorakopoulou K. (2018). Last glacial geomorphologic records in Mt Chelmos, North Peloponnesus, Greece. *Journal of Mountain Science 15*, 948–965. https://doi.org/10.1007/s11629-017-4563-0

Pechoux, P.E. (1970). Traces d'activité glaciaire dans les montagnes de Grèce central. *Revue de géographie alpine 58*, 211-224. https://doi.org/10.3406/rga.1970.3465

Péchoux, P.Y. (1977). Nouvelles remarques sur les versants Quaternaires du secteur de Delphes. *Revue de Géographie Physique et de Géologie Dynamique 19*, 83–92.

Pelletier, L., Vils, F., Kalt, A., Gméling, K. (2008). Li, B and Be Contents of Harzburgites from the Dramala Complex (Pindos Ophiolite, Greece): Evidence for a MOR-type Mantle

in a Supra-subduction Zone Environment. *Journal of Petrology 49*, 2043–2080. https://doi.org/10.1093/petrology/egn057

Pellitero, R., Rea, B.,R., Spagnolo, M., Bakke, J., Hughes, P., Ivy-Ochs, S., Lukas, S., Ribolini, A. (2015). A GIS tool for automatic calculation of glacier equilibrium-line altitudes. *Computer & Geosciences 82*, 55–62. https://doi.org/10.1016/j.cageo.2015.05.005

Pellitero, R., Rea, B.,R., Spagnolo, M., Bakke, J., Ivy-Ochs, S., Frew, C. R., Hughes, P., Ribolini, A., Lukas, S., Renssen, H., 2016. GlaRe a GIS tool to reconstruct the 3D surface of palaeoglaciers. Computer & Geosciences 94, 77-85. https://doi.org/10.1016/j.cageo.2016.06.008

Peña, J.L., Sancho, C., Lewis, C., Mcdonald E.V. (2004) Datos cronologicos de las morrenas terminals del glaciar del Gallego y su relacion con las terrazas fluvioglaciares (Pirineo de Huesca). In: Peña, J.L., et al. (eds.), *Geografia Fısica de Aragon, Aspectos generales y tematicos*, Zaragoza: Universidad de Zaragoza e Institucion Fernando el Catolico, pp 71-84.

Penck, A. (1885). La Période glaciaire dans les Pyrénées. *Bulletin de la Societe d'Histoire Naturelle de Toulouse 19*, 105-200.

Philipson., A. (1892). *Der Peloponnes. Versuch einer Landeskunde auf geologischer Grundlage.* Berlin: Friedlaender & Sohn, pp. 382.

Phillips, F.M., Zreda, M., Gosse, J.C., Klein, J., Evenson, E.B., Hall, R.D., Chadwick, O.A., Sharma, P. (1997). Cosmogenic ^{36}Cl and ^{10}Be ages of Quaternary glacial and fluvial deposits of the Wind River Range, Wyoming. *Geological Society of America Bulletin 109*, 1453-1463. https://doi.org/10.1130/0016-7606(1997)109<1453:CCABAO>2.3.CO;2

Phillips, F., Argento, D., Balco, G., Caffee, M., Clem, J., Dunai, T., Finkel, R., Goehring, B., Gosse, J., Hudson, A., Jull, A., Kelly, M., Kurz, M., Lal, D., Lifton, N., Marrero, S.M., Nishiizumi, K., Reedy, R.C., Schaefer, J.M., Stone, J., Swanson, T., Zreda, M. (2016). The CRONUS-Earth Project: A synthesis. *Quaternary Geochronology 31*, 119-154. https://doi.org/10.1016/j.quageo.2015.09.006

Piccardi, L. (2000). Active faulting at Delphi: seismotectonic remarks and a hypothesis for the geological environment of a myth. *Geology 28*, 651–654

Pirazzoli P.A., Stiros, S.C., Fontugne, M., Arnold, M. (2004). Holocene and Quaternary uplift in the central part of the southern coast of the Corinth Gulf (Greece). *Marine Geology 212*, 35-44. https://doi.org/10.1016/j.margeo.2004.09.006

Pope, R. J. and Millington, A. C. (2000). Unravelling the patterns of alluvial fan development using mineral magnetic analysis: examples from the Sparta Basin, Lakonia, southern Greece. *Earth Surface Processes and Landforms 25*, 601–615. https://doi.org/10.1002/1096-9837(200006)25:6<601::AID-ESP94>3.0.CO;2-M

Pope, R.J. and Wilkinson, K.N. (2006). Reconciling the roles of climate and tectonics in Late Quaternary fan development on the Spartan piedmont, Greece. *Geological Society of London Special Publication 251*, 133-152. https://doi.org/10.1144/GSL.SP.2005.251.01.10

Pope, R.J. (2010). Linking high altitude glacier melting to Late Quaternary sedimentation in environmentally sensitive range-front alluvial fans in the Sparta Basin, southern Greece.

Geophemera *108*, 17-23. https://geomorphology.org.uk/sites/default/files/Geophemera%20108.pdf

Pope, R.J., Hughes, P.D., Skourtsos, E. (2017). Glacial history of Mount Chelmos, Peloponnesus, Greece. IN: Hughes, P.D. and Woodward, J.C. (Eds.), *Quaternary Glaciation in the Mediterranean Mountains.* London: Geological Society of London Special Publications 433, pp. 211-236. https://doi.org/10.1144/SP433.11

Preusser, F., Andersen, B. G., Denton, G. H., Schlüchter, C. (2005). Luminescence chronology of Late Pleistocene glacial deposits in North Westland, New Zealand. *Quaternary Science Reviews 24*, 2207−2227. https://doi.org/10.1016/j.quascirev.2004.12.005

Putkonen, J. and Swanson, T. (2003). Accuracy of cosmogenic ages for moraines.*Quaternary Research 59*, 255-261. https://doi.org/10.1016/S0033-5894(03)00006-1

Putkonen, J. and O'Neal, M. (2006). Degradation of unconsolidated Quaternary landforms in the western North America. *Geomorphology 75*, 408–419. https://doi.org/10.1016/j.geomorph.2005.07.024

Rasmussen, S.O., Andersen, K.K., Svensson, A.M., Steffensen, J.P., Vinther, B.M., Clausen, H.B., Siggaard-Andersen, M.-L., Johnsen, S.J., Larsen, L.B., Dahl- Jensen, D., Bigler, M., Roethlisberger, R., Fischer, H., Goto-Azuma, K., Hansson, K.J., M.E., Ruth, U. (2006). A new Greenland ice core chronology for the last glacial termination. *Journal of Geophysical Research 111 (D06102),* 1-16. https://doi.org/10.1029/2005JD006079

Rasmussen, S.O., Bigler, M., Blockley, S. P., Blunier, T., Buchardt, S.L., Clausen, H. B., Cvijanovic, I., Dahl-Jensen, D., Johnsen, S.J., Fischer, H., Gkinis, V., Guillevic, M., Hoek, W.Z., Lowe, J.J., Pedro, J.B., Popp, T., Seierstad, I.K., Steffensen, J.P., Svensson, A.M., Vallelonga, P., Vinther, B.M.,Walker, M.J.C., Wheatley, J.J., Winstrup, M. (2014). A stratigraphic framework for abrupt climatic changes during the Last Glacial period based on three synchronized Greenland ice-core records: refining and extending the INTIMATE event stratigraphy. *Quaternary Science Reviews 106*, 14-28. https://doi.org/10.1016/j.quascirev.2014.09.007

Rassios, A. E., and Dilek, Y. (2009). Rotational deformation in the Jurassic Mesohellenic ophiolites, Greece, and its tectonic significance. *Lithos 108*, 207–223, https://doi.org/10.1016/j.lithos.2008.09.005

Rassios, A. H. E., and Moores, E. M. (2006). Heterogeneous mantle complex, crustal processes, and obduction kinematics in a unified Pindos– Vourinos ophiolitic slab (northern Greece). IN: A. H. F. Robertson and D. Mountrakis)Eds.), *Tectonic Development of the Eastern Mediterranean Region* (Special Publications 260, pp 237–266). London: Geological Society of London. https://doi.org/10.1144/GSL.SP.2006.260.01.11

Rawson, P.F., Allen, P.M., Brenchley, P.J., Cope, J.C.W., Gale, A.S., Evans, J.A., Gibbard, P.L., Gregory, F.J., Hailwood, E.A., Hesselbo, S.P., Knox, R.W.O'.B., Marshall, J.E.A., Oates, M., Riley, N.J., Smith, A.G., Trewin, N., Zalasiewicz, J.A. (2002). *Stratigraphical Procedure.* London: The Geological Society, pp. 57.

Rea, B.R. (2009). Defining modern day Area–Altitude Balance Ratios (AABRs) and their use in glacier–climate reconstructions. *Quaternary Science Reviews 28*, 237–248. https://doi.org/10.1016/j.quascirev.2008.10.011

Rea, B.R. and Evans, D.J.A. (2007). Quantifying climate and glacier mass balance in north Norway during the YD. *Palaeogeography, Palaeoclimatology, Palaeoecology 246*, 307–330. https://doi.org/10.1016/j.palaeo.2006.10.010

Regato, P. and Salman, R. (2008). Mediterranean Mountains in a Changing World. Guidelines for Developing Action Plans. International Union for Conservation of Nature and Natural Resources, Gland.

Renz., C., 1910. *Stratigraphische Untersuchungen im griechischen Mesozoikum und Paläozoikum.* Wien: Lechner, pp. 131.

Reuther, A.U., Herget, J., Ivy-Ochs, S., Borodavko, P., Kubik, P.W., Heine, K. (2006). Constraining the timing of the most recent cataclysmic flood event from ice-dammed lakes in the Russian Altai mountains, Siberia using cosmogenic in-situ ^{10}Be. *Geology 34*, 913-916. https://doi.org/10.1130/G22755A.1

Reuther, A.U., Urdea, P., Geiger, C., Ivy-Ochs, S., Niller, H.-P., Kubik, P.W. & Heine, K. (2007). Late Pleistocene glacial chronology of the Pietrele Valley, Retezat Mountains, Southern Carpathians constrained by ^{10}Be exposure ages and pedological investigations. *Quaternary International 164–165*, 151–169. https://doi.org/10.1016/j.quaint.2006.10.011

Rhodes, E. J. (2011). Optically Stimulated Luminescence Dating of Sediments over the Past 200,000 Years. *Annual Review of Earth and Planetary* Sciences 39, 461-488. https://doi.org/10.1146/annurev-earth-040610-133425

Ribolini, A., Bini, M., Isola, I., Spagnolo, M., Zanchetta, G., Pellitero, R., Mechernich, S., Gromig, R., Dunai, T., Wagner, B., Milevski. I. (2017). An Oldest Dryas glacier expansion on Mount Pelister (Former Yugoslavian Republic of Macedonia) according to ^{10}Be cosmogenic dating. *Journal of the Geological Society 175*, 100-110. https://do,i.org/10.1144/jgs2017-038

Richards, B.W.M., Benn, D.I., Owen, L.A., Rhodes, E.J. and Spencer, J.Q.G. (2000). Timing of late Quaternary glaciations south of Mount Everest in the Khmubu Himal, Nepal. *Geological Society of America Bulletin 112*, 1621–32. https://doi.org/10.1130/0016-7606(2000)112<1621:TOLQGS>2.0.CO;2

Richmond, G.M. (1959). Report of the Pleistocene Committee, American Commission on Stratigraphic Nomenclature. *American Association of Petroleum Geologists Bulletin 43*, 633–675. https://doi.org/10.1306/0BDA5CCF-16BD-11D7-8645000102C1865D

Richter, D., Mueller, C, Risch, H. (1994). Die Flysch-Zonen Griechenlands IX. Der böotische Oberkreide-Flysch im nördlichen Parnass und im nordwestlichen Kallidromon-Gebirge (Griechenland). *Zeitschrift der geologisches Gesselschaft 145*, 274-285.

Richter, D., Mueller, C, Mihm, A., Risch, H. (1996). Die Flysch-Zonen Griechenlands XII. Das Böotikum und seine Flysche im Bereich des Iti - Parnass - Elikon Gebirges, des nordwestlichen Kallidromon Gebirges und des südwestlichen Othrys - Gebirges

(Mittelgriechenland). *Neues Jahrbook de Geologie und Paläontologie Abhandlung 201*, 267-409.

Robertson, A. H. F. (2002). Overview of the genesis and emplacement of Mesozoic ophiolites in the Eastern Mediterranean Tethyan region. *Lithos 65*, 1–67. https://doi.org/10.1016/S0024-4937(02)00160-3

Rodriguez-Rodriguez, L., Jimenez-Sanchez, M., Dominguez-Cuesta, M.J., Rico, M.T., Valero-Garces, B.L. (2011). Last deglaciation in northwestern Spain: New chronological and geomorphologic evidence from the Sanabria region. *Geomorphology 135*, 48−65. https://doi.org/10.1016/j.geomorph.2011.07.025

Rohling, E.J., Mayewski, P.A., Hayes, A., ABU-Zied, R.H., Casford, J. (2002). Holocene Atmosphere-Ocean Interactions: Records from Greenland and the Aegean Sea. *Climate Dynamics 18*, 573-592. https://doi.org/10.1007/s00382-001-0194-8

Rohling E., Mayewski, P., Challenor, K. (2003) On the timing and mechanism of millennial-scale climate variability during the last glacial cycle. Climate Dynamics 20: 257-267. https://doi.org/10.1007/s00382-002-0266-4

Roucoux, K.H., Tzedakis, P.C., Lawson, I.T., Margari, V. (2011). Vegetation history of the penultimate glacial period (Marine isotope stage 6) at Ioannina, north-west Greece. *Journal of Quaternary Science 26*, 616–626. https://doi.org/10.1002/jqs.1483

Saccani, E., and Photiades, A. (2004). Mid-ocean ridge and supra-subduction affinities in the Pindos ophiolites (Greece): Implications for magma genesis in a forearc setting. *Lithos 73*, 229–253. https://doi.org/10.1016/j.lithos.2003.12.002

Sadori, L., Koutsodendris, A., Masi, A., Bertini, A., Combourieu-Nebout, N., Francke, A., Kouli, K., Joannin, S., Mercuri, A.M., Panagiotopoulos, K., Peyron, O., Torri, P., Wagner, B., Zanchetta, G., Donders, T.H. (2016). Pollen-based paleoenvironmental and paleoclimatic change at Lake Ohrid (SE Europe) during the past 500 ka. *Biogeosciences 13*, 1423–1437. doi:10.5194/bgd-12-15461-2015

Salcher, B. C., Kober, F., Kissling, E., Willett, S. D. (2014). Glacial im-pact on short-wavelength topography and long-lasting effects on the denudation of a deglaciated mountain range. *Global Planetary Change 115*, 59–70, 201. https://doi.org/10.1016/j.gloplacha.2014.01.002

Salvador, A. (1994). *International Stratigraphic Guide: a Guide to Stratigraphic Classification, Terminology and Procedure*. Boulder CO (USA): International Union of Geologic Sciences and The Geological Society of America, pp.137.

Sanchez Goñi, M.F., Harrison, S.P., 2010. Millennial-scale climate variability and vegetation changes during the Last Glacial: concepts and terminology. *Quaternay Science Reviews 29*, 2823-2827. https://doi.org/10.1016/j.quascirev.2009.11.014

Sarıkaya, M.A., Ciner, A., Haybat, H., Zreda, M. (2014). An early advance of glaciers on Mount Akdag˘, SW Turkey, before the global Last Glacial Maximum; insights from cosmogenic nuclides and glacier modelling. *Quaternary Science Reviews 88*, 96-109. https://doi.org/10.1016/j.quascirev.2014.01.016

Sarıkaya, M.A., Çiner, A. (2017). The late Quaternary glaciation in the Eastern Mediterranean. In: Hughes, P. & Woodward, J. (Eds.), *Quaternary Glaciation in the Mediterranean Mountains.* London: Geological Society of London Special Publication 433, pp. 289-305. https://doi.org/10.1144/SP433.4

Sarıkaya, M.A., Stepišnik, U., Žebre, M., Çiner, A., Yıldırım, C., Vlahović, I., Tomljenović, B., Matoš, B., Wilcken , K.M. (2020). Last glacial maximum deglaciation of the Southern Velebit Mt. (Croatia): insights from cosmogenic ^{36}Cl dating of Rujanska Kosa. *Mediterranean Geoscience Reviews 2*, 53–64. https://doi.org/10.1007/s42990-020-00030-9

Sato, T., Yasuda, H., Niita, K., Endo, A., Sihver, L. (2008). Development of PARMA: PHITS-based analytical radiation model in the atmosphere. *Radiation Research 170*, 244-259. https://doi.org/10.1667/RR1094.1

Schimmelpfennig, I., Benedetti, L., Finkel, R., Pik, R., Blard, P. H., Bourles, D., Burnard, P., Williams, A. (2009). Sources of in-situ ^{36}Cl in basaltic rocks. Implications for calibration of production rates. *Quaternary Geochronology 4*, 441–461. https://doi.org/10.1016/j.quageo.2009.06.003

Schimmelpfennig, I., Benedetti, L., Garreta, V., Pik, R., Blard, P-H., Burnard, P., Bourles, D., Finkel, R., Ammon, K., Dunai, T. (2011). Calibration of cosmogenic ^{36}Cl production rates from Ca and K spallation in lava flows from Mt. Etna (38º, Italy) and Payun Matru (36 º S, Argentina). *Geochimica et Cosmochimica Acta 75*, 2611-2632. https://doi.org/10.1016/j.gca.2011.02.013

Schmidt, S., Hetzel, R., Kuhlmann, J., Mingorance, F., Ramos, V.A. (2011). A note of caution on the use of boulders for exposure dating of depositional surfaces. *Earth and Planetary Science Letters 302*, 60–70. https://doi.org/10.1016/j.epsl.2010.11.039

Schomacker, A., Benediktsson, Í.Ö., Ingólfsson, Ó. (2014). The Eyjabakkajökull glacial landsystem, Iceland: Geomorphic impact of multiple surges. *Geomorphology 218*, 98–107. https://doi.org/10.1016/j.geomorph.2013.07.005

Serrano, E., González-Trueba, J.J., González-García, M. (2012a). Mountain glaciation and paleoclimate reconstruction in the Picos de Europa (Iberian Peninsula, SW Europe). *Quaternary Research 78*, 303-314. https://doi.org/10.1016/j.yqres.2012.05.016

Serrano, E., González-Trueba, J.J., Pellitero, R., González-García, M., Gómez-Lende, M. (2012b). Quaternary glacial evolution in the Central Cantabrian Mountains (Northern Spain). *Geomorphology 196*, 65-82. https://doi.org/10.1016/j.geomorph.2012.05.001

Shakun, J.D., Clark, P.U., He, F., Lifton, N.A., Liu, Z., Otto-Bliesner, B.L., 2015. Regional and global forcing of glacier retreat during the last deglaciation. *Nature Communications 6*, 8059. https://doi.org/10.1038/ncomms9059

Sinopoli, G., Peyron, O., Masi, A., Holtvoeth, J., Francke, A., Wagner, B., Sadori, L. (2019). Pollen-based temperature and precipitation changes in the Ohrid Basin (western Balkans) between 160 and 70 ka. *Climate of the Past 15*, 53–71. https://doi.org/10.5194/cp-15-53-2019

Sinopoli, G., Masi, A., Regattieri, E., Wagner, B., Francke, A., Peyron, O., Sadori, L. (2018). Palynology of the Last Interglacial Complex at Lake Ohrid: palaeoenvironmental and

palaeoclimatic inferences. *Quaternary Science Reviews 180*, 177-192. https://doi.org/10.1016/j.quascirev.2017.11.013

Skourtsos, E. and Kranis, H. (2009). Structure and evolution of the western Corinth Rift, through new field data from the Northern Peloponnesus. IN: Ring, U. & Wernicke, B. (Eds.), *Extending a Continent: Architecture, Rheology and Heat Budget.* London: Geological Society of London Special Publication 321, pp 119–138. https://doi.org/10.1144/SP321.6

Skourtsos, E. and Lekkas, S. (2011). Extensional tectonics in Mt Parnon (Peloponnesus, Greece). *International Journal of Earth Science 100*, 1551–1567. https://doi.org/10.1007/s00531-010-0588-0

Smith, G.W., Nance, R.D., Genes, A.N. (1997). Quaternary glacial history of Mount Olympus, Greece. *Geological Society of America Bulletin 109*, 809–824.

Smith, G.R.,Woodward, J.C.,Heywood, D.I., Gibbard, P.L. (1998). Mapping glaciated karst terrain in a Mediterranean mountain environment using SPOT and TM data IN: Burt, P.J.A., Power, C.H., Zukowski, P.M. (Eds.), *Developing International Connections: RSS98 (Proceedings of the 24th Annual Conference and Exhibition of the Remote Sensing Society).* Greenwich: The University of Greenwich, pp. 457–463.

Smith, J.A., Finkel, R.C., Farber, D.L., Robell, D.T., Seltzer, G.O. (2005). Moraine preservation and boulder erosion in the tropical Andes: interpreting old surface exposure ages in glaciated valleys. *Journal of Quaternary Science 20*, 735-758. https://doi.org/10.1002/jqs.981

Spencer, J. Q. and Owen, L. A. (2004). Optically stimulated luminescence dating of Late Quaternary glaciogenic sediments in the upper Hunza valley: Validating the timing of glaciation and assessing dating methods. *Quaternary Science Reviews 23*, 175−191. https://doi.org/10.1016/S0277-3791(03)00220-8

Stavropoulou., N., Papakonstantinou, K., Vantaraki, M., Kizilou, K., Ikonomou, M. (2003). *The wetland of Lake Tsivlos.* Akrata, Greece: Akrata Centre of environmental Education, pp. 3-4.

Sternai, P., Sue, C., Husson, L., Serpelloni, E., Becker, T.W., Willett, S.D., Faccenna, C., DiGiulio, A., Spada, G., Jolivet, L., Valla, P., Petit, C., Nocquet, J.M., Walpersdorf, A., Castelltort, S. (2019). Present-day uplift of the European Alps: evaluating mechanisms and models of their relative contributions. *Earth Science Reviews 190*, 589–604. https://doi.org/10.1016/j.earscirev.2019.01.005

Stewart, S.A. (1996). Influence of detachment layer thickness on style of thin-skinned shortening. *Journal of Structural Geology 18*, 1271–1274. https://doi.org/10.1016/S0191-8141(96)00052-1

Stewart, I. and Vita-Finzi, C. (1996). Coastal uplift on active normal faults: the Eliki fault, Greece. *Geophysical Research Letters 23*, 1853–1856. https://doi.org/10.1029/96GL01595

Stone, J.O.H., Evans, J.M., Fifield, L.K., Allan, G.L., Cresswell, R.G. (1998). Cosmogenic chlorine-36 production in calcite by muons. *Geochimica et Cosmochimica Acta 62*, 433-454. https://doi.org/10.1016/S0016-7037(97)00369-4

Styllas, M.N., Schimmelpfennig, I., Ghilardi, M., Benedetti, L. (2016). Geomorphologic and paleoclimatic evidence of Holocene glaciation on Mount Olympus, Greece. *Holocene 26,* 709-721. https://doi.org/10.1177/0959683615618259

Styllas M.N., Schimmelpfennig, I., Benedetti, L., Ghilardi, M., Aumaître, G., Bourlès, D., Keddadouche, K. (2018). Late-glacial and Holocene history of the northeast Mediterranean mountain glaciers - New insights from in situ-produced 36Cl-based cosmic ray exposure dating of paleo-glacier deposits on Mount Olympus, Greece. *Quaternary Science Reviews 193,* 244-265. https://doi.org/10.1016/j.quascirev.2018.06.020

Sue, C., Delacou, B., Champagnac, J.D., Allanic, C., Tricart, P., Burkhard, M. (2007). Extensional neotectonics around the bend of the Western/Central Alps: an overview. *International Journal of Earth Sciences 96,* 1101−1129. https://doi.org/10.1007/s00531-007-0181-3

Svendsen, J. I., Alexanderson, H., Astakhov, V. I., Demidov, I., Dowdeswell, J. A., Funder, S., Gataullin, V., Henriksen, M., Hjort, Ch., Houmark-Nielsen, M., Hubberten, H. W., Ingo´lfsson, O., Jakobsson, M., Kjær, K. H., Larsen, E., Lokrantz, H., Lunkka, J. P., Lysa˚, A., Mangerud, J., Matiouchkov, A., Murray, A. S., Moeller, P., Niessen, F., Nikolskaya, O., Polyak, L., Saarnisto, M., Siegert, Ch., Siegert, M. J., Spielhagen, R. F., Stein, R. (2004). Late Quaternary ice sheet history of northern Eurasia. *Quaternary Science Reviews 23,* 1229−1271. https://doi.org/10.1016/j.quascirev.2003.12.008

Takaku. J., Futamura, N., Iijima, T., Tadono, T., Shimada, M. (2007). High resolution DSM generation from ALOS PRISM. *International Geoscience and Remote Sensing Symposium (IGARSS), 1974-1977.*

Takaku, J., Tadono, T., Shimada, M. (2008). High Resolution DSM Generation from ALOS PRISM - Calibration Updates-. *IGARSS 2008 - IEEE International Geoscience and Remote Sensing Symposium 2,* 181-184.

Templeton, D.H. (1953). Nuclear reactions induced by high energy particles. *Annual review of nuclear science 2,* 93-104. https://doi.org/10.1146/annurev.ns.02.120153.000521

Toutin, T. (2004). Geometric processing of remote sensing images: models, algorithms and method. *International Journal of Remote Sensing 25,* 1893 - 1924. https://doi.org/10.1080/0143116031000101611

Toutin, T. (2001). Elevation Modelling from Satellite VIR Data: A Review. *International Journal of Remote Sensing 22*, 1097 - 1125. https://doi.org/10.1080/01431160117862

Tsoflias, P. (1973). Geology and Geomorphology of the mount Helmos in the area of Loussi of Kalavryta county (Northern Peloponnisos). Digital Library "Theofrastos", Aristoteleion University of Thessaloniki, Department of Geology, pp 23-25.

Tzedakis, P.C. (1994.) Vegetation change through glacial-interglacial cycles: a long pollen sequence perspective. *Philosophical Transactions of the Royal Society of London 345*, 403-432. https://doi.org/10.1098/rstb.1994.0118

Tzedakis, P.C. (1999). The last climatic cycle at Kopais, central Greece. *Journal of the Geological Society of London 156,* 425-434. https://doi.org/10.1144/gsjgs.156.2.0425

Tzedakis, P.C., Lawson, I.T., Frogley, M.R., Hewitt, G.M., Preece, R.C. (2002). Buffered tree population changes in a Quaternary refugium: evolutionary implications. *Science 297,* 2044-47. https://doi.org/10.1126/science.1080630

Tzedakis, P.C., McManus, J.F., Hooghiemstra, H., Oppo, D.W., Wijmstra, T.A. (2003). Comparison of changes in vegetation in northeast Greece with records of climate variability on orbital and suborbital frequencies over the last 450 000 years. *Earth and Planetary Sciece Letters 212,* 197-212. https://doi.org/10.1016/S0012-821X(03)00233-4

Tzedakis, P.C., Frogley, M,R., Lawson, I.T., Preece, R.C., Cacho, I., de Abreu, L. (2004). Ecological thresholds and patterns of millennialscale climate variability: the response of vegetation in Greece during the last glacial period. *Geology 32,* 109-112. https://doi.org/10.1130/G20118.1

Tzedakis, P.C., Hooghiemstra, H., Palike, H. (2006). The last 1.35 million years at Tenaghi Philippon: revised chronostratigraphy and long-term vegetation trends. *Quaternary Science Reviews 25,* 3416–3430. https://doi.org/10.1016/j.quascirev.2006.09.002

Tzedakis, P.C., Crucifix, M.,, Mitsui, T., Wolff, E.W. (2017). A simple rule to determine which insolation cycles lead to interglacials. *Nature 542*, 427–432. https://doi.org/10.1038/nature21364

Van Asselen, S., Seijmonsbergen A.C. (2006). Expert-driven semi-automated geomorphological mapping for a mountainous area using a laser DTM. *Geomorphology 78,* 309 - 320. https://doi.org/10.1016/j.geomorph.2006.01.037

van Hinsbergen, D. J. J., Edwards, M. A., Govers, R. (2009). Geodynamics of collision and collapse at the Africa–Arabia–Eurasia subduction zone – an introduction. *Geological Society of London, Special Publications 311,* 1-7. https://doi.org/10.1144/SP311.1

Vogiatzakis, I.N. (2012). *Mediterranean Mountain Environments.* Oxford: Wiley-Blackwell.

Wagner, G. A. (1998). *Age Determination of Young Rocks and Artefacts*. Heidelberg: Springer, pp.466.

Wagner, B., Vogel, H., Francke, A. et al., 2019. Mediterranean winter rainfall in phase with African monsoons during the past 1.36 million years. *Nature 573*, 256–260. https://doi.org/10.1038/s41586-019-1529-0

Whipple, K.X., 2009. The influence of climate on the tectonic evolution of mountain belts. *Nature Geoscience 2*, 97–104. https://doi.org/10.1038/ngeo413

Wiche, K. (1956). Beitrag zur Morphologie des Thessalischen Olymp. *Geographischer Jahresberichtus Osterreich 26,* 25-40.

Wirth, S.B. and Sessions, A.L. (2016). Plant-wax D/H ratios in the southern European Alps record multiple aspects of climate variability. *Quaternary Science Reviews 148,* 176-181. https://doi.org/10.1016/j.quascirev.2016.07.020

Woodward, J.C. (2009). *The Physical Geography of the Mediterranean.* Oxford: Oxford University Press.

Woodward, J.C. and Hughes, P.D. (2011). Glaciation in Greece: A New Record of Cold Stage Environments in the Mediterranean. IN: Ehlers J., Gibbard, P.L., Hughes, P.D. (Eds.),

Quaternary glaciations - Extent and chronology. A closer look. (pp. 175-198). Amsterdam: Elsevier. https://doi.org/10.1016/B978-0-444-53447-7.00015-5

Woodward, J.C., Lewin, J., Macklin, M.G. (1992). Alluvial sediment sources in a glaciated catchment: the Voidomatis basin, northwest Greece. *Earth Surface Processes and Landforms 16,* 205–216. https://doi.org/10.1002/esp.3290170302

Woodward, J.C., Lewin, J., Macklin, M.G. (1995). Glaciation, river behaviour and Palaeolithic settlement of upland northwest Greece. IN: Lewin, J., Macklin, M.G., Woodward, J.C. (Eds.), *Mediterranean Quaternary River Environments.* Rotterdam: Balkema, pp. 115–129.

Woodward, J.C., Hamlin, R.H.B., Macklin, M.G., Karkanas, P., Kotjabopoulou, E. (2001). Quantitative sourcing of slackwater sediments at Boila rockshelter: A record of Lateglacial flooding and Paleolithic settlement in the Pindus Mountains, Northwest Greece. *Geoarchaeology 16,* 501-536. https://doi.org/10.1002/gea.1003

Woodward, J.C., Macklin, M.G., Smith, G.R. (2004). Pleistocene glaciation in the mountains of Greece. IN: Ehlers J., Gibbard, P.L. (Eds.), *Quaternary glaciations - extent and chronology. Part I: Europe.* Amsterdam: Elsevier, pp. 155-173. https://doi.org/10.1016/S1571-0866(04)80066-6

Woodward, J.C., Hamlin, R.H.B., Macklin, M.G., Hughes, P.D., Lewin, J. (2008). Glacial activity and catchment dynamics in northwest Greece: long-term river behaviour and the slackwater sediment record for the last glacial to interglacial transition. *Geomorphology 101,* 44–67. https://doi.org/10.1016/j.geomorph.2008.05.018

Wulf, S., Hardiman, M.J., Staff, R.A., Koutsodendris, A., Appelt, O., Blockley, S.P.E., Lowe, J.J., Manning, C.J., Ottolini, L., Schmitt, A.K., Smith, V.C., Tomlinson, E.L., Vakhrameeva, P., Knipping, M., Kotthoff, U., Milner, A.M., Müller, U.C., Christanis, K., Kalaitzidis, S., Tzedakis, P.C., Schmiedl, G., Pross, J. (2018). The marine isotope stage 1–5 cryptotephra record of Tenaghi Philippon, Greece: Towards a detailed tephrostratigraphic framework for the Eastern Mediterranean region. *Quaternary Science Reviews 186,* 236–262. doi:10.1016/j.quascirev.2018.03.011

Žebre, M., Sarıkaya M.A., Stepišnik, U., Yıldırım, C., Çiner, A. (2019). First ^{36}Cl cosmogenic moraine geochronology of the Dinaric mountain karst: velež and Crvanj Mountains of Bosnia and Herzegovina. *Quaternary Science Reviews 208,* 54–75. https://doi.org/10.1016/j.quascirev.2019.02.002

Zreda, M.G., Phillips, F.M., Elmore, D. (1994). Cosmogenic ^{36}Cl accumulation in unstable landforms. 2. Simulations and measurements on eroding moraines. *Water Resources Research 30,* 3127-3136. https://doi.org/10.1029/94WR00760